

AD-766 475

ALASKAN ARCTIC COASTAL PROCESSES AND  
MORPHOLOGY

William J. Wiseman, Jr., et al

Louisiana State University

Prepared for:

Office of Naval Research  
Advanced Research Projects Agency

July 1973

DISTRIBUTED BY:

**NTIS**

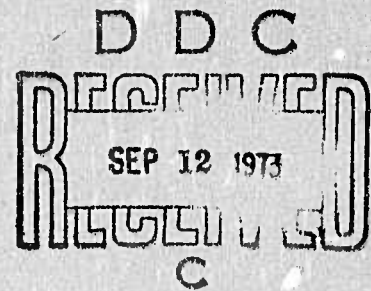
**National Technical Information Service  
U. S. DEPARTMENT OF COMMERCE  
5285 Port Royal Road, Springfield Va. 22151**

AD 766475



Coastal Studies Institute  
Louisiana State University  
Baton Rouge, Louisiana 70803

W. G. McIntire, Principal Investigator  
Phone 504 388-2395



Technical Report No. 149

# ALASKAN ARCTIC COASTAL PROCESSES AND MORPHOLOGY

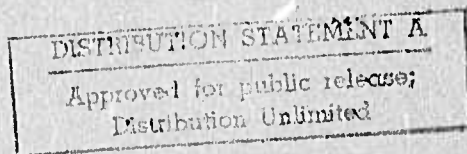
By Wm. J. Wiseman, Jr., J. M. Coleman, A. Gregory, S. A. Hsu,  
A. D. Short, J. N. Suhayda, C. D. Walters, Jr., and L. D. Wright

Scientific Officer: Director, Geography Programs, Earth Sciences  
Division, Office of Naval Research, Department of the Navy,  
800 North Quincy Street, Arlington, Virginia 22217

Contract Duration: May 1, 1971 - June 30, 1973

FINAL REPORT

JULY 1973

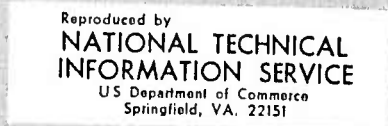


Sponsored by

Advanced Research Projects Agency ARPA Order No. 1783  
(Amount of Contract, \$110,000)

and

Geography Programs (Code 414) Office of Naval Research  
Contract No. N00014-69-A-0211-0C05



Unclassified

Security Classification

DOCUMENT CONTROL DATA - R & D		
<i>(Security classification of title, body of abstract and indexing annotation must be entered when the overall report is classified)</i>		
1. ORIGINATING ACTIVITY (Corporate author) Coastal Studies Institute Louisiana State University Baton Rouge, La. 70803		2a. REPORT SECURITY CLASSIFICATION Unclassified
		2b. GROUP Unclassified
3. REPORT TITLE ALASKAN ARCTIC COAST PROCESSES AND MORPHOLOGY		
4. DESCRIPTIVE NOTES (Type of report and inclusive dates)		
5. AUTHOR(S) (First name, middle initial, last name) Wm. J. Wiseman, Jr., James M. Coleman, Anthony Gregory, Shih-Ang Hsu, Andrew D. Short, Joseph N. Suhayda, Charles D. Walters, Jr., and Lynn D. Wright		
6. REPORT DATE July 1973	7a. TOTAL NO. OF PAGES 171	7b. NO. OF REFS 138
8a. CONTRACT OR GRANT NO. N00014-69-A-0211-0005	9a. ORIGINATOR'S REPORT NUMBER(S) Technical Report No. 149	
b. PROJECT NO. NR 388 110	9b. OTHER REPORT NO(S) (Any other numbers that may be assigned this report)	
c.		
d.		
10. DISTRIBUTION STATEMENT Approved for public release; distribution unlimited.		
11. SUPPLEMENTARY NOTES		12. SPONSORING MILITARY ACTIVITY Geography Programs and Arctic Program Office of Naval Research Arlington, Virginia 22217
13. ABSTRACT A study of the temporal and spatial variability of the physical processes and environments of the Alaskan Arctic Coast was conducted over a 2-year period (May 1971 - June 1973). Micrometeorological studies demonstrated the difficulty of characterizing momentum transfer from air to ice by a single constant drag coefficient but indicated that such a coefficient may characterize air-sea momentum transfer in the nearshore waters. Summer wind-driven currents were far stronger and more variable than those during the winter season. They caused large meteorological tides and subsequent modification of the nearshore water mass characteristics. Major wave energy at the coast resulted from storm-generated waves. A single storm produced 200 times more wave power at the shoreline than was present during nonstorm conditions. Storm waves may be fetch limited by either storm size or width of open water. (U) Statistically significant contrasts were noted between the morphology of the Chukchi and Beaufort coasts. Structural lineaments parallel the Chukchi coast and are perpendicular to the Beaufort coast. Barrier systems are straight and continuous along the western coast and irregular and arcuate along the eastern. Offshore bars are common along both coasts but differ considerably in length and spacing along both coasts. They influence ice grounding, inlet location, subaerial beach characteristics, and erosion. (U) The study demonstrated the dominance of storm-induced modification of the nearshore region and indicated that the arctic coastal environment cannot be adequately characterized from short-term studies conducted during moderate conditions. (U)		

DD FORM 1473 (PAGE 1)  
1 NOV 65  
D/N 0101-807-6811

Unclassified  
Security Classification

A-31408

Unclassified

Security Classification

KEY WORDS	LINK A		LINK B		LINK C	
	ROLE	WT	ROLE	WT	ROLE	WT
Alaska Arctic Nearshore processes Beach processes Waves Currents Storm surges Water masses Boundary layer Micrometeorology Breakup Freezeup Geomorphology Offshore bars						

DD FORM 1473 (BACK)  
1 NOV 65

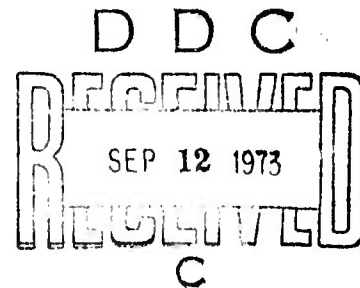
Unclassified

Security Classification

A-11401

ia

Coastal Studies Institute  
Louisiana State University  
Baton Rouge, Louisiana 70803



Technical Report No. 149

## ALASKAN ARCTIC COASTAL PROCESSES AND MORPHOLOGY

By Wm. J. Wiseman, Jr., J. M. Coleman, A. Gregory, S. A. Hsu,  
A. D. Short, J. N. Suhayda, C. D. Walters, Jr. and L. D. Wright

This research was partially supported by the Advanced Research  
Projects Agency of the Department of Defense and was monitored  
and partially supported by ONR under Contract No.  
N00014-69-A-0211-0005.

**DISTRIBUTION STATEMENT A**

Approved for public release;  
Distribution Unlimited

The views and conclusions contained in this document are those  
of the authors and should not be interpreted as necessarily  
representing the official policies, either expressed or implied,  
of the Advanced Research Projects Agency or the U. S.  
Government.

Approved for public release; distribution unlimited.

## ABSTRACT

A study was conducted from May 1971 through June 1973 to improve understanding of the temporal and spatial variability of the physical processes and environments of the Alaskan Arctic Coast. Laboratory study of maps and aerial photographs continued throughout the 2-year period; field investigations were conducted from April through October 1972. Micrometeorological studies demonstrated the difficulty of characterizing momentum transfer from air to ice by a single constant drag coefficient. Similar studies during the summer indicated that a single drag coefficient ( $1.71 \times 10^{-3}$  at 10 meters) may characterize air-sea momentum transfer in the nearshore waters of the entire Arctic. Air-sea interaction was determined to be the dominant feature of the nearshore physical oceanography. Summer wind-driven currents were far stronger and more variable than those during the winter season. These wind-driven currents caused large meteorological tides and subsequent modification of the nearshore water mass characteristics. Major wave energy at the coast resulted from storm-generated waves rather than those generated during more quiescent periods. A single storm produced 200 times more wave power at the shoreline than was present during nonstorm conditions. Storm waves along the Chukchi coast appear to be fetch limited by the storm size; those along the Beaufort coast may be fetch limited by either storm size or width of open water.

Statistically significant contrasts were noted between the morphologic parameters of the Chukchi and Beaufort seacoasts. Structural lineaments parallel the Chukchi coast and are perpendicular to the Beaufort coast. Barrier systems are straight and continuous along the western coast and irregular and arcuate along the eastern coast. Offshore bars are common along both coasts but differ considerably in size, spacing, and pattern along the coast. They influence grounding of nearshore ice, location of inlets, subaerial beach characteristics, and erosion rates.

Seaward flushing of lagoon waters by tidal currents during the freezeup period brings slush ice into the nearshore region, where storm waves may deposit it high on the beach face. This ice, along with snow and frozen swash, is often preserved and incorporated into the beach deposits. Subsequent melting during spring thaw produces a hummocky, irregular, and soft beach surface that persists until reworked by significant wave action.

The study demonstrated the dominance of storm-induced modification of the nearshore region and indicated that the arctic coastal environment cannot be adequately characterized from short-term studies conducted during moderate conditions.

#### ACKNOWLEDGMENTS

This study was supported by Geography Programs and Arctic Program, Office of Naval Research, under Contract N00014-69-A-0211-0005, Project NR 338 110, and Advanced Research Projects Agency Order No. 1783. Logistical and life support was provided by the Naval Arctic Research Laboratory at Barrow, Alaska. Without the help of the director, Mr. John Schindler, and its personnel, the project could not have been successfully completed. Aircraft support alone figured significantly in the project's success, and thanks are due to the pilots, who often performed duties beyond merely piloting the aircraft. The station masters and personnel at the Distant Early Warning (DEW) Line stations LIZ-2 and POW-2 were extremely helpful during the course of the field work and rendered assistance when it was requested. Coastal Studies Institute personnel freely contributed time, advice, and services during the duration of the project. Dr. Harley Walker, Department of Geography, LSU, provided valuable advice throughout the duration of the project. Mrs. Romaine Kupfer, research assistant, and Mrs. Mary Erickson, programmer, provided invaluable help. The successful completion of the project, however, would not have been possible without the help of our field and laboratory technical staff. Messrs. Norwood Rector, Rodney Fredericks, Bob Montgomery, Donald White, and Thomas Alexander were in charge of designing, fabricating, and shipping all the field gear used during the project. In addition, Messrs. Rodney Fredericks, Bob Montgomery, and Don White accompanied the field parties and installed and serviced the instrumentation, most often working under adverse conditions and for periods far beyond the call of duty. Mark Badgley and Douglas Fisher also assisted with the field work.

CONTENTS

	Page
ABSTRACT . . . . .	iii
ACKNOWLEDGMENTS . . . . .	iv
LIST OF FIGURES . . . . .	vii
LIST OF TABLES . . . . .	xiii
PREFACE . . . . .	xiv
CHAPTER I. INTRODUCTION . . . . .	1
Study Area . . . . .	3
Field Sites . . . . .	5
Instrumentation . . . . .	7
CHAPTER II. ATMOSPHERIC PROCESSES . . . . .	11
Introduction . . . . .	11
General Climate . . . . .	11
Surface Boundary-Layer Phenomena at Point Lay Site . . . . .	14
SUMMER SEASON . . . . .	14
WINTER SEASON . . . . .	20
CHAPTER III. NEARSHORE HYDRODYNAMIC PROCESSES . . . . .	25
Introduction . . . . .	25
Sea Level Variation . . . . .	25
Waves . . . . .	30
DATA ACQUISITION AND ANALYSIS . . . . .	31
DISCUSSION OF RESULTS . . . . .	33
Waves with 30- to 1,000-Second Periods . . . . .	33
Waves with 0.5- to 30-Second Periods . . . . .	33
SUMMARY . . . . .	39
Currents . . . . .	39
DROGUES . . . . .	40
Point Lay . . . . .	41
Pingok Island . . . . .	41
CURRENTS UNDER THE ICE . . . . .	42
SUMMER CURRENT METER MEASUREMENTS . . . . .	45
Water Mass Characteristics . . . . .	49
Discussion . . . . .	59
CHAPTER IV. ALASKAN ARCTIC COASTAL MORPHOLOGY . . . . .	61
Introduction . . . . .	61
Macroscale Coastal Geomorphic Variability . . . . .	65
STRUCTURAL LINEAMENTS AND COASTLINE PLAIN . . . . .	67
INFLUENCE OF RIVERS . . . . .	69
MARINE REGIME . . . . .	69
Macroscale Morphologic and Morphometric Variability . . . . .	71
Intermediate-Scale Coastal Variability and Province Descriptions . . . . .	72
THE WESTERN ZONE PROVINCES . . . . .	72
THE EASTERN ZONE PROVINCES . . . . .	83
CHAPTER V. BEACH PROCESS-RESPONSE INTERACTIONS . . . . .	91
Introduction . . . . .	91
Instrumentation and Field Techniques . . . . .	91
Breakup . . . . .	93
RIVER BREAKUP--ITS EFFECT IN THE COASTAL ZONE . . . . .	96

	Page
Point Lay. . . . .	96
Pingok Island. . . . .	96
SEA ICE BREAKUP . . . . .	98
Point Lay. . . . .	98
Pingok Island. . . . .	98
BEACH THAW. . . . .	99
Point Lay. . . . .	99
Pingok Island. . . . .	100
NEARSHORE ICE MOVEMENT. . . . .	103
DISCUSSION. . . . .	106
Open Water . . . . .	106
PINGOK ISLAND . . . . .	107
Beach Sediment Characteristics . . . . .	107
Two-Dimensional Beach Response . . . . .	108
Offshore Bars. . . . .	121
Bar Formation. . . . .	124
Bar Migration. . . . .	127
Beach Modification Associated with Bars. . . . .	127
Inlet Morphology . . . . .	132
Island Migration . . . . .	134
POINT LAY . . . . .	135
Two-Dimensional Beach Response . . . . .	137
Inlet Morphology . . . . .	139
DISCUSSION. . . . .	139
Freezeup . . . . .	141
FROZEN UPPER BEACH SURFACE. . . . .	143
SNOW COVER. . . . .	143
ICE FORMATION . . . . .	143
Ice Cakes. . . . .	144
Lagoon Ice Slush . . . . .	146
Frozen Swash, Foam, and Spray. . . . .	147
FROZEN BEACH FACE . . . . .	147
Observation of a Winter Beach. . . . .	149
LATE FREEZEUP FEATURES. . . . .	150
DISCUSSION. . . . .	153
Summary. . . . .	153
CHAPTER VI. CONCLUSIONS. . . . .	159
REFERENCES. . . . .	163

LIST OF FIGURES

Figure	Page
1. Location map of Alaskan Arctic Coastal Plain. . . . .	4
2. Location map of Point Lay site, Alaskan Arctic Coast. . . . .	6
3. Location map of Pingok Island site, in the Jones Islands, Alaskan Arctic Coast. . . . .	8
4. Alaskan Arctic Coast precipitation and temperature trends . . . . .	12
5. Frequency distribution of wind based on DEW Line data . . . . .	13
6. Schematic cross section of Point Lay barrier island showing location of four wind profile measurement stations during the summer measurement period . . . . .	15
7A. Example of wind profiles on lagoon side of island at Point Lay . . . . .	16
7B. Example of wind profiles at island berm station at Point Lay. . . . .	16
8A. Example of wind profiles at beach station at Point Lay site . . . . .	17
8B. Example of wind profiles at offshore station at Point Lay site. . . . .	17
9A- Shear velocity as a function of 2-meter wind speed at Point 9C. Lay site. . . . .	19
10. Shear velocity as a function of 10-meter wind speed at the offshore (Chukchi Sea) station. . . . .	20
11. Total mean nondimensionalized horizontal wind speed components at each site during winter measurement period at Point Lay. . . . .	22
12. Capacitance tide gage record from Kasegaluk Lagoon, behind Point Lay Island. . . . .	26
13. Tide gage records from lagoons at Point Lay, Point Barrow, and Oliktok Point . . . . .	27
14. Atmospheric pressure at Point Lay during the latter part of July and the early part of August . . . . .	28
15. Progressive vector diagram of surface wind stress at Point Lay drawn from hourly wind observations and assuming an air density of $1.2 \times 10^{-3}$ gm/cm <sup>3</sup> and a drag coefficient of $1.6 \times 10^{-3}$ . . . . .	29

Figure	Page
16. First sixty periodogram estimates of the 596.3-hour tide record from Point Lay. . . . .	30
17A. Long-wave spectra of records taken 4 hours apart on September 3, 1972. . . . .	34
17B. Long-wave spectra of wave records taken 4 hours apart on September 1, 1972 . . . . .	34
18. Long-wave spectra of wave records taken at Pingok Island on September 1 and 3, 1972 . . . . .	35
19. Long-wave spectra of records taken at Pingok Island compared to observations reported by Munk (1963) . . . . .	35
20. Wind wave spectra at 0925 and 1415 on 9/2/72 . . . . .	37
21. Generalized spectrum of wave amplitude in the Arctic Ocean . . . . .	40
22. Scatter diagrams of wind speed versus current speed and wind direction versus current direction relative to true north at Point Lay . . . . .	42
23. Mean drogue velocities for seven experiments in which drogues were released at 2-meter depth . . . . .	43
24. Drogue trajectories for August 18, 1972. . . . .	44
25. Scatter diagrams of wind speed versus current speed and wind direction versus current direction relative to true north at Pingok Island . . . . .	44
26. Mean drogue velocities for seven experiments with drogues released at 2-meter depth. . . . .	45
27. Records of the easterly and northerly components of current at mid-depth in 7.6 meters of water in April 1972 at Point Lay . . . . .	46
28. Three records of current velocity at mid-depth in 9.8 meters of water during open-water season in 1972 at Point Lay . . . . .	47
29. Temperature-salinity diagrams for the nearshore water at Point Lay immediately following breakup. . . . .	51
30A. Temperature section and salinity section from the nearshore waters at Point Lay on 7/12/72 . . . . .	53
30B. Temperature section and salinity section from the nearshore waters at Point Lay on 7/18/72 . . . . .	53
31A. Temperature section and salinity section from the nearshore waters at Point Lay on 7/22/72 . . . . .	54
31B. Temperature section and salinity section from the nearshore waters at Point Lay on 7/26/72 . . . . .	54

Figure	Page
32A. Temperature section and salinity section from the nearshore waters at Point Lay on 7/27/72 . . . . .	56
32B. Temperature section and salinity section from the nearshore waters at Point Lay on 7/29/72 . . . . .	56
33A. Temperature section and salinity section from the nearshore waters at Point Lay on 8/2/72. . . . .	57
33B. Temperature section and salinity section from the nearshore waters at Point Lay on 8/3/72. . . . .	57
34. Temperature section and salinity section from the nearshore waters at Point Lay on 8/15/72 . . . . .	58
35. Location map of Alaskan Arctic Coast showing province divisions and sector numbers . . . . .	62
36. Diagram illustrating definition of morphometric terms. . . . .	64
37. Major structural lineaments of the Alaskan Arctic Coastal Plain. . . . .	68
38. Average ice concentration along the Alaskan Arctic Coast and adjacent waters from May through mid-October . . . . .	70
39. Sequence of lagoon formation and barrier island isolation by thaw-lake coalescence. . . . .	73
40A- Photographs illustrating characteristic features of provinces	
40B. 1 and 2. . . . .	77
41. Diagrammatic representation of process regimes along the western Alaskan Arctic Coast . . . . .	78
42A- Photographs illustrating characteristic features of provinces	
42D. 4, 6, and 7. . . . .	79
43A- Photographs illustrating characteristic features of provinces	
43D. 8, 9, and 10 . . . . .	82
44A- Photographs illustrating characteristic features of provinces	
44D. 11, 12, 15, and 19 . . . . .	85
45A- Photographs illustrating characteristic features of provinces	
45B. 19 and 21. . . . .	89
46. Schematic diagram illustrating definition of parameters used in calculating beach area and volume changes . . . . .	94
47. Mean daily air temperature and breakup sequence at Pingok Island and Point Lay sites during the period May 1 to August 10, 1972. . . . .	95
48A- Photographs illustrating characteristic features during	
48B. breakup. . . . .	99

Figure	Page
49. Beach profile changes across grid I, Point Lay. . . . .	101
50A- Photographs illustrating sequence of	
50D. beach thaw. . . . .	102
51. The beach in the vicinity of grid I, Pingok Island, in July 1972 . . . . .	104
52. Graphs showing relationship between ice movement and wind speed and direction at Point Barrow . . . . .	105
53. Plot of daily averages of selected marine and atmospheric parameters for Point Lay site, May 11 to June 26 and July 15 to August 21, 1972. . . . .	108
54. Plot of daily averages of selected marine and atmospheric parameters at Pingok Island site, July 11 to September 25, 1972 . . . .	109
55. Relationship between mean grain diameter and sorting coefficient, and mean grain diameter and skewness, for Pingok Island beach samples . . . . .	112
56. Variation in grain size distribution across three beach sections on Pingok Island, grid I. . . . .	113
57. Map of Pingok Island showing location of the field camp, beach grids (I, II, and III), profiles A-L, and spits surveyed (I, II, III). . . . .	114
58A- Photographs illustrating details of small-scale beach features	
58B. formed during low wave action . . . . .	115
59. Plot of wave height, swash limit, erosion-deposition node, and beach volume change at Pingok Island, grid I. . . . .	116
60. Schematic diagram showing characteristic sequence of beach profile change. . . . .	117
61. Selected changes in beach configuration along profiles A, B, C, D, and E, grid I, Pingok Island, during the period September 3-25, 1972 . . . . .	118
62. Changes in beach profiles F, G, and H, grid II, Pingok Island . . . . .	119
63. Photograph of recently formed ridge-and-runnel system on Pingok Island. . . . .	120
64. Selected changes in profiles J, K, and L, grid III, Pingok Island . . . . .	121
65. Nearshore bathymetry off Pingok and Leavitt islands (August- September 1972) . . . . .	123
66A- Photographs illustrating the outer bar and shoreline rhythms	
66B. along Pingok Island . . . . .	124

Figure	Page
67. Selective bar profiles showing the pattern of bar development. . . . .	126
68. Pingok and Leavitt islands shown in 1908, 1950, 1955, and 1972. . . .	128
69. Sequential profiles along range 17 showing the onshore migration of two bars. . . . .	128
70. Rates of migration of cusp-type sand waves versus wave length. . . .	129
71. Beach profiles across Spy Island, Leavitt Island, and Bertoncini Island . . . . .	130
72. Beach profiles across Cottle Island and Long Island. . . . .	131
73. Schematic diagram showing migration of outer bar and shoreline rhythm and development of beach ridge-and-swale systems. .	132
74. Spit development at eastern and western ends of Pingok Island. . . .	133
75. The Tapkaluk Islands shown in 1950 and 1955. . . . .	135
76. Eastern Cottle Island, Long Island, and Egg Island, shown in 1908, 1950, 1955, 1970, and 1972. . . . .	136
77. The Maguire Islands, shown in 1908, 1950, and 1955 . . . . .	137
78. Plot of swash limit, erosion-deposition node, and beach volume changes at Point Lay, grid I. . . . .	138
79. Changes in the inlet at the Point Lay site . . . . .	140
80. Relationship between period of morphological response and volume of material per unit time . . . . .	142
81A- Photographs illustrating types of nearshore ice	
81D. accumulations. . . . .	145
82A- Photographs illustrating processes and resulting forms	
82D. during freezeup. . . . .	148
83A. Beach section at Pingok Island made on September 21, 1972. . . . .	149
83B. Beach section at Point Lay made on June 7, 1972. . . . .	149
84A- Aerial photographs illustrating late freezeup features	
84D. on the Alaskan Arctic Coast. . . . .	151
85A. Section across Pingok Island winter beach following complete 1972 freezeup . . . . .	152
85B. View west along the ice boulder ridge at Pingok Island . . . . .	152

LIST OF TABLES

Table	Page
1. Summary of Roughness Length and Drag Coefficient Values. . . . .	21
2. Wind Velocity Ratios for Landward Station. . . . .	23
3. Wind Velocity Ratios for Ridge Station . . . . .	23
4. Wind Velocity Ratios for Seaward Station . . . . .	24
5. Wave Data Acquisition Runs . . . . .	32
6. Province Variability of Wave Power . . . . .	66
7. Summary Statistics and F Ratios for Wave Power and Energy Contrasts between the Western and Eastern Coasts... . . . .	71
8. Summary Statistics and F Ratios for Morphometric Contrasts between the Western and Eastern Coasts . . . . .	74
9. Province Morphology and Morphometry. . . . .	75
10. Instrument Array, Point Lay and Pingok Island, 1972. . . . .	92
11. Summary of Daily Means of Selected Marine and Atmospheric Parameters at Point Lay and Pingok Island. . . . .	110
12. Composite of Pingok Island Beach Sediment. . . . .	111
13. Distinctions Between Outer- and Inner-Bar Rhythmic Topographies. . . .	125

**Preceding page blank**

## PREFACE

The Alaskan coastline from Point Hope to Demarcation Point is a broad stretch of shoreline interacting with a suite of physical processes of variable intensities and scales, both spatial and temporal. Previous studies have been concerned with only a small number of the total physical interrelationships present in this region. This project took the approach that, in order to understand the importance of the fine-structured, small-scale processes, it is necessary first to acquire an understanding of the structure of the broad-scale interactions composing the coastal environment of arctic Alaska. To accomplish this task, scientists in the fields of meteorology, nearshore hydrodynamics, wave mechanics, morphodynamics, and beach dynamics combined efforts in a field and laboratory study. Each of these scientists carried out a program of investigations within his own field of interest but with this basic goal in mind. J. M. Coleman, A. Gregory, A. D. Short, and L. D. Wright conducted the broad-scale map and photo studies of the regional variability of coastal morphology. J. M. Coleman, A. Gregory, A. D. Short, Wm. J. Wiseman, Jr., and L. D. Wright performed the beach dynamics studies, and J. N. Suhayda and Wm. J. Wiseman, Jr., investigated the physical oceanography of the coastal zone. Meteorological processes were investigated by S. A. Hsu and C. D. Walters, Jr.

The format of this report is in keeping with the initial goals. Chapter I, the introduction, sets this study in proper perspective with respect to past efforts. It also contains a summary of the operational characteristics of our instrumentation. On the premise that the basic energy inputs to the coastal environment are meteorological, we have grouped the meteorological studies in Chapter II. Although not the only ones, the most striking responses to the meteorological inputs involve the hydrosphere. Thus, the physical oceanographic studies are discussed in Chapter III. The broad-scale morphological characteristics of the coast are summarized in Chapter IV in an effort to present a basis on which to evaluate the representative nature of the shoreline dynamics investigations, the topic of Chapter V. Chapter VI is a summary of our most salient conclusions.

## CHAPTER I

### INTRODUCTION

The beach and nearshore zone is an area of interaction between marine, atmospheric, and terrestrial forces. The type, magnitude, and frequency of their respective contributions control coastal morphology. Long-term or secular characteristics of numerous processes acting in combination over a relatively broad area define a coastal process environment. Within a coastal environment, short-term changes in marine and atmospheric processes and terrestrial parameters effect variation in the morphology at correspondingly short time scales. The sum of these changes in process and form contributes to the long-term, low-frequency process regime and the morphological environment.

Although a significant fraction of the total coastline of the world lies within polar environments, these coasts have not been intensively studied because of the severe environmental setting and the high cost of logistics. The northern Alaskan coast falls within the polar or arctic environment; land and water surfaces are frozen from fall to spring. Polar coastal environments include numerous processes that differentiate them from temperate or tropical environments: yearly freezing and thawing effects, large Coriolis parameter and resulting Ekman drift, and persistent high winds. This study was designed to examine the variability of coastal process environments and morphology along the entire Alaskan Arctic Coast and to investigate specific nearshore processes and beach responses at two field sites, Point Lay and Pingok Island. More specifically, the intent was to characterize the interactions between the two fluid components of the environment, the ocean and the atmosphere, and the two solid components, the land and the ice. Secular and broad-scale interactions were investigated using published data and aerial reconnaissances. High-frequency interactions were studied at the two field sites.

The first phase of the study involved acquisition, generation, synthesis, and analysis of existing data on the North Slope. In addition, aerial field reconnaissance trips were made along the entire coast during breakup, open-water conditions, and freezeup in 1971 and 1972. The detailed field studies consisted of installing various sensors at each site, sampling numerous environmental processes, and analyzing the resultant data for specific features or parameters.

Scientific investigation of the Alaskan Arctic Coast began in the 19th Century, when explorers began traversing the region, but the first compilation that refers to specific arctic coastal processes and their effects was published in 1918 by Leffingwell. He observed the effects of waves, wind, and sea ice along the coast and concluded that waves and winds, not ice, were the primary morphological controls. Studies specifically involving shoreline processes and responses are meager in number and, inasmuch as they were concentrated primarily around settlements, geographically spotty. Work in the Cape Thompson region by the Atomic Energy Commission (see Wilimovsky and Wolfe, 1966) provides some general data on major process controls along the strand of an arctic beach. Additional studies in the Point Barrow region by MacCarthy (1953), Rex and Taylor (1953), Rex (1955, 1964), Schalk

(1957), and Hume and Schalk (1964b, 1967) contain information on both process and morphological change along the coast at this site. Lewellen (1970, 1972b) discussed erosional processes in the vicinity of Flaxman Island, a barrier island east of the Colville River region, and later (1972a) included some data on other shorelines along the North Slope. Dygas et al. (1972) considered sediment transport and shoreline changes from Oliktok Point to Beechy Point. Hartwell (1971) reviewed and discussed the general coastal conditions for the arctic North Slope; the work was based primarily on a study of air photographs and aerial reconnaissance. Nearshore processes at the mouth of the Colville River have been documented by Walker (1969, 1972).

Additional work on nearshore processes and morphology along arctic coasts has been published by Popov (1959), Nichols (1961), Giddings (1952), McCann and Owens (1969, 1970), Owens and McCann (1970), and McCann (1972). Generally these papers deal with specific small areas, and no attempt has been made to put the studies into an arctic or regional context. None of the studies has systematically delineated the temporal sequence of the breakup, open-water, or freezeup periods or described the salient processes operative in each. Knowledge of the magnitude and frequency of these processes and resultant beach and nearshore response is essential to the understanding of arctic coastal morphology.

Oceanographic studies in the Arctic Ocean basin have been extensive, but few deal with nearshore dynamics. The Arctic Basin report (Sater et al., 1963) and the Proceedings of the Arctic Basin Symposium (1963) provide general background data. The Oceanographic Atlas of the Polar Seas and the U.S. Naval Oceanographic Office "Bird's Eye" reports give summaries of significant oceanographic parameters and have been used extensively in the data compilation. An article by Dietz and Shumway (1961) presents offshore regional physiographic aspects of the Arctic Basin. Water masses in the Arctic Basin have been discussed by Aagaard (1964) and Coachman (1963). Recent work by Barnes (1972), McManus and Creager (1963), and Fleming and Heggarty (1966) on the Chukchi Sea and by Reimnitz et al. (1972) in the Beaufort Sea have increased knowledge of circulation and ice movement in these regions. Wendler (1973) reviews the work on sea ice observations by satellites, a method that will in the future significantly increase knowledge of ice movement and density. Kinney et al. (1972) studied currents in Simpson Lagoon, and Reimnitz (personal communication) has sampled the temperature and salinity in waters east of the Colville River. Beal (1968), Matthews (1972), and J. Dygas (personal communication) have monitored tides at Point Barrow and Oliktok Point.

The most extensive work has been on the Arctic Coastal Plain, and numerous books and articles have been published on geology, geomorphology, pedology, and thermal processes. Geological aspects of the coastal plain are extensively summarized by Miller et al. (1959), Raasch (1961), Adkison and Brosgé (1971), and O'Sullivan (1961). These papers and others provide a rather detailed account of the stratigraphy, structure, and geologic history of the North Slope. The bibliography by Maher and Trollman (1970) lists most of the important contributions to arctic geology. Bird's (1967) *Physiography of Arctic Canada* provides a basis for comparative studies on the North Slope. Thermal processes and permafrost have been amply studied in the coastal plain, but details of variability across the coastal plain are generally lacking. Publications by Black (1951), Lachenbruch (1960), Brewer (1958), Washburn (1956), Scott (1969), and Kelley et al. (1969) provide general background on processes active on the tundra surface. Lakes on the tundra surface have also received considerable attention, but the vast majority of the work has been concentrated around Point Barrow. Few studies deal with the variability in size, shape, orientation, and relationship to other processes across the Arctic Coastal Plain.

To summarize, it appears that numerous and significant investigations have been completed along the Arctic Coastal Plain but that few of them treat nearshore dynamics and shoreline responses. Information on regional distribution and variability of coastal landforms would add significantly to our understanding of the coastal plain. Studies of nearshore circulation, as well as of circulation in lagoons and through inlets, are almost completely lacking. Wave dynamics and sediment movement along the shoreline are other areas in which few studies have been attempted. Even though such processes operate only during a short period of the year, they obviously play important roles in controlling the coastal morphology and consequently are responsible for many of the changes observed. This study was initiated to fill some of the gaps in the existing knowledge but has raised as many questions as it has answered. The report is segmented into four major topics: atmospheric processes, coastal hydrodynamic processes, coastal geomorphic characteristics, and beach processes and responses. These categories roughly indicate the areas of interest of the personnel conducting the study.

#### Study Area

The study was undertaken along the Alaskan Arctic Coast between Point Hope and Demarcation Point, a distance of 1,441 km (Fig. 1). This area lies entirely within the Arctic Circle, between lat. 68°15' and 71°20'N and long. 141° and 167°W.

The coast may be divided into two sectors: the eastern coast, extending from Point Barrow (the northernmost point of the United States) 816 km ESE to Demarcation Point; and the western coast, extending southwest from Point Barrow 625 km to Point Hope. The Chukchi Sea borders the western coast, the Beaufort Sea the eastern coast. The coastline is the northern boundary of the Arctic Coastal Plain, which extends from 50 km west of Demarcation Point in the east to Cape Beaufort in the west (Fig. 1). To the west of Cape Beaufort, the western extension of the Arctic Foothills dominates the topography.

The Arctic Coastal Plain is shaped like a triangle; it measures approximately 900 km across the base and 175 km at its broadest point and covers an area of 70,000 km<sup>2</sup>. It is a gently undulating region, seldom higher than 15 meters at the coast, rising slowly to its southern boundary with the Arctic Foothills, where it is generally between 60 and 180 meters in elevation.

Tundra soils, vegetation, and patterned ground cover the surface of the plain. Numerous beaded and meandering streams and rivers traverse the plain, and innumerable lakes, usually oriented, exist in the region.

The plain is composed of unconsolidated Quaternary sediments overlying Cretaceous or Tertiary sediments (Black, 1964). The sediments are part of the Gubik formation, a series of lenses and admixtures of silt and fine-grained sands and some clays and gravels. Eolian and frost processes were involved in both their deposition and their modification. The Gubik has three lithologic units: (1) the Skull Cliffs unit, the oldest, resting on the Cretaceous bedrock and only 7 meters in maximum thickness; (2) the Meade River unit, the thickest (65 meters maximum), dominant in the southern and southeastern region; and (3) the Barrow unit, the youngest, generally interfingering with the Meade River unit and dominant in the northern part of the plains (Black, 1964).

The entire plain is affected by permafrost, which acts as a cement for the sediments. Annual freezing and thawing produce a thin active layer at the surface. Polygons displaying a wide variety of dimensions give the tundra surface its characteristic patterned appearance. The surface has also been modified by fluvial,

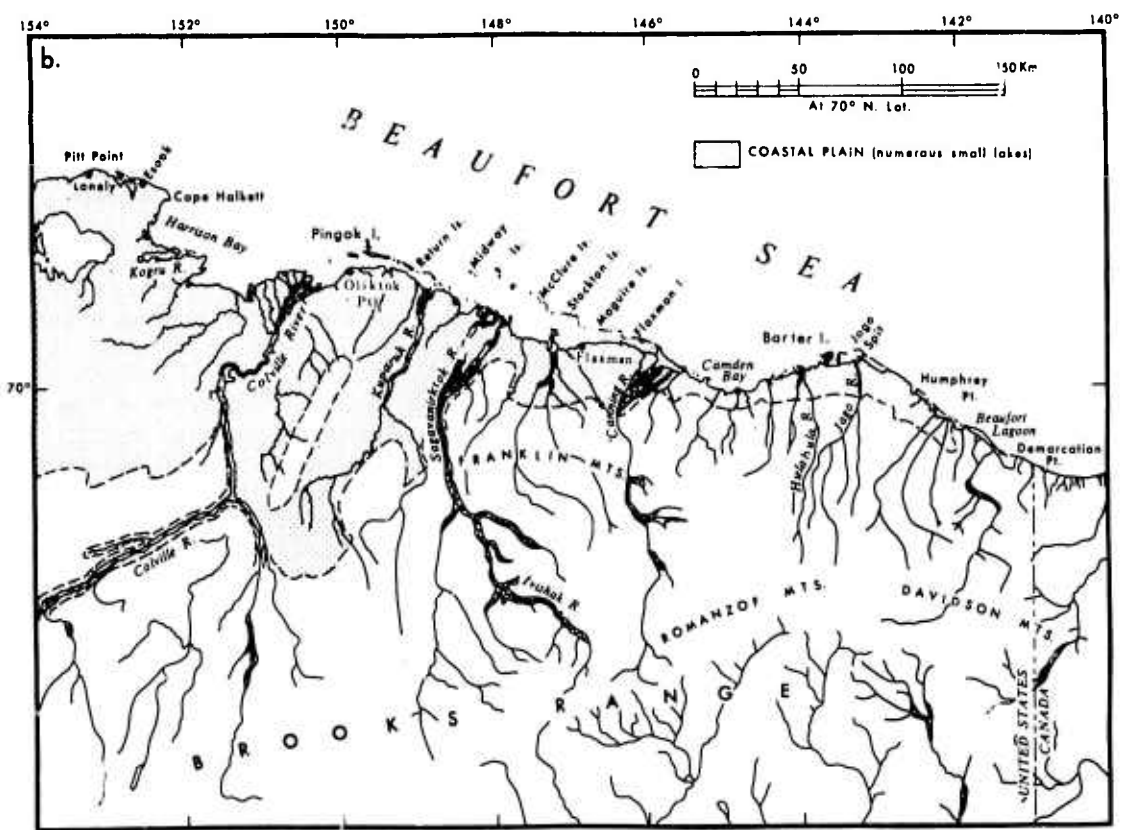
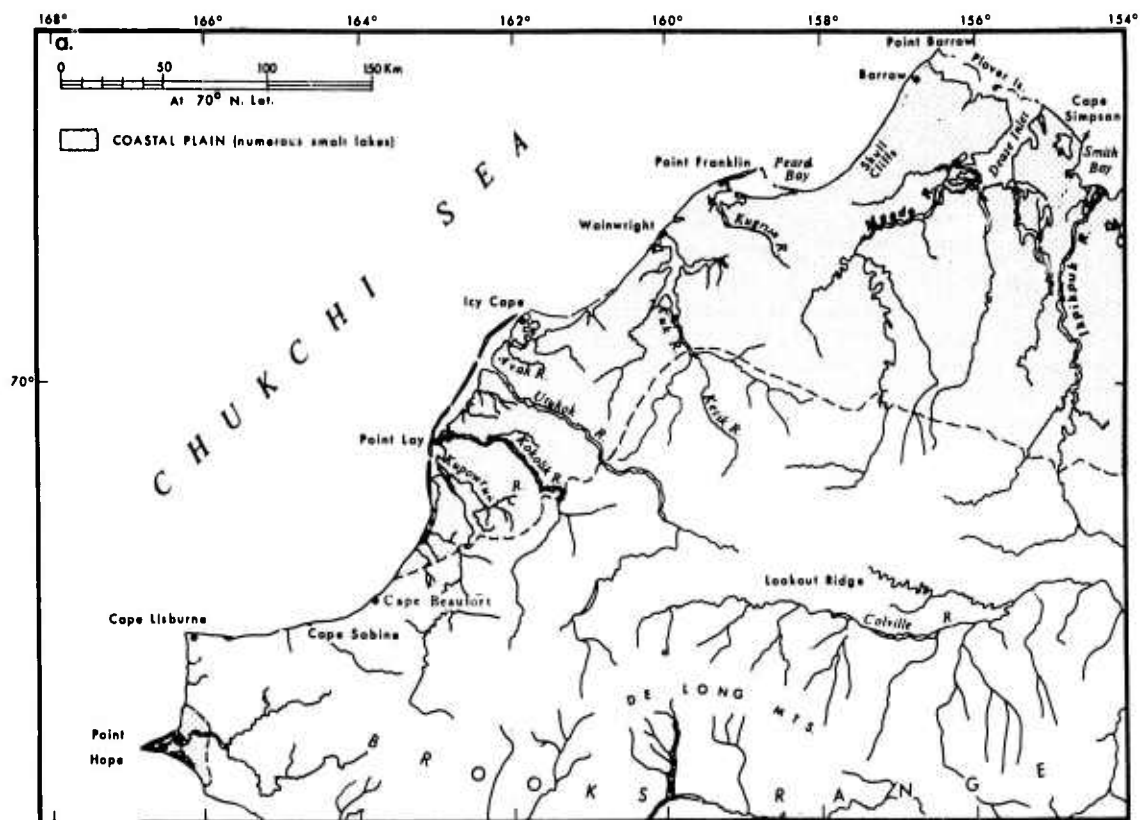


Figure 1. Location map of Alaskan Arctic Coastal Plain.

lacustrine, deltaic, and eolian reworking, as well as tundra soil development. Along the coast, thermal, fluvial, and marine processes erode the tundra bluffs and rework the nearshore sediments to produce sand and gravel barrier islands and beaches. Muds and silts are dominant in the coastal lagoons.

Lineaments have marked effects on the structural geology. The primary lineaments of  $35^\circ$  and  $310^\circ$  (Voronov et al., 1970) affect both local and regional drainage patterns and coastal orientation.

The climate of the coastal plain is characterized by low winter temperatures, very short summers, and low precipitation (20-30 cm). Temperatures drop below 0 C in late September and do not rise above freezing until May. At Barrow the minimum mean temperature is less than -25 C from December through March. The snow cover begins to melt in May, the shorefast ice breaking up between June and July. Removal of the shorefast ice, coupled with onshore winds, produces fog and low clouds along the eastern coast during July and August. Summer temperatures remain low; at Barrow the mean for June, July, and August (the warmest months) is 3.3 C, and the mean diurnal range is 5.5 C. Summer temperatures are lowest along the eastern coast and become increasingly warmer down the western coast. Summer rainfall is scattered and light, though the annual maximum occurs in June and July. Snow accompanies freezing temperatures in September. October is the period of transition from summer to winter.

The pressure and wind fields are dominated by the Polar High, resulting in prevailing northeasterly winds, particularly during the winter. During summer, cyclonic low-pressure cells crossing Alaska produce southwesterly winds approximately 30 percent of the time and occasionally severe southwesterly storms in late summer (September and October).

The Beaufort and Chukchi seas are ice covered 6-7 months of the year. Open water begins in June near Cape Lisburne, decreasing in width and duration toward the east. Coastal currents in the Beaufort Sea set to the west, driven by the polar easterlies. Nearshore currents are wind dominated; they reverse in summer with the occurrence of westerly winds. Water temperatures remain low year-round, reaching a maximum of 5 C in August. The Chukchi Sea has northerly flowing coastal currents along the western coast, and there is evidence of the occurrence of large coastal eddies between Cape Lisburne and Icy Cape (Barnes, 1972). At Point Lay water temperatures rise during the summer to a maximum of 15 C. Along the entire coast salinities range from 20 ‰ to 32 ‰. River and lagoon flushing, coastal upwelling, and snow and ice melt have important local effects on the salinity. A 15-30-cm lunar tide is common along the entire coast; however, aperiodic wind- and pressure-induced sea level fluctuations dominate the astronomical tide, and ranges are as great as 1 meter or more.

#### Field Sites

For the examination of specific process-response systems two sites, Point Lay on the western coast and Pingok Island on the eastern coast, were chosen as representative of their respective coasts.

Point Lay (lat.  $69^\circ 45' N$ , long.  $163^\circ W$ ) lies 240 km southwest of Barrow (Fig. 1). The site (Fig. 2) is part of the long barrier fronting Kasegaluk Lagoon and is adjacent to one of the eight inlets that cut the barrier. The barrier is capped with tundra and averages 250 meters in width and 3 meters in maximum height. The active beach averages 40 meters in width. Except for the shoal seaward of the inlet, no offshore bars were present during the study. A series of outer bars become

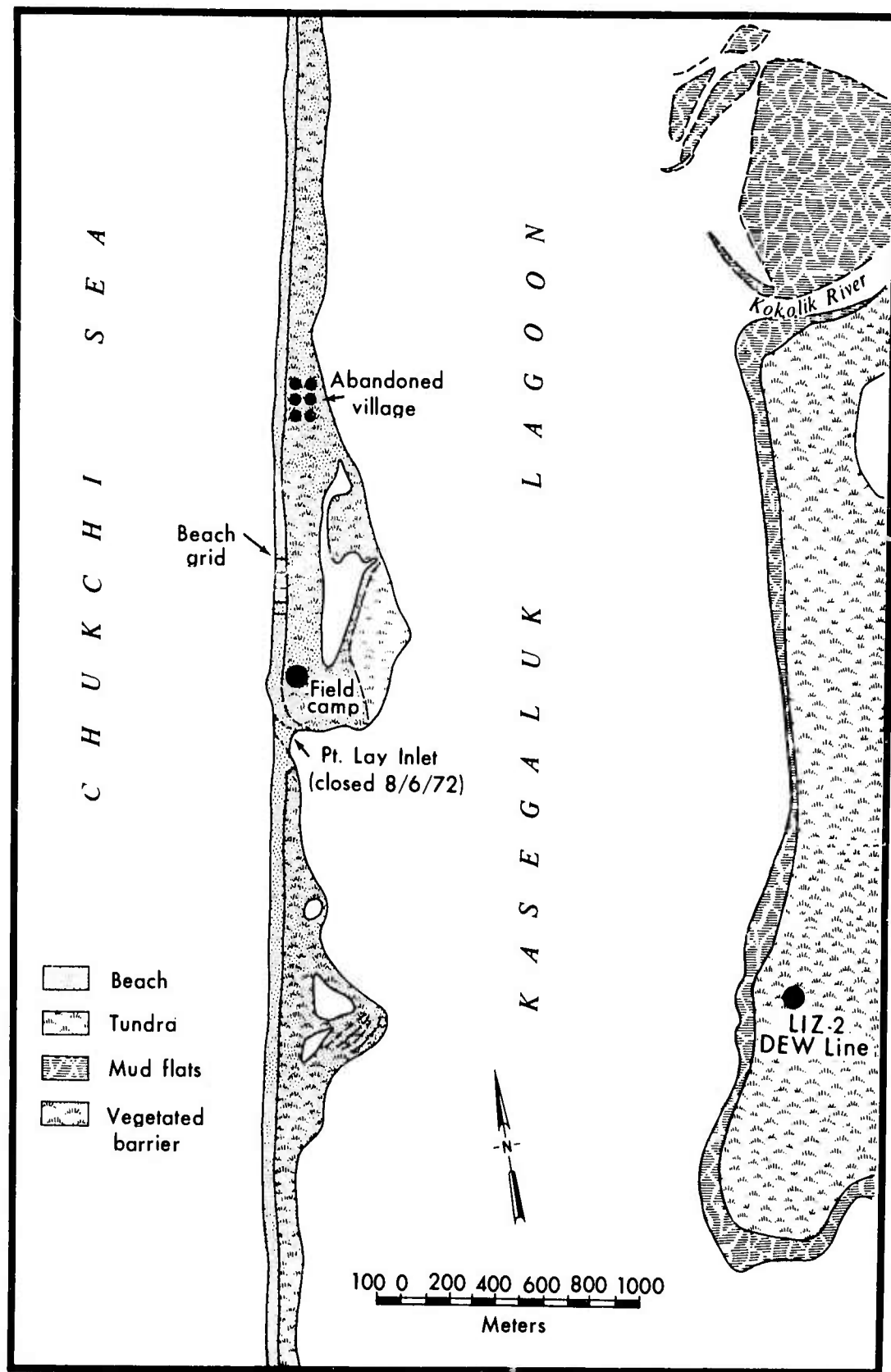


Figure 2. Location map of Point Lay site, Alaskan Arctic Coast.

dominant 60 km to the north. The barrier is oriented  $12^\circ$  and is exposed to both southwesterly and northerly waves and associated currents. The southwest waves are less frequent, but, being larger, are a dominant control on the morphology. In form the island is typical of the barrier islands and beaches west of Barrow, though it lacks the bars prevalent to the north.

Pingok Island (lat.  $70^\circ 31'N$ , long.  $139^\circ 40'W$ ) lies 220 km ESE of Barrow, in the center of the eastern coast (Fig. 1). The island is a single tundra remnant and is the largest of the Jones Islands and Return Islands group (Fig. 3). The island is 6.5 km long, 250-800 meters wide, and has a maximum elevation of 5 meters. Two prominent tundra points project into the lagoon. The tundra is straight on the northern side and is fronted by a sand-and-gravel beach, which varies in width from 5 to 165 meters. Outer bars and associated shoreline rhythms dominate the beach and nearshore morphology. Both easterly and westerly oriented process regimes actively affect the beach.

West of Pingok Island lie Leavitt, Spy, and Thetis islands, all of which are low sand-and-gravel barrier islands. To the east lie tundra remnants (Bertoncini, Bodfish, and Cottle islands) and barrier islands (Long, Egg, and Stump). Relatively wide, shoal inlets (average width 500 meters) separate the islands.

Backing all the islands is Simpson Lagoon, which averages 10.7 km in width and 2-3 meters in depth. Actively eroding tundra bluffs and projecting tundra points lie along the mainland lagoon shoreline. The Colville and Kuparuk rivers lie 27 and 28 km to the southwest and southeast, respectively.

Pingok Island is therefore ideally suited to represent the west coast, having within the study area barrier and tundra islands, tundra bluffs, numerous inlets, and a broad lagoon and being adjacent to two large rivers and their deltas. In addition, outer bars identical to those occurring around parts of the entire coast dominate the nearshore zone. Its east-west orientation permits influence from both easterly and westerly process regimes.

#### Instrumentation

A wide variety of sensors were employed during the field studies with differing degrees of success. Because of the remoteness of the region and the expense of logistics, we feel that it would be useful to future investigators to indicate the success or lack of it concerning equipment. Three types of mechanical current meters were used during the project; none of these worked as desired.

The Marine Advisers Model B-3c Roberts current meter failed to produce accurate data because in such high latitudes the horizontal component of the earth's magnetic field is significantly less than at lower, temperate latitudes. The Roberts current meter transfers direction information from a compass to a recorder as an electrical signal through wipers. The compass assembly is contained within an oil-filled housing. Thus, the earth's magnetic field must realign the compass while working to overcome the frictional effects of the wiper assembly and the viscous drag of the oil on the compass. We found that our Roberts meter did not respond to a change in current direction, even after the normal oil in the housing was replaced by a low-viscosity oil. This problem is, undoubtedly, partially due to the small horizontal component of the earth's magnetic field.

The second meter, a Bendix Marine Advisers Model Q-15, gave a similar performance. This ducted meter has its compass in an oil-filled housing, and consequently the direction sensor did not respond properly. The oil in the original meter was

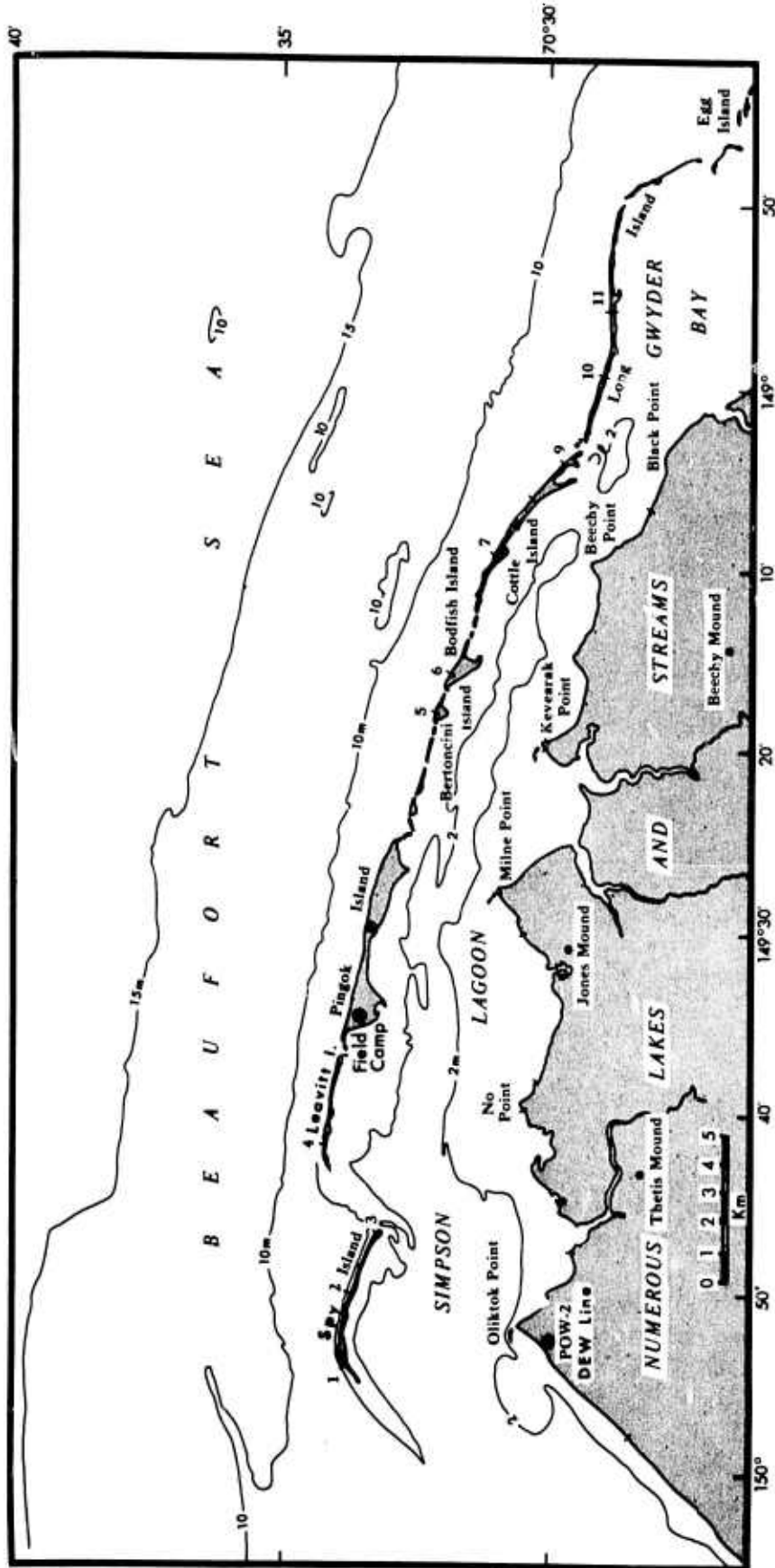


Figure 3. Location map of Pingok Island site, in the Jones Islands, Alaskan Arctic Coast. Numbers indicated along the seaward side of the islands refer to locations of beach survey grids.

replaced by Dow Corning 200 fluid (20 cs viscosity), but no improvement resulted.

The third current meter was a Braincon Corporation Type 1381 histogram meter. This meter was moored, and it recorded in situ for about 1 month. Direction is sensed by a viscous-dampened, permanent magnet similar to a ship's magnetic compass. Direction information is recorded photographically, and the system worked well. Unfortunately, the drive mechanism on the film advance did not function properly, and, rather than a continuous record, several short records with poorly defined absolute time bases were produced.

The final technique used for determining currents was drogue tracking, for which a Raytheon Company Model 2900 Mariner's Pathfinder Radar, a 3-cm radar, was utilized. The drogues were 60-X60-X0.015-cm PVC crosses suspended from a 3-meter-long aluminum conduit; polyurethane was used for flotation. Atop the pole was a radar reflector made of aluminum foil. Within 3.5 km of the radar, and when few ice cakes were in the vicinity, the return was excellent. Drogue depths were made variable by changing the suspension. This technique provided the most dependable method utilized during the project.

Two different conductivity-temperature-salinity systems were employed, an Interocean CSTD probe and a Beckman RS5-3 salinometer. The first instrument was never satisfactorily operated inasmuch as electrical failure precluded its use. The Beckman Instruments, Inc., RS5-3 portable salinometer was used successfully throughout the open-water season. Surface water samples were collected for precise calibration of the salinity circuit. Immediately after breakup, when water temperatures were below 0 C, thermometers were used to estimate water temperatures because the Beckman instrument does not measure negative temperatures. Accuracy of the system appeared to be well within 0.5 ‰, and precision on any particular day was much better.

Two types of tide gage were employed. A commercial gage, a Hydroproducts Model 521 in situ wave and tide recorder, was used at both sites. The system utilized a pressure transducer to sense the water level and sampled twice an hour onto a Rustrak recorder. The major drawback of the instrument is the short lifetime of its battery, which must be serviced once a week. The second type of meter was a capacitance tide gage constructed at CSI (Rector et al., in preparation). The system was able to operate in a 30-minute sampling mode for a period of about 1 month. A stilling well was constructed around the probe to dampen out high-frequency oscillations. Although the gage itself worked well, three failures occurred owing to the mounting support design. The design was for 0.5-1-meter waves and not for the 2-3-meter breakers actually encountered.

Fathometers used were Raytheon Company Model DE-731 recorders. These units performed satisfactorily throughout the project. A malfunction in the motor drive circuitry caused failure in one of the units.

Waves were sensed by resistance-wire wave staffs. The output signal from these staffs was recorded on a Gould, Inc., Brush Instruments Division, Mark 260 recorder, a six-channel analog strip-chart recorder. The system worked well, and cost was kept to a minimum. Again, the support upon which the wave staffs were mounted did not weather the environmental stresses well. Large wave motions tended to undercut and tilt the structures. All five staffs were lost at Pingok Island during a storm, when drifting ice cakes knocked over the support towers and snapped the signal cables.

Wind speed profiles were measured with a C. W. Thornthwaite Associates wind

profile register system, Model 106, 12 VDC, CWT-1088B, and recorded with a C. W. Thornthwaite Associates digital printout recorder, Model 706, CWT-1038A. The recorder utilizes a Polaroid camera, which presented a significant problem because the Polaroid film has a threshold temperature below which it will not develop. Atmospheric pressure was monitored at both sites with a Weather Measure Corporation B211 microbarograph. These systems were rugged and easy to operate. They functioned well during the entire season. Wind speed and direction were measured at both sites with a Climet Instruments Company Model CI-26 wind recording system and recorded on an Esterline Angus Model A602C two-channel recorder. These systems also worked well throughout the season except for occasional freezing of the speed sensor.

Other equipment used consisted of optical surveying instruments, cameras, and small radios. All of it functioned well and caused few problems during the project. Battery life is lessened considerably in that cold environment, and large supplies were used.

CHAPTER II  
ATMOSPHERIC PROCESSES

Introduction

Characterization of the general climate of the Alaskan Arctic North Slope requires extensive research with regard to precipitation, temperature, and wind as well as the resultant effects of these phenomena on the geomorphology of the coastal region. Meteorological records of some of the relevant parameters are available for a number of years from Alaska's Distant Early Warning (DEW) Line stations, but in many cases these records do not exhibit consistency or continuity. A multiyear summary of the precipitation and temperature observations is, therefore, abstracted from the climatological records of the state. An approach to an investigation of the wind variability along the Arctic coastal region is also presented. The time available for reduction of the massive amount of data from the DEW Line stations did not permit full analysis of the data.

The micrometeorological or surface boundary-layer wind structure study at Point Lay was designed with two objectives. The first was to determine mean values of the aerodynamic roughness length and wind stress drag coefficient over various surfaces during the ice-free summer season. The second objective, undertaken during the winter season, was to determine the effect of a sea ice pressure ridge or hummock on the two-dimensional wind structure as the wind flows over the ridge.

General Climate

The precipitation and temperature data presented in Figure 4 are abstracted from climatological observations presented by Searby (1968). These observations extend over the 22-year period from 1931 through 1952. It is apparent that the mean annual precipitation accumulations are, in general, less in the Arctic coastal region than in the interior of the mainland. The region between Barter Island and Barrow is apparently cooler, on a mean annual basis, than the region between Cape Lisburne and Barrow during the summer month of July, whereas the opposite is true during the winter month of January.

There was insufficient time to perform a comprehensive study of the near-surface wind variability for the Alaskan Arctic Coast; however, an initial approach to this problem was implemented by selecting the eastern and western extremes of the coast (i.e., Barter Island and Cape Lisburne, respectively). At Barter Island, the frequency distribution of wind direction and speed was determined for January and August of the years 1957-1964 (Figs. 5A and 5B). The distribution at Cape Lisburne was determined for January of 1957 through 1965 (Fig. 5C) and for August of 1956 through 1965 (Fig. 5D). The wind roses were computed from DEW Line station observations made at 6-hour intervals for each period of analysis. The thicker lines at the extremities of the easterly-westerly direction winds illustrated in Figure 5A indicate the percentage occurrence of winds 5-10 m/sec. There was no record of any occurrence above 10 m/sec. All other lines give the percentage occurrence of wind in a particular direction. "North" of each figure is to be

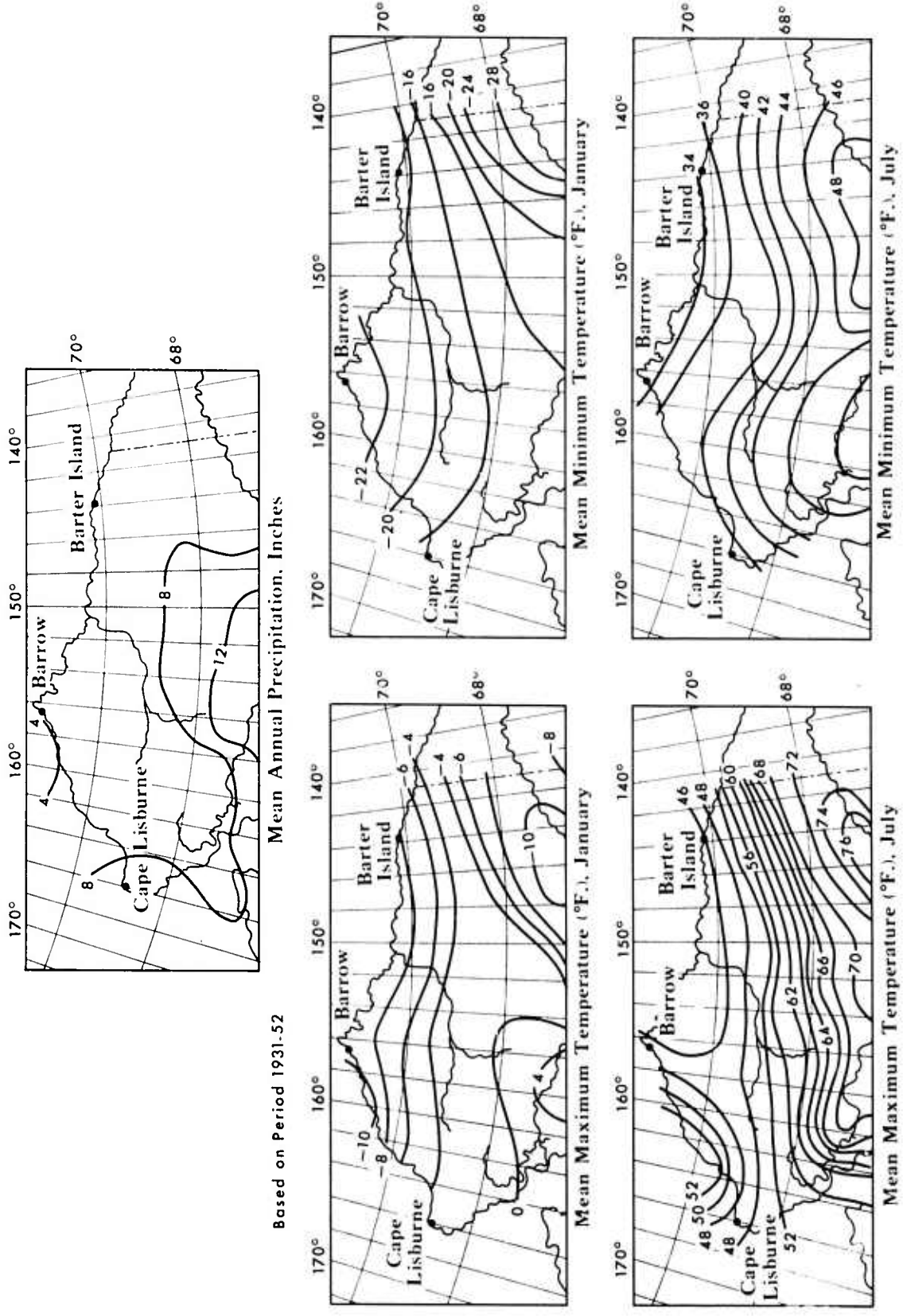


Figure 4. Alaskan Arctic Coast precipitation and temperature trends.

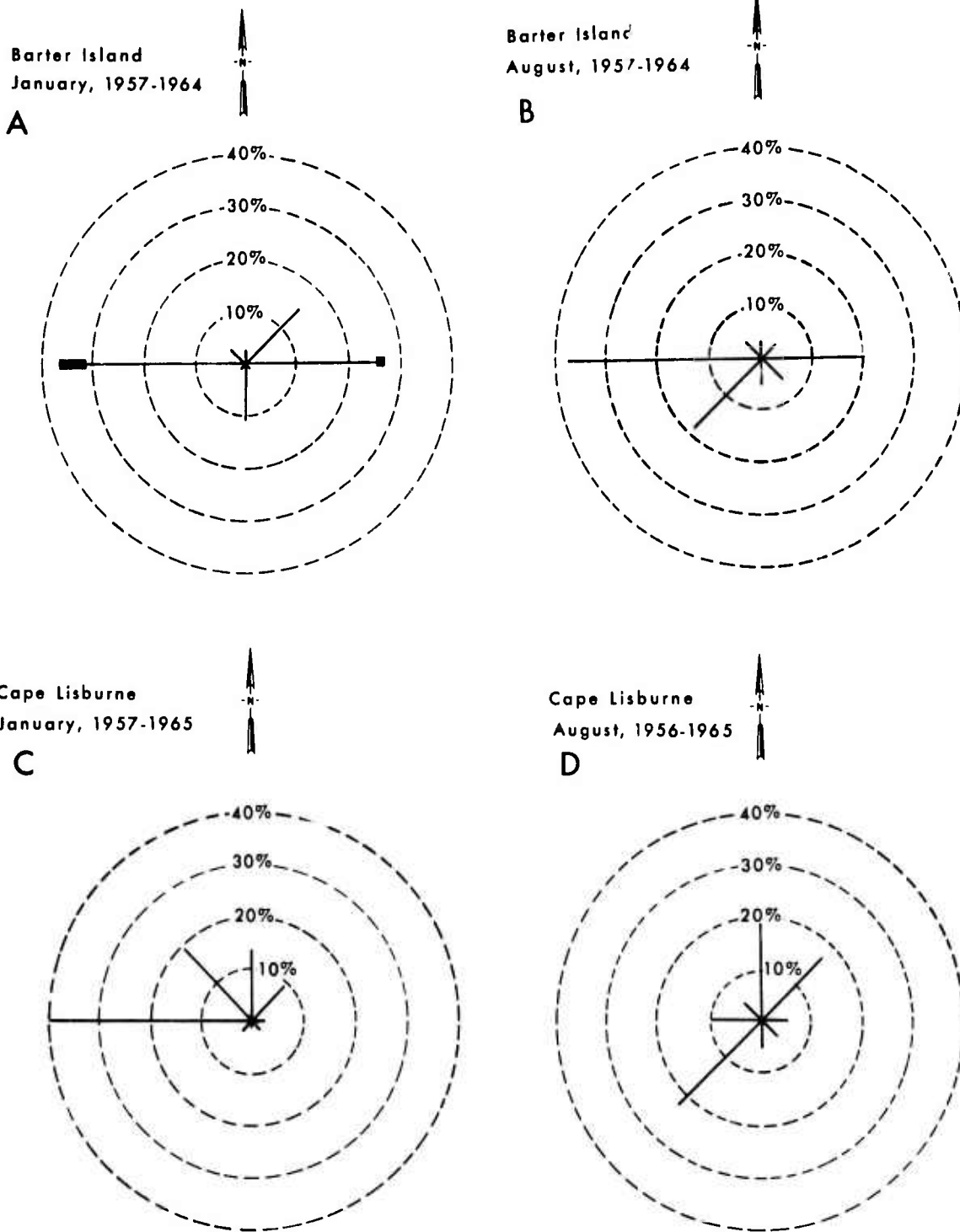


Figure 5. Frequency distribution of wind based on DEW Line data. A and B roses represent Barter Island, and C and D represent Cape Lisburne.

interpreted as geographic north.

It should be emphasized that a comprehensive study of the spatial and temporal characteristics of winds on the Alaskan Arctic Coast would require 2 years minimum time if all the available DEW Line station data were reduced and appropriately analyzed.

#### Surface Boundary-Layer Phenomena at Point Lay Site

##### SUMMER SEASON

The generally accepted definition of the atmospheric surface boundary layer is that layer within which the wind shearing stress is approximately constant with height (Munn, 1966). There have been very few significant wind profile measurements in the region above the Arctic Circle, but the results of Banke and Smith (1971) are of extreme interest with respect to this study because of the almost identical latitudes of the two study sites.

The objective of the summer phase of this study was to determine mean values of the aerodynamic roughness lengths and the wind stress drag coefficients over three different surfaces on Point Lay Island and over the Chukchi Sea. The aerodynamic roughness length,  $Z_0$ , is defined as that height above the surface where the horizontal wind speed,  $U_z$ , is equal to zero. The wind stress drag coefficient at height  $Z$  is defined by

$$C_D = \left( \frac{U_*}{U_z} \right)^2 \quad (1)$$

where  $U_*$  is the wind shear velocity. The wind shear velocity is determined from the logarithmic wind profile equation,

$$U_* = k U_z / \ln \left( \frac{Z}{Z_0} \right) \quad (2)$$

where  $k$  is the von Karman constant ( $\approx 0.4$ ). Equation 2 is valid only when there is a predominance of mechanical turbulence which is neither augmented nor suppressed by thermally induced turbulence or stratification in the surface boundary layer (Hess, 1959). This is commonly known as the neutral buoyancy condition and is a necessary characteristic in order for the horizontal wind speed to increase logarithmically with height, as is specified by equation 2.

Knowledge of the wind stress drag coefficient and aerodynamic roughness length is of considerable importance. These parameters play an essential role in models of momentum transfer across the air-sea interface, the surface heat budget over land and water, eolian sand transport along a beach, onshore penetration of aerosols from the sea to land, and the development of micro- and meso-scale prediction models for synoptic coastal phenomena.

Four wind profile measurement stations were monitored during the summer phase of the study. Three of these stations were over land and one was over water, as shown in Figure 6. Each station utilized a Thornthwaite six-unit, three-cup, fast-response anemometer system with a portable Thornthwaite Wind Profile Register System (Model 106). The cup assemblies at stations 1-3 were placed 20, 40, 80, 160, 240, and 320 cm above the surface. At station 4, they were 63, 83, 123, 202, 282, and 361 cm above the mean water level during the experiment.

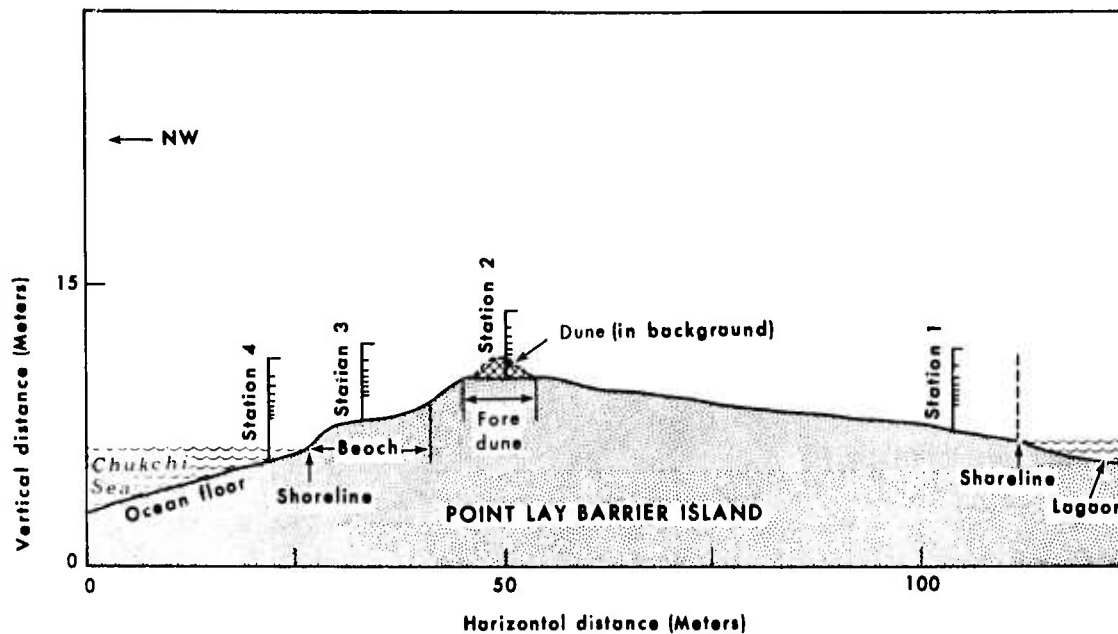


Figure 6. Schematic cross section of Point Lay barrier island showing location of four wind profile measurement stations during the summer measurement period.

Station 1 was located approximately 20 meters from the lagoon over a moist, short-grass and gravel surface and was operational from 0940 Alaska Daylight Time (ADT) on July 13 until 0940 ADT on July 15, 1972. Station 2 was located on the foredune crests which ran parallel to the island shoreline. The crests of the foredunes were spaced at intervals of approximately 40 meters and lay along a line about 50 meters from the Chukchi Sea shoreline. The surface, a mixture of dry sand and gravel, was covered by short grass. This station was in operation from 1050 ADT on July 17 until 1050 ADT on July 19, 1972. Station 3 was located on the beach face approximately 10 meters from the shoreline. The surface was primarily sand interspersed with gravel. This station was operational from 1145 ADT on July 17 until 1230 ADT on July 19, 1972. Station 4 was located over the Chukchi Sea naviface approximately 10 meters from the island shoreline and was operational from 1410 until 1855 ADT on July 19, 1972. Visual observations indicated wave activity to be small (significant wave height less than 20 cm) during this period.

Mean horizontal wind speed observations were made over 15-minute intervals at each of the six levels at each station. Mean horizontal wind speeds were plotted against height on a semilogarithmic scale, and the assumption was made that a correlation coefficient of 0.92 or greater is sufficient to justify the use of equation 2. This assumption is based on previous study criteria in separating log-linear from nonlog-linear profiles (e.g., see Ruggles, 1969). Examples of mean wind profile observations selected according to this criterion are shown for each station in Figures 7 and 8. There were 141, 163, 175, and 17 observations made whose wind profiles were logarithmic for stations 1, 2, 3, and 4, respectively.

The wind shear,  $U_{*}$ , was first determined for each of these observations by the statistical application of

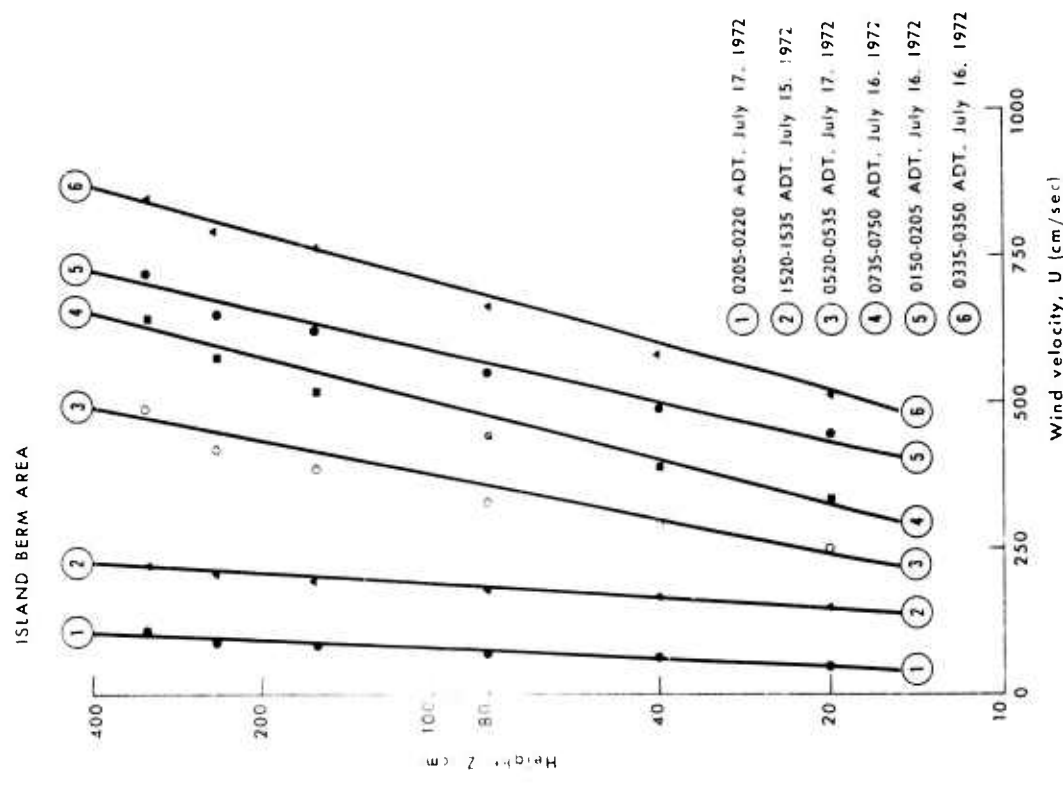


Figure 7A. Example of wind profiles on lagoon side of island at Point Lay. Vertical scale is logarithmic.

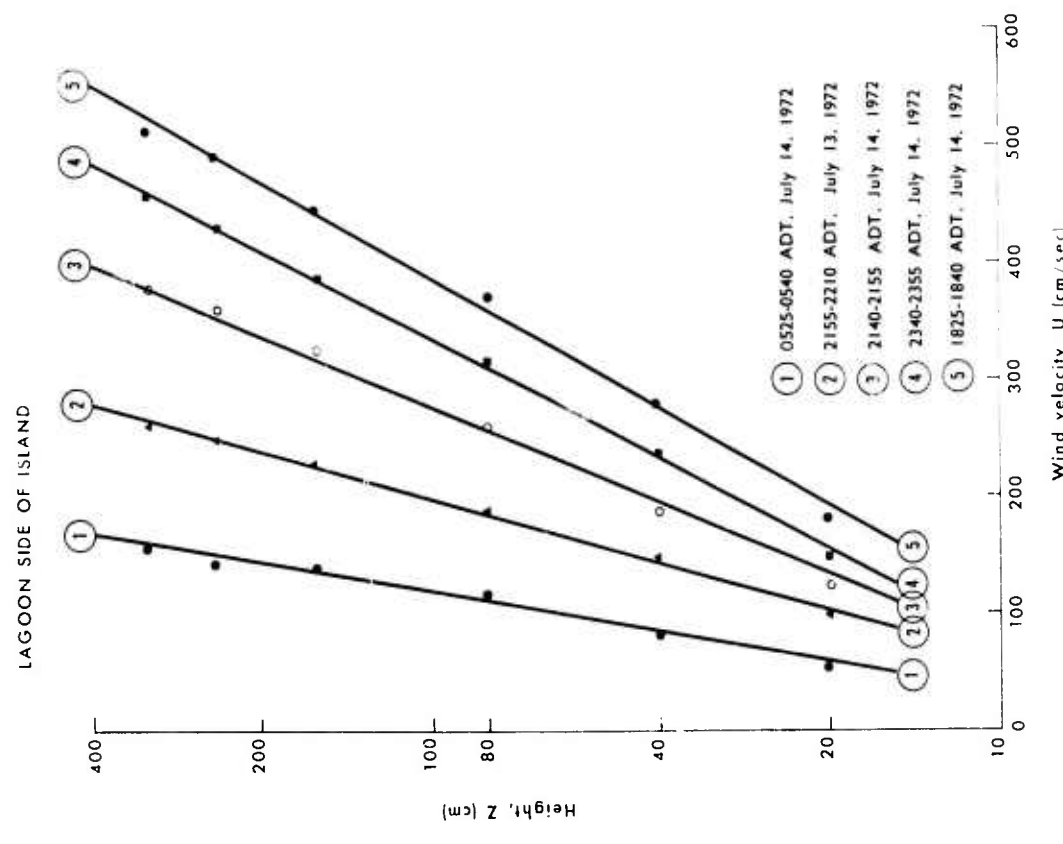


Figure 7B. Example of wind profiles at island berm station at Point Lay. Vertical scale is logarithmic.

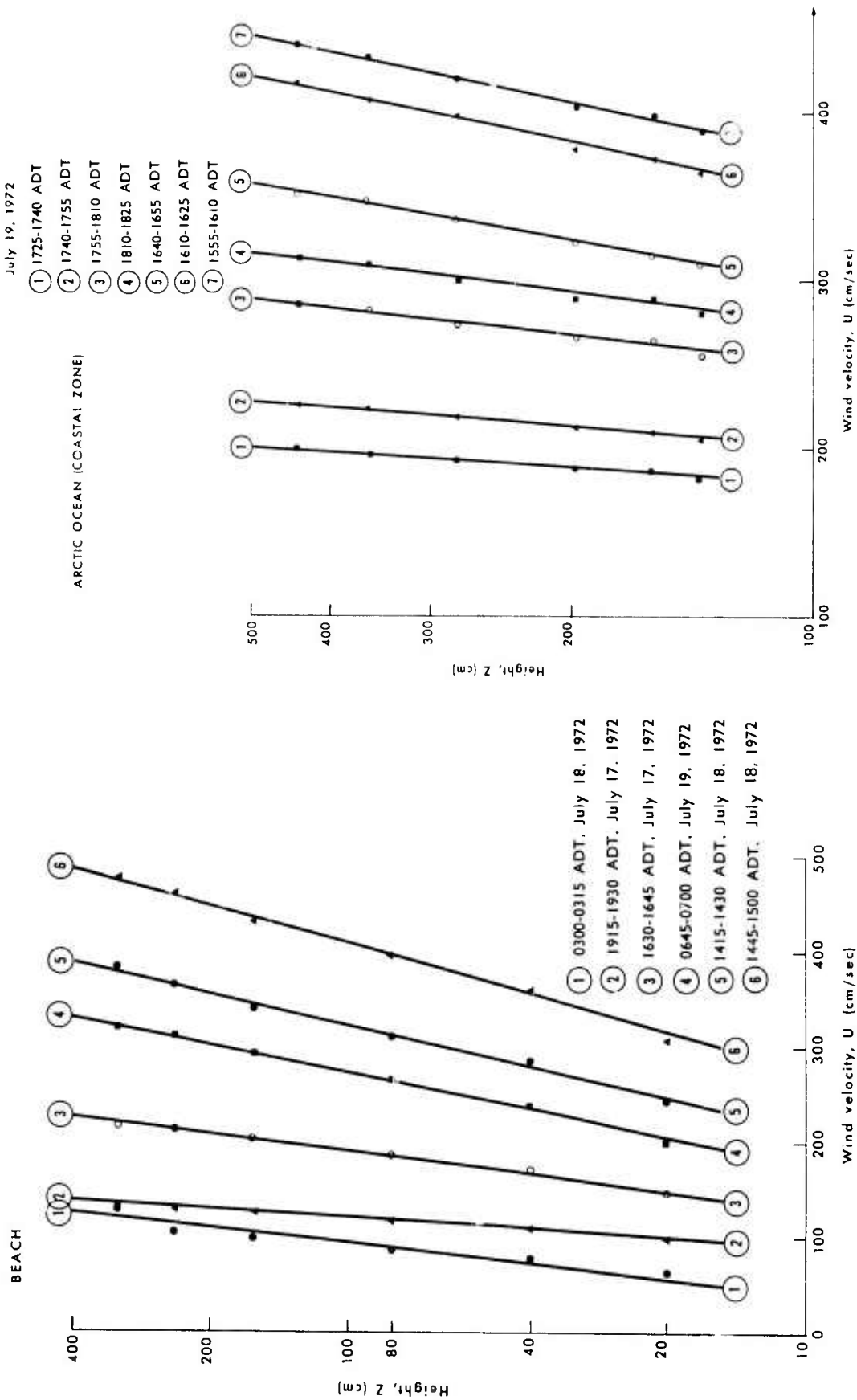


Figure 8A. Example of wind profiles at beach station at Point Lay site. Vertical scale is logarithmic.

Figure 8B. Example of wind profiles at offshore station at Point Lay site. Vertical scale is logarithmic.

$$U_* = \frac{k(U_{z_i} - U_{z_j})}{\ln\left(\frac{z_i}{z_j}\right)} \quad (3)$$

where  $i$  and  $j$  are indices which represent different heights. Then, the mean wind speeds at 2- and 10-meter heights for each of these observations were estimated from the least-squares fit line given from the mean wind speed versus height plot (e.g., see Figs. 7 and 8). Pairs of the calculated  $U_*$  and  $U_{2m}$  (mean wind speed at 2-meter height) which were made over the same 15-minute period were plotted against one another for stations 1-3 and are shown in Figure 9A-9C. Wind speed observations at 2-meter height are conventional for weather stations over land. In the same manner, the mean wind speed at 10-meter height,  $U_{10m}$ , versus  $U_*$  determinations for station 4 are plotted in Figure 10. Wind speed observations at 10-meter height are conventional over a sea surface. The correlation coefficient,  $\gamma$  (e.g., see Snedecor and Cochran, 1967), of  $U_*$  with  $U_{2m}$  or  $U_{10m}$  is given in Figures 9 and 10. The equation for a straight line

$$U_* = a + b U_z \quad (4)$$

is the least-squares fit to the data in Figures 9-10. In equation 4  $a$  is the  $U_*$  intercept when  $U_z = 0$  and  $b$  is the slope of the line. Theoretically, the value of  $a$  will be zero because there should not be any shear velocity when there is no wind velocity. The actual value of  $a$  is very close to zero in each case, and any difference may be attributed to experimental error. Thus, it follows that the value of  $b$  which gives the ratio of  $U_*$  to  $U_z$  is equivalent to the square root of the drag coefficient,  $C_D$ , given by equation 1. The results of the drag coefficient determinations are shown in Table 1. The surface shear stress,  $\tau$  (force per unit area), may be calculated from  $C_D$ , using the wind speed at the corresponding height, by

$$\tau = \rho C_D U_z^2 \quad (5)$$

where  $\rho$  is the air density.

The  $C_D$  values obtained over the land are dependent upon the local topography and are, therefore, not easily comparable to other studies made over land. The value obtained over the sea is, however, presumed to be comparable to other studies made over water. The value of  $C_D = 1.71 \times 10^{-3}$  at 10-meter height obtained in this study is in excellent agreement with the Arctic Region value of  $1.42 \times 10^{-3}$  obtained by Banke and Smith (1971) in their study conducted in the Beaufort Sea during July 1970.

Having obtained  $U_*$  from equation 3, the statistical application of equation 2 may then be used to obtain the mean value for the aerodynamic roughness length,  $Z_0$ , for a particular surface. The mean values, along with the 95 percent confidence limits, are shown for each station in Table 1. The 95 percent confidence limits give the range which has a 0.95 probability of including the true value of  $Z_0$  under a Gaussian hypothesis.

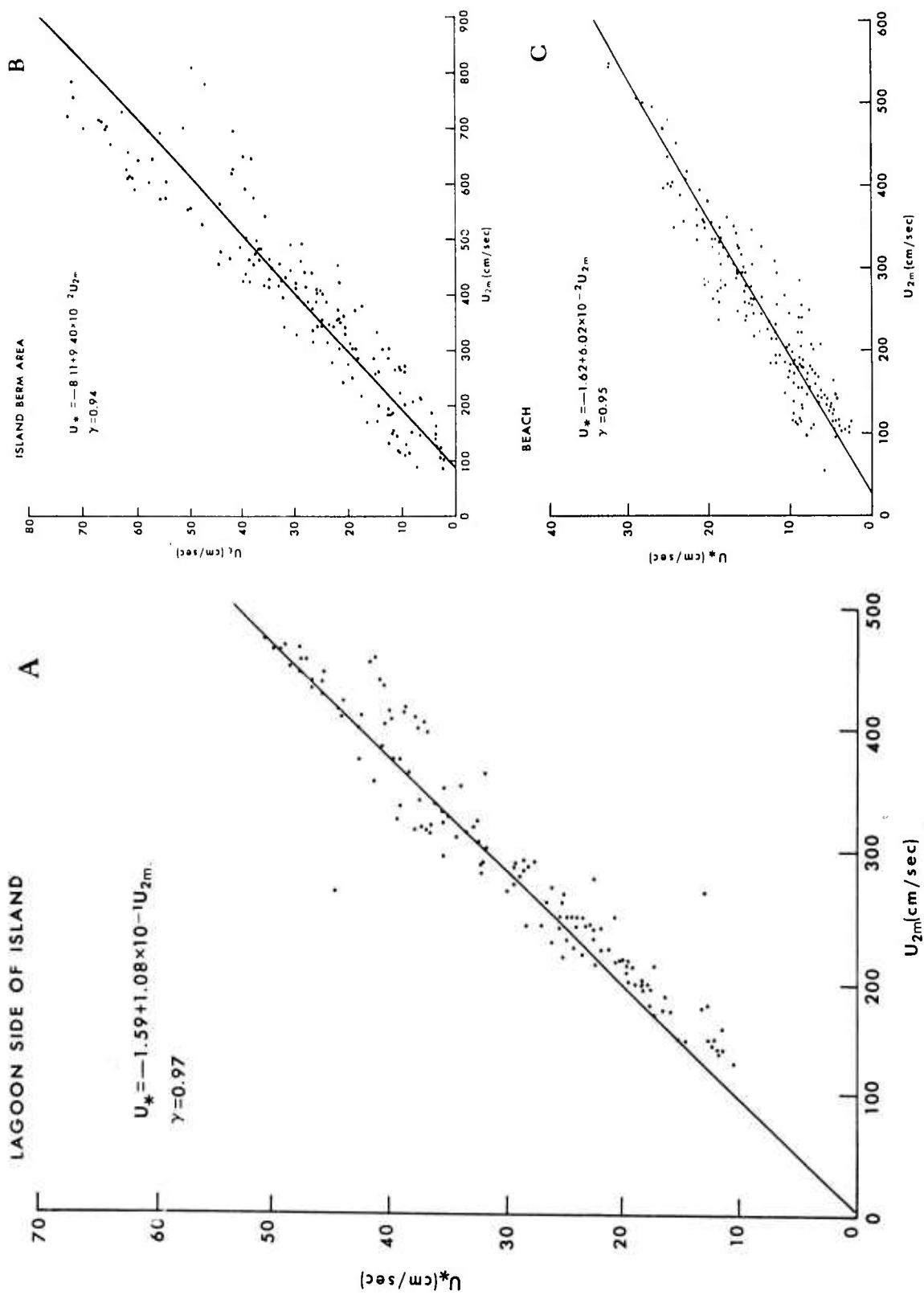


Figure 9A-9C. Shear velocity as a function of 2-meter wind speed at Point Lay site. A. Lagoon side of island. B. Island berm station. C. Beach station.

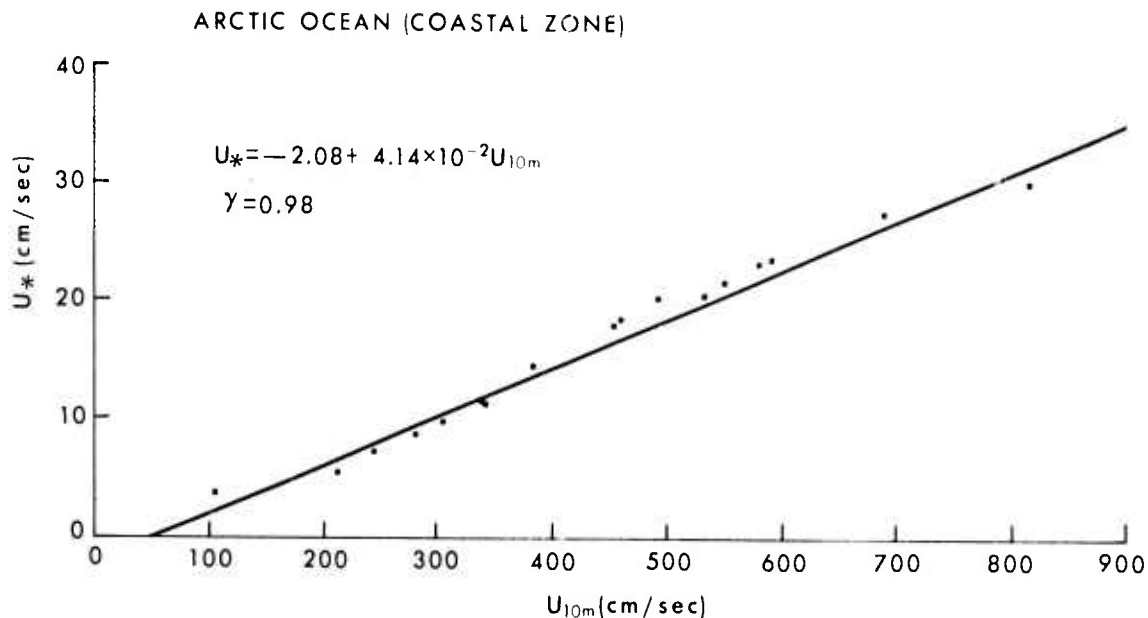


Figure 10. Shear velocity as a function of 10-meter wind speed at the offshore (Chukchi Sea) station.

The values obtained for  $\bar{Z}_0$  over the land are dependent upon the local topography, as was the case with  $C_D$ . The value obtained for the Chukchi Sea surface is, however, almost identical to that obtained in Banke and Smith's previously quoted study (0.025-0.027 cm) over the Beaufort Sea.

#### WINTER SEASON

The objective of the winter phase of this study was to determine the change in the vertical structure of the wind as it passes across a nearshore sea ice pressure ridge or hummock. This study was undertaken during April, long before breakup occurred. It is important to understand the wind structure modification resulting from flow across a coastal pressure ridge because there must exist a horizontal stress gradient which is a function of the abrupt change in the local ice topography. It is very possible that this gradient may influence the opening of leads, which result in local weather modification. Also, there may be analogous applications to nonshorefast, high ice objects such as bergs and ice "islands" which affect hydrodynamic turbulence and wave behavior. While Smith (1972) and Arya (1973), among others, have studied air flow and form drag over flat ice floes and pressure ridges, respectively, it is the main purpose of this study to investigate specifically the possible low-level jet phenomenon induced by the arctic pressure ridge.

The pressure ridge under consideration was located on the shorefast ice of the Chukchi Sea approximately 250 meters from the Point Lay Island shoreline. This ridge varied from approximately 3.5 to 10 meters in height along its length, which ran parallel to the coastline. There was roughly a  $45^\circ$  slope from the ridge crest to the flat ice surface on either side of the ridge. Fairly compact snow formed short, drifting mounds on the flat ice.

Table 1

## Summary of Roughness Length and Drag Coefficient Values

Station	$\bar{z}_o$ (cm)	95% Confidence Limits about $\bar{z}_o$ (cm)	$C_D$
1	4.16	3.79 to 4.52	$1.71 \times 10^{-2}$ (2 meters)
2	1.06	0.90 to 1.23	$8.84 \times 10^{-3}$ (2 meters)
3	0.221	0.16 to 0.28	$3.63 \times 10^{-3}$ (2 meters)
4	$2.53 \times 10^{-2}$	$1.52 \times 10^{-2}$ to $3.54 \times 10^{-2}$	$1.71 \times 10^{-3}$ (10 meters)

Three stations were placed in a straight line; the seaward and landward stations were located on opposite sides of the ridge at 152 and 122 meters, respectively, from the center of the ridge base, and the center or ridge station was located on a 3.8-meter-high portion of the ridge crest. This layout is illustrated in Figure 11; the ratio of the height to surface distance is illustrated as 20 to 1.

Each of the stations used multilevel, three-cup, fast-response Thornthwaite anemometer systems similar to those used in the summer study, the only difference being the sampling heights. At the landward station, cup assemblies were placed 91, 144, 224, 351, 546, and 851 cm above the surface; and at the seaward station, cup assemblies were placed 144, 224, 351, 546, and 851 cm above the surface. The ridge station cup assemblies were 20, 40, 80, 160, 240, and 320 cm above the crest. Observations were made simultaneously for each of the stations at 15-minute intervals on the portable Wind Profile Measurement System (see p. 14) from 2135 AST (Alaska Standard Time) on April 27 to 0235 AST on April 28, 1972. During this period a wind direction recorder (Climet Instrument Company, Model CI-26) indicated a constant direction from land to sea at  $45^\circ$  from the northeasterly trend of the ridge.

The horizontal wind speeds measured at each level of each station during the simultaneous operation of the three stations were normalized by dividing each observed mean horizontal wind speed by  $U_R = 600$  cm/sec because no observed mean wind speed exceeded this value. Normalized values were used in order to present the data clearly within the scale of Figure 10. The normalized mean wind speed values are listed for each level of the landward, ridge, and seaward stations in Tables 2, 3, and 4, respectively. The values are given opposite the twenty corresponding times which began each of the 15-minute intervals of observation. In addition, the normalized mean wind speed value for the entire time period, along with the standard deviation among each of the individual normalized 15-minute wind speeds, is given for each level at the bottom of each table. In Figure 11 the normalized horizontal mean wind speed values averaged over the entire 5-hour time period are represented by arrows of lengths drawn to scale located at each cup assembly sensor position. These lengths can be referenced to the arrow, which has a length of unity ( $\bar{U}_z/U_R = 1$ ), located in the upper right-hand corner of the figure. It should be kept in mind that the arrows also represent the component direction of the wind flow normal to the ridge. Note the vertical increase in wind speed as a function of height at both the landward and seaward stations as opposed to the somewhat hyperbolic profile over the pressure ridge. This clearly illustrates that

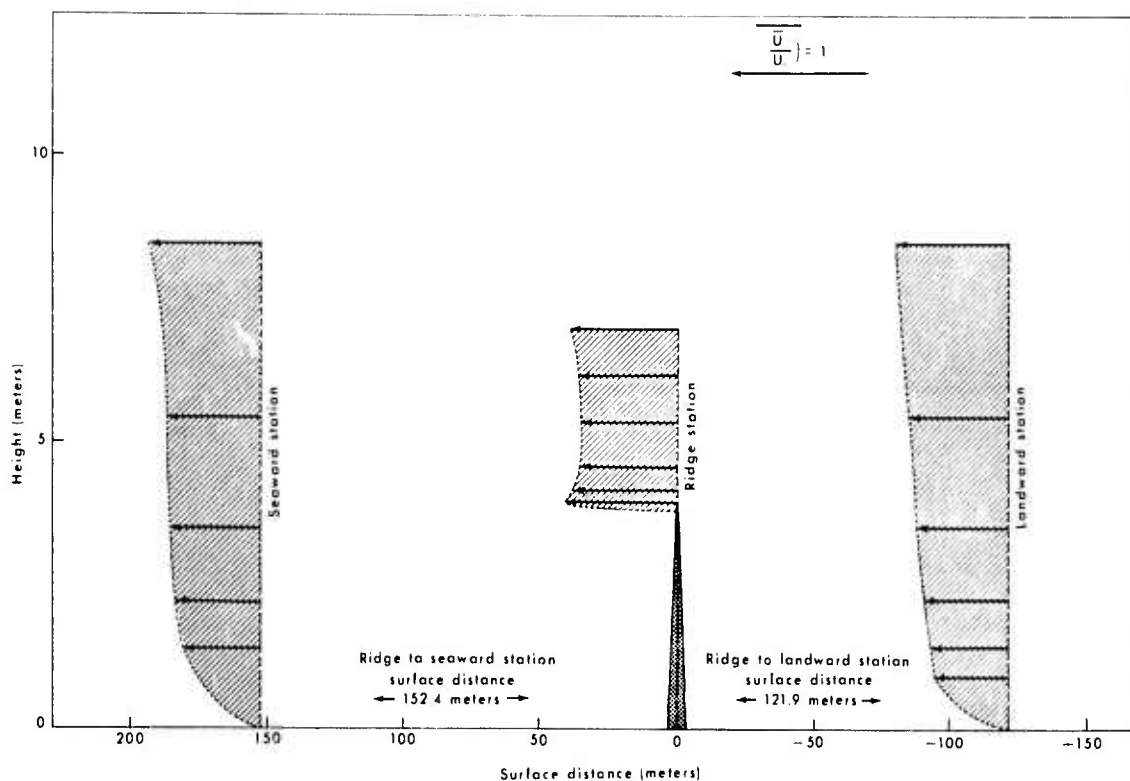


Figure 11. Total mean nondimensionalized horizontal wind speed components at each site during winter measurement period at Point Lay. The vertical to horizontal distance representation is 20:1.

a region of air flow of relatively high velocity has formed close to the crest of the ridge. The landward and seaward station profiles are, in fact, logarithmic, whereas the pressure ridge station profile indicates the formation of a low-level jet between the crest of the ridge and approximately 1 meter above it.

Examination of the values for each individual 15-minute observation yields results which are essentially identical, as to each profile shape, with the mean profiles. Thus, averaging the values over the entire 5-hour period had no effect on the basic results set forth and illustrated in Figure 11.

The effect of the formation of a jet over the pressure ridge can be partially attributed to the fact that mass must be conserved in any type of flow (e.g., see Hess, 1959). A comprehensive method for predicting the magnitude of such a flow must include knowledge of the vertical thermal stratification and resulting density gradient in the region. In order to construct a more explicit illustration of the air flow modification, it is recommended that additional stations be located on either side of the pressure ridge within those of this study so that isotachs of the air flow may be constructed. There may also be some value in constructing a high-frequency experiment wherein the data might be taken at extremely short time intervals (for example, 1 second or less). This would enable one to inhibit the effects of filtering out the high-frequency components of the wind energy spectrum and perhaps get a better overall picture of the effect of the ridge on turbulence.

Table 2

Wind Velocity Ratios for Landward Station

Time (AST)	$\frac{\bar{u}_{z_1}}{U_R}$	$\frac{\bar{u}_{z_2}}{U_R}$	$\frac{\bar{u}_{z_3}}{U_R}$	$\frac{\bar{u}_{z_4}}{U_R}$	$\frac{\bar{u}_{z_5}}{U_R}$	$\frac{\bar{u}_{z_6}}{U_R}$
April 27						
2135	0.5094	0.5557	0.5806	0.6530	0.7045	0.8311
2150	0.5866	0.6368	0.6609	0.7226	0.7760	0.8805
2205	0.5817	0.6327	0.6550	0.7228	0.7700	0.8615
2220	0.5450	0.5908	0.6138	0.6793	0.7311	0.8322
2235	0.5373	0.5798	0.6053	0.6593	0.7023	0.7924
2250	0.5338	0.5809	0.6091	0.6648	0.7102	0.8007
2305	0.5670	0.6135	0.6434	0.7053	0.7461	0.8327
2320	0.5412	0.5826	0.6080	0.6623	0.7073	0.7850
2335	0.4716	0.5146	0.5373	0.5927	0.6245	0.7223
2350	0.4836	0.5216	0.5472	0.6009	0.6511	0.7174
April 28						
0005	0.5231	0.5626	0.5913	0.6527	0.6971	0.7889
0020	0.5568	0.6012	0.6272	0.6859	0.7267	0.8122
0035	0.4625	0.4987	0.5206	0.5672	0.6028	0.6796
0050	0.4177	0.4526	0.4746	0.5209	0.5565	0.6327
0105	0.4973	0.5363	0.5615	0.6012	0.6560	0.7401
0120	0.4962	0.5310	0.5557	0.6234	0.6442	0.7179
0135	0.4650	0.5042	0.5406	0.6086	0.6493	0.7431
0150	0.4894	0.5267	0.5546	0.6154	0.6615	0.7615
0205	0.5423	0.5812	0.6067	0.6587	0.6974	0.7796
0220	0.5412	0.5817	0.6091	0.6683	0.7056	0.7946
$\left( \frac{\bar{u}_{z_1}}{U_R} \right)$						
$\sigma \left( \frac{\bar{u}_{z_1}}{U_R} \right)$						
$U_R = 6 \text{ m/sec}$						

Table 3

Wind Velocity Ratios for Ridge Station

Time (AST)	$\frac{\bar{u}_{z_1}}{U_R}$	$\frac{\bar{u}_{z_2}}{U_R}$	$\frac{\bar{u}_{z_3}}{U_R}$	$\frac{\bar{u}_{z_4}}{U_R}$	$\frac{\bar{u}_{z_5}}{U_R}$	$\frac{\bar{u}_{z_6}}{U_R}$
April 27						
2135	0.8440	0.8007	0.7530	0.7593	0.7839	0.8259
2150	0.8866	0.8420	0.7839	0.7879	0.8083	0.8508
2205	0.9056	0.8607	0.7982	0.7960	0.8190	0.8639
2220	0.8711	0.8275	0.7681	0.7683	0.7927	0.8352
2235	0.8190	0.7771	0.7231	0.7242	0.7478	0.7861
2250	0.7885	0.7478	0.6976	0.6998	0.7256	0.7661
2305	0.7664	0.7237	0.6763	0.6804	0.7048	0.7426
2320	0.7253	0.6889	0.6472	0.6554	0.6863	0.7212
2335	0.7470	0.7089	0.6628	0.6626	0.7002	0.7264
2350	0.7231	0.6828	0.6387	0.6417	0.6601	0.6935
April 28						
0005	0.7804	0.7407	0.6894	0.6900	0.7091	0.7461
0020	0.8818	0.8352	0.7755	0.7768	0.7861	0.8218
0035	0.7251	0.6848	0.6439	0.6434	0.6645	0.6985
0050	0.5932	0.5620	0.5313	0.5371	0.5598	0.5913
0105	0.6976	0.6609	0.6209	0.6215	0.6448	0.6826
0120	0.7604	0.7165	0.6735	0.6757	0.7029	0.7302
0135	0.7587	0.7144	0.6689	0.6763	0.7004	0.7379
0150	0.7648	0.7201	0.6793	0.6801	0.7031	0.7390
0205	0.8138	0.7642	0.7146	0.7160	0.7376	0.7730
0220	0.8383	0.7716	0.7256	0.7237	0.7445	0.7774
$\left( \frac{\bar{u}_{z_1}}{U_R} \right)$						
$\sigma \left( \frac{\bar{u}_{z_1}}{U_R} \right)$						
$U_R = 6 \text{ m/sec}$						

Table 4

## Wind Velocity Ratios for Seaward Station

Time (AST)	$\frac{\bar{U}_{z_1}}{U_R}$	$\frac{\bar{U}_{z_2}}{U_R}$	$\frac{\bar{U}_{z_3}}{U_R}$	$\frac{\bar{U}_{z_4}}{U_R}$	$\frac{\bar{U}_{z_5}}{U_R}$
April 27					
2135	0.5535	0.5911	0.6483	0.7242	0.8637
2150	0.5664	0.6048	0.6593	0.7286	0.8492
2205	0.6026	0.6426	0.7050	0.7771	0.8979
2220	0.6187	0.6552	0.7097	0.7664	0.8818
2235	0.6146	0.6505	0.7059	0.7524	0.8767
2250	0.5826	0.6165	0.6738	0.7204	0.8420
2305	0.5609	0.5968	0.6486	0.6856	0.7990
2320	0.5053	0.5387	0.5872	0.6231	0.7357
2335	0.4850	0.5141	0.5571	0.5919	0.7012
2350	0.5206	0.5513	0.5993	0.6374	0.7497
April 28					
0005	0.5099	0.5404	0.5921	0.6187	0.7283
0020	0.5676	0.5968	0.6448	0.6716	0.7924
0035	0.5974	0.6322	0.6850	0.7015	9.8089
0050	0.5269	0.5582	0.6069	0.6258	0.7187
0105	0.4414	0.4697	0.5154	0.5417	0.6464
0120	0.4927	0.5226	0.5708	0.5902	0.6952
0135	0.5615	0.5897	0.6341	0.6426	0.7374
0150	0.5779	0.6091	0.6582	0.6697	0.7733
0205	0.5741	0.6028	0.6467	0.6593	0.7552
0220	0.6012	0.6324	0.6785	0.6902	0.7927
$\left(\frac{\bar{U}_{z_i}}{U_R}\right)$	0.5530	0.5858	0.6363	0.6709	0.7823
$\sigma\left(\frac{\bar{U}_{z_i}}{U_R}\right)$	0.048	0.050	0.053	0.063	0.070

$U_R = 6 \text{ m/sec}$

## CHAPTER III

### NEARSHORE HYDRODYNAMIC PROCESSES

#### Introduction

Of the many hydrodynamic phenomena active in the nearshore zone, four were selected for close scrutiny: sea level variations from periods of a few hours to a few days; wave motion, both local wind-generated waves and swell; mesoscale currents; and mesoscale water mass variability.

Existing literature concerning each of these phenomena is briefly reviewed at the beginning of the appropriate sections and found to be inadequate for characterizing the environment. Our goals were to describe the mesoscale variability of sea level, nearshore currents, wave characteristics, and water mass characteristics at the two field sites and to determine possible causative mechanisms for the observed variations.

Point Lay was selected for the site of the most extensive investigations because it was expected to be logistically more accessible to instrumentation. During the Pingok Island study, however, wave conditions were more variable, and thus more interesting for this study, than at Point Lay.

#### Sea Level Variations

Only a modest amount of literature is available concerning tides in the Arctic. Hunkins (1965) gives a brief review of this information, and Sverdrup (1927) proposes a map of cotidal lines and describes the dynamics of tides in the Chukchi Sea. Beal (1968) studied seasonal sea level variations at Point Barrow, and Matthews (1970, 1971) presented preliminary results of analysis of a long record of sea level from Point Barrow. Hunkins (1965) and Hume and Schalk (1967) describe aspects of meteorological tides or storm surges in the Chukchi Sea. The few data available from this area seem to confirm Sverdrup's (1927) description of the astronomical tides: they are primarily semidiurnal; they enter from the Atlantic; they are severely influenced by the Coriolis force inasmuch as, at these latitudes, the inertial period is very close to that of the semidiurnal tide; and tidal range is small but velocities are amplified.

At Point Lay, two capacitance tide gages were installed, one inside Kasegaluk Lagoon and one offshore, and a pressure-sensing gage was bottom mounted offshore. The offshore capacitance gage was damaged during a storm, and the pressure gage did not function continuously. The capacitance gage within the lagoon gave a good record, which is reproduced in Figure 12. For those periods when the pressure gage was operational, it matched, qualitatively, the capacitance record. Water level was read visually a number of times during the season to within 2 cm, and these data were used to compute a calibration equation for the capacitance gage. The standard deviation of the calibration was 4.2 cm. The gage sampled water level every 27.3 minutes.

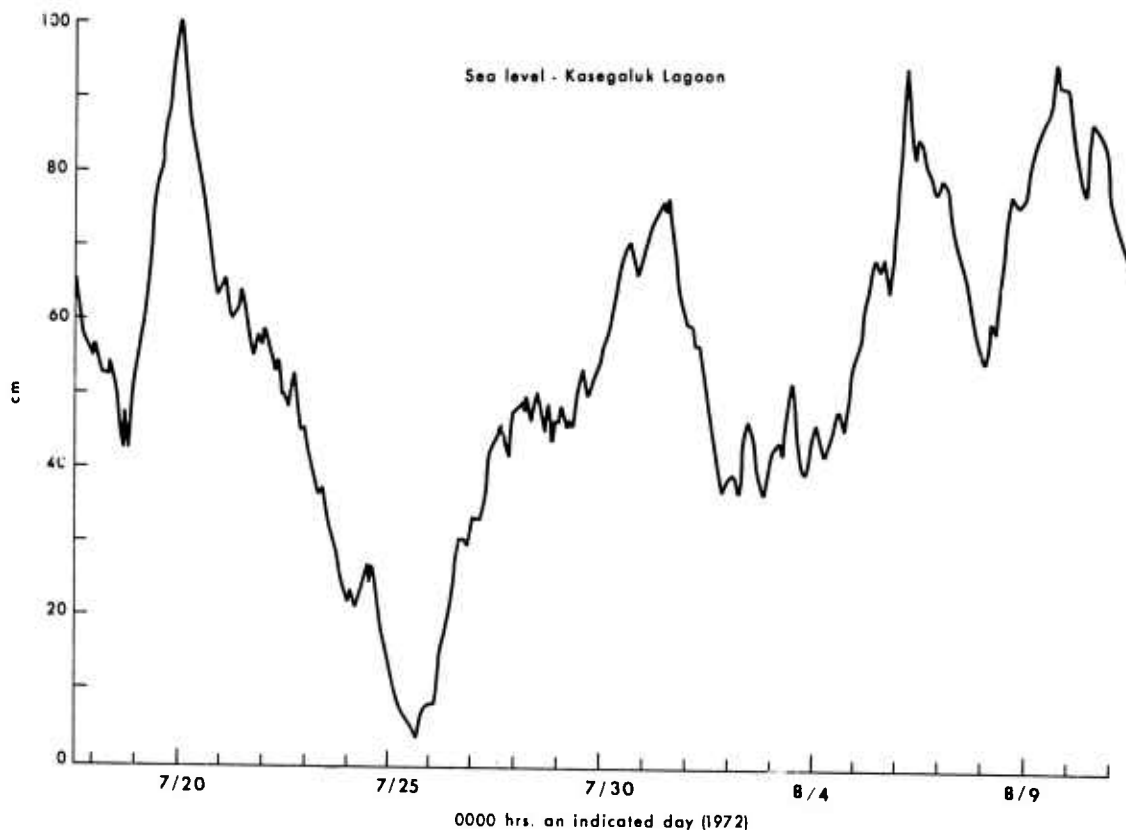


Figure 12. Capacitance tide gage record from Kasegaluk Lagoon, behind Point Lay Island. Time marks refer to 0000 ADT on the indicated day. The gage was not tied into a geodetic leveling net.

It is obvious that the meteorological tides are far more important in the record shown in Figure 12 than the astronomical. Hunkins' and Matthews' records show astronomical tides much more clearly, but they were taken closer to the deep water of the Beaufort Sea, the source of the astronomical tides in the Chukchi Sea. The Point Lay record and tide records from Point Barrow and Oliktok Point supplied by J. B. Matthews may be compared in Figure 13. The two latter stations are also located in lagoons, but they face the Beaufort Sea and its narrow shelf, and the inlets to the lagoons are large. Both features will reduce nonlinear distortion and frictional dampening of the tidal wave. This may explain the well-developed astronomical signal in both these records. Strong meteorological tides are also present at the latter two sites, as in the Point Lay record.

Explanation of the anomalous changes in sea level at Point Lay must be sought in meteorological forcing of the coastal waters. The problem is nonlinear and very difficult to solve, even with extensive data of high quality (Groen and Groves, 1962). With small amounts of data of modest quality, it is next to impossible. Certain conclusions may be drawn, however. Figure 14 shows the barometric pressure at Point Lay during the summer field work converted to centimeters of water, assuming that 1 mb of pressure corresponds to 1 cm of water. There is reasonably good correlation of the larger features of both the sea level (Fig. 12) and the pressure (Fig. 14) records, indicating an inverted barometer effect. When a correlation function was computed, though, the best correlation was obtained between the sea

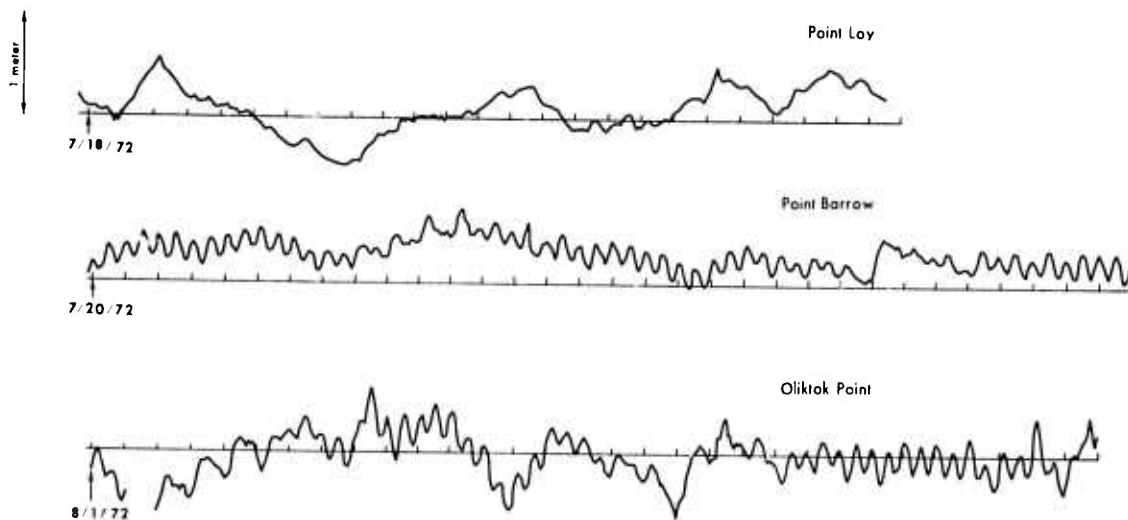


Figure 13. Tide gage records from lagoons at Point Lay, Point Barrow, and Oliktok Point. The time marks refer to 0000 ADT on the indicated day. Note that the records begin at different times. The vertical scale is the same for the three records. The records from Point Barrow and Oliktok Point were obtained through the courtesy of Dr. J. B. Matthews, University of Alaska.

level record and the pressure 2.8 days earlier. However, with a basin the size of the Chukchi Sea, one would not expect a perfect barometric effect (Groen and Groves, 1962), especially with forcing by moving storm systems. It seems more likely that the sea level is influenced by the intense winds which were observed during the field program. Figure 15 is a progressive vector diagram of the wind stress. The winds were read from the anemometer record every hour and assumed to be representative of the next hour-long interval. Stress was computed using a quadratic formula and assuming an air density of  $1.2 \times 10^{-3} \text{ gm/cm}^3$  and a drag coefficient of  $1.6 \times 10^{-3}$ . The scale in the figure represents a stress of 20 dynes/cm<sup>2</sup> blowing for 1 hour. The record begins at 0900 Alaskan Daylight Time (ADT) on July 15. The large dots represent 0000 ADT on the indicated days. Three major reversals of the wind stress are shown. There is also a period of approximately zero stress from July 28 until August 1. The major storm periods were from the northeast from July 23 through 26 and from the southwest from August 5 through 11; a lull occurred on August 7. Southerly winds are generally associated with onshore (westerly) winds and northerly winds with offshore (easterly) winds.

Correlation functions of the sea level with the east-west and north-south wind stress (directions are magnetic) show that when a peak occurs sea level leads the stress by about 4 hours. The correlation is slightly better between the east-west stress and the water level than between the north-south stress and the water level; but, considering the short records and the strong correlation of easterly with northerly winds, it is hard to draw meaningful conclusions from this. When the stress is correlated with the sea level record, corrected for pressure assuming an inverted barometer effect, peak correlation occurs when sea level lags the stress by about 16 hours. Again, considering the short nature of the records these lag times are probably not very meaningful. At best, it may be said that sea level correlated well with wind stress at very short lags. Qualitatively, these

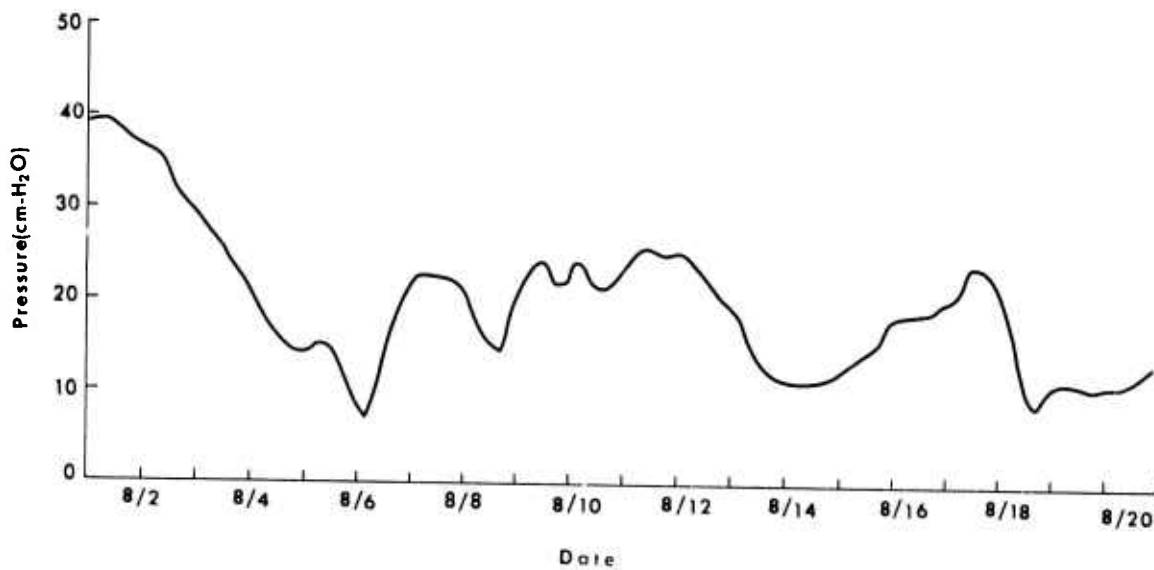
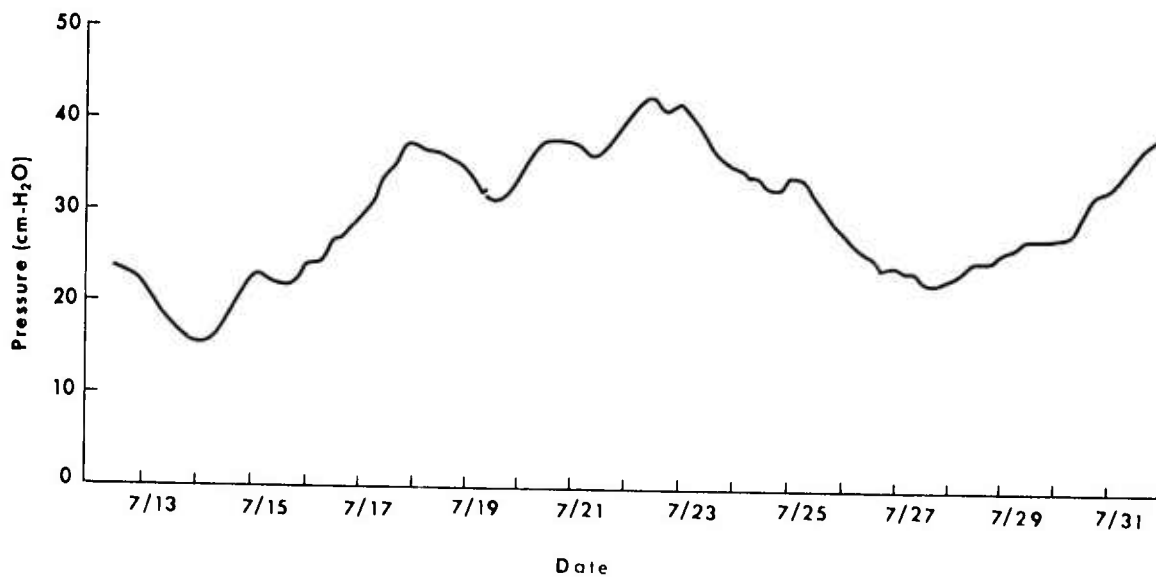


Figure 14. Atmospheric pressure at Point Lay during the latter part of July and the early part of August. Pressure is shown in centimeters of water. Time marks refer to 0000 ADT on the indicated day.

correlations would be predicted by application of linear Ekman theory to the near-shore region (Murray, in preparation). The mechanics of a storm surge, however, are known to be nonlinear.

Figure 16 shows the periodogram computed using a Fast Fourier Transform program. The first sixty harmonics are shown. The entire record was used in the computation. No averaging has taken place. Thus, from a statistical point of view, each estimate has 2 degrees of freedom. The periodogram was considered, though, to represent the distribution of energy actually present in the record measured, making

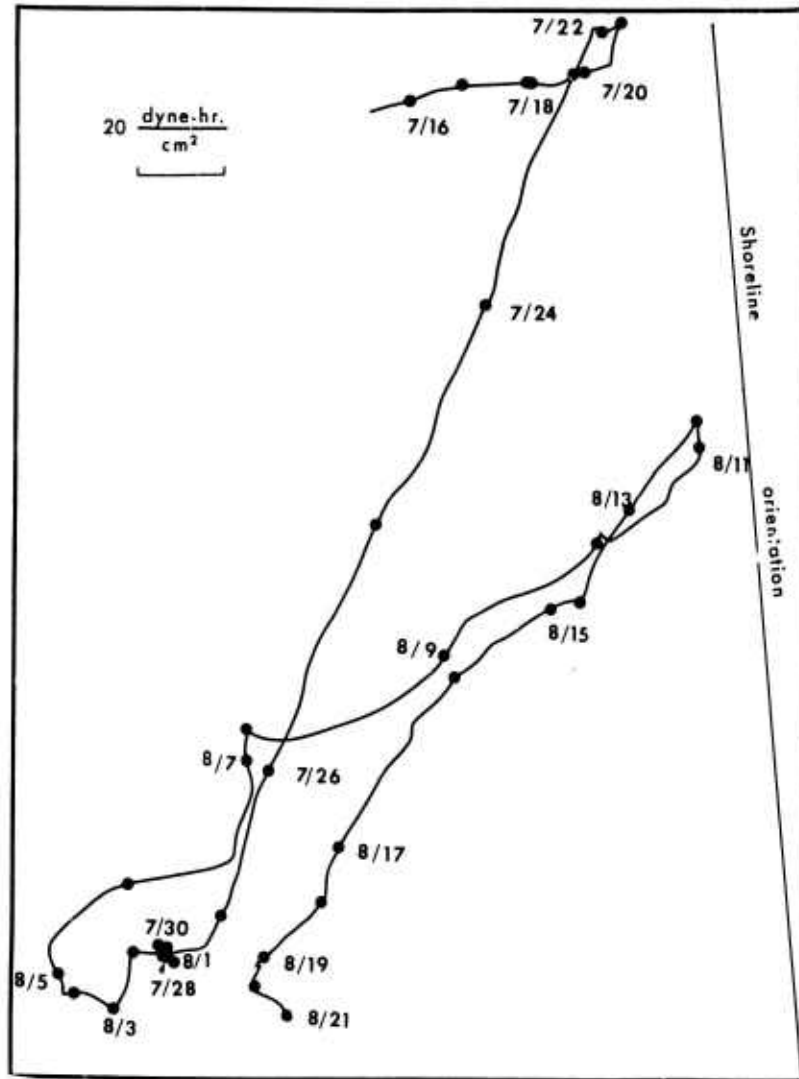


Figure 15. Progressive vector diagram of surface wind stress at Point Lay drawn from hourly wind observations and assuming an air density of  $1.2 \times 10^{-3} \text{ gm/cm}^3$  and a drag coefficient of  $1.6 \times 10^{-3}$ . The record begins at 0900 ADT on July 15, 1972, and black dots refer to 0000 ADT on the indicated day. The local trend of the shoreline is also shown.

no inferences about an underlying process. The frequencies of the diurnal and semidiurnal tides are marked on the figure. There is a flattening of the periodogram estimates near the diurnal frequencies. There is also a definite peak near the semidiurnal frequencies. The high values at low frequencies are associated with storm surges. If this figure were converted to a power spectrum and plotted on log-log paper, these peaks would appear more pronounced. There is also an obvious peak in the periodogram corresponding to a period of 18.07 hours. If it is assumed that Kasegaluk Lagoon, from its southern tip to Icy Cape, where it is blocked by sand flats, has a centerline distance of 125 km and a mean depth of 1.5 meters, not unreasonable numbers, then, using Merian's formula, we find a fundamental

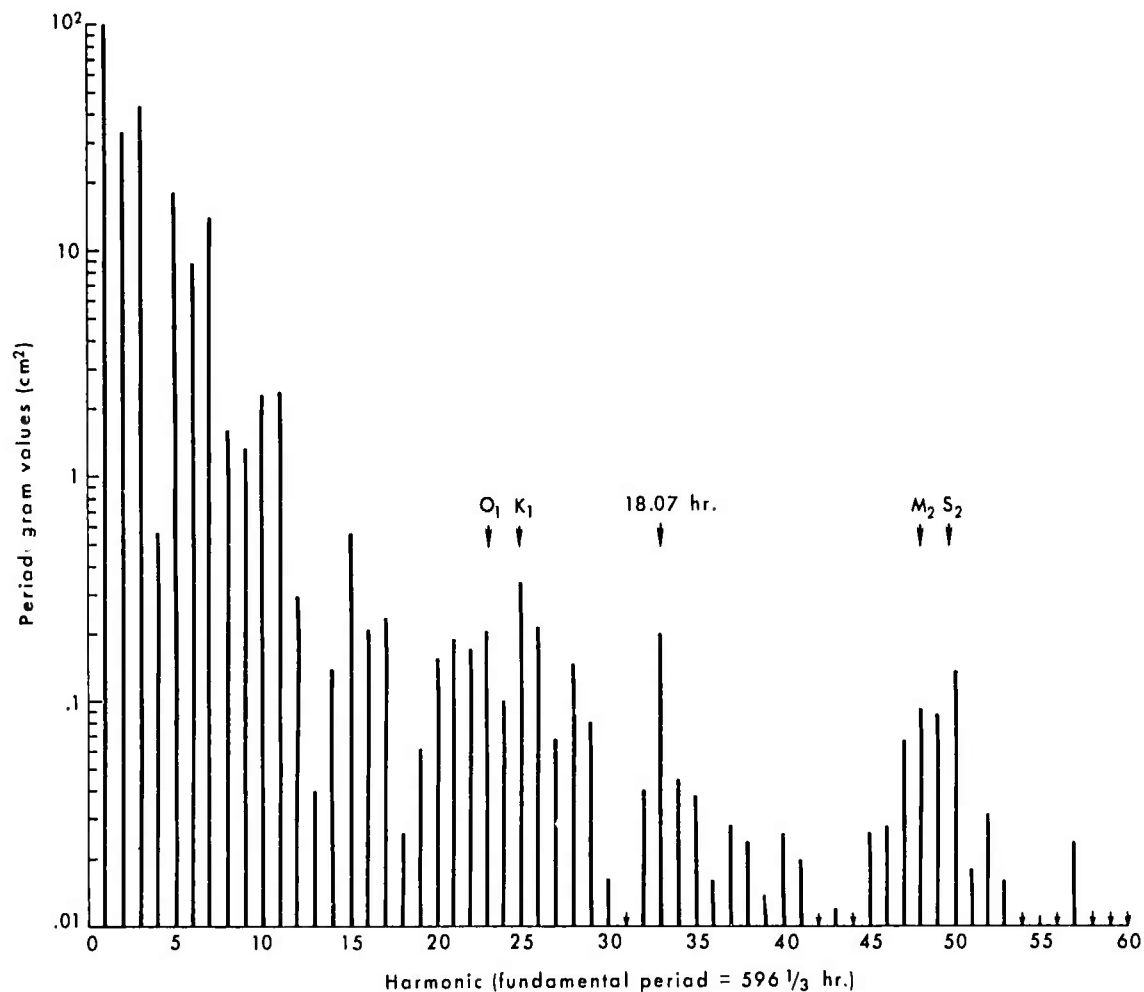


Figure 16. First sixty periodogram estimates of the 596.3-hour tide record from Point Lay. Small arrows on the horizontal axis indicate values less than  $0.01 \text{ cm}^2$ . The frequencies of the two major semidiurnal and diurnal astronomical tides are indicated, as well as a seiche period of 18.07 hours.

seiche period of 17.9 hours. The strong atmospheric disturbances in this region would be expected to initiate seiche motion in a large body of water such as Kasegaluk Lagoon. This seems to be the explanation for the anomalous energy peak in the periodogram.

#### Waves

The current understanding of arctic wave action is based on a very limited data base, and no systematic survey of wave processes exists in the literature. Yet there is abundant evidence that wave action is, as in lower latitude coastal environments, a primary factor controlling beach and coastline morphology (Moore, 1966; Hume and Schalk, 1964b; Hume and Schalk, 1967).

Hunkins (1962) studied surface waves during the winter season from floating ice stations. Measurements were made of ice surface oscillations over a broad

range of frequencies. These results will present an interesting contrast to those reported here for summer wave conditions. Recently the University of Alaska has been engaged in an extensive data-gathering program in the nearshore area. Wave data are included, and some results have been published.

Visual observations have been more frequent. Hartwell (1971) has presented some wave climate statistics for the Barrow area, and Short (1973), for the Pingok Island area. Large-amplitude wave observations have been reported by Hume and Schalk (1967). These reports indicate that wave heights have reached 6 meters in the Point Barrow area.

#### DATA ACQUISITION AND ANALYSIS

The general location and characteristics of the field sites, Pingok Island and Point Lay, were described earlier in this report. Selection of these sites was determined partly by the feasibility of locating a camp close to the shoreline for an extended period of time. The Point Lay site is on a relatively straight section of coastline oriented nearly north-south, and the open Arctic Ocean is to the west. There the prevailing northeast winds blow offshore. The continental shelf is very wide (distance to the nearest shelf break is approximately 275 km), and the nearshore bathymetry is rather regular on a large scale; that is, there are no submarine canyons cutting the shelf, nor are there any troughs or shoals offshore which would produce complex wave refraction patterns. The pack ice is about 200 km offshore during maximum open water.

The Pingok Island site presented numerous contrasts to the Point Lay site. It is located along a rather irregular coastline whose general trend is east-west, and the Arctic Ocean is to the north. There the prevailing winds blow with an onshore component. The shelf is narrower than at Point Lay, averaging about 90 km in width. The pack ice is of the order of 10 km offshore during maximum open water.

Equipment used in measuring waves consisted of resistance-wire wave staffs, a low-pass filter, and an analog strip-chart recorder. The resistance-wire wave staffs were described by Truxillo (1970). When recording wind waves and swell, the signals from the wave staffs are transmitted by cable directly to the recorder. At Pingok Island, when long waves were measured RC filters were used to attenuate the higher frequency wind waves and swell. The filters had time constants of about 30 seconds. The strip-chart recorder was a six-channel Mark 260 Brush Recorder.

The field set-up at both sites was basically the same. Each wave staff was mounted on land to a portable tripod tower. These towers were hand carried into 2-meter water depth and placed in a line array parallel to and about 10 meters from the shoreline. At Point Lay, the array had four wave staffs whose separations were 3, 9, and 6 meters. At Pingok Island, five wave staffs were used in the array, and the separations between staffs were 1, 3, 2, and 4 meters. The locations of the sites are shown in Figures 2 and 3. The wave data taken at each site during the field experiments consisted of continuous recordings of signals from one or more wave staffs for a certain period of time. The wind wave and swell records varied from 30 minutes to 180 minutes (3 hours) in length. The long-wave records varied from 90 minutes to 510 minutes (8 1/2 hours) in length. The time interval between these individual recordings was generally about 8 hours, and measurements continued for about 1 week. The wave data taken at both field sites are catalogued in Table 5. In addition to the wave data recordings, calibration records were made by filming simultaneously the wave staff and an attached meter scale. Visual observations of wave height and period were made during storm conditions at each site, when the wave staffs were inoperative.

Table 5  
Wave Data Acquisition Runs

Data Acquisition No.	Date (1972)	Starting Time (ADT)	Length of Record (Min)	Wave Type Measured
<u>Point Lay</u>				
95	August 13	1157	180	Wind Waves
96	August 14	2000	225	Wind Waves
97	August 15	1040	190	Wind Waves
98	August 15	1653	150	Wind Waves
99	August 16	0006	100	Wind Waves
100	August 16	1000	80	Wind Waves
101	August 16	1625	150	Wind Waves
102	August 17	0025	60	Wind Waves
103	August 17	1020	100	Wind Waves
104	August 17	1800	135	Wind Waves
105	August 18	0130	90	Wind Waves
106	August 18	1920	30	Wind Waves
<u>Pingok Island</u>				
107	August 29	1900	40	Wind Waves
108	August 30	1308	60	Wind Waves
109	August 31	1402	27	Wind Waves
110	August 31	1525	90	Long Waves
111	August 31	1714	40	Wind Waves
112	August 31	1830	90	Wind Waves
113	August 31	2045	180	Long Waves
114	September 1	1106	520	Long Waves
115	September 1	2130	60	Wind Waves
116	September 2	0915	70	Wind Waves
117	September 2	1330	70	Wind Waves
118	September 3	1006	520	Long Waves
119	September 3	2110	30	Wind Waves
120	September 4	0830	60	Swell
121	September 4	0947	250	Long Waves
122	September 4	1400	60	Swell
123	September 4	1512	360	Long Waves
124	September 5	0900	30	Swell

Analysis of the recorded field data has been partially completed. The calibration factor for the wave sensors at each site was determined and applied to each record. The wave data were analyzed for significant wave height and period from a 20-minute section of each wave record. Wave records were also digitized, and power spectra were computed for some wave records, including wind waves and long waves. Problems with the digitizer hardware limited the amount of wave data which was spectrally analyzed. The long-wave spectra were corrected for the effects of the RC filter. Wave spectra were calculated, estimates having equivalent degrees of freedom of 7 for the long waves and 10 for the wind waves.

## DISCUSSION OF RESULTS

### Waves with 30- to 1,000-Second Periods

Energy spectra for waves in the frequency range 0.001-0.033 cps (periods of 1,000 to 30 seconds) are shown in Figures 17A and 17B. Figure 17A shows two spectra of records taken 4 hours apart at Pingok Island, and Figure 17B shows another pair of spectra taken 4 hours apart 2 days later. A general increase in energy level with period is noticeable in all records. This is the same property noted by Hunkins (1962). Superimposed on the general trend is a fine structure that is closely reproduced in the records taken the same day.

The general decrease of wave energy with increasing frequency is a major feature of the spectra. Figure 18 shows spectra for both days, and the similar form of the spectra can be seen. This is not typical behavior for waves in this frequency range. Figure 19 shows a spectrum observed at Pingok compared to spectra taken at Guadalupe Island, Mexico, and Camp Pendleton, California, reported by Munk (1963). At the other locations the rise in energy at about 0.0025 cps and the peak that occurs at about 0.01 cps are much larger than at Pingok Island. Also, the energy levels above 0.007 cps are considerably higher at the other locations than at Pingok Island.

The slopes of the Pingok spectra are about  $f^{-3.3}$ , where  $f^{-4}$  would denote constant acceleration. Hunkins (1962) reported similar behavior for wave spectra between 0.016 cps and 0.1 cps. A constant acceleration of about  $10^{-5}$  m/sec<sup>2</sup> was reported to fit his data. His measurements were made on an ice island during the winter season, and the amplitude of the waves was found to be correlated with wind speed. The Pingok observations extend to lower frequency than those of Hunkins; however, the trend of the spectra is the same. The Pingok measurements were taken during the summer, when nearshore waters were ice free, yet the amplitudes where the measurements overlap are nearly identical. The Pingok amplitudes are larger by about a factor of 2 than the average reported by Hunkins, though the effects of shoaling, which increase shallow-water wave heights over deepwater values, could account for this.

It appears, then, that long waves are generated by the action of wind on the pack ice. The ice pack appears to filter out the high-frequency wave components. The long waves propagate to the shorelines of the Arctic Ocean. Open water during summer, representing only a fractional change in the area of the pack ice, is of little consequence for these waves.

The fine structure of long wave spectra is generally reproduced within the same days, and, although there is some difference between the frequency of the peaks of September 1 and September 3, the general positions are the same. The peaks on September 1 are at about 0.005 and 0.01 cps; on September 3 the peak is at about 0.004 cps. Long waves are highly reflected from the shoreline and are very strongly influenced by bathymetry, inasmuch as the waves are in relatively shallow water. Trapping and resonance of these waves by nearshore bathymetry is a possible explanation for these peaks. The offshore bars (see Chapter V) are of the proper order of magnitude, in their distance from the shoreline, to produce this effect. Also, nonlinear interactions of wind waves can produce "surf beats" which have frequencies in the long wave range, which may be the source of the spectral peaks.

### Waves with 0.5- to 30-Second Periods

Wind wave data taken at Point Lay are rather disappointing. The wind during

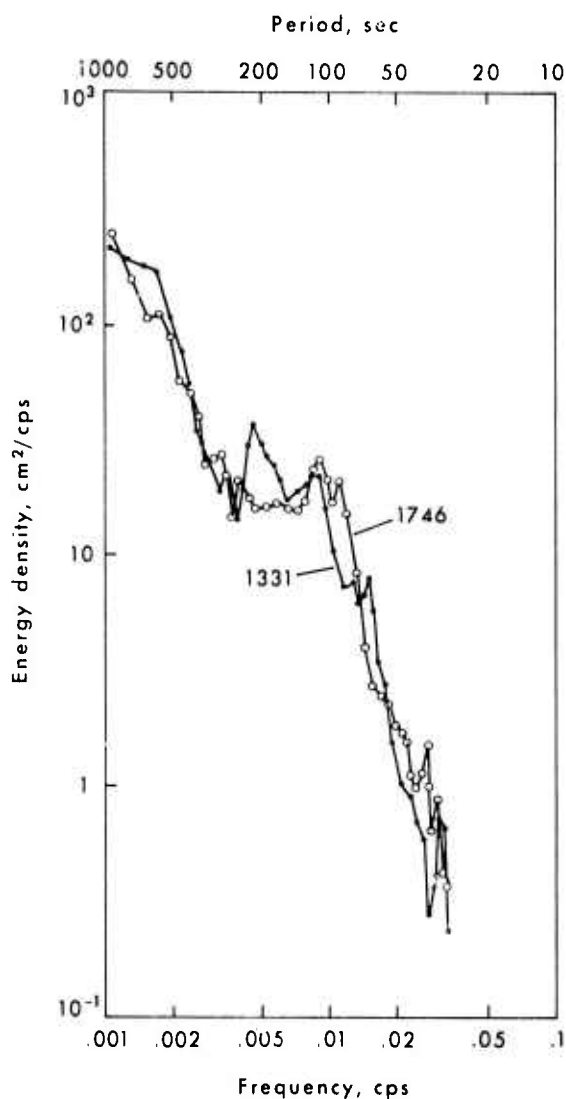


Figure 17A. Long-wave spectra of records taken 4 hours apart on September 1, 1972. General trend and fine structures are reproduced in each spectrum. Numbers refer to time of sample (Alaska Daylight Time).

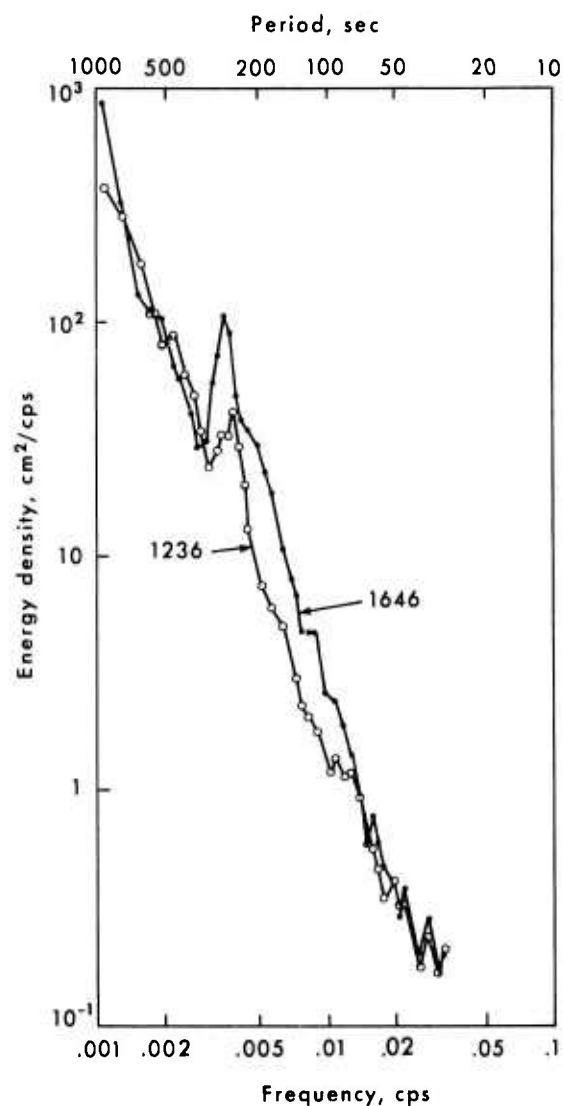


Figure 17B. Long-wave spectra of wave records taken 4 hours apart on September 3, 1972. Spectral peak at 0.004 cps and general trend of decreasing energy with increasing frequency are shown in each spectrum.

the observation period generally blew alongshore, with a slight offshore component in a WSW direction, at about 4.5 m/sec. Wave heights increased offshore where the wave crests were observed to be aligned perpendicular to the shore. At the shoreline, wave height varied between 10 and 30 cm and periods were between 2 and 3.5 seconds. The waves approached the shoreline from the north at a steep angle; the angle between the wave crest and the line of sensors varied from about  $10^\circ$  to  $20^\circ$ . The waves generated offshore were refracted into the shoreline so that they were propagating at approximately  $90^\circ$  to the winds.

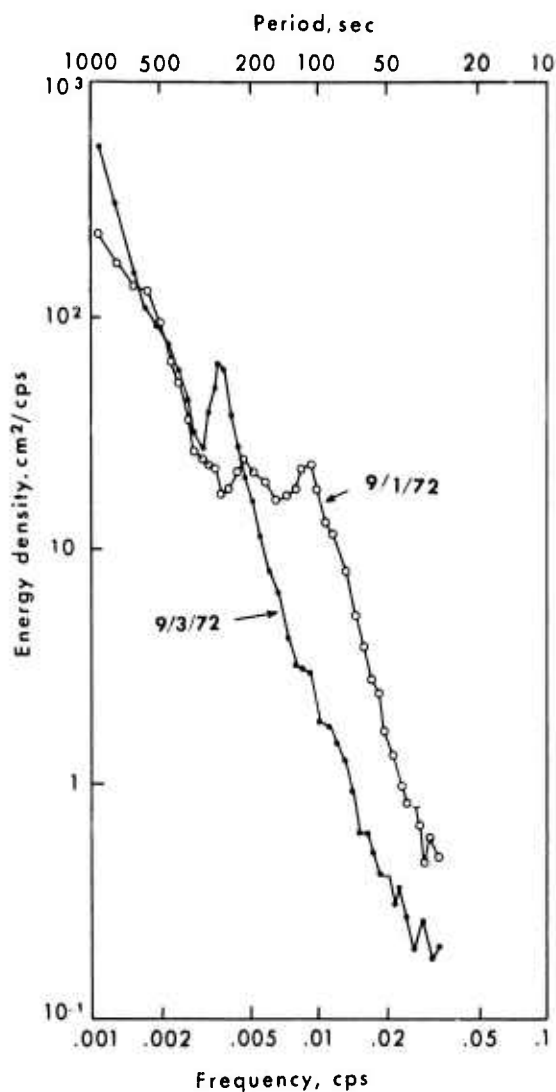


Figure 18. Long-wave spectra of wave records taken at Pingok Island on September 1 and 3, 1972. Both spectra show similar general features of a decrease in energy with increasing frequency.

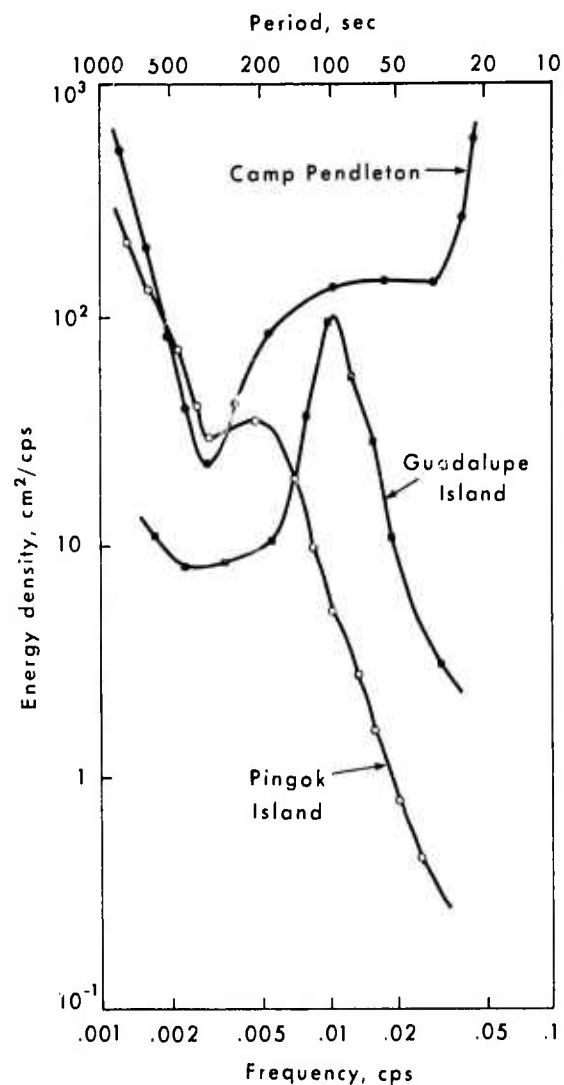


Figure 19. Long-wave spectra of records taken at Pingok Island compared to observations reported by Munk (1963). The Pingok Island spectrum shows much lower energy at high frequencies.

A period of strong orshore winds and large waves occurred between August 5 and 11. Visual wave observations recorded the waves as arriving from the southwest and to be about 2 meters in height and about 5 seconds in period. During a 36-hour period of time, beach sediment was moved alongshore to the north and closed the inlet (see Chapter V). To fill the inlet required a minimum of 10,000 m<sup>3</sup> of sediment. This storm occurred before the wave sensors were deployed.

Komar and Inman (1970) have determined that the immersed-weight longshore transport rate of sand,  $I_1$ , and the longshore component of wave energy flux,  $P_1$ , are

$$I_1 = 0.77 P_1 \quad (6)$$

The data from Point Lay can be compared to this relation. The immersed-weight longshore transport rate is given by

$$I_1 = (\rho_s - \rho) g a' S_\ell \quad (7)$$

where  $\rho_s$  and  $\rho$  are the density of the sediment and water, respectively,  $g$  is gravity,  $a'$  is a pore factor taken as 0.6, and  $S_\ell$  is the alongshore volume transport rate. The alongshore power is given by

$$P_1 = (E C_n)_b \sin \alpha_b \cos \alpha_b \quad (8)$$

where  $E$  is the energy density of the waves,  $C_n$  is the group velocity, and  $\alpha$  is angle of the wave approach relative to normal to the shoreline. The alongshore wave power is evaluated at the break point.

The storm waves at Point Lay, assuming a wave 2 meters in height approaching the shoreline at  $10^\circ$  at the break point, produced an alongshore wave power of  $2.0 \times 10^8$  ergs/sec/cm. The immersed-weight transport rate, according to equation 6, would be  $1.5 \times 10^8$  dynes/sec. The average transport rate needed to supply the  $10,000 \text{ m}^3$  in 36 hours that closed the inlet is  $0.8 \times 10^8$  dynes/sec, or about one-half that predicted by equation 6.

The sediment transported alongshore to the south by the average wave conditions observed during the week of wave measurements can be contrasted with the storm rate. Taking the average height of the waves as 20 cm and assuming that they arrived at  $20^\circ$ , the alongshore power is  $1.0 \times 10^6$  ergs/sec/cm, or about 0.7 percent of the storm rate. Put another way, the storm transported the same amount of sediment in one day as average waves would transport in 142 days.

The storm waves observed and the known wind allow for some understanding of the importance of fetch versus duration as the determining factor on the wave field. The wind speed at the Point Lay site was 9-13.5 m/sec, thus corresponding to an 11-16 m/sec wind at sea. Taking the waves at 2 meters and 5 seconds, and using wave forecast graphs, the required fetch is a minimum of 32-48 km and the duration is 3-4 hours. Because the wind speed was above 9 m/sec for much longer than this, the wave must have been fetch limited at about 32-48 km. The pack ice was clearly much farther offshore than this at Point Lay, and thus does not appear to have limited the fetch. Although this cannot be known for sure, evidently the wind field itself had a limited length scale for winds directed toward Point Lay.

The wave measurements at Pingok Island provided a good set of data for waves between 15 and 30 seconds in period. A variety of onshore wind conditions occurred, and during the last period of measurement swell was observed. Consideration of one period of wind-wave generation and the swell will be given below.

Wave spectra for two different times on September 2 are shown in Figure 20; the first spectrum was taken at 0925 ADT, the other at 1415 ADT. The wind field had started at 1.3 m/sec on September 1 at 1830 ADT and slowly increased until, at

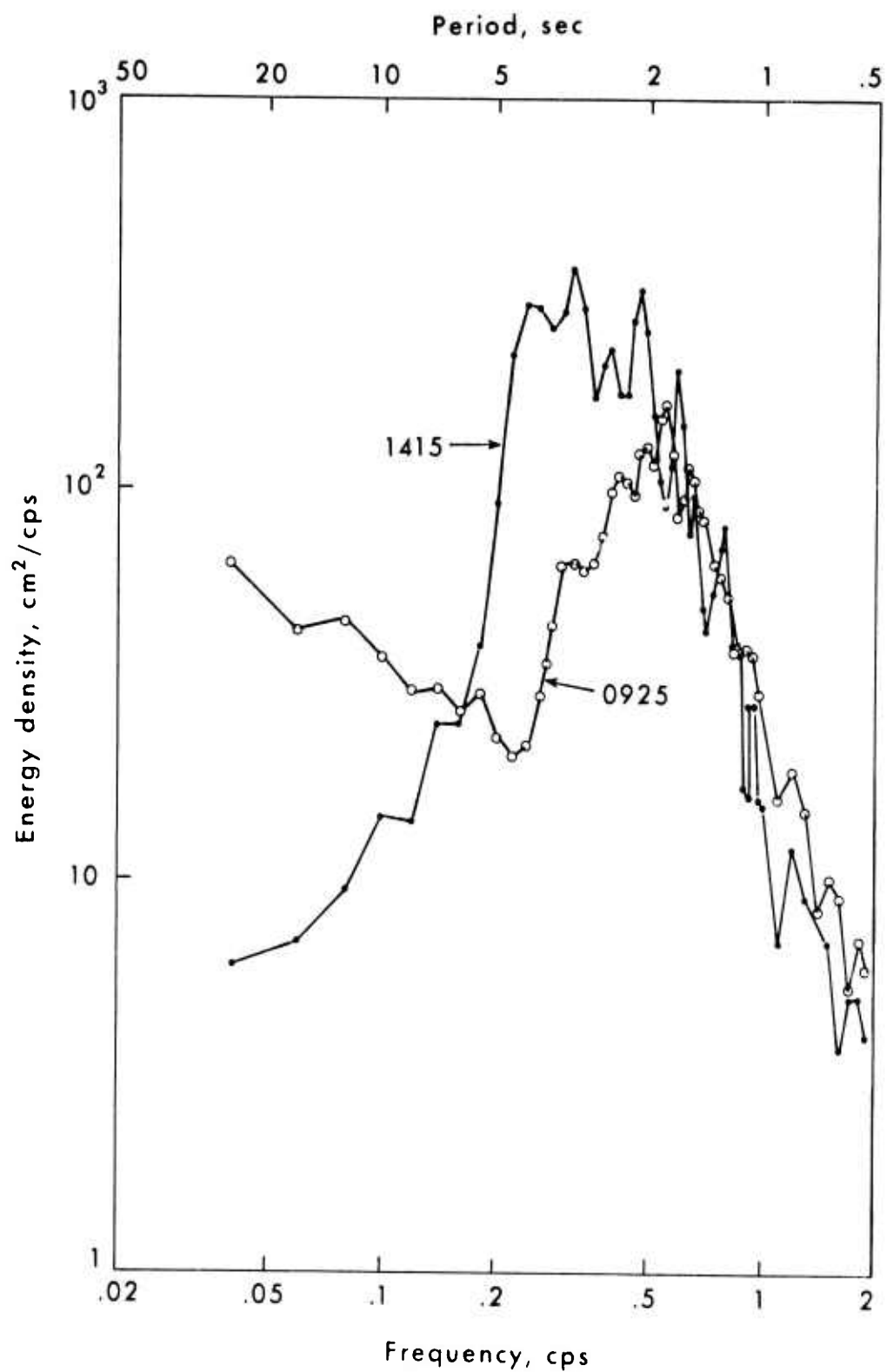


Figure 20. Wind wave spectra at 0925 and 1415 on 9/2/72. Spectra show the equilibrium range at frequencies above 0.5 cps and the change of peak energy and frequency resulting from a steady 11 m/sec wind.

0925 ADT on September 2, it had reached 11 m/sec. For the next 5 hours it blew at a nearly constant rate of 11 m/sec. The second spectrum was taken as the wind started to slacken. The wind direction changed from 60° to about 75° during this time. Thus, between the two spectra, the wind was constant at 11 m/sec and at about 70° heading.

Both wave spectra show an equilibrium range at high frequency. The slopes of the spectra are -3.3 on log-log plots, indicating an  $f^{-3.3}$  dependence on frequency. When corrected for aliasing, or foldback of energy, about 2.0 cps, the dependence is steepened to  $f^{-4}$ . The energy spectrum in this equilibrium range generally has an  $f^{-5}$  dependence on frequency, although Garrett (1969) has shown this to be only generally valid.

The peak of the spectrum at 0925 ADT is at 0.45 cps, whereas at 1415 ADT the peak is at 0.30 cps. The change in peak frequency reflects the growth of the wave field under wind. For a duration, D, the equivalent fetch, F, is given by

$$F = \frac{DC}{2} \quad (9)$$

where C is the phase velocity of the waves. For the waves under consideration  $C \approx 4.8$  m/sec, and so the fetch equivalent to a 5-hour duration is 43 km, from equation 9. This is of the same magnitude as the distance to the pack ice.

During the period September 4-6 large-amplitude swell was observed at Pingok Island. Strong alongshore currents and ice cakes eventually toppled the wave towers and ended data acquisition at Pingok Island, but prior measurements revealed that the swell had a period of 9-10 seconds and an average height of 1-1.5 meters. The direction of approach was from the east, and the wave angle of incidence at the array was about 10°. The swell increased in height to about 2 meters. This brought the wave sensors into the surf zone and resulted in their destruction.

The observed swell would have had a deepwater height about twice that at the shoreline, owing to refraction. The deepwater swell characteristics can give some general clues as to the wind wave generation conditions at the source. The wind speed in the area of wave generation was about 9 m/sec (determined from radio communication with Barter Island). A minimum fetch of about 300 km and minimum duration of 16 hours would generate 2- to 3-meter, 8- to 9-second waves. This fetch is consistent with the open water to the east, where the maximum possible was 1,000 km, to Banks Island. The high-pressure system which generated the swell was formed over Victoria Island at 0600 GMT on September 3, and by September 5 at 0600 GMT the wind field had a possible maximum duration of 48 hours. Thus the waves would have certainly been fetch limited by the pack ice had the wind blown onshore, but were probably fetch limited by the wind system in this case.

Continuous visual observations of wave height and wave period at Pingok Island, reported in Chapter V, permit the relative roles of these swells for the whole open-water period to be assessed. As at Point Lay, swell contributed the predominant amount of wave energy to the nearshore zone, or approximately 90 percent. Thus the really important wave conditions are those associated with infrequent moderate wave heights. At Pingok these waves would appear to be limited by the open-water fetch and the angle of the wind relative to the open water.

## SUMMARY

The limitations of this single set of wave data in interpreting wave properties in a relatively unknown area cannot be overstressed. It is possible that the summer measurement period was atypical and therefore unrepresentative. However, the findings of this study indicate the following:

- (1) The average nearshore wind-wave field is primarily determined at both locations by local winds and has energy peaks at periods in the 2- to 3-second range and heights of 10-30 cm. The pack ice on both coastlines was generally too far away to act as a fetch limit for these waves.
- (2) The extreme wave conditions and principal form of nearshore wave action are determined by infrequent storms whose wind speed, fetch, and duration determine the wave field. The ice pack does not seem to play a role in limiting the fetch at Point Lay, although at Pingok the ice pack may limit the wave field.
- (3) Wave action at very low frequencies, periods of 1,000 seconds to 30 seconds, decreases with wave periods from 2 to 3 cm at 1,000 seconds to 0.5 cm at 30 seconds. This behavior is nearly identical to observations made during winter on the ice and supports the conclusion that wind blowing over the pack ice is the process responsible for the source of these waves. Nearshore bathymetry may determine the fine structure of the wave spectrum in this frequency range.

A general schematic representation of the Pingok data is given in Figure 21. In the figure the generalized spectrum has a peak at 3-second period representing wind waves, a peak at 9-second period representing the swell, and the long-wave spectrum at lower frequencies. The winter data reported by Hunkins (1962) is also shown. It can be seen that the variability of wave action between winter and summer conditions above 10 cps is extremely great, and below 10 cps it is very small.

## Currents

Few measurements of coastal water velocities have been made in the Alaskan Arctic north of Cape Lisburne. Spot measurements from icebreakers (e.g., Ingham and Rutland, 1973) and university research vessels (e.g., Fleming and Heggarty, 1966), have been reported from the shelf waters of the Chukchi and Beaufort seas. The University of Washington recently attempted to place a current meter mooring in Barrow Canyon off Point Franklin but was unable to retrieve it (K. Aagaard, personal communication). Other moorings by the University of Washington and the U.S. Coast Guard in the Beaufort Sea will be recovered in 1973 (G. Hufford, personal communication). However, these are outside the nearshore region. Closer to shore, even less current data are available. The U.S. Geological Survey (E. Reimnitz, personal communication) is continuing a program of short-term moorings near the Kuparuk River and the Jones Islands. Kinney et al. (1972) report on surface drifter and drogoue data collected in the region near Oliktok Point and a current meter record from Simpson Lagoon. Hume and Schalk (1964b) show data collected near Barrow using ice cakes as drogues. Similar data are described in Chapter V. All these studies were performed during the open-water season. No successful studies of nearshore currents under the ice were found in the literature.

There is, as yet, no useful theory for predicting nearshore currents in the Arctic. In fact, there does not even exist a reasonable body of literature

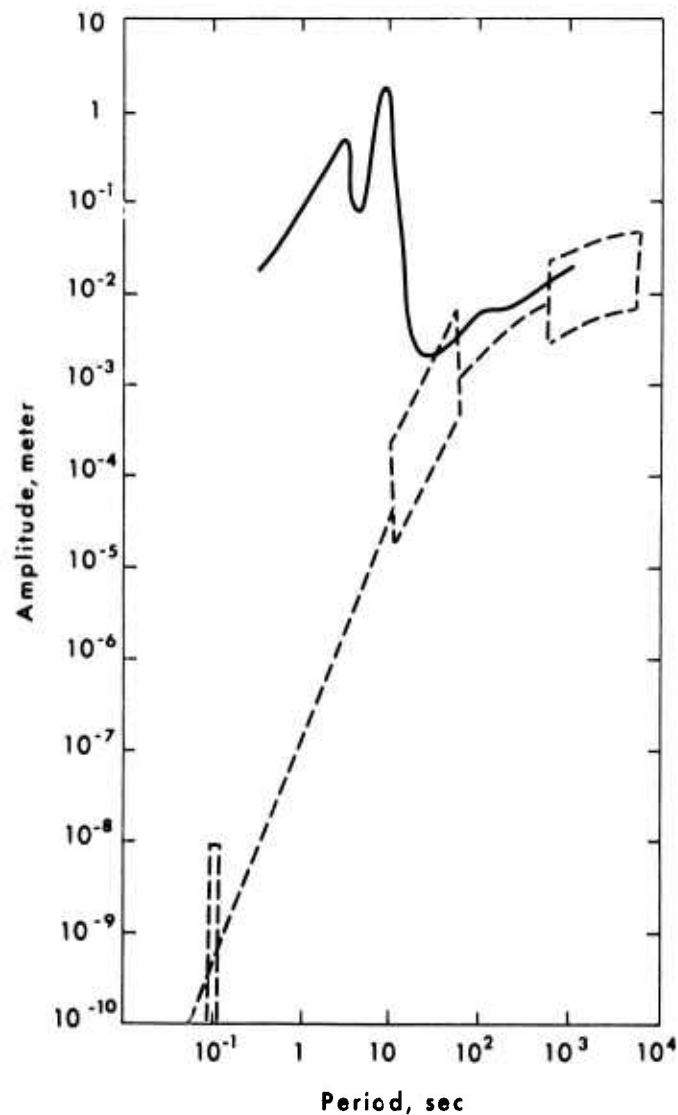


Figure 21. Generalized spectrum of wave amplitude in the Arctic Ocean. Solid line indicates observed summer data. Dashed lines indicate winter data and interpolation of winter data (after Hunkins, 1962).

describing these currents. Our study is an attempt to fill some of this void.

#### DROGUES

The drogues described in Chapter I were tracked at both the Point Lay and the Pingok Island sites using the Raytheon radar mounted atop a wanigan on the foredune crest of each island. Seven acceptable runs were obtained at each site. During all runs, the drogues were at 2-meter depth, i.e., within the surface mixed layer. Numerous restrictions were imposed on the drogue tracking, primarily radar equipment

failure and rough offshore seas. Ice cakes gave spurious returns on the radar and were difficult to separate from the drogue returns, and most runs were confined to nearly ice-free days. We attempted to use the ice cakes themselves as drogues, but the deep draft of the larger cakes, which gave the best returns, and the rough nearshore topography caused by the offshore bars resulted in grounding of these cakes. Thus, they were not good indicators of the mean velocity of the water. A further difficulty lay in the fact that, because of the low level at which the radar had to be mounted, it was possible to track the drogues to a maximum distance of approximately 3.2 km from the radar. This precluded the possibility of obtaining any extremely long records of drogue motion.

It was initially hoped that the drogue records could be used to determine certain characteristics of the turbulent velocities in the areas studied. This was not possible. The three probable sources of difficulty are as follows: (1) the records are not long enough to permit a sufficient number of samplings for statistical reliability, (2) the local topography is sufficiently rough to preclude an assumption of homogeneity, and (3) the response time of the water to atmospheric changes is sufficiently short and the wind sufficiently variable to preclude an assumption of stationarity. Therefore, only the mean motion of the drogues will be discussed in the following sections.

#### Point Lay

Scatter diagrams for wind speed versus current speed and wind direction versus current direction at Point Lay are shown in Figure 22. The data plotted are the means of three drogues at each sampling interval. Although there is an obvious qualitative correlation between high wind speed and high current speed, the data do not justify any attempt to fit a curve through the sample points. The direction diagram is somewhat more informative. Current direction was primarily north-south. Those samples which do not follow this pattern were taken during weak or variable wind conditions. Figure 23 shows the mean velocity of each drogue for each run and the mean wind during that run. These two figures indicate that the surface currents generally followed the coastline, as one would expect from Ekman dynamics (Ekman, 1905; Murray, in preparation).

The runs made on August 18 under varying wind conditions present an interesting sequence (Fig. 24). Early in the afternoon, under a strong easterly wind the drogues were moving offshore. The offshore transport of water would probably set up a water level gradient tilting up in an offshore direction. The wind then swung around to a southeasterly origin and dropped in speed continuously for 4 hours. Initially, the drogues continued to move offshore, but under the reduced wind stress the offshore waters began to flow back onshore to compensate for the reduction in stress. The small southerly wind component was sufficient to direct the waters in a northerly direction after they began to feel the influence of the coast. Later in the evening, the winds began to pick up from a slightly more southerly direction to almost their initial speed. The drogues responded by moving off rapidly to the north along the coast. The other interesting run was on August 14, when, under a moderate northwesterly wind, the drogues initially moved onshore and, as they began to feel the influence of the coast, veered to the south. These measurements agree well with Murray's (in preparation) modifications of Ekman's theory in the presence of a coast.

#### Pingok Island

The Pingok Island data were taken over a longer period of time than the Point Lay data. The scatter diagrams for wind versus current speed and direction are

### Point Lay

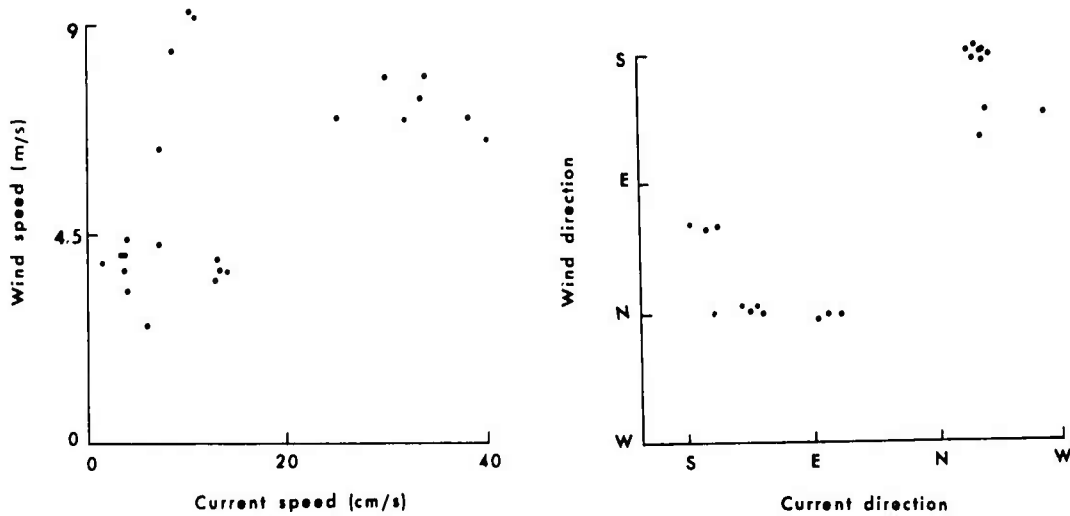


Figure 22. Scatter diagrams of wind speed versus current speed (left) and wind direction versus current direction (right) relative to true north at Point Lay. Current parameters were estimated from drogue trajectories at 2-meter depth. Each data point is an average derived from three drogue trajectories.

shown in Figure 25. Again, for the speed diagram there is a qualitative relation between wind speed and current speed, with both increasing together. However, the data do not warrant curve fitting. Kinney et al. (1972) found similar results for their measurements in Simpson Lagoon and a few data they took off the Jones Islands. The direction data are confined to two small regions of the scatter diagram. Easterly winds are associated with westerly currents and westerly winds with easterly currents. The pattern is much tighter than in the Point Lay data, but this may be due simply to fortuitous sampling. In general, the easterly currents have a slight onshore component and the westerly currents a slight offshore component (Fig. 26) (Murray, in preparation), but the observations from September 10, a rather short run, belie this.

#### CURRENTS UNDER THE ICE

In April 1972 we moored a Braincon 1381 histogram current meter under the ice off Point Lay. The meter uses a Savonius rotor (full size) to sense speed and a  $0.37 \text{ m}^2$  vane to measure direction. The instrument records 15-minute averages of speed and direction on photographic film. We installed the meter under the ice in 7.6 meters of water at mid-depth. The instrument was left in place from 1742 AST on April 22, 1972, until 1110 AST on April 30, 1972. The data were reduced manually at CSI. Figure 27 is a plot of the northward and eastward components of the hourly butt-averaged record. The data were converted from rotor revolutions to speed using a linear fit of  $v = 37.5 w$ , where  $v$  is current speed in centimeters per second and  $w$  is the rotation rate of the rotor in revolutions per second. This conversion is conservative at low speeds inasmuch as the instrument has a threshold of approximately 2 cm/sec. At higher rotation rates, the fit is a reasonably good approximation to the response of the Savonius rotor, barring an independent calibration.

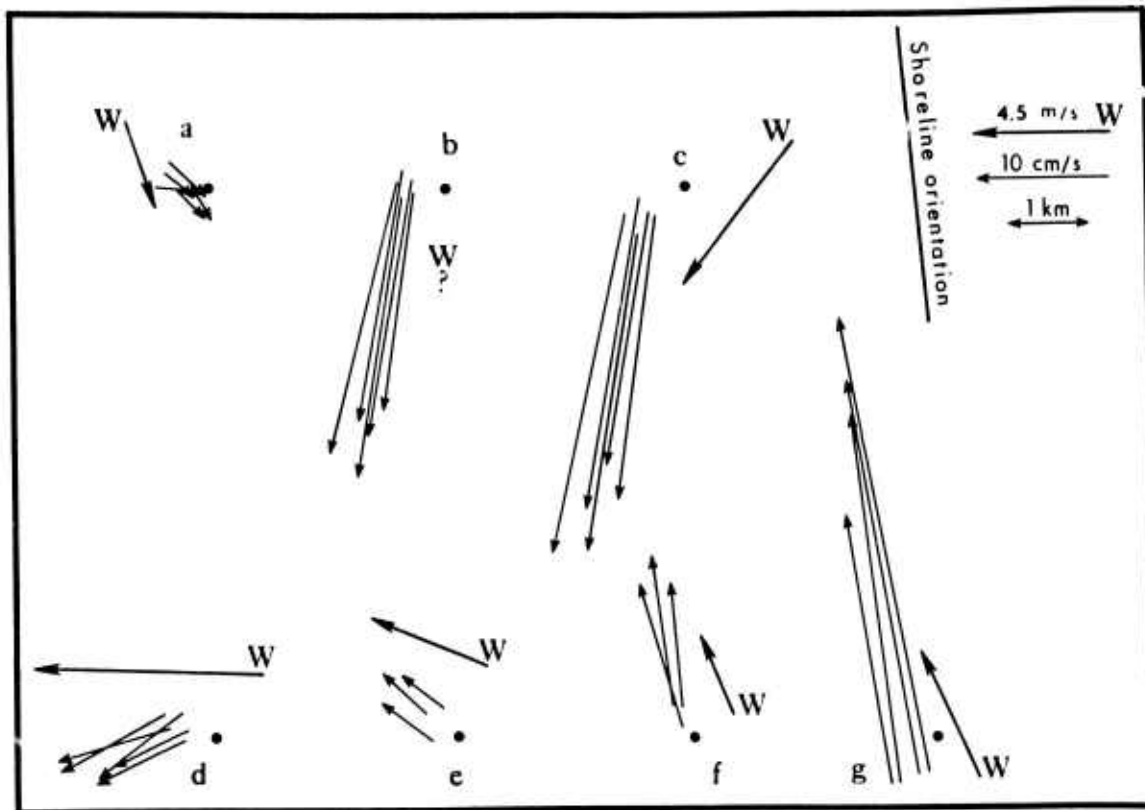


Figure 23. Mean drogue velocities for seven experiments in which drogues were released at 2-meter depth: (a) 8/14/72, 1522-1637 ADT; (b) 8/15/72, 1416-1446 ADT; (c) 8/15/72, 1450-1550 ADT; (d) 8/18/72, 1348-1422 ADT; (e) 8/18/72, 1450-1850 ADT; (f) 8/18/72, 2113-2143 ADT; (g) 8/18/72, 2227-2307 ADT. The round dot in each figure represents the location of the tracking radar atop the foredune crest. Drogue velocity vectors originate at the release points of the drogues. When available, local wind velocity is indicated. Shoreline orientation and scales for wind velocity, drogue velocity, and initial distance to the radar are shown in the upper right of the diagram.

The current was predominantly northerly except for a 2-day period from April 26 to 27, but during this time the current speed was so low that we were experiencing conditions near or below the meter threshold and the data are suspect. A slight westerly component is apparent throughout the major portion of the record. Two things stand out in the north-south component time series. There is a definite semidiurnal oscillation present toward the end of the record and an indication of one in the first third of the record. The other major feature of the record is the drop in speed on April 26-27. The explanation for this is not readily apparent, but these were days when the winds were southwesterly rather than northeasterly, the more common case. This was also a time of rising atmospheric pressure. A periodogram of the northerly component of flow was computed. The semidiurnal oscillation stands out well, as would be expected at this latitude, where the inertial response is resonant with the semidiurnal period. The diurnal tidal periods do not correspond with strong periodogram peaks. A strong unexplained peak in the periodogram appears at a period of about 8 hours. It is not known

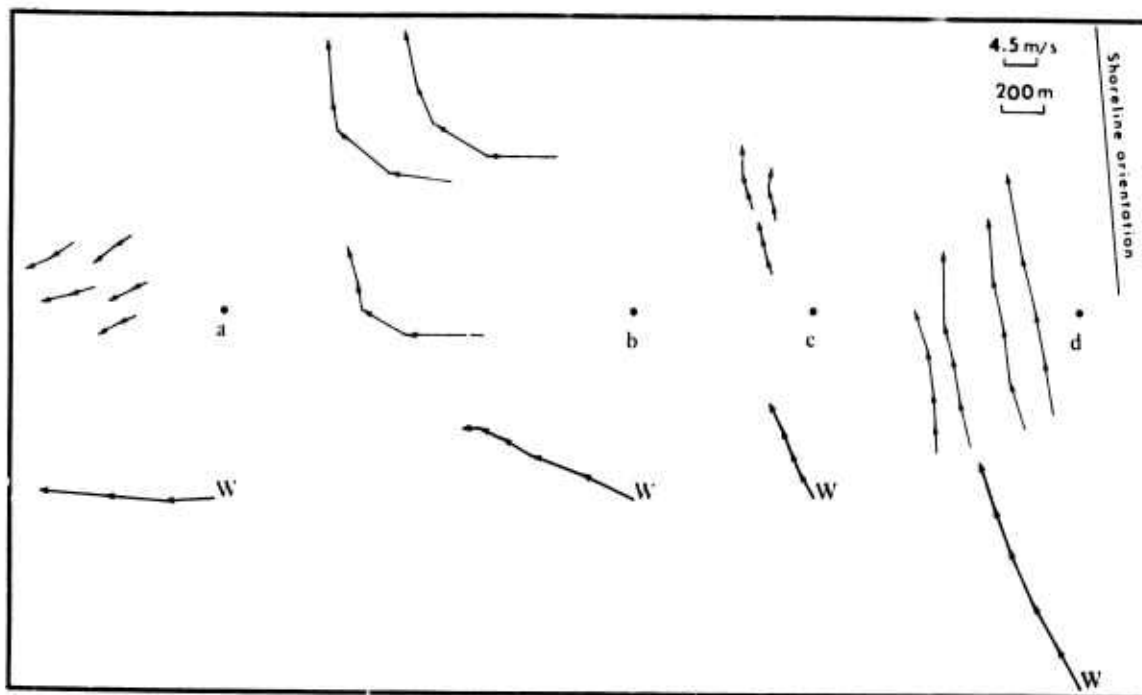


Figure 24. Drogue trajectories for August 18, 1972. Successive sightings of the drogues are connected by arrows indicating direction of movement. Sightings were at (a) 1348, 1403, 1422 ADT; (b) 1450, 1550, 1650, 1750, 1850 ADT; (c) 2113, 2123, 2133, 2143 ADT; and (d) 2227, 2237, 2247, 2257, 2307 ADT. Wind velocities at the time of each sighting are indicated in the lower part of each diagram. Black dots represent the location of the tracking radar atop the foredune crest. Shoreline orientation and scales for wind speed and distance are shown in the upper right of the diagram.

### Pingok Island

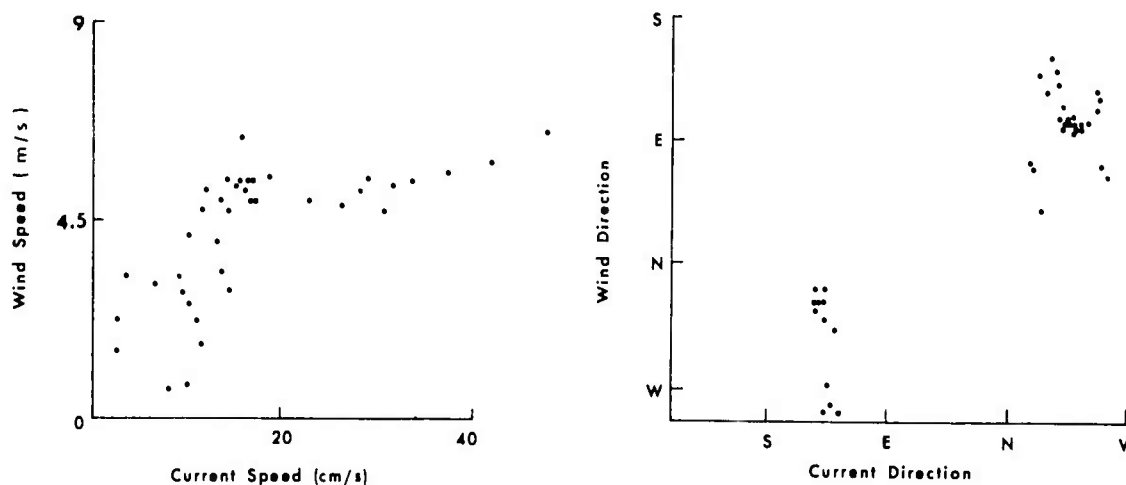


Figure 25. Scatter diagrams of wind speed versus current speed (left) and wind direction versus current direction (right) relative to true north at Pingok Island. Current parameters were estimated from drogue trajectories at 2-meter depth. Each data point is an average derived from three drogue trajectories.

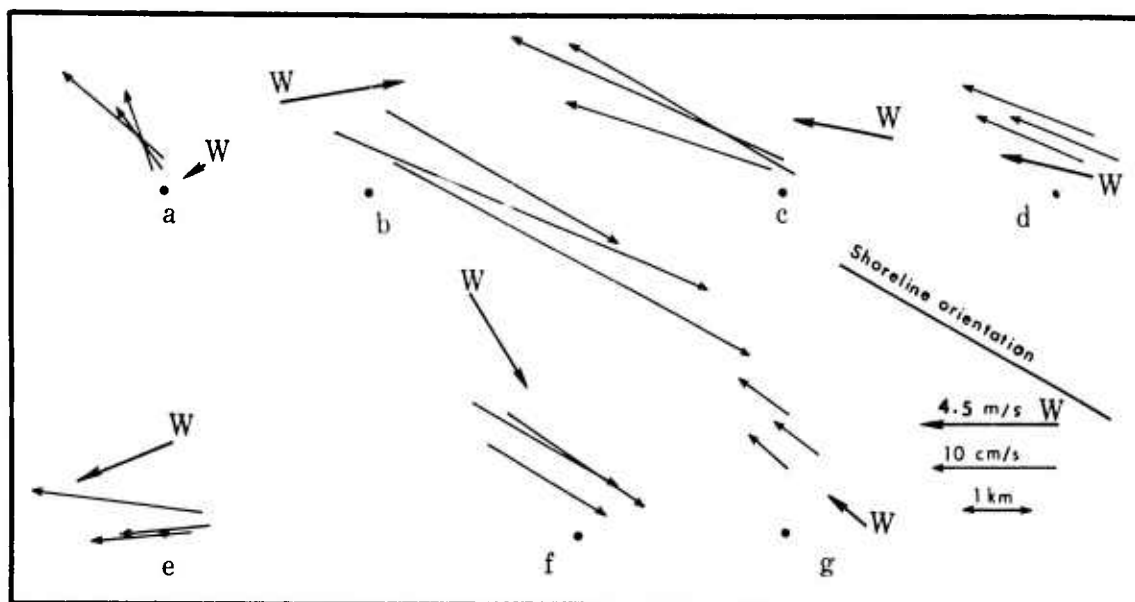


Figure 26. Mean drogue velocities for seven experiments with drogues released at 2-meter depth: (a) 8/30/72, 1536-1421 ADT; (b) 8/31/72, 1610-1732 ADT; (c) 9/3/72, 1627-1657 ADT; (d) 9/4/72, 1631-2128 ADT; (e) 9/10/72, 1330-1350 ADT; (f) 9/11/72, 1305-1833 ADT; (g) 9/14/72, 1429-2256 ADT. The round dot in each figure represents the location of the tracking radar atop the foredune crest. Drogue velocity vectors originate at the release points of the drogues. Local wind velocities are indicated. Shoreline orientation and scales for wind velocity, drogue velocity, and initial distance to the radar are shown in the lower right of the diagram.

whether or not this is real. It should be mentioned that the amplitude of the semidiurnal oscillation is very small. It appears to be only of the order of 1 cm/sec. It is possible that this low value is due to intense dampening of the tidal current by the ice cover. It should be noted that the winter mooring was such as to place the meter at about the 4.3-meter depth, but there was 1.6 meters of ice present and thus the meter was only 2.7 meters under the ice. Frictional drag on the ice may have significantly reduced the currents measured.

Over the record length, the mean speed and direction of the current velocity are 2.1 cm/sec and  $-6.7^\circ$  magnetic. This is a very slow drift which follows the coastline orientation almost exactly. But again it should be stressed that because of the low speeds, particularly those on April 26-27, these estimates are conservative.

#### SUMMER CURRENT METER MEASUREMENTS

During the summer operation the meter was moored at mid-depth in 9.8 meters of water. Thus it was at approximately the same depth and distance offshore as during the winter operation. As was mentioned in Chapter I, the film advance in the meter had a tendency to stick. Thus, instead of a single long record, a series of shorter records was obtained. Also, after the first occasion when the advance mechanism stuck, an absolute time base for the record was lost and information from

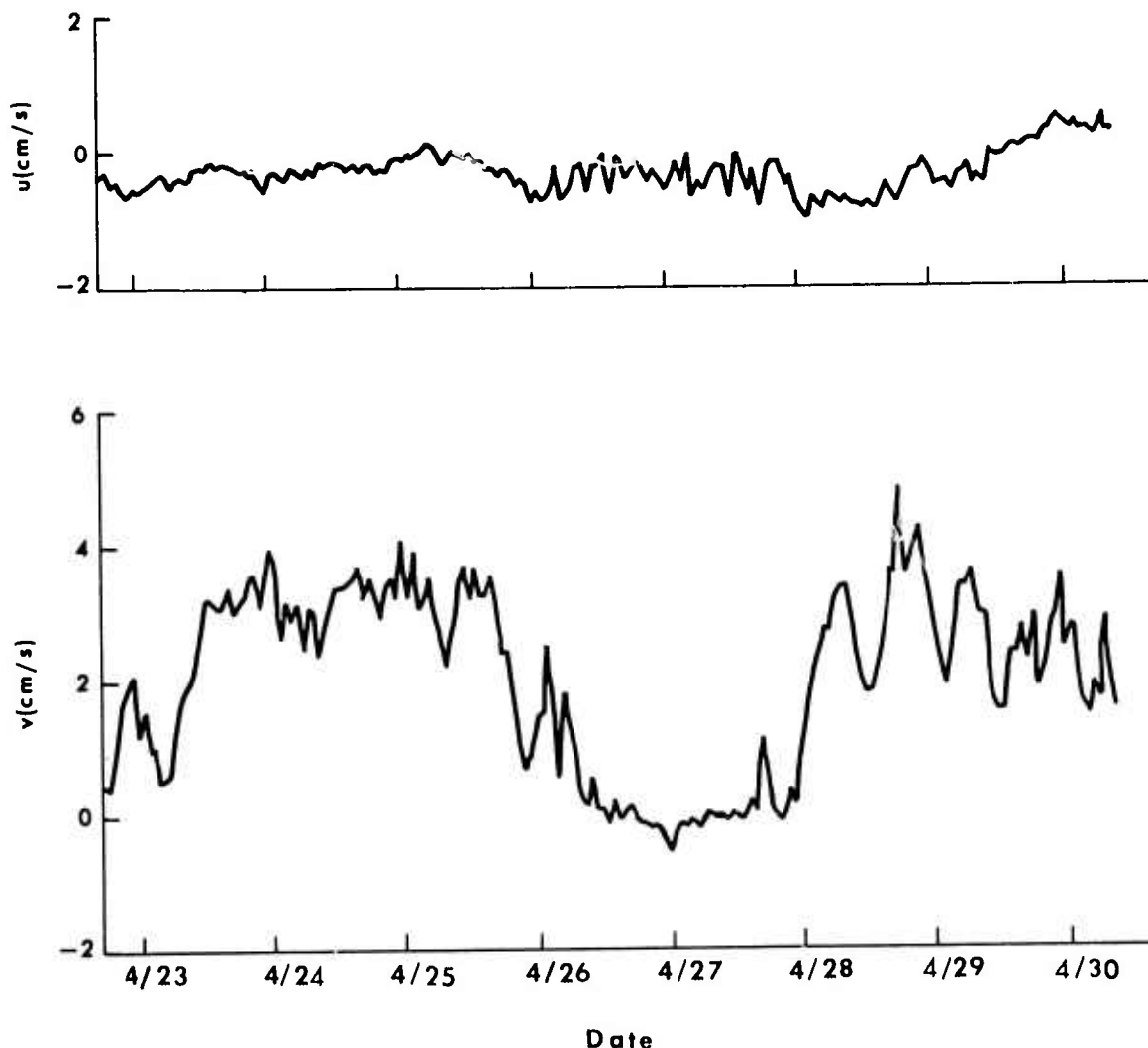


Figure 27. Records of the easterly (upper) and northerly (lower) components of current at mid-depth in 7.6 meters of water in April 1972 at Point Lay. The meter was moored under 1.6 meters of ice. Time marks refer to 0000 AST on the indicated day. All directions refer to magnetic north.

the meter could not be correlated with weather patterns. Three of the longest continuous records are shown in Figure 28. The values plotted are hourly butt-averages of the 15-minute averages actually sampled. Before discussing these records, particularly the u-components, it should be mentioned that the film on which the data were recorded showed significantly more turbulence during the summer than during the winter. On the winter film the direction trace was contained within very narrow bounds. On the summer film the direction trace during any one 15-minute sampling period indicated a large variation (at times as much as  $150^\circ$ , although more often much less). Because of the recording technique used, the film exposure tends to give a frequency distribution of current directions during a sampling interval. We estimate that we were able to read the modal direction to within  $\pm 15^\circ$  in the worst cases and much better when the directional variability was less. Much of the induced variability is undoubtedly due to waves.

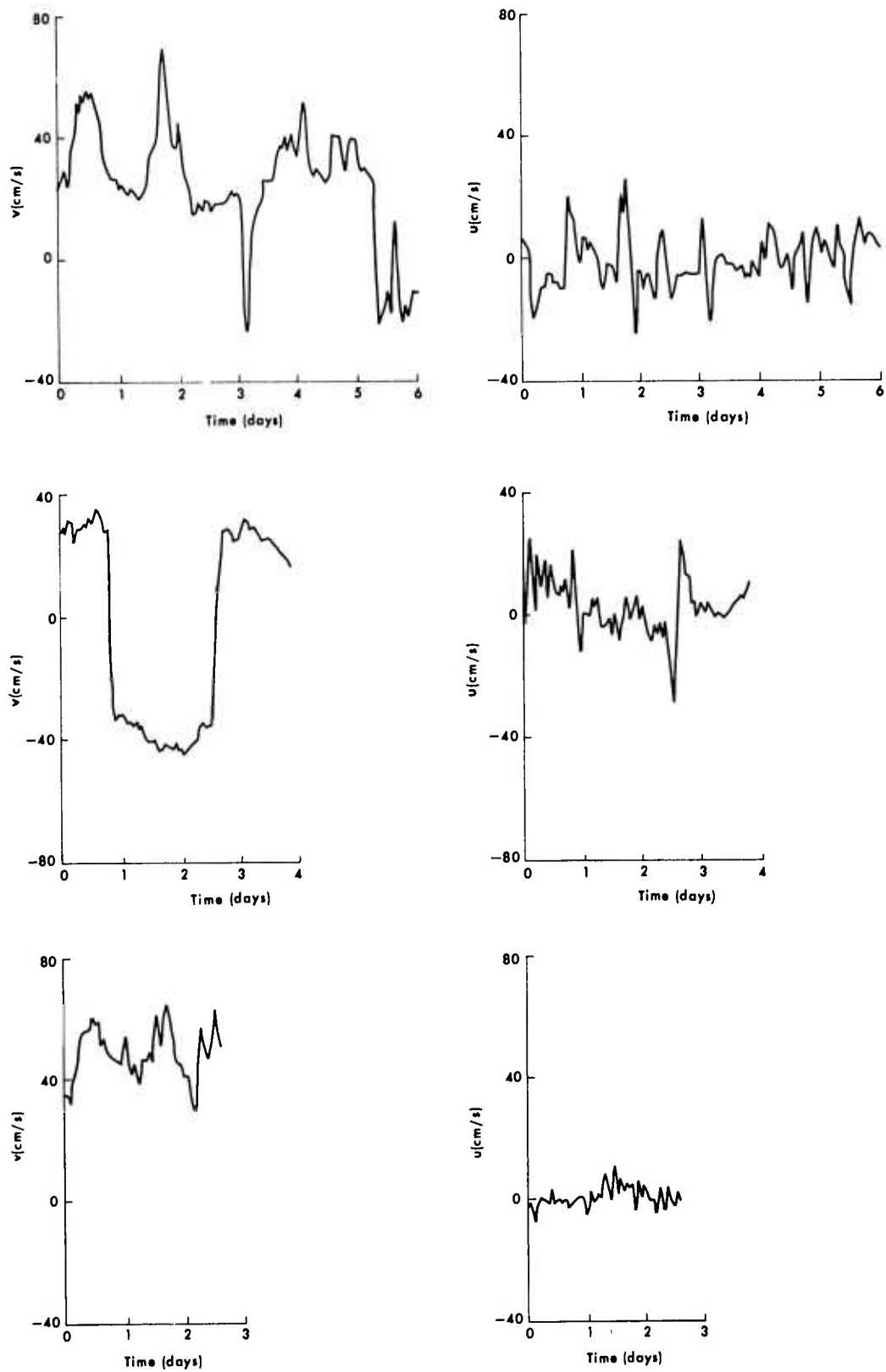


Figure 28. Three records (upper, middle, and lower) of current velocity at mid-depth in 9.3 meters of water during open-water season in 1972 at Point Lay. The northerly components are shown on the left and the easterly components on the right. All directions refer to magnetic north.

The first thing to notice on the records in Figure 28 is that the mean speeds are much greater during the summer open-water season than during the frozen winter season. Also, the day-to-day variability is far greater. Strong reversals of the current are present in two of the three records presented. The weighted mean current for the three records shown sets at  $2^\circ$  magnetic at a speed of 21.8 cm/sec. The direction is approximately the same as that of the winter currents, but the speed is 10 times as great. The speeds recorded by the meter were also far larger than those measured with the current drogues, sometimes reaching 60 or 70 cm/sec. This, though, is not unreasonable inasmuch as the drogues were used only on calm days, when the currents, assuming they were primarily wind driven, would probably have been significantly reduced. In fact, the last few days of record indicate speeds of 20-30 cm/sec. This section of film probably corresponds to the period when the drogue runs were made, and the speeds are much more compatible. A periodogram of the north-south component of the first record in Figure 28 shows a peak at the semi-diurnal frequency. Another peak is present near a period of 7 hours. A similar peak was seen in the winter record. These may be indications of a shelf wave, but the data are not of sufficient quality to warrant further investigation of the possibility at this time.

Pollard (1973) has suggested the possibility of strong contamination of current meter records as a result of mooring motion. Our strongest observed winds occurred for only a few hours during an intense storm. These never exceeded 16 m/sec, and winds were generally less than 8 m/sec. According to Pollard's Figure 1, the contamination resulting from vertical motion of a surface-following buoy under these wind conditions would be less than 10 cm/sec and generally less than 2 cm/sec if the sea were fully developed.

Let us assume a buoy motion which tracks horizontal rather than vertical particle motion. This is probably more representative of a subsurface float. For deep water, vertical and horizontal particle displacements have the same amplitude, and we can still use Pollard's Figure 1.

To estimate the change resulting from the fact that the mooring was in shallow water, note that the ratio of shallow-water to deepwater horizontal particle speed is  $[kh \exp(kz)]^{-1}$ , where  $h$  is the water depth, 10 meters,  $k$  is the wave number, and  $z$  is the meter depth, -5 meters. For a Pierson spectrum, the frequency,  $\sigma$ , of maximum energy is given by  $1.23 g/U$ , where  $g$  is the acceleration resulting from gravity and  $U$  is the wind speed in m/sec. A 16-m/sec wind then corresponds to a shallow-water wave length of 80 meters, which implies a horizontal velocity twice that for deep water. An 8-m/sec wind implies a horizontal particle velocity at 5 meters approximately 1.5 times the deepwater value. If, then, we may use the waves of maximum energy in the Pierson spectrum as defining a length scale for the energy-containing portion of the spectrum, we can estimate that, under the worst conditions assumed by Pollard concerning a buoy absolutely tracking the horizontal particle motion, we will have a contamination velocity of 20 cm/sec and generally less than 3 cm/sec. Our mooring probably responded far less than the hypothetical buoy in the preceding analysis. Our record was, therefore, less contaminated. Thus, most of the preceding comparison of winter and summer records holds, although some of the peak summer speeds may be slightly overestimated.

Coachman and Tripp (1970) describe a 4-day current meter record through the ice about 190 km NNE of Bering Strait. Their meter was moored 15 meters below the ice floe in approximately 22 meters of water. The mooring was approximately 97 km from the nearest land. Their conclusion, from comparison with previously obtained data, was that the currents in this area were essentially the same during summer and winter in their mean characteristics. We find, on the contrary, at Point Lay and

much closer to shore, that the mean flow during summer is much stronger and more variable than in winter, although in the same direction. Pressure changes can be transmitted through the ice, but wind stress cannot, if the ice is shorefast. Thus it would appear that the basic feature causing the change in current pattern from summer to winter is the wind stress. This does not, though, rule out the possibility of a wind stress influence on winter currents from a distance where stress may be transmitted to the water through the movement of the pack ice.

#### Water Mass Characteristics

Nearshore temperature and salinity studies in the Alaskan Arctic have been extremely spotty, both in time and space. Most of the data have been collected outside the nearshore region (e.g., Lafond and Pritchard, 1952; Fleming and Heggarty, 1966; Ingham and Rutland, 1972). For instance, the U.S. Coast Guard has had numerous icebreaker cruises to both the Chukchi Sea and the Beaufort Sea, but these ships are restricted to waters deeper than 10 fathoms. The 1960 cruise of the M.V. Brown Bear to the Chukchi Sea (Fleming and Heggarty, 1966) did take one station near shore just north of Point Lay, and on the 1937 and 1938 summer cruises of the U.S.C.G.C. Northland to the Chukchi Sea a number of stations were occupied close to shore between Point Lay and Icy Cape. These few sets of data show modest variability of both the temperature and the salinity characteristics of nearshore waters but give no indication of the time scales of these variations. Farther offshore, great variability is seen in the coastal waters, but it is difficult to distinguish spatial changes from temporal changes owing to nonsynoptic sampling (Ingham and Rutland, 1972). Recently, the U.S.G.S. has been sampling the nearshore waters between Point Barrow and Demarcation Point. These data have not yet been published. The University of Alaska has also been involved in sampling the waters near Oliktok Point, just west of the Colville River delta. The data presented here represent an initial effort to define and describe the time scales and mechanisms of nearshore temperature and salinity variability on the Alaskan Arctic Coast.

The primary temperature and salinity measurements were made in the vicinity of Point Lay. Four sections were run at Pingok Island, but the results are of doubtful use.

Measurements were made in the nearshore waters from a 16-foot Boston Whaler with a Beckman RS5-3 salinometer, described in the introductory section. Measurements were also made in Kasegaluk Lagoon with the same instrument, but from a Cessna 180 floatplane. The Beckman salinometer has a quoted accuracy of  $\pm 0.3$  ‰ in salinity and  $\pm 0.5$  C in temperature. The precision of the instrument is quoted at  $\pm 0.05$  ‰ in salinity and  $\pm 0.05$  C in temperature. The instrument was compared in the field to a laboratory thermometer which could be read to 0.1 C, and the two devices were in agreement to within 0.2 C. Field calibration of the conductivity circuit was maintained with a conductivity loop. Water samples were also taken in the field and titrated for salinity. The titrated values and the values read for salinity from the Beckman instrument were least-squares fitted to give a correction formula for the field data. The standard deviation for the correction curve was 0.42 ‰. The error in the low-precision titration technique used to process the salinity samples was about 0.2 ‰. Thus, the instrument seems to have operated well within the stated specifications.

Data were collected at Point Lay during three different occupations of the camp: in April, during the period when the micrometeorological study was being made over the ice; in June, just after breakup had begun but before the nearshore waters were ice free; and in July and August, during the open-water period. No measurements were made in October, when the site was again occupied for 10 days.

In April, attempts were made to take a few sporadic samples of the salinity of the waters under the ice, both within Kasegaluk Lagoon and outside the lagoon. Only two were actually obtained, one within the lagoon and one offshore. Most of the lagoon was frozen all the way to the bottom, i.e., 1.5-2 meters of ice. One water sample was obtained in the deep channel, near the inlet, under the ice (i.e., just behind the tundra remnant). The salinity of this water was 38.0 ‰. Water sampled offshore of the island but near the inlet had a salinity of 35.7 ‰. The value 38.0 ‰ seems to be relatively low for the lagoonal salinity considering the large volume of ice present within the lagoon. Expulsion of salt molecules from the ice lattice as the seawater freezes should significantly increase the salinity of an isolated water body. In order for the relatively low salinities to be accounted for, one must assume that the waters within the lagoon were in moderately free communication with the nearshore waters for at least most, if not all, of the winter. The salinity value found outside the lagoon seems to be rather higher than might be expected. Two reasonable explanations come to mind. Possibly the sample was taken inside the bar which lay offshore of the tidal inlet and the water sampled had been trapped in a pond behind the bar. The pond lacking free connection with the nearshore waters, its salinity could be enhanced by the same mechanism which one would assume to be active in increasing the salinity of the lagoon. The other possibility is that the sample was taken near one of the channels whereby the lagoon waters connect with the nearshore waters and thus the water sampled was not pure nearshore water but a mixture of nearshore water and the more saline lagoon water.

Breakup began at Point Lay on May 24, 1972. For the next 2 days, river water from the Epizetka or Kukpowruk rivers slowly crept northward, over the lagoon ice, toward Point Lay. On May 27 the lagoon was flooded from the north, probably from the Kokolik or Utukok rivers. It was not until June 13 that water flowed through the inlet into Kasegaluk Lagoon; that is, the freshwater head overpowered any tidal inflow tendencies until this date.

The first temperature and salinity measurements were made in the nearshore waters on June 10 (Fig. 29). There were two basic types of water present: warm, fresh water and cold, salty water. Offshore, the fresh surface layer was about 4 meters thick. This water originates in the river freshets and in the melt of the shorefast ice. Below this layer was the local coastal water. The Beckman salinometer was not calibrated to read below 0 C. We have assumed, however, that, to a good approximation, the calibration can be linearly extrapolated. It is from such an assumption that the cold, saline water characteristics plotted in Figure 29 were obtained. Within the lagoon and the tidal inlet, the pycnocline tended to be less intense than offshore, probably as a result of mixing by bottom-induced turbulence.

On June 19, the waters behind the tundra remnant were saltier than on June 10. The water was also homogeneous. Offshore of the inlet the waters were much saltier and slightly warmer on the surface than they had been 9 days earlier. The pycnocline region extended from about 1.5 to 4 meters depth, i.e., destruction of the pycnocline had begun. The bottom layer maintained the same characteristics as it had had earlier (Fig. 29).

By June 21-22 the shorefast and nearshore ice had broken up sufficiently so that the Boston Whaler could be utilized offshore to the south of Point Lay. The nearshore and lagoon temperature and salinity structure were sampled for a distance of about 18.5 km south of the camp. Again, the deep layer offshore had the same characteristics as on the first day sampled. By this time, though, the influence of the rivers within the lagoon was well localized. Also, the pycnocline offshore was rising toward the surface. Of most interest for what will follow is the fact that there was a definite, noticeable dependence of surface salinity on proximity to an

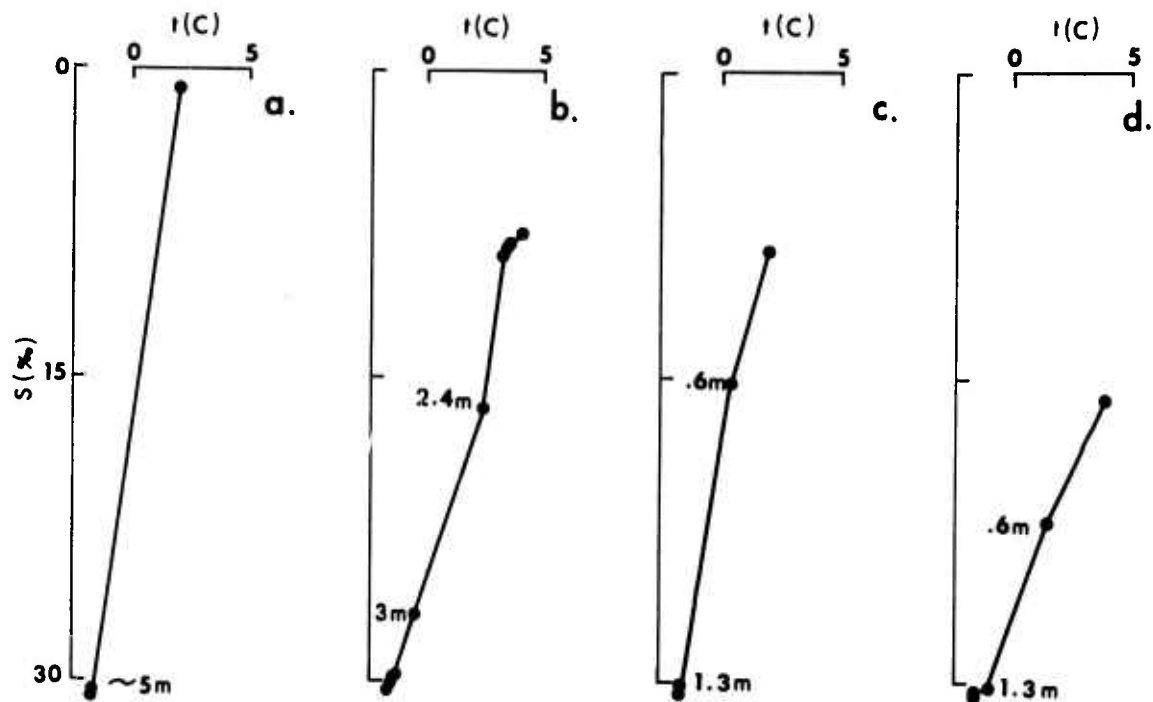


Figure 29. Temperature-salinity diagrams for the nearshore water at Point Lay immediately following breakup: (a) 6/10/72, offshore of Point Lay inlet; (b) 6/19/72, offshore of Point Lay inlet; (c) 6/22/72, offshore of Point Lay inlet; (d) 6/22/72, offshore of barrier island 4 km south of Point Lay inlet.

inlet. Samples taken immediately off an inlet (0.4 km from shore) had surface salinities of 8 or 9 ‰, and those taken midway between inlets (4 km from an inlet) had surface salinities of 15 ‰ (Fig. 29). By 1-2 meter depth, however, the inlet influence was no longer noticeable.

It seems, then, that immediately following breakup the nearshore waters are divided by an intense halocline into a warmer surface layer of low salinity derived from river runoff and ice melt and a deeper, cold, saline layer which is probably the remnant of the water which lay in the nearshore zone under the shorefast ice. As the spring freshet decreases, the pycnocline breaks down through turbulent mixing. The deep pycnocline initially measured was possibly in the center of a strong effluent such as Wright (1970) has measured at South Pass, Mississippi River delta, rather than an indication of conditions all along the coast. As the flow through the inlet drops off, the depth of influence of this flow also becomes less. The influence of the freshet, though, is undoubtedly felt all along the coast.

During the period July 12 - August 3, numerous temperature and salinity sections were run in the nearshore region and two surveys of the temperature and salinity structure in the lagoon behind the barrier island. Five sections were sampled which spanned a distance 2.2 km alongshore, encompassing the tidal inlet. Samples were taken every meter from the surface to the bottom. Sampling locations were determined by the bottom contours, samples being taken at 3.1-, 6.1-, 7.6-, 9.1-, 10.7-, and 12.2-meter depth contours when weather permitted. This took the sections

to a maximum distance of 4 km offshore. Sampling locations were determined from U.S.C.&G.S. Chart 9457. The five sections were sampled together three times, and noticeable differences were seen between sections. It is not known, though, if these differences were due to true spatial variations or to temporal variations which occurred during the time necessary to sample the grid. Undoubtedly some spatial variation did exist. The temporal variation at the same section on different days, though, far exceeded any spatial variation noted between sections on the same day. Therefore, emphasis was placed on sampling a particular section as often as possible. The section chosen ran offshore at a bearing of 260° magnetic from just south of the Point Lay schoolhouse. Most of the discussion to follow deals with this section, although, at times, when data from this section are missing, we have assumed that other sections are representative of the large-scale features of the entire area sampled.

Figures 30-34 are temperature and salinity sections from the nearshore waters at Point Lay. Each diagram pair contains a temperature section (upper diagram) and a salinity section (lower diagram). Figure 33B was drawn from data taken along section I, the southernmost section. All other figures were drawn from data taken at section M, off the Point Lay Village schoolhouse, the northernmost section. Temperature is contoured in degrees Celsius, salinity in parts per thousand. At times, half-degree contours and half-part-per-thousand contours were drawn to aid in visualizing distribution patterns. Locations of data points on the figures have been corrected for changes in sea level.

On July 12 (Fig. 30A) numerous stations were sampled within the nearshore region and the lagoon to obtain an idea of the variations in water structure. Temperatures ranged from 1 C to 9 C and salinities from 28 ‰ to 30.5 ‰. The warm, low-salinity water seemed to be contained within a narrow band close to shore similar to that described by Csanady (1972) as a wedge-shaped pycnocline associated with a coastal jet and winds blowing with the coast to their right. The surface waters of the lagoon at this time were fresh and warm (16.2 C, 18.6 ‰).

On July 17 the waters within the lagoon had temperatures varying between 11 and 15.5 C and salinities ranging from 21 to 23 ‰. When the waters began to flow out of the lagoon on July 18 (Fig. 30B), this warm, low-salinity water formed an intense pycnocline in the nearshore area. Over the next few days, the waters in the nearshore region and those within the lagoon mixed through tidal exchange (both astronomical and meteorological). By July 22 (Fig. 31A) the nearshore waters were fairly homogeneous in temperature, but a strong halocline still existed.

From July 22 to 26 strong northeasterly winds blew along the coast. On July 26 (Fig. 31B) the waters in the nearshore region were totally renewed. The waters were extremely homogeneous in both temperature and salinity. Temperatures ranged from 3 to 5 C and salinities from 31 to 31.5 ‰. It is unfortunate that the spatial coverage of our stations does not permit determination of the source of this water. It can be speculated that its source was offshore, since water of these characteristics was found at lat. 69°48'N, long. 163°34'W (20 km WNW of Point Lay), on July 4 between the surface and the 5-meter depth (G. Hufford, personal communication). The wind stress for the 4 days prior to July 26 was from the correct direction to cause upwelling. On July 24 a temperature and salinity survey of Kasegaluk Lagoon was conducted. With the strong northeasterly winds, water was being flushed out of the lagoon at all the inlets except Icy Cape Inlet, where 5.9-C, 30.5-‰ water was entering the lagoon to satisfy continuity. Thus a source of cold and salty water must have existed close to shore at Icy Cape. This water, which was probably associated with that seen earlier offshore of Point Lay, may have been blown along the coast to replace the nearshore water at the field site.

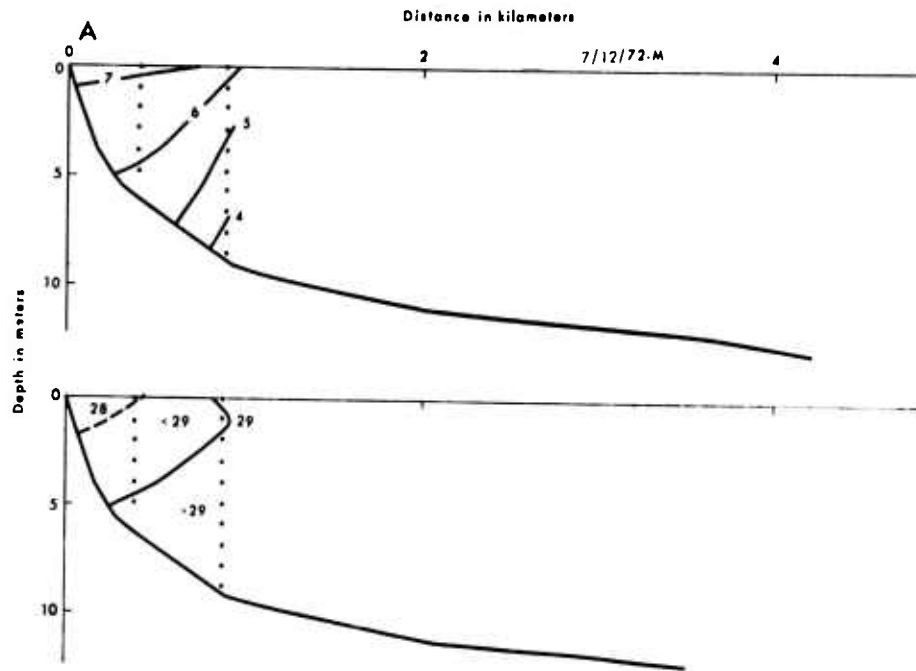


Figure 30A. Temperature section (upper) and salinity section (lower) from the nearshore waters at Point Lay on 7/12/72. Temperature is contoured in degrees Celsius and salinity in parts per thousand. Sample points are indicated by dots.

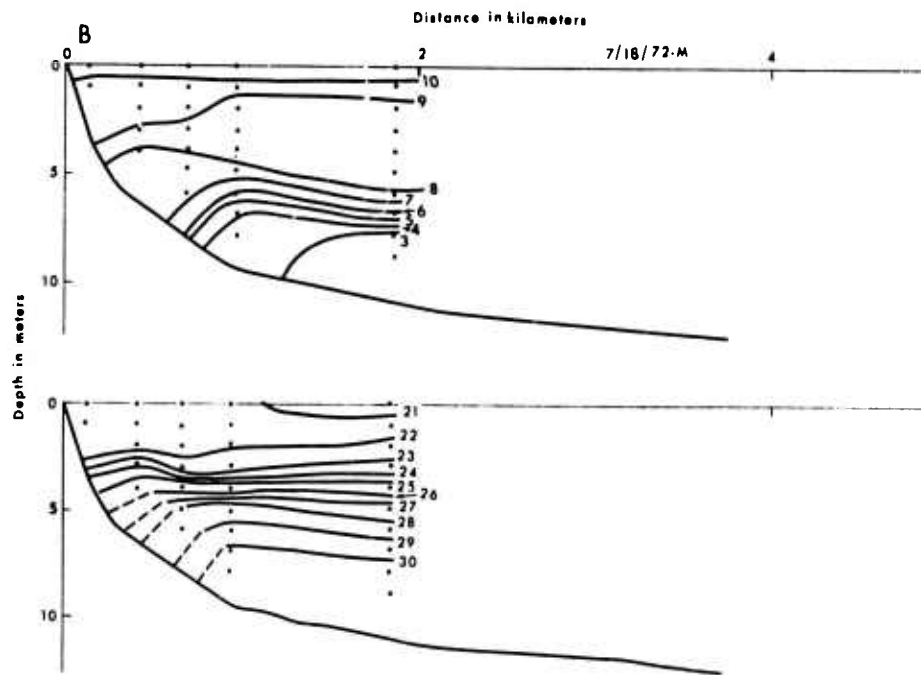


Figure 30B. Temperature section (upper) and salinity section (lower) from the nearshore waters at Point Lay on 7/18/72. Temperature is contoured in degrees Celsius and salinity in parts per thousand. Sample points are indicated by dots.

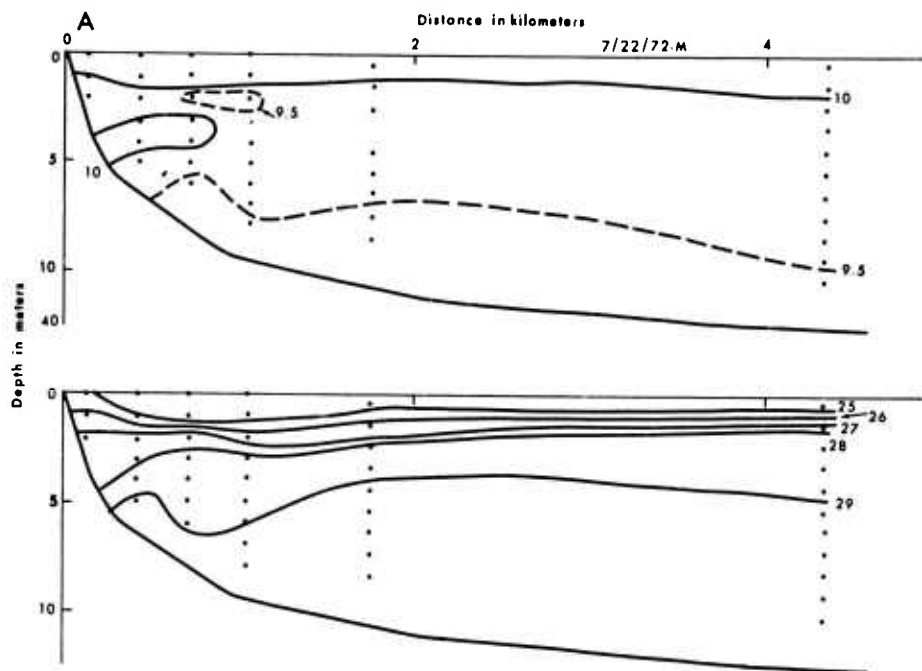


Figure 31A. Temperature section (upper) and salinity section (lower) from the nearshore waters at Point Lay on 7/22/72. Temperature is contoured in degrees Celsius and salinity in parts per thousand. Sample points are indicated by dots.

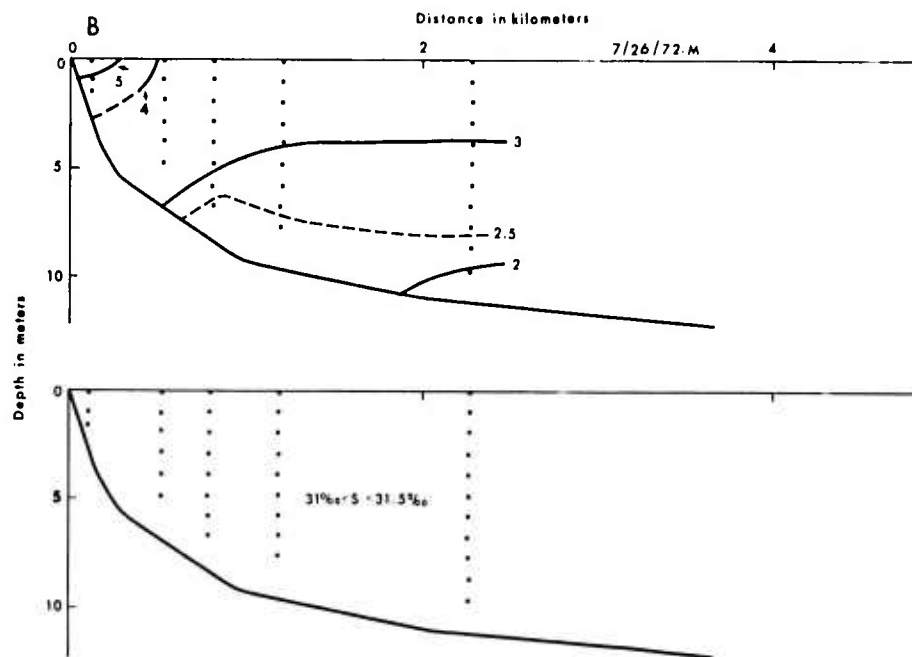


Figure 31B. Temperature section (upper) and salinity section (lower) from the nearshore waters at Point Lay on 7/26/72. Temperature is contoured in degrees Celsius and salinity in parts per thousand. Sample points are indicated by dots.

By July 27 (Fig. 32A) the winds were slackening but were still northeasterly. The waters nearshore were still cold but were somewhat less salty than on the day before. There was an indication in the surface layers of a lens of water offshore, again similar to a feature which Csanady (1972) describes as a lens-shaped pycnocline associated with a coastal jet and winds blowing with the coast to their left.

Between July 27 and 29 (Fig. 32B) the waters in the nearshore region and those within the lagoon exchanged and mixed under the influence of tidally and meteorologically induced motion. The waters freshened somewhat in the nearshore and warmed significantly. The fact that only a slight freshening occurred indicates that by that time of the year only a slight input of fresh water is supplied to the lagoon by the local rivers. The freshet influence is over.

From July 31 until August 1, water level dropped within the lagoon. For the next 3 days (Figs. 33A and 33B) it oscillated about a mean level with an amplitude of 5 cm or less. The induced mixing of the lagoon and nearshore waters tended to further freshen the latter and to significantly warm them.

In early August, two strong southwesterly storms passed through the area, closing the inlet near our camp. Waves from these storms prohibited any further data collection until August 15 (Fig. 34), when the nearshore waters were very homogeneous (9-10 C, 28-29 ‰). The camp was abandoned 5 days later; therefore, it is uncertain whether the homogeneous conditions were due to the intense wave-induced mixing or to the fact that an inlet was no longer in the immediate vicinity to influence the water characteristics.

It was often possible to observe visually the turbid plume of effluent flowing from the inlet into the nearshore waters. This plume had well-defined boundaries and was extremely narrow. It was not visually observed to spread immediately alongshore as far as the section studied. It is possible that the section was influenced by alongshore spreading, as described by Sonu et al. (in preparation). They describe nonlinear, recirculating eddies just outside an inlet which spread alongshore under the action of buoyancy forces. The large number of inlets present along the Alaskan coast from Icy Cape to the southern end of Kasegaluk Lagoon lead to the belief that the processes observed at Point Lay were indicative of processes affecting the nearshore waters of large sections of the coast. The measurements were undoubtedly influenced by the proximity to an inlet. The waters somewhat farther from the inlet would be expected, though, to be influenced in a similar fashion, albeit possibly with some time delay and to an attenuated degree. Although the data did not extend through the freezeup season, the pattern of variability near an inlet, and possibly in the entire nearshore region from Icy Cape to the southern end of Kasegaluk Lagoon, is believed to be the following. The spring freshet and the melt of the shorefast ice produces an intense pycnocline, primarily a halocline. Gradually, through wind-induced and tidal mixing, this pycnocline dissipates. If a major storm passes through the area, wave-induced mixing may also contribute to the destruction of the pycnocline. Subsequent to this, the nearshore waters are influenced by impoundment in the lagoon, where they are heated by solar radiation and freshened by mixing with any fresh water flowing from the rivers entering the lagoon. When meteorological conditions permit, these waters flow out of the lagoon and form a new pycnocline in the nearshore region. This discontinuity layer will be dissipated, as was that formed by the spring freshet. Catastrophic renewal of the nearshore waters may also occur under the influence of strong winds, possibly indicating an upwelling process.

Parentetically, the results of the two surveys of Kasegaluk Lagoon should be mentioned. The surveys were flown on July 24 and August 17. In both cases a

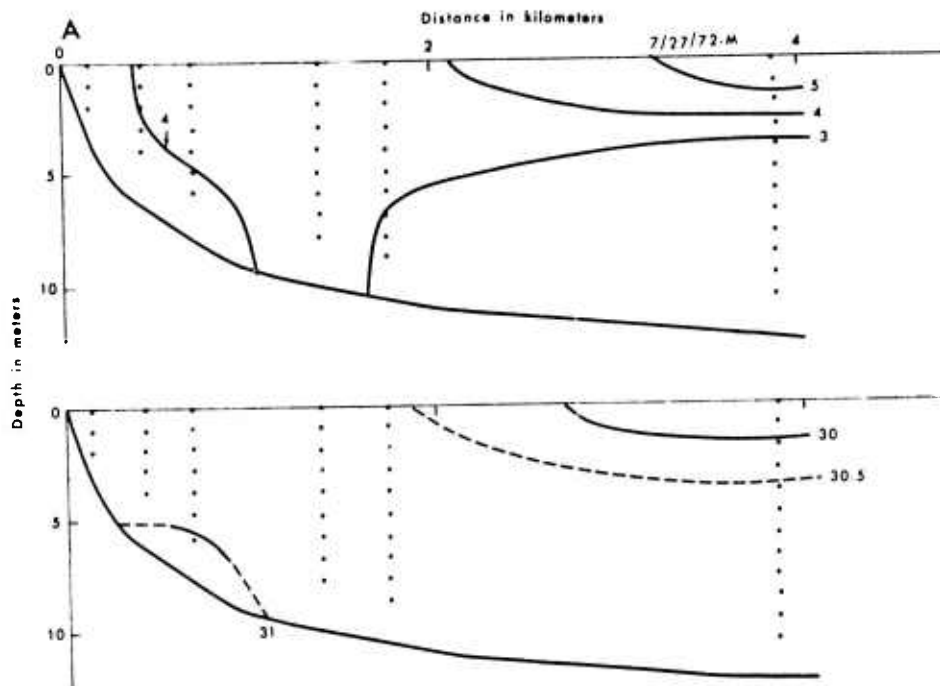


Figure 32A. Temperature section (upper) and salinity section (lower) from the nearshore waters at Point Lay on 7/27/72. Temperature is contoured in degrees Celsius and salinity in parts per thousand. Sample points are indicated by dots.

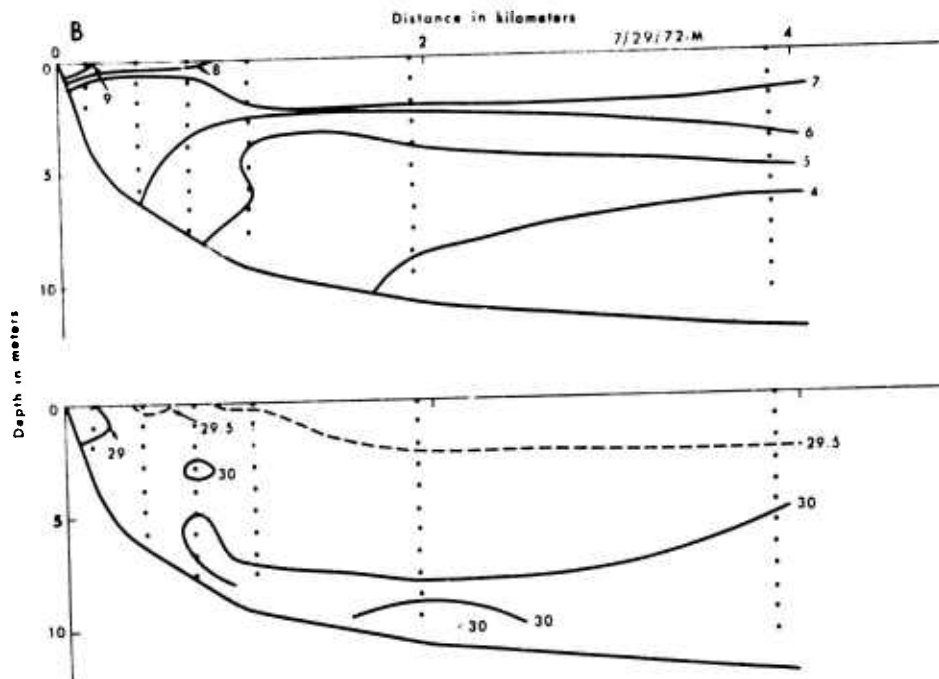


Figure 32B. Temperature section (upper) and salinity section (lower) from the nearshore waters at Point Lay on 7/29/72. Temperature is contoured in degrees Celsius and salinity in parts per thousand. Sample points are indicated by dots.

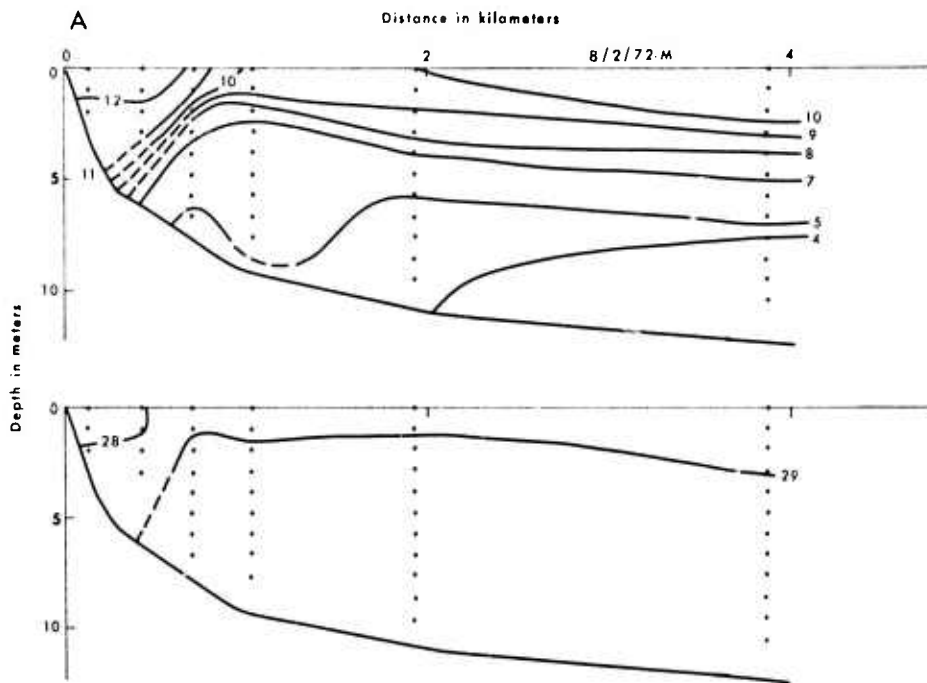


Figure 33A. Temperature section (upper) and salinity section (lower) from the nearshore waters at Point Lay on 8/2/72. Temperature is contoured in degrees Celsius and salinity in parts per thousand. Sample points are indicated by dots.

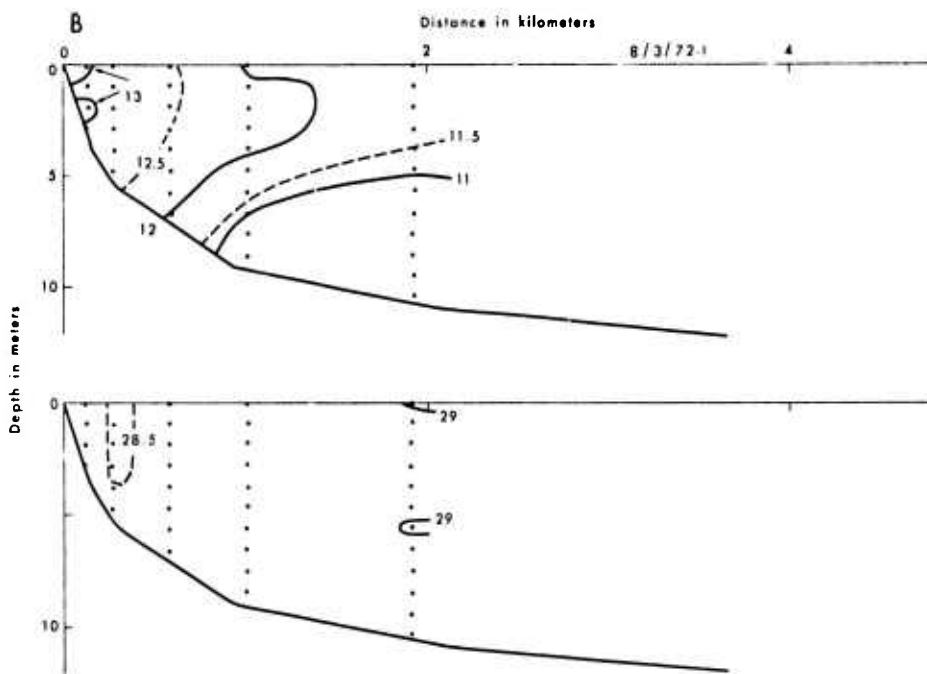


Figure 33B. Temperature section (upper) and salinity section (lower) from the nearshore waters at Point Lay on 8/3/72. Temperature is contoured in degrees Celsius and salinity in parts per thousand. Sample points are indicated by dots.

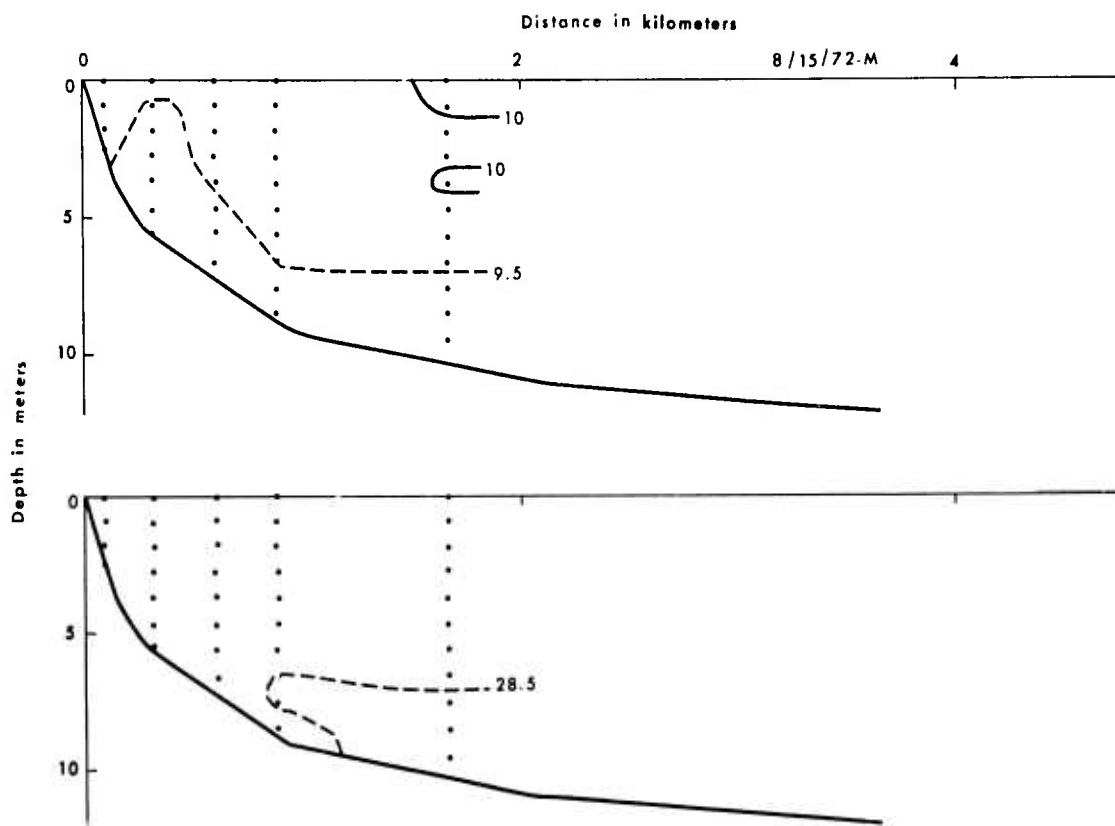


Figure 34. Temperature section (upper) and salinity section (lower) from the near-shore waters at Point Lay on 8/15/72. Temperature is contoured in degrees Celsius and salinity in parts per thousand. Sample points are indicated by dots.

northeasterly wind stress was present, although it was more intense on the earlier date. Certain features were common to both surveys. There were no definitive, cross-lagoon gradients. Temperatures warmed and salinities freshened to the south, thus density decreased to the south. Wind stress seemed to push water out of the southern inlets, and continuity required a compensating inflow through the northern inlet. No surveys were made during a southerly wind stress, and the influence of such a condition cannot be evaluated. But it is reasonable to assume that with a southerly wind the pattern would reverse, and light lagoon waters would flow out of the northern inlets and heavy nearshore waters would enter through the southern inlet.

The situation at Pingok Island is not as clear from the data as that at Point Lay. A single section, perpendicular to shore, was occupied four times from August 29 until September 12. By that time of year, the nearshore waters were nearly at their freezing point, never being warmer than 1 C and generally being colder than 0 C. Salinity values also showed very little variation (27.7-30.4 ‰). Measurements of the waters in the lagoon just behind Pingok Island showed variations from 0.5 to 2 C and 19.5 to 22.5 ‰. Discussions with G. E. Hall, of the University of Alaska, indicate that the major variability of the lagoon waters is caused by westerly winds, which blow fresh water from the Colville River into Simpson Lagoon.

This water forms a layer of almost totally fresh water on the surface of Simpson Lagoon, but the layer is only a meter or two thick. Another source of fresh water to the lagoon is the Kuparuk River, which is being studied by the U.S. Geological Survey. For the past few years, the U.S.G.S. has operated small boats in the near-shore waters near Pingok Island. Among other data, temperature and salinity samples from the surface and bottom have been collected at numerous stations. Although these data are not fully analyzed and their interpretation is not yet clear, there are indications that there exists a quasi-permanent intrusion of cold, clear, high-salinity water from offshore into the coast near Oliktok Point. Farther offshore, as the pack ice is approached, the waters become less saline owing to ice melt (E. Reimnitz and P. Barnes, personal communications).

The tidal fluctuations within Simpson Lagoon at astronomical frequencies are much more noticeable than in Kasegaluk Lagoon (Fig. 13). This would seem to indicate a freer exchange of water between the lagoon and the nearshore than was seen at the western site. Such an exchange would probably tend to subdue intense changes in water characteristics such as observed at Point Lay.

#### Discussion

As has been mentioned throughout this report, there is very little published data concerning physical processes in the nearshore region of the Alaskan Arctic. This study has added some data to the body of descriptive knowledge but has probably raised more questions than it has answered. The oceanographic processes in the nearshore region during the open-water months appear to be predominantly controlled by atmospheric processes, primarily wind stress and solar heating. Wind-driven currents cause set-up and set-down at the shoreline, resulting in sea-level variations far in excess of those produced by the astronomical tides. These meteorological tides, in turn, strongly influence the water mass properties in the nearshore area, at least near inlets. They also determine the section of beach subjected to wave action.

The intense wind stress during storm conditions causes a fetch-limited sea to develop, which is responsible for the primary reworking of the coastline. The duration-limited seas present during average wind conditions deliver only modest power to the shoreline. Long, infragravity waves (Kinsman, 1965) of moderate energy also appear to be generated as the wind blows over the pack ice.

More work is definitely called for on comparisons of currents during the frozen winter and open-water seasons and on the processes which cause their variability. The Chukchi Sea, with its strong wind stress, shallow water, and large Coriolis parameter, is a perfect laboratory for the study of storm surges. Such studies should be encouraged in the future inasmuch as the problem of surge prediction still needs substantial work.

More work is also needed to identify the processes responsible for the variability of coastal water masses and their spatial scales. A first step has been made in the vicinity of a tidal inlet, but the spatial extent of the influence of such a process is not yet known. There are indications of processes similar to upwelling in our data from the Chukchi Sea. Although we have no data to substantiate the conjecture, in the Beaufort Sea, with its strong winds from the east and north-east, large Coriolis parameter, and narrow shelf, coastal upwelling would be expected to be an important process. This, too, should be investigated.

## CHAPTER IV

### ALASKAN ARCTIC COASTAL MORPHOLOGY

#### Introduction

The Alaskan Arctic Coast studied in this project extends from Point Hope to Demarcation Point, a total shoreline distance of 1,441 km. Although this coast is influenced primarily by an arctic environment, it exhibits a range of coastal landforms comparable to those found throughout the world. Of the total coastline length, 805 km (56 percent) consists of Recent barrier islands and associated inlets backed by lagoons of various widths. Tundra bluffs (primarily Pleistocene in age) fronted by narrow beaches prevail along 381 km (27 percent) of the coastline, and delta shorelines total 135 km (9 percent). The remaining 120 km (8 percent) is dominated by rocky cliffs. More significant than this broad variability of general landform types, however, is the large range of landform configurations and combinations. These variations reflect differences in local structure, exposure aspect, offshore slope, sediment supply, and relative intensity of various hydrodynamic and aerodynamic forces. In addition to spatial variability, the coast also experiences secular as well as short-term changes. This chapter is concerned with the nature, range, and causes of this variability.

Coastal geomorphic characteristics and their variability were determined from analyses of hydrographic and topographic maps, aerial photographs, and several aerial photographic and reconnaissance flights made during different seasons over the period June 1971 - November 1972.

In order to characterize the coastline geometry and its variability, morphometric measurements were made from maps and aerial photographs. The coastline was divided into one hundred fifty-seven 8-km segments. For convenience of description these segments were grouped into twenty-two provinces displaying similar landform suites. Province boundaries were identified on the basis of abrupt changes in coastal landform suites. The salient geomorphic characteristics of each province were recorded during air and ground reconnaissances and from photographs. The provinces and sector numbers along the coastline are shown in Figure 35.

To facilitate the measurements of the shoreline geometry, a Fortran IV program (ARCMAP) was written in which digitized shoreline configurations were reduced into predefined parameters. The shoreline and the lagoons were digitized on a CALMA electronic digitizer, and the tapes were processed by the ARCMAP program. The following shoreline parameters were then determined (see Fig. 36 for definitions).

- (1) Coastline trend length ( $L_t$ ) - the length, in kilometers, of the coastline, including both land and open-water (i.e., inlets, etc.) distances.
- (2) Shoreline length ( $L_s$ ) - the length, in kilometers, of the shoreline that is a land-water boundary.
- (3) Open water ( $L_w$ ) - the length, in kilometers, of the open-water distance

**Preceding page blank**



along the general coastline length.

- (4) Ratio  $L_S/L_W$  - the ratio of shoreline (land portion) length to open water.
- (5) Coastline crenulation ( $C_T$ ) - the ratio of the coastline trend length ( $L_T$ ) of a province to the chord connecting the boundaries of the province. The higher the number, the more crenulated or embayed the shoreline.
- (6) Average shoreline crenulation ( $\overline{C_T}$ ) - the average value of the ratios of the shoreline length to the chord of all sectors within the province. The coefficient of variability is also indicated.
- (7) Barrier length ( $L_B$ ) - the average length, in kilometers, of barriers within each province.
- (8) Barrier width ( $W_B$ ) - the average width of all barriers within a province. The width was measured at 1.6-km intervals along each barrier. The coefficient of variability is also given.
- (9) Barrier length/chord ( $L_B'$ ) - the average ratio of the barrier length ( $L_B$ ) to the chord connecting the ends of each barrier. The higher the number, the more arced is the barrier.

In addition, the following measures of lagoon shape were determined:

- (1) Length ( $L_\ell$ ) - the centerline length, in kilometers, of each lagoon.
- (2) Width ( $W_\ell$ ) - the average width of each lagoon, in kilometers. Width was measured at 19.4-km spacings. The coefficient of variability is also indicated.
- (3) Length/Width - the ratio of the length to the width is given.
- (4) Area ( $A$ ) - the area, in square kilometers, is given for each lagoon.
- (5) Perimeter ( $P$ ) - the perimeter, in kilometers, is given for each lagoon.
- (6)  $\alpha$ Crenulation ( $\alpha C_L$ ) - the ratio of the barrier-side lagoon shoreline length ( $L_\alpha$ ) to the lagoon chord.
- (7)  $\gamma$ Crenulation ( $\gamma C_L$ ) - the ratio of the landward-side lagoon shoreline length to the lagoon chord. The higher the value, the more indented and crenulated is the shoreline.

Owing to the general lack of detailed nearshore bathymetry data, few detailed morphometric parameters could be determined for the offshore region except near field sites where repeated offshore surveys were made. In order to obtain some morphometric measures of this region, a Fortran IV program (CALMOR) was used to obtain the subaqueous hypsometric integral (HI) for each sector. The offshore contours were digitized and the HI for each sector was obtained from the digitized data by:

$$HI = \int_{Z_{\max}}^0 (A/A_{\max}) d(Z/Z_{\max})$$



In addition to the HI, the slopes,  $\beta$  (ratio of vertical to horizontal distances), and distances to offshore contours have been measured each mile along the shoreline. The slope plays an important role in wave processes; a very low offshore slope tends to permit frictional attenuation and consequently reduction in the energy working on the shoreline.

Secular wave climate and its provincial variations were determined by means of comprehensive Fortran IV programs developed to compute refraction, shoaling, and frictional dissipation effects for any given set of wave conditions and for any bottom configuration, and the resulting wave power regime for all input wave sets combined. Deepwater wave statistics were computed by hindcasting techniques using DEW Line meteorological data. Bathymetric data from 1:50,000-scale hydrographic charts are input from magnetic tape in digital form by a CALMA electronic digitizer. From this input, wave height, length, period and angle, shoaling and refraction coefficients, new wave height resulting from frictional loss (calculated by the equations derived by Bretschneider, 1954, and Bretschneider and Reid, 1954), wave steepness, group velocity, onshore and alongshore wave power, and coastline power gradients are calculated for any depth from deep water to the coastline. Any number of input positions offshore can be specified. This program is described in detail in Coastal Studies Institute Technical Report 95 (Coleman and Wright, 1971). Because detailed deepwater wave statistics are lacking in the Arctic, hindcasting techniques had to be relied upon for computation of the deepwater wave conditions. In addition, the presence of ice in the offshore severely limits the fetch, and average offshore ice boundaries were taken at numerous points alongshore to obtain fetch distance. The wind statistics were reduced from 8-year records at the DEW Line stations to determine wind velocity, direction, and frequency. Resulting wave power levels at the 10-meter contour and at the shore are presented for each province in Table 6. Owing to the poor quality of input data and the highly variable fetch lengths, the absolute values of these data probably have little meaning. However, they should indicate the general contrasts in energy environments.

Owing to limited degrees of freedom, statistical analyses were restricted to analysis of variance, performed on wave power and morphometric parameters in an effort to test for significant contrasts between the Chukchi Sea coast and the Beaufort Sea coast. The canned analysis of variance routine of the Statistical Analysis System (SAS) program was used. The model was based on a randomized block design and on the assumptions of sample independence and a normally distributed error term. The 0.10 confidence limit was taken as the cutoff between significant and nonsignificant F ratios.

#### Macroscale Coastal Geomorphic Variability

The coastal geomorphology of the Alaskan Arctic exhibits variability on several scales. On a macroscale, the overall coastal landscape and general coastline configuration along the Chukchi Sea coast to the west of Point Barrow contrasts appreciably with the landscape and configuration of the Beaufort Sea coast to the east of Point Barrow. On the intermediate scale, individual provinces have distinctive landform combinations, geometries, and orientations. On a microscale there are variations in the type of landform present at a given location, as well as variations in the size, plan, and profile shape of the landforms. Macroscale variability and its causes will be considered first.

Macroscale variability of the coast is attributable to a combination of influences, including the geologic structure underlying the coastal plain, the distribution of major rivers, major features of the oceanic circulation system, general contrasts in thermal regime, major differences in the proximity of the ice pack and

Table 6

## Province Variability of Wave Power

Province	June Wave Power x 10 <sup>7</sup> ergs/sec			July Wave Power x 10 <sup>7</sup> ergs/sec			August Wave Power x 10 <sup>7</sup> ergs/sec			September Wave Power x 10 <sup>7</sup> ergs/sec			Annual Wave Power x 10 <sup>7</sup> ergs/sec			Total Energy x 10 <sup>14</sup> ergs		
	10 m Shore			10 m Shore			10 m Shore			10 m Shore			10 m Shore			10 m Shore		
	1-15	16-30	10 m	1-15	16-30	10 m	1-15	16-30	10 m	1-15	16-30	10 m	1-15	16-30	10 m	1-15	16-30	10 m
1	Mean S.D.	5.2 4.3	0.497 0.569	17.00 7.56	2.22 1.80	270.17 151.14	51.23 44.51	248.47 174.38	42.57 46.02	95.49 48.18	21.01 20.19	114.44 41.31	31.66 26.0	96.60	18.92	101.0	20.2	
6	Mean S.O.	21.73 20.95	2.196 2.11	33.94 29.39	6.08 5.09	33.94 29.39	6.08 5.09	33.94 29.39	6.08 5.09	44.49 41.08	9.09 12.58	44.49 41.08	9.09 12.58	33.39	5.79	26.8	4.63	
7	Mean S.D.	8.98 9.23	2.94 3.87	16.01 12.86	3.77 5.09	13.91 4.14	12.33 13.91	2.81 4.14	19.32 21.63	2.48 2.39	14.16	3.00	7.65	1.61				
8	Mean S.O.	4.68 0.960	0.447 0.12	8.66 2.25	1.11 0.294	17.31 5.14	11.20 17.31	2.86 5.14	17.83 28.65	5.38 9.87	10.59	2.45	5.72	1.18				
9	Mean S.D.	3.90 1.80	0.290 0.165	9.26 4.27	0.755 0.76	40.83 20.00	6.96 8.29	65.32 34.18	13.61 15.84	29.83	5.40	16.1	2.88					
10	Mean S.O.	3.73 5.36	0.614 1.27	22.23 27.92	9.96 14.47	52.68 59.31	24.72 33.49	186.22 367.11	26.21 31.09	66.22	15.38	36.1	8.28					
11	Mean S.O.	117.54 44.53	12.14 24.59	188.60 86.39	14.54 20.00	153.1	13.34	41.3	3.58									
12	Mean S.D.	1.58 1.72	0.180 0.569	50.51 70.91	0.383 0.498	31.20	0.500	32.48	0.316	13.0	0.128							
13	Mean S.O.	1.609 1.873	0.00205 0.00264	11.94 4.97	0.00624 0.06651	8.28	0.0192	9.63	0.0063	3.89	0.003							
14	Mean S.O.	0.724 0.219	0.044 0.056	3.30	0.493	2.99	0.292	8.73	0.387	3.52	0.155							
15	Mean S.O.	18.93 9.39	0.304 0.168	38.62 21.02	0.591 0.433	44.44 22.16	0.471	33.99	0.484	13.4	0.191							
	Mean S.O.	6.45 0.384	0.166 0.084	2.02	0.351	2.61	0.202	11.35	0.258	4.6	0.097							
17	Mean S.O.	4.58 1.68	0.216 0.266	8.88 3.63	0.236 0.259	4.47	0.065	8.11	0.236	3.29	0.096							
18	Mean S.O.	48.84 43.85	6.96 5.74	51.35 52.16	6.29 4.80	49.18 37.57	7.78 6.14	49.79	7.01	20.2	2.85							
19	Mean S.D.	36.02 32.34	5.136 4.235	37.87 38.47	3.54	36.27 27.71	5.74 4.53	36.72	5.172	14.4	2.05							
20	Mean S.D.	32.44 6.31	8.6 0.943	24.76 5.08	6.55 0.325	35.10 7.74	9.498 0.86	30.76	8.22	12.2	3.27							

duration of the open-water period, and resulting gross contrasts in the coastal wave power. Since the astronomical tide range is relatively uniform over the entire study region, tide is not a primary source of variability.

#### STRUCTURAL LINEAMENTS AND COASTLINE PLAIN

Inspection of topographic maps and aerial photographs indicates the presence of a system of surface lineaments. Voronov et al. (1970) define lineaments as "a geometrically regular network of fissuring which extends over the earth's crust and is manifested in geostructural and geomorphological planar configurations." These lineaments are identifiable from linear coastline trends, stream courses, and contour trends. The pattern of the major lineaments is illustrated in Figure 37. The most conspicuous set of lineaments has an average azimuthal trend of 35°, or NNE, whereas a secondary, less pronounced set of lineaments displays an average trend of 312°, or northwest. This lineament pattern agrees generally with the patterns described by Voronov et al. (1970) for the world as well as for both sides of the Bering Straits. The primary lineaments of the Bering Straits area trend 50° and 310° (Voronov et al., 1970). However, the 35° azimuth of the primary lineaments of the North Slope corresponds to one of the six major global lineament trends described by Voronov et al. Although Voronov et al. (1970) postulate that the global lineaments are the result of solid-earth tidal stresses, the actual causes of the patterns present on the surface of the Alaskan Arctic Coastal Plain remain to be established. The important point here is the role that these lineaments play in controlling the macroscale coastal configuration.

The coastline to the west of Point Barrow, between Cape Beaufort and Point Barrow, is highly regular and includes a series of three capes (Icy Cape, Point Franklin, and Point Barrow). South of each cape are long, linear coastal stretches averaging 90 km in length. These straight regions are successively offset from each other by distances of about 25 km. Although the fringing barrier and depositional features locally reflect the dynamic wave and current regimes, the general trends of the coast appear to be closely associated with the lineament patterns: the long, straight regions are parallel to and represent surface manifestations of the major 35° lineaments, whereas the offsets tend to occur along the secondary 312° lineaments. The net result has been to produce a regular system of "Carolina capes" similar to those described by Nolan and Ferm (1968) along the eastern seaboard of the U.S. and a consistent coastline trend of 35° for a total distance of 350 km. The secondary 312° lineaments control the courses of small streams which debouch along the coast between Cape Beaufort and Point Barrow.

Between Cape Beaufort and Point Hope structural control of the coastline is even more pronounced but is related to a large structural block of the Brooks Range which reaches the coast in this vicinity. In this case coastline lineaments are oriented east-west and north-south to produce an orthogonal pattern. At Cape Lisburne the coast abruptly changes orientation from east-west to north-south.

The coastline east of Point Barrow is oriented approximately perpendicular to and, hence, truncates the major 35° lineament system. For this reason, among others, this eastern coast is far more irregular and indented than that to the west of Point Barrow, where the major lineaments reinforce the coastline trends. However, several coastline stretches are aligned parallel to the 312° lineaments, as indicated by Figure 37, and, although the effect is far less conspicuous than along the western coast, a series of offset linear regions and associated capes are present. The numerous capes and points which occur along this coast are typically located on primary lineaments. The 35° lineaments also appear to correlate well with the directions of the lower courses of numerous large rivers which debouch

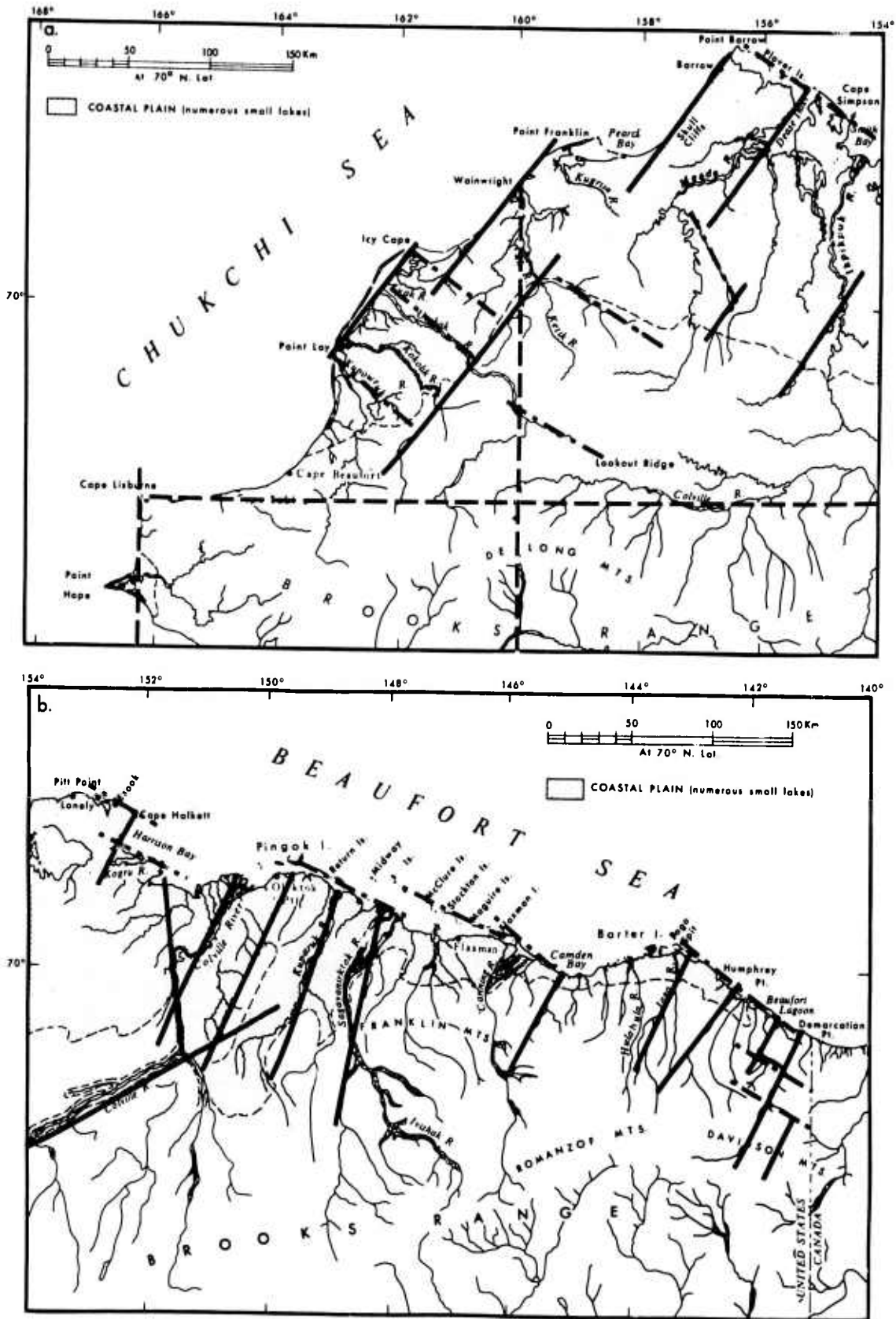


Figure 37. Major structural lineaments of the Alaskan Arctic Coastal Plain. Lineaments interpreted from photographs and maps.

into the Beaufort Sea.

#### INFLUENCE OF RIVERS

One of the more salient differences between the western and eastern coastal zones lies in the fact that all the major rivers of arctic Alaska debouch along the latter coast. This tendency is partially attributable to the fact that the Brooks Range, the northern slopes of which provide the catchment for the rivers, has appreciably greater elevation and relief to the east of Point Barrow than to the west. The courses of the rivers are correlated with the major northeast lineaments just described.

Together these rivers discharge large quantities of sediment into the near-shore zone, causing local flattening of the offshore slope and resulting in the accumulation of large coastal deltas. Whereas deltas are relatively insignificant features along the western coastal zone, they account for 135 km or 9 percent of the coast to the east of Point Barrow.

Warmer fresh water introduced to the coastal zone by these rivers during spring floods exerts local influences on sea ice breakup and is a likely contributor to the intense thermal erosion of the tundra shorelines. In the fall, decreased salinity of the coastal waters permits more rapid freezeup.

#### MARINE REGIME

Point Barrow is the convergent point of two major current systems and marks the coastal boundary between the Chukchi and Beaufort seas. Offshore currents along the western coast transport moderately warm water from the Bering Straits north-eastward toward Point Barrow. As a result, summer water temperatures near Point Hope are as high as 10 C and decrease progressively to about 2 C near Point Barrow. East of Point Barrow, in the Beaufort Sea, weaker offshore currents set to the northwest. However, because the waters of the Beaufort Sea are confined to higher latitudes than those of the Chukchi Sea, water temperatures are appreciably lower, ranging from -2 to +2 C. Breakup begins earlier and the pack ice recedes farther in the Chukchi Sea than in the Beaufort Sea. The average annual ice limits and concentrations for six 2-week periods between spring and fall are shown in Figure 38. The western coast has a longer open-water period and longer fetch than the eastern coast, with its short, ice-congested summer. Hence, on the average, the former coast receives greater wave power over a longer period of the year than the eastern coast. The coastline to the west of Point Barrow experiences significant wave power by late June or early July, whereas along the eastern coast wave power is normally negligible prior to mid-August. Weighted mean wave power values at the 10-meter contour and at the shore average  $41.8 \times 10^7$  ergs/sec and  $8.5 \times 10^7$  ergs/sec along the western coast; corresponding values to the east of Point Barrow are  $37.5 \times 10^7$  ergs/sec and  $3.5 \times 10^7$  ergs/sec, respectively. More significant contrasts are exhibited by the values of total wave energy for the open-water season because of the appreciable differences in duration of wave activity. Total energy values at the 10-meter contour and at the shore average  $32.2 \times 10^{14}$  ergs and  $6.5 \times 10^{14}$  ergs west of Point Barrow and  $13.0 \times 10^{14}$  ergs and  $3 \times 10^{14}$  ergs east of Point Barrow. Analysis of variance performed on the weighted mean power and total energy values revealed that the tendencies for wave power and total energy to be higher along the western coast than along the eastern coast are highly significant (Table 7) and that the wave climate differences existing between the two macroscale coastal zones are more important than those occurring between individual provinces. Accordingly, wave-built features such as beaches, barriers, and spits are well developed and relatively continuous to the west of Barrow but are irregular and highly discontinuous to the east.

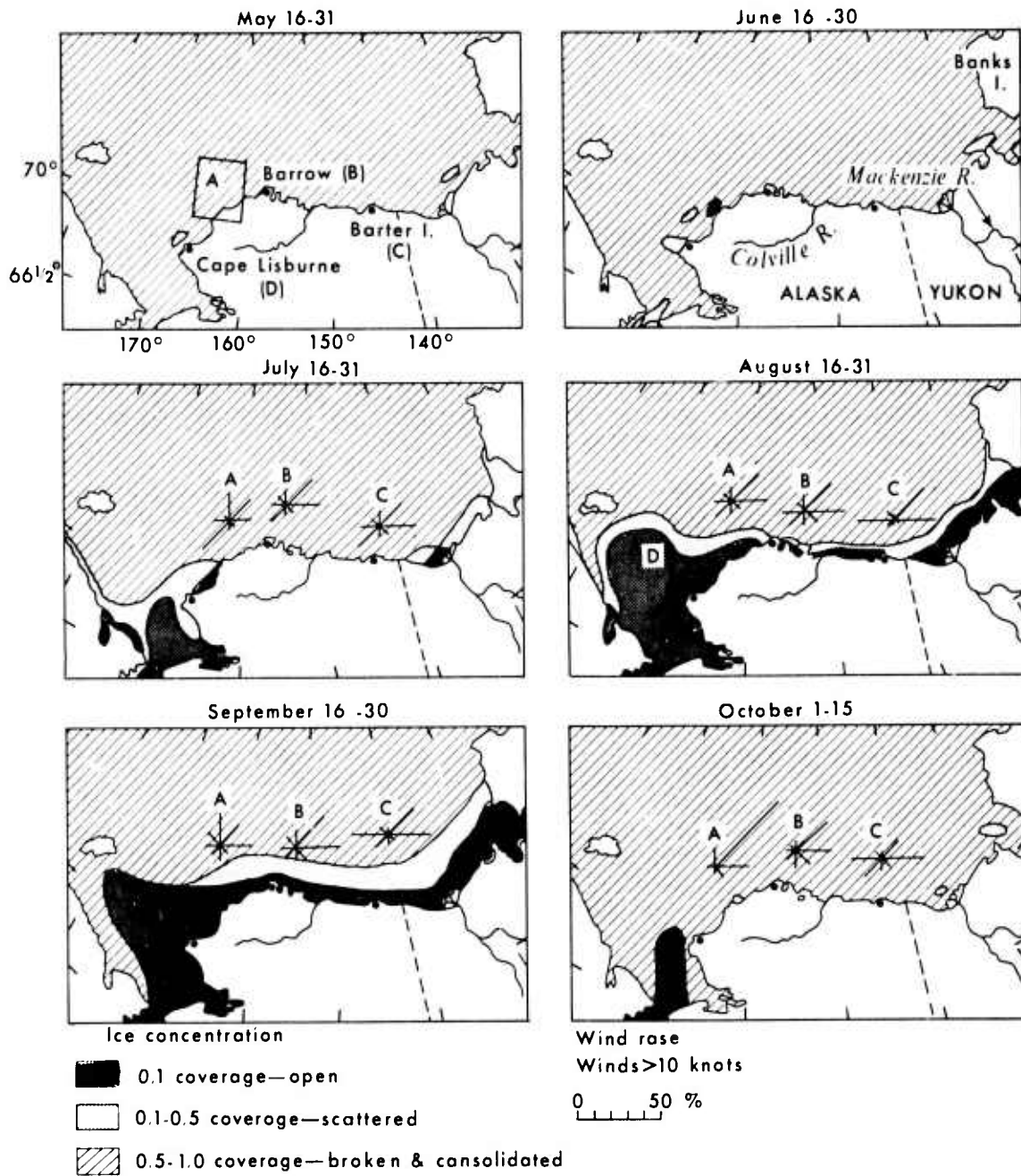


Figure 38. Average ice concentration along the Alaskan Arctic Coast and adjacent waters from May through mid-October. Wind roses show frequency of winds exceeding 10 knots at three sites: A, Point Lay region; B, Point Barrow; and C, Barter Island. Data compiled from U.S. Navy Hydrographic Office Publication No. 122A.

Both of the coastal zones are subject to occasional severe storms and resulting intensified wave energy. Along the western coast, storms arrive predominantly from the southwest, the direction of the longest fetch. The onshore winds produce appreciable set-up, and many barrier formations are capped with storm berms to elevations of over 3 meters above mean sea level. To the east of Point Barrow,

Table 7

Summary Statistics and F Ratios for Wave Power and Energy Contrasts  
Between the Western and Eastern Coasts

	10-Meter Wave Power $\times 10^7$ ergs/sec	Shore Wave Power $\times 10^7$ ergs/sec	10-Meter Open-Water Energy $\times 10^{14}$ ergs	Shore Open- Water Energy $\times 10^{14}$ ergs
Total n	16	16	16	16
Overall Mean	39.09	4.39	20.2	3.2
Standard Deviation	38.61	5.93	24.4	5.05
Western Coast				
n	6	6	6	6
Mean	41.79	8.49	32.2	6.46
Standard Deviation	33.32	6.92	35.6	7.20
Eastern Coast				
n	10	10	10	10
Mean	37.47	3.54	13.0	3.04
Standard Deviation	43.14	4.67	11.5	6.16
Degrees of Freedom				
Zone	1	1	1	1
Error	14	14	14	14
Total	15	15	15	15
F Ratio	0.044 NS	2.95 *	2.58 *	5.10 *

NS = Nonsignificant

\* = Significant above the 0.10 confidence level

westerly storms cause sea level rises of up to 3 meters (Schalk, 1957, 1963; Reimnitz et al., 1973), onshore movement of ice (which tends to reduce wave height), and easterly setting currents. Strong easterly winds, on the other hand, cause a drop in the nearshore sea level and offshore movement of ice owing to the effects of Ekman drift.

#### Macroscale Morphologic and Morphometric Variability

The effects of the structural lineaments, the riverine regimes, and the marine agents just described have reinforced each other to divide the Alaskan Arctic Coast into two distinct dynamic and morphologic zones: the "western" coast, from Point Hope to Point Barrow, and the "eastern" coast, from Point Barrow to Demarcation Point. The western coast is generally characterized by straight, regular coastlines with relatively continuous and linear wave-built beaches, barriers, and spits. The coast of the eastern zone is irregular and is characterized by a combination of arcuate barrier islands separated by broad expanses of open water and backed by wide lagoons, numerous large deltas, embayments of various sizes, and low-energy, thermally eroding tundra shorelines.

Thermal erosion appears to play a particularly important role in determining the morphology of this coast. Lagoons backing the larger barrier chains appear to

have originated through the erosion and coalescing of thaw lakes. Various stages in the possible sequence of lake erosion and lagoon formation are shown in Figure 39. If this mode of lagoon formation is correct, the barrier arcs represent residuals which are very likely related to the secondary  $312^\circ$  lineaments, which they approximately parallel (Fig. 37). Thermal erosion of the landward lagoon shores has proceeded at different rates, leaving behind a series of cusped points (e.g., Oliktok Point, Fig. 39C). These points show a consistent tendency to be situated on primary  $35^\circ$  lineaments and are presumably associated with increased resistance along these lineaments.

In addition to the coastal landscape contrasts just described, several morphometric properties also exhibit significant differences between the western and eastern coastal zones, as suggested by an analysis of variance performed on all morphometric variables previously described. Location in the eastern or western coastal zones served as the classifier in the analysis of variance. Morphometric values from each province were used as data points. Means and standard deviations for each zone and F ratios and significance levels for the macroscale treatment are presented in Table 8.

The most significant zonal contrasts are displayed by the lateral open-water distances ( $L_W$ ) separating barriers, the ratio of barrier length to chord length ( $L_B$ ), and lagoon width ( $W_L$ ). Owing to the discontinuity of barrier formations to the east of Point Barrow,  $L_W$  has a mean of 15.7 km, as opposed to a mean of 1.32 km along the western coast. The difference is highly significant; the F ratio is 11.5. The greater "arcuateness" of the eastern barriers is indicated by the significant tendency for  $L_B$  to be greatest along the eastern coast. Lagoon width is also significantly greater to the east, averaging 2.51 km along the eastern coast as contrasted with a value of 1.16 to the west. Other significant tendencies include a greater value of  $L_S/L_W$  to the west; appreciably greater lagoon area along the eastern coast; and a flatter offshore slope between the shoreline and the 15-meter contour to the east. Surprisingly, although the offshore slope configurations, as indexed by HI, varied considerably between provinces, the variation between zones was negligible, a mean value of 0.36 characterizing both zones.

#### Intermediate-Scale Coastal Variability and Province Descriptions

Within each of the two zones just described the shoreline morphology and associated process regimes exhibit appreciable variability. Many parameters exhibit greater variability between provinces than between zones. Along both coastal zones local differences in geology, exposure aspect, offshore slope conditions, and proximity to river mouths have created contrasts in dynamic forces, sediment supply, and morphologic response. In order to describe this variability, the coast has been divided into provinces largely on the basis of distinctive suites of coastal landforms. The qualitative and quantitative (morphometric) characteristics of each province of the western and eastern zones are listed in Table 9. Because of insufficient degrees of freedom, and because the salient characteristics of the provinces are primarily qualitative, there has been no attempt to test the province boundaries statistically. Thus province divisions are solely for purposes of describing the salient characteristics of the coast.

#### THE WESTERN ZONE PROVINCES

Variations between the ten provinces west of Point Barrow reflect structural control and alternations in the directions of littoral drift and dominant wave power.

The entire coastline of province 1, the southernmost province, consists of an

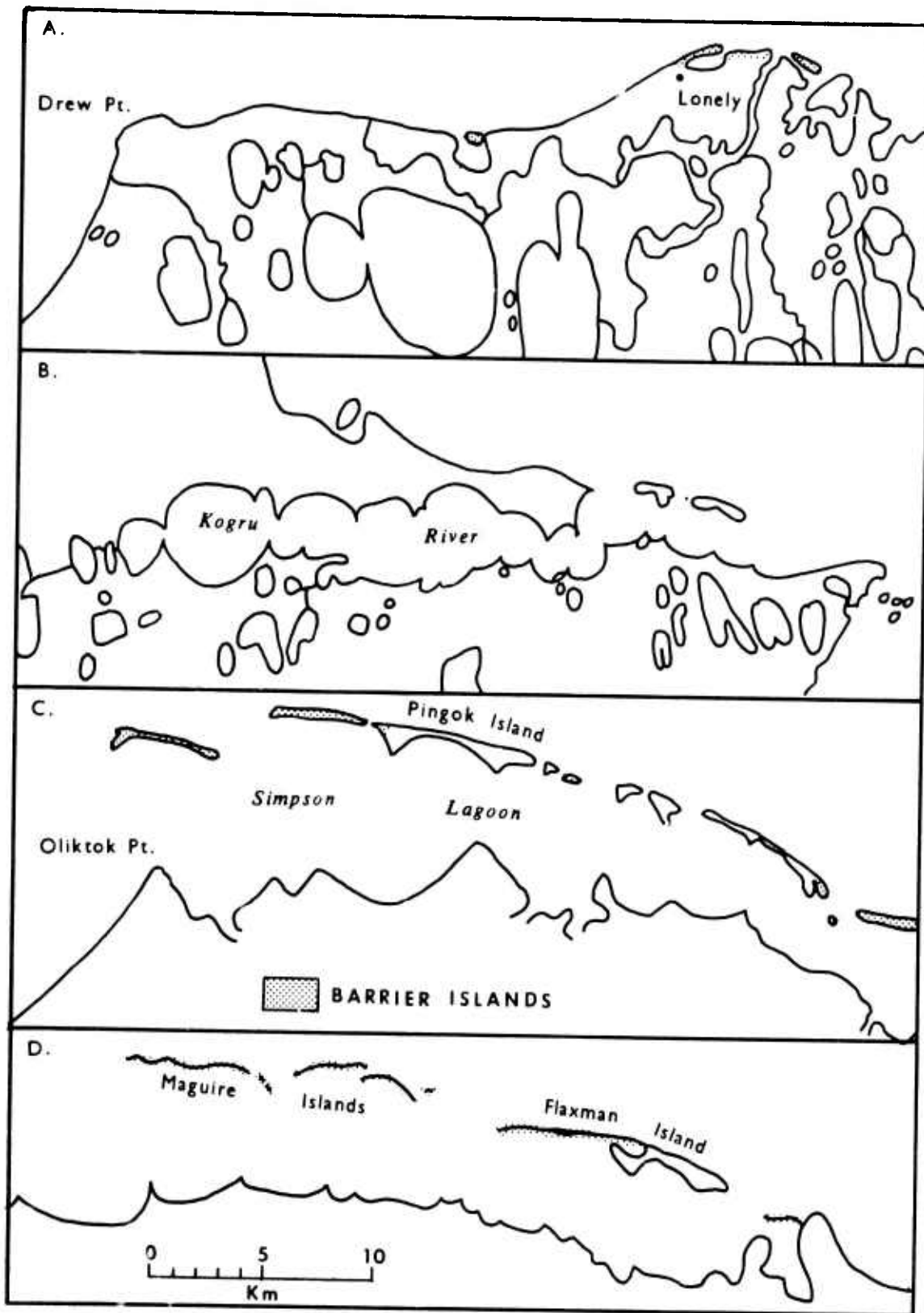


Figure 39. Sequence of lagoon formation and barrier island isolation by thaw-lake coalescence. A. Initial tapping, draining, and coalescing of lakes. B. Continued coalescing of lakes and thermal erosion of shoreline. C. Continuing thermal erosion and isolation of offshore tundra remnants. D. Erosion of tundra remnants and reworking of sand and gravel into offshore barriers.

Table 8

Summary Statistics and F Ratios for Morphometric Contrasts  
Between the Western and Eastern Coasts

	$L_S$	$L_W$	$L_S/L_W$	$C_r$	$\overline{C_r}$	$L_B$	$W_B$	$L_B'$	$L_\ell$
Total n	20	20	17	20	20	29	29	29	17
Overall Mean	51.4	9.3	204	1.36	1.13	8.03	0.192	1.05	33.4
Standard Deviation	33.4	10.5	463	0.49	0.13	6.6	0.24	0.23	36.1
Western Coast									
n	10	10	8	10	10	10	10	10	8
Mean	54.9	1.32	472	1.40	1.07	11.7	0.28	1.05	28
Standard Deviation	27.9	2.4	731	0.67	0.12	8.0	0.35	0.038	73
Eastern Coast									
n	10	10	9	10	10	10	10	10	9
Mean	66.5	15.7	16.3	1.31	1.18	5.8	1.4	1.16	21.8
Standard Deviation	41.7	14.9	34.4	0.18	0.15	3.8	0.09	0.06	25.1
Degrees of Freedom									
Zone (W or E)	1	1	1	1	1	1	1	1	1
Error	18	18	15	18	18	18	18	18	15
Total	19	19	16	19	19	19	19	19	16
F Ratio	0.09 NS	11.5*	4.0*	0.16 NS	8.0*	1.95 NS	0.93 NS	4.10*	1.45 NS
	$W_\ell$	$L_\ell/W_\ell$	$A_\ell$	$\alpha C_\ell$	$\gamma C_\ell$	HI	$\beta_3$	$\beta_{15}$	
Total n	17	17	17	17	17	20	20	20	
Overall mean	3.6	9.56	232.6	1.15	1.45	0.36	0.012	0.003	
Standard Deviation	3.3	6.69	320.9	0.37	0.51	0.06	0.009	0.002	
Western Coast									
n	8	8	8	8	8	10	10	10	
Mean	1.16	9.19	42.2	1.22	1.51	0.364	0.01	0.04	
Standard Deviation	1.47	7.09	102.7	0.51	0.67	0.07	0.005	0.003	
Eastern Coast									
n	9	9	9	9	9	10	10	10	
Mean	2.51	8.14	128	1.37	1.70	0.361	0.015	0.003	
Standard Deviation	2.58	7.14	252	0.48	0.68	0.06	0.012	0.003	
Degrees of Freedom									
Zone (W or E)	1	1	1	1	1	1	1	1	
Error	15	15	15	15	15	18	18	18	
Total	16	16	16	16	16	19	19	19	
F Ratio	4.89*	0.24 NS	3.61*	0.19 NS	0.16 NS	0.005 NS	0.99 NS	2.68*	

NS = Nonsignificant

\* = Significant above the 0.10 confidence level

Table 9  
Province Morphology and Morphometry

Province	1	2	3	4	5	6	7	8	9	10	11
	Barrier Lagoon	Rocky	Barrier Lagoon	Rocky	Tundra	Barrier Lagoon	Barrier Lagoon	Tundra Barrier Lagoon	Barrier Lagoon	Tundra	Barrier Lagoon
L <sub>t</sub>	74.68	48.27	18.91	85.25	29.97	121.69	94.91	37.37	48.01	76.22	114.55
L <sub>s</sub>	74.65	48.27	18.91	85.12	29.16	118.75	92.35	37.37	39.29	76.07	91.37
L <sub>w</sub>	0.04	0	0	0.13	0.81	2.94	2.55	0	8.71	0.15	23.18
L <sub>s</sub> /L <sub>w</sub>	2017.5	-	-	657.3	35.82	40.37	36.17	-	4.51	514.00	3.94
C <sub>r</sub>	2.27	1.01	2.98	1.08	1.17	1.01	1.31	1.01	1.16	1.01	1.36
C <sub>r</sub>	1.40	1.13	1.01	1.01	1.06	1.04	1.04	1.01	1.07	1.01	1.07
L <sub>B</sub>	30.53	-	7.05	4.22	17.25	18.87	18.37	3.26	13.02	3.74	5.75
W <sub>B</sub>	0.33	-	0.07	0.06	1.35	0.35	0.13	0.20	0.17	0.20	0.09
L <sub>B</sub>	1.04	-	1.01	1.02	1.02	1.12	1.03	1.10	1.04	1.03	1.15
L <sub>z</sub> n	5	0	2	3	1	1	5	2	1	0	5
mn	9.55	-	4.81	2.66	2.44	129.87	14.34	3.05	38.33	-	14.84
σ	4.61	-	1.84	0.86	-	-	13.64	0.62	-	-	13.59
W <sub>z</sub> n	5	-	2	3	1	1	5	8	1	-	5
mn	1.95	-	0.37	0.37	0.76	4.16	2.47	0.40	7.01	-	6.47
σ	0.44	-	0.16	0.27	-	-	0.60	0.01	-	-	1.63
L <sub>z</sub> /W <sub>z</sub>	4.90	-	8.02	7.19	3.21	31.22	5.81	7.63	5.47	-	2.30
A <sub>z</sub> n	5	-	2	2	1	1	5	2	1	-	4
mn	9.16	-	1.50	1.59	1.05	301.29	19.46	0.59	128.95	-	68.71
σ	4.77	-	0.88	0.69	-	-	22.73	0.11	-	-	69.87
Total	45.79	-	3.00	3.18	1.05	301.29	97.27	1.18	128.95	-	274.84
P n	5	-	2	1	1	-	5	2	1	-	3
m	23.88	-	5.72	8.75	7.70	-	33.36	3.92	87.76	-	12.49
σ	9.31	-	3.91	-	-	-	30.74	0.97	-	-	7.61
Total	119.45	-	11.43	8.75	7.70	-	15.80	7.83	87.76	-	37.48
αC <sub>z</sub>	1.35	-	1.02	1.34	1.03	1.19	1.16	1.08	1.03	-	1.26
γC <sub>z</sub>	1.68	-	1.20	1.25	1.99	1.30	1.45	1.15	1.25	-	1.97
III	0.357	0.447	0.282	0.411	0.357	0.251	0.302	0.419	0.405	0.409	0.345
β <sub>3</sub>	0.0035	0.0038	0.0094	0.00086	0.0059	0.0114	0.0123	0.0133	0.0073	0.0133	0.0057
β <sub>15</sub>	0.0020	0.00234	0.00252	0.00083	0.00105	0.00175	0.00274	0.0082	0.00253	0.00651	0.001061

Province	12	13	14	15	16	17	18	19	20	21	22
	Indented Tundra, Delta	Delta	Broken Barrier-Tundra-Lagoon	Broken Barrier-Lagoon	Barrier-Tundra-Lagoon	Barrier-Delta	Tundra	Broken Barrier-Delta-Lagoon	Barrier-Lagoon-Tundra	Barrier-Lagoon-Delta	Barrier-Lagoon-Tundra
L <sub>t</sub>	189.81	87.41	75.63	86.58	47.36	47.18	18.83	56.50	27.92	61.27	19.39
L <sub>s</sub>	159.56	84.45	59.20	26.33	24.61	27.25	15.56	39.72	27.79	54.65	16.32
L <sub>w</sub>	30.25	2.96	17.43	60.25	22.76	19.92	3.27	16.78	0.13	6.62	3.07
L <sub>s</sub> /L <sub>w</sub>	5.27	28.53	3.34	0.40	1.08	1.37	4.75	2.37	214.57	8.25	5.31
C <sub>r</sub>	1.50	1.50	1.40	1.38	1.36	1.02	1.42	1.12	1.02	1.11	1.08
C <sub>r</sub>	1.25	1.53	1.12	1.30	1.19	1.06	1.07	1.22	1.02	1.03	1.06
L <sub>B</sub>	3.81	5.22	14.76	3.74	5.40	-	2.22	5.70	8.92	18.97	4.46
W <sub>B</sub>	0.09	0.11	0.37	0.11	0.28	0.06	0.31	0.11	0.11	0.07	0.17
L <sub>B</sub>	1.21	1.19	1.14	1.26	1.12	1.12	1.16	1.18	1.03	1.04	1.26
L <sub>z</sub> n	2	1	1	1	1	1	0	2	1	3	0
mn	3.52	51.25	100.29	100.29	100.29	43.70	-	12.43	37.74	21.40	-
σ	1.13	-	-	-	-	-	-	0.56	-	15.22	-
W <sub>z</sub> n	2	1	1	1	1	1	-	2	1	3	-
mn	1.21	4.55	12.34	12.34	12.34	2.61	-	2.25	2.50	1.83	-
σ	0.26	-	-	-	-	-	-	0.49	-	0.36	-
L <sub>z</sub> /W <sub>z</sub>	2.91	11.26	8.13	8.13	8.13	16.74	-	5.52	15.10	11.69	-
A <sub>z</sub> n	2	1	1	1	1	-	-	2	1	3	-
mn	2.13	192.23	645.98	645.98	645.98	-	-	14.15	38.65	20.48	-
σ	1.07	-	-	-	-	-	-	3.43	-	16.18	-
Total	2.30	192.23	645.98	645.98	645.98	-	-	28.29	38.65	61.42	-
P n	2	1	-	-	-	-	-	-	1	3	-
m	8.42	149.17	-	-	-	-	-	-	82.40	51.23	-
σ	2.57	-	-	-	-	-	-	-	-	36.78	-
Total	16.84	149.17	-	-	-	-	-	-	82.40	153.66	-
αC <sub>z</sub>	1.18	1.49	1.45	1.45	1.45	-	-	1.13	1.13	1.14	-
γC <sub>z</sub>	1.18	1.99	1.82	1.82	1.82	-	-	1.50	1.31	1.50	-
III	0.397	0.510	0.290	0.295	0.407	0.343	0.318	0.366	0.342	0.358	0.274
β <sub>3</sub>	0.00043	0.0007	0.0042	0.0267	0.0062	0.0084	0.01333	0.00533	0.02286	0.1000	0.05333
β <sub>15</sub>	0.00058	0.0074	0.00148	0.00207	0.00300	0.00225	0.00137	0.00240	0.00456	0.00429	0.00932

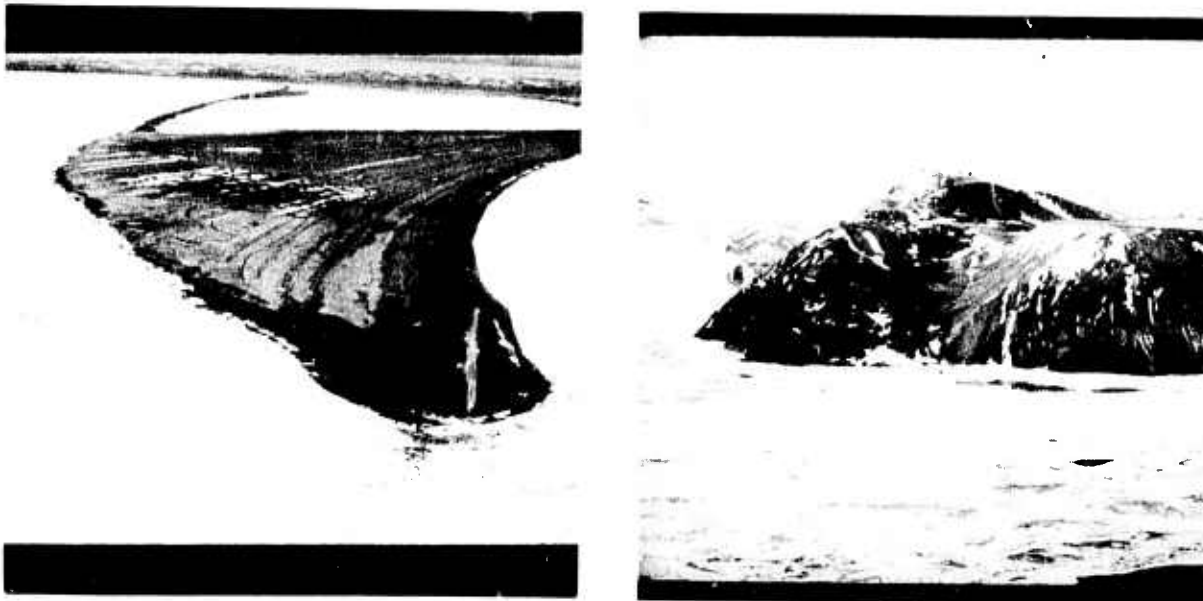
essentially unbroken sand-and-gravel barrier in the form of a long, symmetrical cusped foreland (Fig. 40A) backed by narrow lagoons. The Kukpuk River enters a lagoon on the northern side and is responsible for extensive shoaling in the lagoon. At the tip of Point Hope, numerous beach ridges, some slightly recurved, are present on the southern side, creating a beach ridge plain over 1 km wide. Washover fans are present on the back side of the barrier ridges, indicating topping by storm tides. This results in a highly crenulated lagoon shoreline. This province experiences significant wave power from early June through September. The highest wave power and total energy occur on the southern shore of the foreland, where the ice-free season is of longest duration.

Province 2 is dominated by steep rocky cliffs (Fig. 40B) up to 300 meters in height associated with the western extremities of the Brooks Range. Highest relief is in the vicinity of Cape Lisburne, where the Lisburne Hills form the prominent cape. Numerous small creeks drain the mountains and debouch into the sea via narrow valleys that are choked with sediment. Prominent beaches exist at each point at which a small stream intersects the coastline. Elsewhere along the coast, only narrow beaches are found at the foot of the steep cliffs. Structural control is evidenced by the extremely straight coastline segments and abrupt 90° change in orientation at Cape Lisburne. Aerial reconnaissance indicates numerous slump scars on the cliffs. Mass wasting of the steep slopes is augmented by freezing and thawing activity.

Province 3, though quite small, is distinguished from neighboring provinces by the fact that a barrier has impounded several small lagoons which have cliff scarps on their landward sides. Several creeks empty into the ocean along the shoreline and have fed sediment to the nearshore region, allowing wave action to construct relatively straight barrier islands. The barrier has numerous small inlets that appear to be ephemeral because their positions differ on two sets of photographs. The cliffs bordering the lagoon shoreline are not especially steep, and few slump scars are apparent on the photos. A marshy tundra behind the barrier appears to have formed as a result of deposition by the creeks emptying into and filling the lagoons.

Northeastward from Province 3, variations in nearshore circulation and wave properties are associated with the "Carolina cape" systems (Fig. 41) previously described. The long, NNE-trending shorelines separating successive capes have their greatest exposure to the higher energy westerly winds and waves. The shorter northwest-trending segments immediately north of each cape, as well as the east-west trending coastline between Cape Lisburne and Cape Beaufort, are sheltered from the westerly forces and receive their dominant energy from the more frequent but less intense northerly waves (Fig. 41). The strength of these northerly waves decreases toward Point Barrow owing to increasing proximity to the ice pack and the resulting reduction in fetch. Hence, littoral drift and sediment transport converge toward the capes, as indicated by Figure 41, causing accumulation of extensive shoals, bars and spits, and barriers. Divergence of drift approximately midway between the capes causes sediment deficiencies; beaches tend to be narrow and are frequently backed by eroding tundra scarps.

These wind and wave effects are probably augmented by the local current systems. Evidence of current separation and eddy formation past capes occurs around Cape Prince of Wales, 350 km south of Lisburne (McManus and Creager, 1963). Formation of clockwise eddies in the zones immediately northeast of the capes in the study region may result from separation of the north-flowing offshore current at the capes. South-flowing coastal currents along the coast between Cape Lisburne and Icy Cape were recorded by Fleming and Heggerty (1966) and Barnes (1972) and



A. View east during winter season at Point Hope showing beach ridge development.

B. View east during winter season at Cape Lisburne showing rocky cliff characteristic of province 2.

Figure 40. Photographs illustrating characteristic features of provinces 1 and 2.

were observed during the present study at Point Lay accompanying northerly winds (see Chapter III).

Province 4 lies within the southernmost zone of southerly drift and extends from the eastern end of Aycigatals Lagoon to a point just northeast of Cape Beaufort. The coastline is relatively straight but is sediment deficient. Although some small sand-and-gravel barriers are present, most of the shoreline exhibits cliffs and bluffs. On the western edge of the province, Sapumik Ridge parallels the coast and results in cliffs that attain heights of 60 meters. Very narrow gravel-and-cobble beaches are present at the foot of the cliffs. East of this ridge several small creeks enter the sea between bluffs 15 meters high. At the mouth of each creek, broad gravel beaches form slightly recurved spits. Bluffs exhibit steep slopes and are fronted by small gravel beaches (Fig. 42A). Near Cape Beaufort several other small creeks drain into the sea, forming coalescing alluvial fans with bluffs up to 15 meters high at the shoreline. These bluffs do not show any evidence of massive slumping, but the irregular, angular appearance of the shoreline suggests that thermal erosion of patterned ground is a major process responsible for shoreline changes. This type of morphology continues to the eastern boundary of the province.

Province 5 is essentially a narrow transition 25 km long separating the cliffs to the south from the barrier coastline to the north. Bluffs are generally low, less than 8 meters, and quite often broad gravel beaches are found along the shoreline. Wave action and thermal erosion of the tundra surface are the major processes responsible for shoreline erosion. Ice-pushed features along the shoreline are generally absent. The tundra surface behind the shoreline is highly irregular, and many small, poorly oriented lakes dot the surface. Thermal erosion of a large polygon pattern on the tundra surface has produced a highly irregular shoreline.

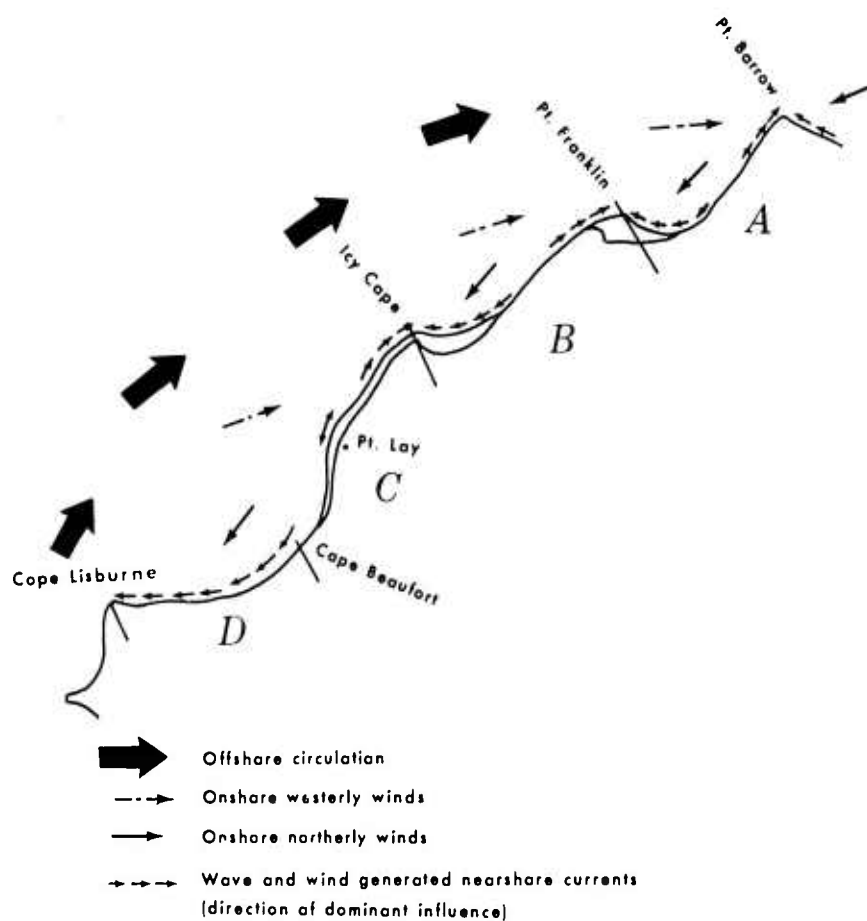


Figure 41. Diagrammatic representation of process regimes along the western Alaskan Arctic Coast. Areas A, B, and C are similar to "Carolina cape" systems, and area D has rocky shoreline. Note divergence of littoral currents along straight sectors and convergence of currents at the capes.

Narrow but nearly continuous barrier formations, backed by a narrow lagoon, dominate the shoreline landscape of province 6, which extends from the southern end of Kasegaluk Lagoon to Icy Cape.

Along most of its length the back side of the barrier consists of very low, marshy tundra displaying predominantly rectangular polygonal patterns. Irregular polygonal patterns are apparent on occasional tundra surfaces. Small, shallow lakes on the tundra behind the sand-and-gravel barrier show no significant orientation. The barrier island is interrupted by numerous narrow inlets along its length. The tundra surface and the creeks and rivers thaw before the ocean does, and during breakup splays of sediment spread onto the shorefast ice (Fig. 42B).

Recurved spits frequently occur on the lagoon side of the inlet. Although such features are common on both sides of the passes, the ones on the southern tip are usually more prominent. This might indicate a dominant migration of the passes to the northeast. In the northeastern part of the province, several abandoned



A. Sand beach deposits fronting erosional bluffs in province 4. Note drainage channels across the beach.



B. View north of Kukpowruk Pass in province 6. Note recurved spits protruding into Kasegaluk Lagoon and flushing of lagoon sediment over sea ice.



C. View onshore of low barrier island northeast of Icy Cape in province 7. Note the presence of two offshore bars and rhythmic cuspate features along lagoon shoreline.



D. View seaward showing storm washover fans characteristic of lagoon side of low barrier islands in province 7.

Figure 42. Photographs illustrating characteristic features of provinces 4, 6, and 7.

passes with relict spits are prominent. Tidal bars and deltas on both sides of the barrier exist off the passes, but the tidal delta built into the lagoon is usually larger and displays a more complex channel pattern.

The barrier varies in height, averaging from 3 to 4 meters in the southern part of the province and generally becoming lower to the northeast. Near Icy Cape the barrier is broad and is approximately 2.5-3.0 meters high. Gravel is common along the entire shoreline, but more sand appears to be present in the northern part, giving the foreshore areas a firmer surface.

The tundra surface behind the barrier is better developed near the southern part of the province and becomes less well developed in the northern region. Washover fans are much more abundant where the barriers are low (predominantly in the northern region). Offshore bars are normally present, and north of Point Lay one offshore bar is commonly persistent along the entire shoreline. As the offshore bar approaches a tidal pass, it moves seaward from the beach and gradually merges with the tidal delta bar. In the northernmost part of the province, particularly north of Akanuk Pass, two relatively continuous, straight offshore bars are present. In some places a third offshore bar can be seen, but it appears to have poor lateral continuity. Along the entire length of Solivik Island, the northernmost barrier in the province, two well-developed offshore bars are present, and the most characteristic strandline morphology is ridge-and-runnel topography. This morphologic pattern is presumably associated with the net decrease in northerly littoral drift and corresponding accumulation of sediment in the nearshore zone. Point Lay, one of the two sites of detailed field observations, is located approximately in the middle of this province and is described in detail elsewhere in this report. This site was selected for more intensive field investigations because it possesses most of the geomorphic and dynamic properties characteristic of the western zone.

Province 7 encompasses a shoreline distance of 82 km, extending from Icy Cape to Wainwright. This province lies within one of the regions of northerly exposure and southerly drift previously described and experiences lower wave energy than province 6. It extends northward to the postulated position of drift divergence.

The shoreline exhibits a broad concave-seaward arc with a coastline crenulation of 1.31. The entire province is characterized by a long, narrow barrier island (Fig. 42C) backed by a broad lagoon near its western edge which tapers to the northeast and terminates near the center of the province. Northward from this point the barrier impounds numerous small lagoons. The widest portions of the barrier are in the vicinity of the tidal passes which cut across the island and through which recurved spits protrude into the lagoon from both sides of the passes. Near the western end of the province the tidal passes show migration to the east, but elsewhere both directions of migration are evident. Flood-tide deltas are well developed, and there is some indication that a poorly developed ebb delta and bars exist.

Near the western end of the province the lagoon is infilled with algae-covered mudflats. Here the barrier is quite low, and numerous washover fans are evident (Fig. 42D). Ridge-and-runnel topography is characteristic along the strand, and at least two offshore bars are prominent. Farther northeast, elevations increase with increasing wave power. Sand and gravel are present, and gravel is concentrated at the berm and in the washover fans. Rhythmic cusped topography prevails along the lagoon side of the barrier, especially near the northeastern end of the province (Fig. 42C). Two offshore bars, well-developed ridge-and-runnel topography, and rhythmic topography along the lagoon side of the barrier are common. This type of rhythmic topography is most prominent in the smaller lagoons. Along the shores of the larger lagoons, long, high-angle spits are more common. In several instances

lobate features, probably washover fans (Fig. 42D), are present behind the barrier. These features are not inundated during normal high tide; so they must result from storm tide or high wind set-up within the lagoon. The landward lagoon shoreline shows bluffs 3 to 12 meters high and many small drainage channels emptying into the lagoons. Lowest scarps are found near the western and northeastern ends of the provinces.

A shoreline morphology reflecting littoral drift divergence and sediment deficiency typifies the 36 km of province 8. The coastline is relatively straight, apparently controlled by a primary 35° lineament, and has tundra bluffs 1.5-8.0 meters in height (Fig. 43A). Deep snow accumulations against the scarp insulate it against thermal erosion during breakup. Numerous small drainage channels, following thawed ice wedges, deliver sediment to narrow graveliferous beaches which front the tundra bluffs. Ridge-and-runnel topography characterizes the strandline, and at least two linear offshore bars are present throughout.

Northeast from the abandoned Atanik Village to Point Nalimut, littoral drift convergence has resulted in the accumulation of a long barrier system enclosing Peard Bay, a broad lagoon. This barrier system comprises province 9. The barrier consists of two basic units: the western portion has the form of a nearly continuous northeast-trending barrier spit influenced by northeasterly drift which terminates at Point Franklin; the eastern unit lies to the southeast of Point Franklin, where the shoreline abruptly changes direction to a southeast-northwest alignment.

The western portion of the province is exposed to the high westerly wave energy and displays a straight shoreline and few tidal passes. There are at least two prominent offshore bars. Ridge-and-runnel topography is characteristic at the shoreline, and at least two stranded berms are apparent (Fig. 43B).

The barrier is quite wide, having widths of up to 1.2 km. Barrier elevations are variable, but heights up to 2.5 meters are common. A flat, gravel-littered wind-deflation zone at the barrier crest is normally well developed. Dunes are found along the entire length but are better developed in the vicinity of the tidal passes. Most of the dunes consist of hummocky surfaces, and individual dunes rarely attain heights greater than 3 meters. Recurved spits at tidal passes curve abruptly into the adjacent lagoon (Fig. 43C). Beach ridges normally occur on both sides of the passes but are usually better developed on the southwestern side. This possibly indicates slow migration of the passes to the northeast. The size and depth of Peard Bay allow higher wave action in this lagoon than in more restricted lagoons to the south. Straight, low beaches, composed primarily of gravel and debris, flank most of the back side of the barrier shoreline.

The lower energy eastern portion of the province consists of many broken and irregular short barriers and shoals separated by numerous wide openings. The tidal passes are very shoal and rarely have depths greater than 3 meters. Inspection of aerial photographs indicates that the shoals have a tendency to change position constantly. The barrier islands are very low, rarely attaining elevations greater than 1.5 meters above sea level, and are composed primarily of gravel. Two offshore bars and ridge-and-runnel topography characterize the nearshore zone.

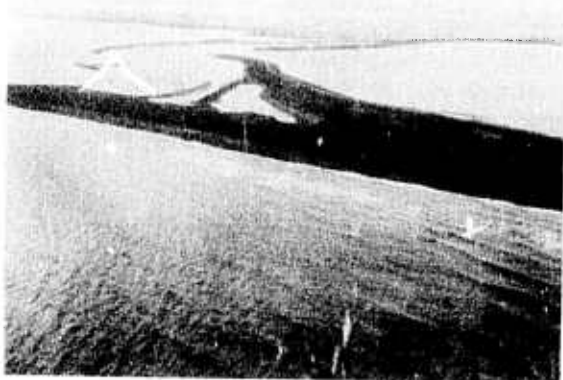
Peard Bay is 14.4 km wide at its widest point; depths commonly exceed 6 meters. Broad tidal passes allow exchange of water with the offshore. This lagoon is one of the largest along the North Slope. The landward lagoon shoreline displays low bluffs with heights of 3 to 4 meters. Numerous small drainage channels debouch into the lagoon; most are the result of thawed ice wedges. The tundra surface does not display great relief, most of the surface having an elevation of 15 meters, but isolated



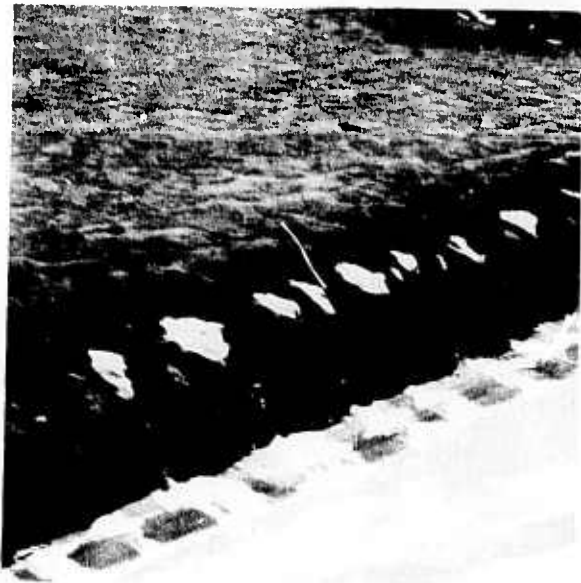
A. Tundra shoreline bluffs northeast of Wainwright, in province 8, during summer season. Note the narrow beach and offshore bar fronting the scarp.



B. Ridge-and-runnel topography on Seahorse Islands, in province 9. Note offshore bar indicated by breaking waves.



C. View of barrier island near Tachinisok Inlet, in province 9, during summer season. Note high-angle spits emanating from both lagoon shores.



D. View of tundra bluffs (Skull Cliffs) in province 10. Note sawtooth dissection associated with ice wedge thaw and development of "microfans" on beach.

Figure 43. Photographs illustrating characteristic features of provinces 8, 9, and 10.

hummocks reach elevations of 25 meters near the shoreline. Oriented lakes are not numerous near the shoreline, but farther inland they account for a high percentage of the tundra surface. Marshy areas representing drained lake basins are quite numerous near the shoreline. A very narrow gravel, debris-littered beach is present at the foot of the bluffs. Where the drainage channels intersect the shoreline, small sand flats offshore are exposed at low tide.

The Skull Cliff region comprises province 10, which extends from the eastern end of Peard Bay to a point near the Naval Arctic Research Laboratory. This province lies within the northernmost drift divergence region and is sediment deficient. The entire shoreline displays high bluffs backed by a relatively high tundra surface. Bluffs are about 8 meters high near the southwestern boundary and gradually increase in height toward the central part of the coast, where they attain heights of 15 meters.

The bluffs have a saw-toothed appearance as a result of differential thermal erosion of the ice wedges in the polygons (Fig. 43D). High-centered polygons are the most characteristic polygonal type near the shoreline. During the ice-bound season, shorefast ice abuts abruptly against the scarp, and a drape of snow often completely masks the scarp. At the foot of the bluffs there is commonly a narrow gravel beach (Fig. 43D) with a rather straight berm; only occasionally is ridge-and-runnel topography present. One prominent offshore bar exists nearly continuously along the entire shoreline. About thirty drainage channels empty into the sea along the shoreline. These vary in size from those that drain only a few polygon basins to those that extend 8-15 km inland and drain large areas of the tundra surface. The channels follow ice wedges, producing an angular drainage pattern. These channels deliver large sediment loads to the coast during the period of breakup. Subsequent wave action and tidal currents rework the material and disperse it along the coast. Where channels intersect the shoreline, well-developed, broad sand-and-gravel beaches occur. In most instances, a small channel cuts across the sand-and-gravel beach, and some runoff continues to occur throughout the summer period. In such cases, small bars seaward of the channel can be discerned. In other instances, wave action completely seals off the channel and will impound water behind the beach. In these regions the beach surface is extremely soft and in many instances will not support the weight of a man.

#### THE EASTERN ZONE PROVINCES

As along the western coast, the eastern zone experiences variations in wave intensity and direction of littoral drift and coastal currents associated with variations in exposure aspect. Four major barrier island chains and occasional segments of tundra coast are aligned parallel to the 312° lineaments and have an oblique exposure to the dominant northeasterly winds and waves (which prevail for about 70 percent of the time during open water). The associated westerly littoral drift is responsible for westerly migration of bars, spits, and inlets. Embayed sections to the west of barrier island arcs are partially sheltered from the easterly forces and face the less frequent but often intense westerly storms which appear to cause significant tundra erosion. However, the total energy of the eastern coast is considerably less than that of the western coast, and the changes in coastline orientation are less abrupt. Hence contrasts in coastline energy and littoral drift direction are much more subdued in the eastern zone.

Province 11 encompasses the Point Barrow spit and the northwest-southeast trending coastline between Point Barrow and Cape Simpson. The morphology of this province reflects the convergence of the northeasterly drift of the western zone and the northwesterly drift of the eastern zone. Although the extreme western portion

of the province lies within the western zone, it has been included with province 11 because its short length (<8 km) does not warrant isolation as a separate province and because of the geomorphic attributes it shares with the easterly portions.

From the western boundary of the province to Point Barrow the coastline has the form of a nearly continuous barrier spit. This system is moderately wide, averaging 0.3 km. Height varies considerably but averages about 2 meters. Numerous beach ridges with recurved segments are common near the point (Fig. 44A). The beaches are predominantly graveliferous, and one or two berms can be discerned. One prominent offshore bar exists, and a second, poorly developed one is sometimes present. Ridge-and-runnel topography is rarely present. Dunes are not especially common, and only small hummocks are present near the top of the barrier.

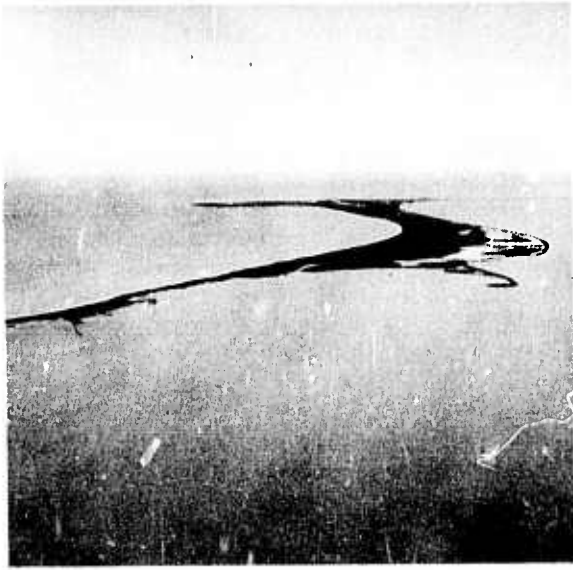
East of Point Barrow the barrier changes its character drastically as it abruptly assumes a northwest-southeast alignment. The barrier breaks up into numerous small, highly arched segments separated by numerous broad, shallow tidal passes. Barrier elevations are low, rarely exceeding 2 meters above sea level. Washover fans are common, and ice-pushed features are present on nearly every island. A prominent berm scarp exists, and rarely is ridge-and-runnel topography present. The barriers have a length-to-chord ratio of 1.15, which is higher than that of any barriers to the west.

At the point where it rejoins the mainland at McKay Inlet, the barrier narrows significantly and forms a beach at the foot of a tundra scarp 2-3 meters high. At points where the shoreline has eroded into an old lake, small barriers have formed, impounding saline water behind the beach. On the back side of the barriers, spitlike rhythmic features are common.

The barriers are backed by two large lagoons, Elson Lagoon and Dease Inlet, which have depths of about 3 meters throughout. The landward lagoon shoreline is highly crenulated (Table 9) and has numerous small inlets, eroded lake margins, and cusped headlands along the shoreline. The tundra bluffs behind the lagoon shores are not exceptionally high, averaging 2 meters. The polygons on the surface are relatively small, and the sawtoothed pattern is quite fine. Thermal erosion and subsequent slumping of the tundra surface are the major processes responsible for shoreline retreat. Numerous drained oriented lake basins have been truncated, resulting in lower scarps and mudflats along the shoreline. Both high- and low-centered polygons are found adjacent to the shoreline. A very narrow beach, composed of both sand and gravel, is occasionally found at the foot of the scarp. A few rhythmic features are seen along the shoreline, most commonly where a small drainage channel debouches into the lagoon. Storm debris lines are seen on top of the tundra surface at numerous spots along the coast.

The ice pack normally lies quite close to the shoreline during the summer season. Its position is dependent on wind conditions, and it can quickly move onto the beach area with a westerly wind. Small ice floes are common and can nearly always be seen in the nearshore region. Quite often they are grounded on the offshore bar and prevent any wave action from reaching the beach face.

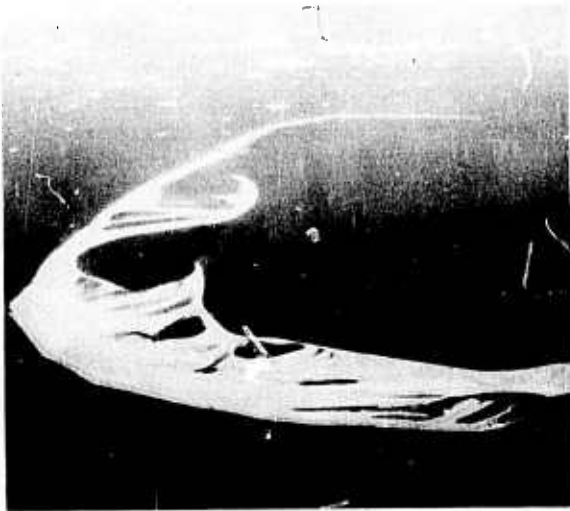
The highly indented shoreline between Cape Simpson and a point near the delta of Fish Creek comprises province 12. The crenulate shoreline is 165 km long and owes its irregularity in large part to coalescing oriented thaw lakes which are now truncated by the coast. There are few offshore barriers or shoals; most of the shoreline consists of tundra scarps fronting the Beaufort Sea. Just south of Cape Simpson the shoreline trends north-south fronting Smith Bay. This shoreline consists of a very low tundra scarp with an elevation of only 1.5 meters (Fig. 44B).



A. View north of Point Barrow in province 11.



B. View of tundra shoreline in the vicinity of Cape Simpson, in province 12.



C. View east of Cross Island, in province 15. Note arcuate form of the barrier and high-angle easterly deflected spits on the lagoon shoreline.



D. View seaward during winter of tombolo connecting Manning Point to the mainland.

Figure 44. Photographs illustrating characteristic features of provinces 11, 12, 15, and 19.

Much of the shoreline has truncated oriented lake basins, and smooth, rounded indentations mark the shoreline. In many instances little or no scarp exists, and the low tundra surface simply merges with the bay waters. Thermal erosion is the most active process in this region, and beaches are essentially nonexistent at the foot of the scarp.

The delta of the Ikpikpuk River is building into and filling Smith Bay. Broad sand flats crossed by multiple braided channels are the most common landform. Algal flats with a variety of types of ice-pushed and drag features are quite common. No beaches are apparent, and little wave energy is expended on the coast because of the very flat offshore subaqueous slope. Comparisons of photographs indicate that the channels are prone to change their positions often and the shoreline is in constant flux.

From the Ikpikpuk River to Fish Creek the shoreline trends in a variety of directions and is highly indented. The bluffs vary considerably in height, ranging from 1 to 5 meters. As elsewhere in this province, the truncation of large lake basins results in rounded indentations along the coast, and thermal erosion is the major process causing coastal retreat. Near Drew Point the shoreline is composed of rectangular slumped peat blocks, indicating the rapid retreat of this shoreline. Farther east, near Esook Trading Post, more irregular polygons are present on the tundra surface, and the slumped peat blocks are more triangular. Sand and silt have been pushed back over the tundra surface by high storm waves.

Farther east, a few small barrier formations occur at the mouths of truncated oriented lakes (e.g., Pogik Bay). These barriers are narrow and arcuate, and there are numerous recurved spits on the lagoon shores.

The Colville Delta and its marginal coasts make up province 13. This province has been described in detail by Walker (1969, 1973) and Walker and McCloy (1969). Owing to deltaic progradation and the presence of numerous distributary mouths, the coast is highly crenulate.

The entire shoreline is composed of broad mud and sand flats and intervening highly braided channels. The river mouths are bell shaped and have well-developed offshore river-mouth bars and shoals. Algal flats are extensive, and a variety of types of ice-pushed and scour features are common on the flats. Occasionally, small beaches composed almost entirely of reworked peaty material are present along the strand. The interior of the delta consists of both highly braided and meandering channels, and there are numerous abandoned channel scars. Irregular lakes are quite common between the river channels. The channels are unstable and change their courses constantly. Thermal erosion during high river stage results in deep notches being cut into the peaty tundra material, and slumped peat blocks are common. In many instances these blocks are carried into the central part of the channel and incorporated into the channel deposits. Longitudinal eolian dunes up to 10 meters high occur along the eastern channel banks opposite large midchannel bars.

Offshore, the subaqueous profile is flat or slightly convex ( $HI = 0.51$ ) owing to abundant sediment supply. These offshore profile characteristics are common to many deltas. As a result of this flat profile and consequent attenuation of wave power, the shoreline wave power is lower than in any other province.

Province 14 extends from Oliktok Point to Point McIntyre, 65 km to the east, and encompasses the Jones Islands and associated Simpson Lagoon. Although the Jones Islands are among the highest of the eastern barrier islands, they generally typify the beach and barrier morphology of the eastern zone. For this reason Pingok Island,

the largest island in the Jones group, was selected as the eastern field site for more intensive investigation. Pingok and neighboring islands are described in detail elsewhere in this report. Pingok Island and other larger members of the Jones group consist of graveliferous beaches and spits anchored to tundra remnants which average about 5-7 meters in elevation. The latter appear to have been isolated from the mainland by the process of thaw lake coalescing and truncation previously described. Relatively narrow inlets exhibiting rapid easterly migration separate the barriers. The strandline is characterized by a variety of forms, including ridge-and-runnel topography, rhythmic beach topography, and linear berms.

Simpson Lagoon, which separates the island from the mainland, averages 4 km wide and rarely exceeds 3 meters in depth. The landward lagoon shoreline is highly crenulate as the result of intensive thermal erosion and displays numerous headlands which appear to be related to the 35° lineaments. Shoreline bluffs attain elevations of 6 meters. The Kuparuk River empties into the lagoon and probably supplies much of the material composing the offshore barriers.

Province 15 extends from Point McIntyre to Bullen (or Savakvik) Point. Prudhoe Bay, the deltas of the Sagavanirktok, Kadleroshilik, and Saviovik rivers, and numerous small offshore barrier islands compose the landscape of this province.

Three offshore barrier island chains, the Midway, McClure, and Stockton islands, are situated on a linear offshore shoal at an average distance of 10 to 12 km from the mainland shore. These islands and the shoal on which they lie are aligned parallel to the northwest-southeast trending lineaments. The majority of the islands have crest elevations of only 1-2 meters. The barriers are highly arcuate and widely spaced. The western ends of the islands display recurved spits suggestive of westerly migration; however, high-angle spit features on the lee shores of the islands appear to be migrating eastward (Fig. 44C). Ridge-and-runnel topography is prominent, particularly in the Stockton group.

Owing to the greater fetch between the offshore islands and the mainland shoreline, the latter receives somewhat greater wave energy than that of province 14. As a result, narrow beaches and spits have accumulated at the bases of tundra bluffs to smooth the shorelines, except in the vicinity of delta lobes. Wherever the shoreline is unaffected by the presence of deltas, correlation with lineaments is strongly evident. The eastern shores of Prudhoe Bay (near the western province boundary) and Mikkelson Bay (near the eastern province boundary) are nearly linear and coincide with 35° lineaments, whereas two linear segments of tundra coastline flanking the Kadleroshilik River trend northwest-southeast.

The morphologies of the Sagavanirktok and other smaller deltas are similar to that of the Colville Delta. Multiple branching, bell-shaped distributaries are separated by sand and mud flats and numerous small lakes.

Province 16 extends from Bullen Point to the westernmost distributary of the Canning River. The Maguire Islands comprise a moderately continuous chain of barrier formations lying approximately 5 km seaward of a crenulate mainland shore. Like the other barriers of the eastern zone, the islands are arcuate and are separated by frequent inlets; however, the average unbroken barrier length is greater than in province 15, and inlets are narrower. Like Pingok Island, Flaxman Island, the largest of the chain, consists of a tundra remnant on which gravel beaches and spits have become anchored. The islands are fronted in the nearshore zone by numerous oblique littoral bars. Well-developed rhythmic beach topography is associated with these bars. The eastern distributary of the Canning River, which debouches near the eastern boundary of the province, presumably supplies much of the

the largest island in the Jones group, was selected as the eastern field site for more intensive investigation. Pingok and neighboring islands are described in detail elsewhere in this report. Pingok Island and other larger members of the Jones group consist of graveliferous beaches and spits anchored to tundra remnants which average about 5-7 meters in elevation. The latter appear to have been isolated from the mainland by the process of thaw lake coalescing and truncation previously described. Relatively narrow inlets exhibiting rapid easterly migration separate the barriers. The strandline is characterized by a variety of forms, including ridge-and-runnel topography, rhythmic beach topography, and linear berms.

Simpson Lagoon, which separates the island from the mainland, averages 4 km wide and rarely exceeds 3 meters in depth. The landward lagoon shoreline is highly crenulate as the result of intensive thermal erosion and displays numerous headlands which appear to be related to the 35° lineaments. Shoreline bluffs attain elevations of 6 meters. The Kuparuk River empties into the lagoon and probably supplies much of the material composing the offshore barriers.

Province 15 extends from Point McIntyre to Bullen (or Savakvik) Point. Prudhoe Bay, the deltas of the Sagavanirktok, Kadleroshilik, and Saviovik rivers, and numerous small offshore barrier islands compose the landscape of this province.

Three offshore barrier island chains, the Midway, McClure, and Stockton islands, are situated on a linear offshore shoal at an average distance of 10 to 12 km from the mainland shore. These islands and the shoal on which they lie are aligned parallel to the northwest-southeast trending lineaments. The majority of the islands have crest elevations of only 1-2 meters. The barriers are highly arcuate and widely spaced. The western ends of the islands display recurved spits suggestive of westerly migration; however, high-angle spit features on the lee shores of the islands appear to be migrating eastward (Fig. 44C). Ridge-and-runnel topography is prominent, particularly in the Stockton group.

Owing to the greater fetch between the offshore islands and the mainland shoreline, the latter receives somewhat greater wave energy than that of province 14. As a result, narrow beaches and spits have accumulated at the bases of tundra bluffs to smooth the shorelines, except in the vicinity of delta lobes. Wherever the shoreline is unaffected by the presence of deltas, correlation with lineaments is strongly evident. The eastern shores of Prudhoe Bay (near the western province boundary) and Mikkelson Bay (near the eastern province boundary) are nearly linear and coincide with 35° lineaments, whereas two linear segments of tundra coastline flanking the Kadleroshilik River trend northwest-southeast.

The morphologies of the Sagavanirktok and other smaller deltas are similar to that of the Colville Delta. Multiple bifurcating, bell-shaped distributaries are separated by sand and mud flats and numerous small lakes.

Province 16 extends from Bullen Point to the westernmost distributary of the Canning River. The Maguire Islands comprise a moderately continuous chain of barrier formations lying approximately 5 km seaward of a crenulate mainland shore. Like the other barriers of the eastern zone, the islands are arcuate and are separated by frequent inlets; however, the average unbroken barrier length is greater than in province 15, and inlets are narrower. Like Pingok Island, Flaxman Island, the largest of the chain, consists of a high tundra remnant on which gravel beaches and spits have become anchored. The islands are fronted in the nearshore zone by numerous oblique littoral bars. Well-developed rhythmic beach topography is associated with these bars. The eastern distributary of the Canning River, which debouches near the eastern boundary of the province, presumably supplies much of the



A. View landward of Hulahula River delta, in province 19, with Brooks Range in background. Note the braided patterns characteristic of these rivers.



B. View northwest of barrier in the vicinity of Humphrey Point, in province 21. Note alternating concave and convex (plan view) beach ridge patterns of the barrier.

Figure 45. Photographs illustrating characteristic features of provinces 19 and 21.

To the east of Jago Spit the coast (provinces 20-22) is aligned to a northwest-southeast lineament. In addition, higher wave energy, resulting from a larger fetch to the east, has produced a relatively continuous, straight shoreline backed by narrow lagoons and fronted by occasional multiple outer bars. This section is similar in process and form to parts of the western coast.

Province 20 extends from Tapkaurak Entrance to Polok Bay. A long, straight barrier, Tapkaurak Spit, continues to Polok Lagoon, where it joints the tundra. The barrier is backed by a narrow lagoon (average width 2.50 km) and an irregular tundra shoreline. A single outer bar parallels the shore for several kilometers; however, most of the province has no offshore bars. Between Polok Lagoon and Polok Bay straight tundra bluffs are undergoing active thermal and wave erosion.

Province 21 begins at Humphrey Point and extends as a series of long, straight barriers across the coalesced deltas of the Aichilik, Egaksrak, and Korgakut rivers. Beaufort, Egaksrak, and Siku lagoons, parts of a narrow (average width 1.83 km), shallow lagoon, separate the delta front from the barrier. A series of three to four rhythmic offshore bars parallels the barrier (Fig. 45B).

Reconnaissance did not extend east of Icy Reef and hence did not include province 22. This province is dominated by Demarcation Bay, a relatively large, deep (average depth 3 meters) embayment with two irregular recurved spits extending from either side of the embayment mouth. Tundra bluffs extend the remaining 9 km to the U.S.-Canadian border.

## CHAPTER V

### BEACH PROCESS-RESPONSE INTERACTIONS

#### Introduction

Two field sites, Pingok Island and Point Lay, were chosen for more detailed studies of higher frequency beach process-response interactions. These sites were selected because the regional variability study and aerial reconnaissance indicated drastically different morphological landforms at the two sites and because they appeared to be representative of the two major coastal segments east and west of Point Barrow. The results of the study will be discussed in the context of the three major events that occur along the Alaskan Arctic North Slope: breakup, open water, and freezeup. Each site will be presented separately inasmuch as far more information was obtained at the Pingok Island site. The period of occupation at each site and the type and extent of field instrumentation and techniques employed are listed in Table 10. Much of the data in this chapter is contained in a dissertation by Short (1973).

#### Instrumentation and Field Techniques

Instrument arrays were deployed in the immediate vicinity of each camp area to record atmospheric pressure, air temperature, and wind speed and direction. Atmospheric pressure and air temperature sensors were placed in a climate hut 180 cm above the ground; pressure was recorded continuously on a Weather Measure Corporation B211 microbarograph, and temperature, on a Bendix thermograph. Wind-recording equipment has been previously described.

At Pingok Island a capacitance tide gage was installed but was lost during a period of strong wave action. Tide data were, however, read from June 17 to August 20 on a calibrated staff placed seaward of the swash bar in front of the camp. This method was reliable until sea ice breakup, when wave activity and ice movement made maintenance of the staff impossible.

Wave characteristics were recorded by visual observation, except for a short period at each site when four resistance wave staffs were set up off the beach. The results of these studies have been presented in a previous section.

Nearshore currents at 2-meter depths were measured by tracking the movement of drogues, as discussed in Chapter III.

Variations in beach elevation were monitored by placing an array of steel beach stakes (1 meter long, 6 mm in diameter) at set intervals (3.05-6.1 meters) across the beach. Each stake was pushed 60-70 cm into the beach surface. The initial elevation of the surface at the stake relative to sea level and the position of the stake across the beach were recorded. Subsequent beach changes were noted by measuring the distance from the top of the stake to the beach surface. Stakes lost during beach erosion were replaced and the surface elevation resurveyed. Beach grids were established by arranging the sections in parallel rows. This permitted monitoring

Table 10

Instrument Array, Point Lay and Pingok Island, 1972

	April	May	June	July	August	September	October
Occupation	—	—	—	—	—		—
Cup Anemometers	—		.....	.....	.....	.....	
Climet, Microbarograph, and Thermograph	—	—	—	—	—	.....	—
Wave Gages					—	.....	
CSI Tide Staff				—	—		
Braincon	—			—	—		
Drogue Releases					.....	.....	
Salinity- Temperature Profiles	•	••	••	.....	.....	.....	
Beach Profiles and Surveys		—	—	—	—	.....	—
Fathometer Profiles				•	•	•	•
Aerial Reconnaissance	•	••	••	•	•	•	•

— • • Point Lay  
..... • • Pingok Island

of lateral variation in beach elevation. Four beach grids were established on Pingok Island: three on the ocean beach, one with five rows and two with three rows of stakes; and one on the lagoon beach. In addition, eighteen separate profiles were surveyed across the adjacent Jones and Return islands and on the mainland tundra shoreline. At Point Lay one five-row beach grid was established. The frequency of grid surveys ranged from daily on the five-row grids to twice weekly on the three-row grids. Three spits at either end of Pingok Island and on the western end of Leavitt Island were surveyed several times during the study. A theodolite and surveyor's staff were used to make all surveys.

A Raytheon Company Model DE-731 fathometer depth recorder was used to run offshore depth profiles at Pingok and Leavitt islands. Thirty-five ranges were established along the islands and a depth profile run off each. Distance offshore was monitored with a sextant or fixed by radar.

Data reduction and analysis were completed in the laboratory using Wang Calculators, Model 700 Series, a Calma VIP 303 electronic digitizer, and an IBM 360 computer.

Wind speed and direction and air temperature and pressure were read at hourly intervals (6-hourly in the case of DEW Line data) and reduced to daily and monthly averages.

Individual beach profiles were plotted using a Varian plotter. Changes in beach area,  $A$ , between two successive stakes on a profile were calculated by

$$A = (a_1 - a_2)L + \{[(a_1 - a_2) - (b_1 - b_2)] L/2\} \quad (10)$$

The changes in beach volume,  $V$ , between two parallel sets of beach stakes were calculated by

$$V = d(A_1 + A_2)/2 \quad (11)$$

Figure 46 schematically defines the parameters referred to above.

The area and volume changes between each set of measurements were calculated for each beach grid. The volume changes were tabulated into negative, positive, and cumulative totals for the area and volume changes between each two or four beach stakes (see Fig. 46).

Sand samples were dried and sieved at 1/4  $\phi$  intervals. Sediment characteristics were determined by the method described by Inman (1952).

Surveys of spits and nearshore morphology were plotted by hand and contoured at 0.5- and 1-meter intervals, respectively. The maps were digitized on a Calma VIP 303 electronic digitizer. A computer program then transformed these data to net and cumulative area and volume figures at each contour interval.

#### Breakup

Breakup refers to the period of time during which snow and ice cover and frozen ground begin to thaw and be destroyed. This is initiated when air temperatures consistently remain above 0 C for a significant period of time. The melt begins in May and continues through July, accelerating in accordance with the rate of temperature increase above 0 C. By early August, surface melt and breakup on the coastal plain, rivers, and nearshore zone are usually complete, although retreat of the pack ice and thaw of the permafrost continue until September, when the freeze-up period is initiated.

Along the Alaskan Arctic Coast, initiation, duration, and extent of breakup vary both regionally and annually. In general, the timing of breakup is related to latitude; the lower the latitude, the earlier the warming trend. Regionally, ice in the relatively warmer inland areas and southwestern coast breaks up before that on the northwestern and eastern coast. On the western coast, breakup begins in May at Point Hope, reaches Point Lay by mid-June, and arrives at Point Barrow by late July. On the eastern coast, it begins in July at Demarcation Point and reaches Pingok Island and points west by late July.

Previous studies of breakup pattern are limited. The only maps showing the extent of breakup along the Alaskan Arctic Coast are contained in the Oceanographic Atlas of the Polar Seas, Part II (U.S. Navy Hydrographic Office, 1958). However,

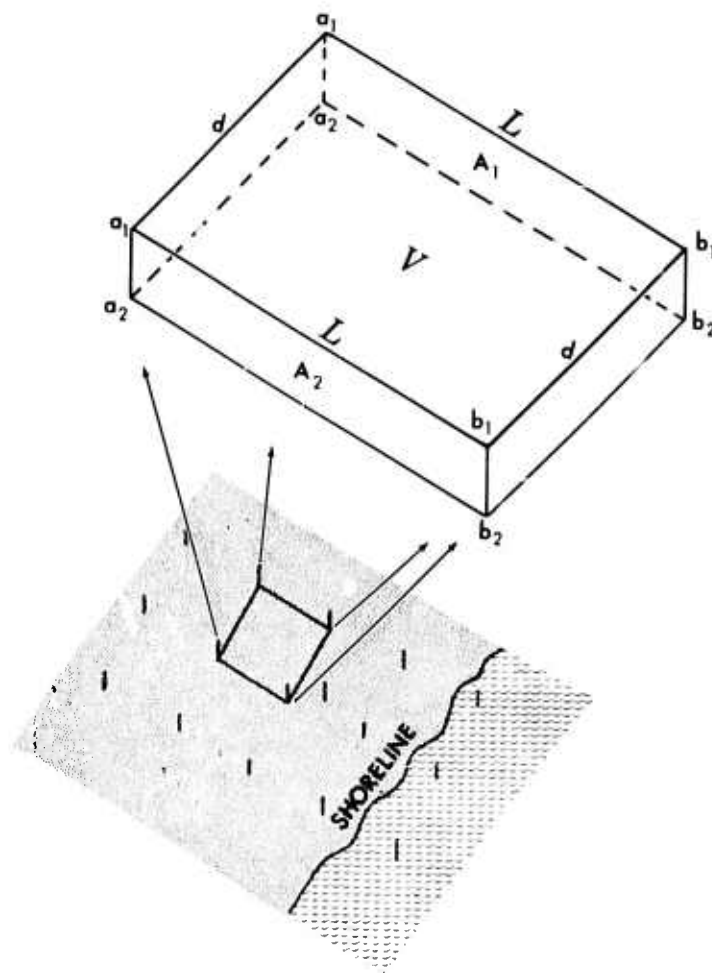


Figure 46. Schematic diagram illustrating definition of parameters used in calculating beach area and volume changes.  $L$  is distance between stakes perpendicular to shoreline and  $d$  is distance parallel to shoreline.

the atlas is based on only 5 years of data, and our 1972 observations indicate that they should be interpreted with caution. Locally the effect of river breakup in the coastal zone has been studied off the Colville (Walker, 1972; Reimnitz and Bruder, 1972) and the Kuparuk (Barnes and Reimnitz, 1972). No work has yet described the regional breakup pattern and its relation to the beach and nearshore morphology.

Breakup will be examined in three interrelated and roughly sequential phases: (1) river breakup, in particular its effect on the lagoons and nearshore zones; (2) sea ice breakup in the coastal zone; and (3) beach thaw. Figure 47 plots the mean daily temperature at Point Lay and Pingok Island for the breakup period. Significant periods of melt or ice movement are recorded in the adjacent columns: Point Lay in the right-hand column, Pingok Island in the left-hand column. The figure indicates that breakup is closely related to the arrival of above 0 C temperatures



and to the subsequent rise in temperature. At Point Lay, where temperature rose earlier and higher above 0 C than at Pingok Island, breakup began earlier and was more rapid.

#### RIVER BREAKUP--ITS EFFECT IN THE COASTAL ZONE

Earlier inland warming initiates melt of the snow cover and subsequent river flow several days to weeks before thaw of the coastal zone. Much of the rivers' annual discharge and suspended sediment load may be delivered to the receiving basin during this period. The Colville delivers half of its discharge and 75 percent of its suspended sediment load during the first 3-4 weeks of river flow (Arnborg et al., 1967; Walker, 1969). Much of this sediment bypasses the ice-covered nearshore area and is deposited seaward of the 2-meter contour (Reimnitz and Bruder, 1972), where the meltwater begins to flow under the sea ice. The relatively warmer sediment-laden river water not only directly melts the ice but also decreases the albedo.

#### Point Lay

On May 24, 1972, the Kukpowruk River, 18 km south of Point Lay, was flowing from its mouth onto frozen Kasegaluk Lagoon (R-1, Fig. 47). The following day, this water had spread 8 km north between the lagoon shore and the seaward barrier. On May 27 (R-2), flow from the Kokolik or Utukok rivers (20 and 45 km north of Point Lay, respectively) had combined with flow from the Kukpowruk, flooding the Point Lay section of the lagoon. This combined meltwater began flowing through the Point Lay inlet onto the nearshore fast ice, forming a lobate pool several hundred square meters in size seaward of the inlet. The pool grew slowly in size, its area not accounting for the magnitude of flow through the inlet. Obviously fractures had formed in the sea ice, allowing flow to continue under the ice. Reimnitz and Bruder (1972) referred to these drainage holes as strudel. The pool reached its maximum size on May 29, drained, and exposed a veneer of sediment on the sea ice. On June 3 (RS-2), an open lead appeared off the inlet and grew rapidly seaward approximately 400 meters. Within 24 hours the lead extended 200 meters north and 500 meters south of the inlet, running along the outer side of the inlet bar pressure ridge.

The lagoon level dropped significantly on June 4 (R-3), exposing the remaining bottomfast ice. Lagoon outflow continued and the inlet lead grew rapidly, extending 2 km seaward and 1 km laterally by June 9. Flow out of the inlet continued until June 13, when a 15-cm rise in sea level caused reverse flowage and seawater flowed into the lagoon, carrying ice cakes with it (SR-1). Figure 48A (page 99) shows the extent of the lead and general breakup on June 13.

On June 17 the remaining lagoon bottomfast ice disintegrated, leaving the southern part of Kasegaluk Lagoon ice free (R-4). Air reconnaissance on June 26 indicated the presence of ice only along the northern reaches of the lagoon.

#### Pingok Island

Pingok Island and the surrounding region had an initial breakup pattern noticeably different from that of the Point Lay region. The difference resulted from variation in the thermal and fluvial regimes and regional morphology. Situated between the largest river in northern Alaska, the Colville (to the southwest) and the Kuparuk and Sagavanirktok rivers (to the east), it lies in an area of large freshwater inflow.

Breakup in the Colville River has been reported by Walker (1972, 1973) and Reimnitz and Bruder (1972) and in the Kuparuk River by Barnes and Reimnitz (1972).

Meltwater flows from the rivers over the lagoon bottomfast ice. In 1971 flow from the Kuparuk advanced as a lobate front at rates of 15-30 cm/sec, accelerating through the inlet between Long and Egg islands (Barnes and Reimnitz, 1972). In Simpson Lagoon, river flow covered the lagoon ice as far east as Bertoncini Island (P. Barnes, personal communication). The weight of the water initially depresses the sea ice, soon breaking through it and flowing seaward under the ice. In 1971 the surface flow of the Colville advanced up to 12 km over bottomfast ice in Harrison Bay before draining under sea ice. It then flowed seaward at a rate of about 45 cm/sec, advancing as far as 35-40 km seaward (Walker, 1972).

In 1972 the Colville was flowing by May 30 (R-1), but the Kuparuk did not begin flowing until June 1 (R-2) (E. Reimnitz, personal communication). The Sagavanirktok had flooded Prudhoe Bay by June 6 (R-3) (C. Lund, personal communication). The Colville floodwater had advanced within 2 km of Thetis Island (RS-1) by June 7. The eastern edge of the Colville flood, from Oliktok Point toward Thetis Island, remained fairly stationary. On June 7 open water extended from the Colville across Harrison Bay to Kogru River (RS-3), an area of approximately 1,000 km<sup>2</sup>. The eastern edge remained in a line from Oliktok Point to Spy Island. The eastern edge is possibly held stationary by the greater depth of Simpson Lagoon, which permits the floodwater to flow under the lagoon ice, where westerly currents can redirect it. On the night of July 13-14 the ice at the eastern edge of the floodwater plume began breaking up, and during July 14 the remaining ice in Simpson Lagoon, considerably weakened by melt, began moving westward under an 8-15-knot northeast wind (R-4). By afternoon less than 1 percent ice was visible on the lagoon. The large open-water areas in Harrison Bay no doubt acted as a receiving basin for the moving ice, facilitating its rapid breakup.

The inlet between Pingok and Leavitt islands was unaffected by the initial river outflow (May 30-June 27). A lead appeared on June 27 (RS-2) and coincided with the 2.5-meter-deep inlet channel. This lead was initiated by surface melt and tidal flushing below the ice. By July 12 the lead extended 2 km along the southwestern shore of Pingok Island and 200 meters seaward. Prior to lagoon breakup (July 14) the lagoon shoreline of Pingok Island was almost surrounded by leads from the eastern and western inlets. At the time of lagoon breakup, the lead extended 1 km seaward.

Inlet leads initiated by tidal action rather than river outflow appear to be dominant along the entire eastern coast. Aerial reconnaissance during this period and examination of aerial photographs taken during breakup in 1955 indicate that the majority of inlets are opened by tidal flushing similar to that observed in the Pingok Island inlet. Inlets affected by river floodwaters lie in areas immediately seaward of the rivers or along the western coast, such as described at Point Lay. These two types of breakup in inlets are significantly different and deserve greater study in future projects.

Breakup of the rivers and flooding of the adjacent lagoon and sea ice with relatively warm river water has considerable local effect on coastal breakup. Along the western coast, the small number and size of streams and rivers and the presence of relatively continuous barrier islands off most rivers and two embayments confine the river breakup to a section of the lagoon and adjacent inlets. The river water therefore has little direct effect on the regional sea ice breakup. Along the eastern coast, rivers are far more numerous and greater in size. Their effect is considerably greater, the surface flow of the Colville extending up to 12 km seaward and under-ice flow up to 40 km (Walker, 1972). In the vicinity of the river mouths, hundreds of square kilometers of bottomfast and sea ice are broken up by river meltwater. However, much of the breakup effect is contained by the generally wider nature of the lagoons and the presence of wide embayments, such as Smith Bay and Dease

Inlet. Therefore, most of the outer shoreline remains unaffected by river water and must wait for breakup of the sea ice. The influx of warm river water under the sea ice does, however, accelerate sea ice melt. To the east, the large discharge of the Mackenzie River appears to effect early breakup of several thousand square kilometers of sea ice.

#### SEA ICE BREAKUP

##### Point Lay

Sea ice breakup is initiated by melt once air temperatures rise above 0 C. At Point Lay this occurred sporadically in early May (S-1, Fig. 47) and continuously after May 31. This is some 2 1/2 to 3 weeks earlier than at Pingok Island. The ice melt and salt water seeping through tidal shear fractures rapidly gather in surface pools (S-3). Sediment blown onto the ice decreases the albedo and accelerates melting. By May 27 most of the snow cover had melted and melt pools (approximately 50 meters by 10 meters in size) had formed, exposing fractures in the sea ice (Fig. 48A). Air reconnaissance on June 13 showed approximately 30 percent of the sea ice covered by interconnected pools. Except near the inlet, shorefast ice deposited above sea level during the 1971 freezeup formed a boundary between the beach and the pools. Meltwater from the beach face ran under this ice, depositing sediment in the pools (BS-1).

Sea ice begins moving out only after it has been weakened and fractured by the melt, when enough open water is available for the ice to move into, and when winds generate offshore Ekman drift. On June 18 (S-4), 12-knot NNE winds began actively moving ice southwest, and by midafternoon all ice just south of the camp had been moved out. Only a 20-meter band of shorefast ice remained. Boat reconnaissance on June 21 indicated no visible pack ice 25 km south of Point Lay, although scattered ice cakes were common. Hartwell (1971) gives June 24 as the average date for breakup at Point Lay on the basis of a 4-year record. On June 26 aerial reconnaissance showed that ice had moved out as far north as Inuvik Pass and was not present between Icy Cape and Wainwright (S-5). On July 6, the ice had moved out as far north as Point Franklin (S-6).

The time elapsed between initiation of continuous ice melt and sea ice breakup was approximately 5 weeks. The ice, weakened by melt, moved out rapidly under north and northeast winds. Open water south and west also facilitated this movement. In the absence of offshore bars, no hindrance to ice movement existed, and open water extended immediately to the outer edge of shorefast ice. In the presence of bars, nearshore ice will ground and ice movement will be drastically restricted. Figure 48B shows grounded ice on offshore bars in the vicinity of Icy Cape on July 16, 1949.

##### Pingok Island

Sea ice breakup began with sporadic melt in early May (S-1). Not until June 9 (S-2), nearly 3 weeks later than at Point Lay, was melt continuous. Melt pools rapidly developed, and by June 19 had made contact with the beach face (SB-1). The absence of extensive shorefast ice permitted a continuous melt lead 1-20 meters wide to form along the shoreline by July 14 (SB-2), and by July 19 melt pools covered most of the sea ice. At this stage, breakup lagged approximately 4 weeks behind that at Point Lay.

Offshore ice movement was initially observed on July 20 (S-3), when a large lead formed several kilometers offshore. On the morning of July 24 (S-4) the



A. Aerial view of Point Lay on June 13, 1972. Note the relatively ice-free lagoon (upper right), inlet lead (center), muddy melt pools on the sea ice (aligned to the northeast), and reactivated sea ice fractures.

B. Sea ice grounded on outer bars to the east of Icy Cape on July 16, 1949. Note the decrease in size of the ice cakes toward the shore.

Figure 48. Photographs illustrating characteristic features during breakup.

offshore ice began moving west, driven by a 20-knot northeast wind. By late afternoon the outer edge of the ice lay approximately 10 km offshore. Throughout the next day, 25-knot northeast winds continued to move the ice westward at an accelerating rate. By July 26 there was between 10 and 100 meters of open water immediately seaward of the beach. A 600-meter-wide band of scattered fast ice which was grounded on the bars (ice coverage  $\approx$  50 percent) lay seaward of this open-water zone. It took from July 24 to August 6 before all the grounded ice had disintegrated (S-6). Thus the period required between continuous ice melt and sea ice breakup was approximately 7-8 weeks, considerably longer than at Point Lay.

#### BEACH THAW

Melt of the snow- and ice-covered beaches at Point Lay and Pingok Island was coincident with melt of the sea and lagoon ice (Fig. 47). At Pingok the surface of the beach was completely ice free the first week in July, 3 weeks before sea ice breakup. At Point Lay, however, the beach still contained buried ice and shorefast ice following sea ice breakup. The difference in the two melt patterns was a result of the 1971 freezeup conditions at both sites.

#### Point Lay

Freezeup processes at Point Lay the previous year (1971) resulted in

accumulation of alternating layers of snow, ice, and sediment (Fig. 49). This structure continued alongshore over a distance of several kilometers. In addition, a gravel-covered storm ice foot (Rex, 1964) was present on the lower beach face (a, Fig. 49), and a 20-30-meter-wide, 2-3-meter-thick body of shorefast ice covered the nearshore zone to a depth of 2 meters. Tidal and/or storm action had pushed new winter ice onto the fast ice, building a 1-2-meter-high ice ridge paralleling the outer edge of the shorefast ice (b, Fig. 49). Figure 50A is a photograph illustrating this ice ridge. The entire beach area and nearshore zone were covered with a 1-1.5-meter blanket of snow. A minimum of 15 m<sup>3</sup> of ice per unit width was incorporated into or over the beach surface.

Melt was initiated in early May (B-1, Fig. 47), and by May 13 the foredune and gravel crest of the ice foot were exposed (B-2). Figure 50B shows the crest of the ice foot and its gravel-coated and pitted surface on May 29. The sandy surface of the foredune thawed rapidly, permitting the surface water to sink into, rather than flow over, the surface. As a result, no water or streams flowed across the beach surface, except under the fast ice on the lower beach face.

Beach thaw was monitored on the surveyed beach grid, and eight surveys were made between May 25 and June 25. The beach was trenched on June 5, revealing alternate layering of ice, sand, and gravel to a maximum depth of 1.5 meters. The surveys indicate that melt of the buried ice layers caused the beach sediment to collapse an average of 50 cm, the depth ranging from 25 cm on the upper beach to at least 1 meter under the ice foot. The average volume decrease was 10 m<sup>3</sup> per meter width of beach. A similar volume of ice was deposited on the Pingok Island beach in fall 1972 and preserved through the winter.

By June 1 the beach was still 50 percent snow covered, but by June 9 the upper beach was free of surface snow (B-3) and the ice foot had thawed to a level lower than that of the adjacent beach surface. Figure 50C shows the depression formed by the melted ice foot; it is flanked by angular scarps, and gravel piles overlie the remaining ice cores. Continued thaw of the ice foot lowered the depression, increased the height of the scarps to a 10-40-cm maximum, and left gravel piles 10-60 cm in height (Fig. 50D). Similar melt features have been described by Greene (1970).

The fast ice seaward of the ice foot gradually retreated down the beach face, exposing an irregular stream-eroded surface. On June 18 the remaining shorefast ice was lifted off by a rise in sea level (SB-1), thus exposing the beach face to wave action for the first time during the study.

By June 20 the ice foot was almost completely thawed, except where overlain by thick gravel deposits. The removal of the ice layers and subsidence caused increased distortion of the sedimentary layers toward the surface. This resulted in an upper beach layer (up to 1.5 meters thick) containing mottled and complex interbedding (Short and Wiseman, 1973).

On the surface, however, eolian action was already smoothing the angular surface expression of the ice melt and subsidence. On June 26 only subdued surface forms and a little subsurface ice remained to attest to the frozen landscape existing just 6 weeks earlier (B-5).

#### Pingok Island

At Pingok Island, the beach thaw sequence varied significantly from that at Point Lay as a result of the duneless tundra backing and variation in the 1971

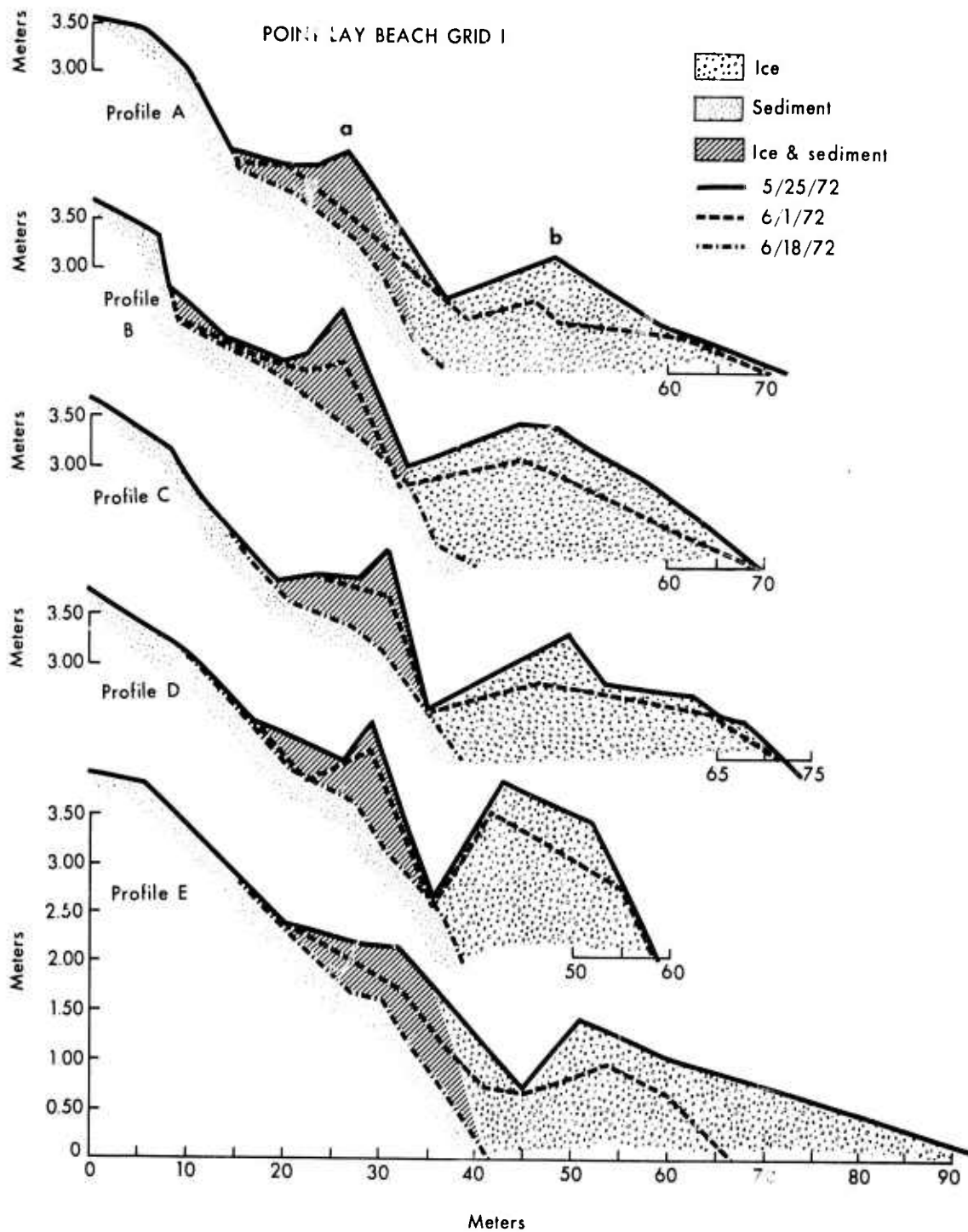


Figure 49. Beach profile changes across grid I, Point Lay. The subsidence of the beach surface is a result of melt of the ice and ice-sediment structures. The letter a indicates storm ice foot; b, shoreline pressure ridge.



A. View landward of shoreline pressure ridge and exposed foredune just north of Point Lay. Photograph taken from 15-meter-high ice-pushed ridge on May 25, 1972.



B. Ground-level view toward south at Point Lay of exposed foredune (left), exposed crest of gravel-covered ice foot (center), and shoreline pressure ridge (right). Snow has leveled the depression between these forms. Photograph taken May 25, 1972.



C. Point Lay beach on June 9, 1972. Note the subsiding gravel-covered ice foot (center); the thawing ice-sediment layers (left); the lower beach face still partially ice covered (right); and the foredune (far left).



D. Gravel piles, up to 60 cm high, following partial thaw of the ice foot. The larger piles have ice cores. Note the prominent scarp between the ice foot depression and the lower beach face. Point Lay, June 20, 1972.

Figure 50. Photographs illustrating sequence of beach thaw.

freezeup processes. Snow had begun melting during the first week in June. By June 8 small streams of meltwater were flowing onto the still-frozen beach surface and under the snow cover (B-2, Fig. 47). Flow from the streams continued until June 12, by which time the streams had built "microfans" extending from the foot of the tundra several meters across the upper beach (a, Fig. 51). In areas protected from wave action, fans covering tens of square meters of beach are developed over a period of years. Similar forms have been described by Greene (1970), who termed them "microdeltas." However, this term does not distinguish the "fans" from melt-stream deltas deposited at the shoreline by larger tundra streams flowing right across the beach.

The 1971 freezeup at Pingok Island and along much of the eastern coast had been accompanied by calm sea conditions. The flotsam lines mark the upper limit of swash activity during 1971 (b, Fig. 51) and 1970 (c, Fig. 51). In addition, no sea ice was deposited on the beach face during freezeup. During the winter, relatively little snow accumulated on the beach face (average snow thickness 0.5-1.0 meter) inasmuch as it lies on the windward side of the island. Consequently, little ice or snow covered the beach.

#### NEARSHORE ICE MOVEMENT

The movement of ice floes in the nearshore zone (shoreline to approximately 2 km offshore) has not been monitored to any great extent along the Alaskan coast. It was intended to monitor the ice movement during this study by utilizing the radar unit at both Point Lay and Pingok Island. However, at Point Lay the unit was not installed and operating properly until after breakup and after strong offshore winds had moved the ice offshore. As a result, currents were monitored by drogue-tracking, as discussed in Chapter III. At Pingok Island, also, the ice moved far offshore prior to installation of the radar unit, and thus little information was obtained on ice movement at the two sites. When ice was in the nearshore region, intermittent grounding prevented use of the ice cakes as natural current drogues.

The Naval Arctic Research Laboratory made available four canisters of 1,700-foot, 16-mm color time-lapse movies taken by Mr. Don Stephens of the Naval Electronic Laboratory. These time-lapse movies were taken during the period June through November 1958 at three sites at Point Barrow. One site was atop the gymnasium at the NARL site, and the camera was pointed 300° true north. This orientation is approximately at right angles to the shoreline trend. The camera station viewed the beach and nearshore area, and ice could be tracked as it moved across the viewing area. Exposures were taken at 1-minute intervals during the entire period except when film change was necessary. In addition to the photography, DEW Line and U.S. Weather Bureau meteorological data (wind direction, intensity, temperature, etc., at 6-hour intervals) at Point Barrow were available over the same period of time. Thus the movement of the ice could be correlated with wind direction, and any deviation from wind direction is undoubtedly the result of nearshore currents.

A 16-mm motion analysis projector was used to analyze ice movement. A single offshore bar was present in the nearshore, and the ice movement was tabulated in two zones: (a) between the shoreline and the offshore bar and (b) from the offshore bar seaward to the limit of view (estimated to be 2 km offshore). Each frame was projected individually; ice floes in the respective zones were marked, then the next frame was projected and the same floes marked again. A total of 60 frames or 1 hour real time was thus projected. The number of frames or time it took individual floes to cross the field of view were then counted and averaged for the entire hour. It must be realized that this gives only relative rates of motion inasmuch as flows farther seaward will take longer to cross the field of view.



Figure 51. The beach in the vicinity of grid I, Pingok Island, in July 1972. Note the shoreline melt: microfan (a); 1971 flotsam line (b); and 1970 westerly storm flotsam (c).

Figure 52 shows the results of this film analysis for the period July 9 through July 27, when most of the ice had disappeared from the nearshore. The bottom curves show the northern or southern movement of the ice between the shoreline and offshore bar. The scale is relative; the number of frames (or minutes) it took ice floes to cross the field of view averaged over an hour. The second curve from the bottom shows the northern or southern movement of ice floes in the zone seaward of the outer bar. The two upper curves are wind direction and velocity. Winds from the southern quadrants should move ice north, alongshore, whereas northerly quadrant winds should produce southerly ice drift. Any deviation from this pattern is caused by currents in the water mass that apply stress on the subaqueous portion of the ice floes.

The net movement of ice during the entire period is to the north, but major reversals to the south occurred on July 10, 11, 18, 23, and 24. In many instances, ice floes seaward of the offshore bar would be moving north, and ice floes in the zone between the outer bar and the shoreline (July 14) would be moving south. The results of this analysis include the following:

- (1) Over the entire period, ice floes generally follow the wind direction, but periods of reversals do occur for short times.
- (2) Direction and velocity of ice movement between the shoreline and offshore bar are quite different from the movement of the ice seaward

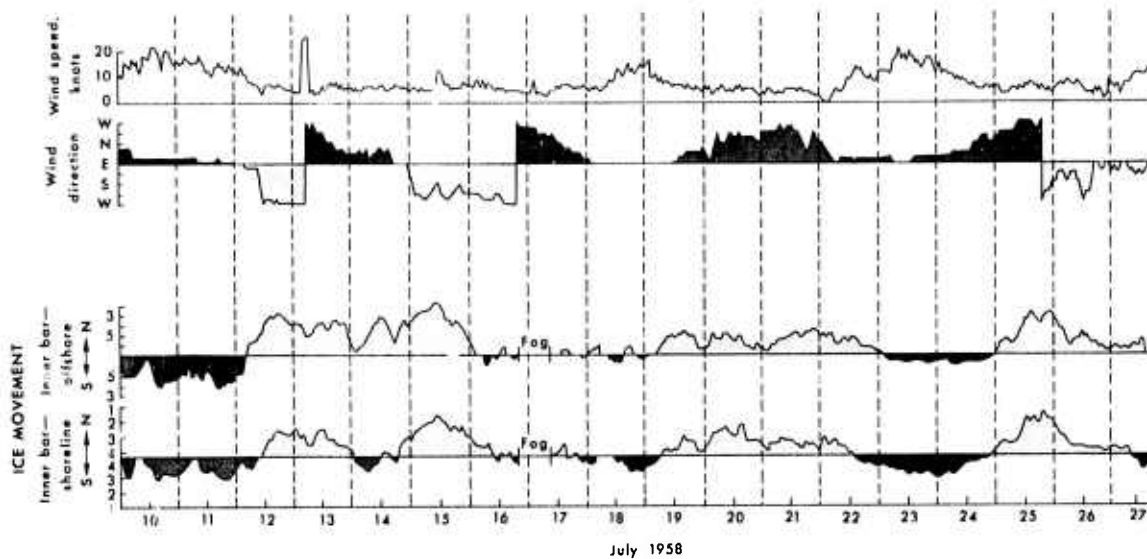


Figure 52. Graphs showing relationship between ice movement (lower two curves) and wind speed and direction (upper two curves) at Point Barrow. Subsequent to July 27 there was little or no ice in the nearshore region.

of the offshore bar. This difference is associated with circulation induced by wave and tidal processes interacting with bottom topography between the shoreline and offshore bar. In a following discussion, this circulation will be described in relation to the bar configurations.

- (3) Smaller ice floes react more quickly and follow wind pattern more closely than do larger floes. If wind direction remains constant for 4-6 hours at moderate intensities (12-15 knots), larger ice floes will parallel wind direction after a lag of 2-3 hours. However, during periods of low wind intensity the larger floes follow and react more to residual currents in the water mass than do the smaller floes.
- (4) During periods of low wind intensity, ice floes generally move more slowly in both zones and display a more erratic drift pattern (July 16, 17, 18, Fig. 52).
- (5) In the zone seaward of the offshore bar, ice floes, both large and small, drift at a significantly faster rate when the offshore pack ice is near the coast than when it is farther offshore.
- (6) Initiation of a strong onshore wind results in initial movement (after a 1- to 2-hour lag) of the ice onshore, but when it moves to within a few hundred meters from the offshore bar it tends to parallel the coast, and only the smaller floes will move directly onshore and ground on the bar.
- (7) During onshore wind conditions, ice floes between the offshore bar and

the shoreline will move parallel to the coast and then move directly offshore through breaks in the bar. In many instances, ice floes in this zone would be moving both north and south alongshore until a break in the bar occurred (one break was within the view of the camera) and then would drift through this gap.

- (8) Low wind velocities associated with an offshore wind direction cause extremely erratic drift directions and velocities. Ice floes can be seen moving in all directions during such periods.

## DISCUSSION

Breakup along the Alaskan Arctic Coast can be separated into three inter-related areas of influence: (1) the rivers; (2) sea ice; and (3) the beach.

River breakup affects the coastal area immediately adjacent to river mouths. The area of influence depends on several factors: (1) breakup discharge of the river, which determines the volume of relatively warm fresh water delivered to the coastal zone; (2) nearshore morphology, especially the distance to the 2-meter contour, which determines the extent of bottomfast ice over which the river water must pass before flowing under the sea ice; (3) the presence of barriers and inlets adjacent to the rivers which confine or channel the flow; and (4) the coastal currents, which will redirect the flow once it is under the sea ice. River breakup locally effects breakup of lagoon and nearshore ice 1-10 weeks before sea ice breakup.

Sea ice breakup is dependent on above 0 C temperatures' melting and weakening the pack ice; wind-generated offshore Ekman transport to drive weakened ice seaward; an area of open water downwind to receive the ice; and, locally, on the presence of bars which ground ice, delaying final breakup by up to 2 weeks.

Beach thaw begins when above 0 C temperatures initiate melt and continues until all ice on or in the beach has melted. The presence of ice in the beach deposits will prolong thaw and upon melting will generate unique beach forms, including gravel piles, pits, kettle holes, distorted bedding, depressions, and scarps. In the absence of dunes, tundra meltwater flows onto and across the beach, building microfans at the tundra-beach interface and microdeltas at the shoreline.

### Open Water

Open water occurs when less than one-tenth of the water surface is covered by floating ice. In this study, the term is more generally used to refer to the period between breakup and freezeup, when the edge of the pack ice is seaward of the shore. The removal of the ice permits wind and pressure systems to interact with the water and land surfaces, generating waves, currents, sea level fluctuations, eolian action, and saltwater-freshwater mixing. These processes, coupled with the thermal effects of above 0 C temperatures, are here called the open-water processes. Open water is therefore a period when the purely arctic nature of the environment, the ice cover, is partially removed, and processes common to all coastal environments--waves, currents, tides, and eolian activity--may act. The influence of the high latitude remains, however, in the presence of a large Coriolis parameter, pronounced Ekman transport, and the effect of proximity of the pack ice on wave generation.

Open-water processes and the associated responses of the beach and nearshore zones at Point Lay, Pingok Island, and selected sites will be discussed in this

section. The morphological response in the study area is examined in several frequency ranges, from daily beach changes to island migration.

The atmospheric and marine processes operative during the 1972 open-water period at Point Lay and Pingok Island are summarized in Figures 53 and 54 and Table 11.

At Point Lay, westerly winds (mean direction  $230^\circ$ ) arrived during 30-50 percent of the July-August period and northerly winds (mean direction  $50^\circ$ ) during 50-60 percent (Table 11). Westerly winds generated moderately high wind waves (average height 1 meter, period 4-6 seconds), and northerly winds generated lower waves (average height 30 cm, period 2-3 seconds). Three westerly storms occurred during the period of site occupation, the first two from August 5 to 7 and 8 to 11, the third from October 8 to 12. Wind-generated nearshore currents ranged in velocity to 50 cm/sec or more. Sea level fluctuations related to wind and pressure effects (Fig. 53, plot of July/August tides) had a maximum range of 100 cm. No ice returned to the shore following breakup.

At Pingok Island northeasterly winds, associated with high-pressure systems, arrived 63 percent of the time during the open water months, August and September. The resulting wind-generated waves, currents, and eolian action dominate the morphology. In addition, the northeast winds caused offshore movement of ice, lowered sea level and air temperature, and produced coastal fogs. One severe easterly storm, coincident with an exceptionally long fetch of several hundred kilometers, occurred from September 4 to 9. Westerly winds associated with low-pressure systems arrived 37 percent of the period. These winds generated westerly waves and east-flowing currents, raised sea level and air temperatures, and produced onshore movement of sea ice. Sea level had a maximum range of at least 90 cm. During August the waves were low, averaging 16 cm in height and having a period of 1.8 seconds. In early September the pack ice moved out, enabling higher waves to be generated (average height and period of 60 cm and 5.4 seconds, respectively).

#### PINGOK ISLAND

Beach responses were continuously monitored during the open-water period at Pingok Island; less frequent monitoring was conducted at Point Lay. The various frequencies of responses and their relation to input energy conditions form the following discussion on the Pingok Island site.

##### Beach Sediment Characteristics

Thirty-six sediment samples were collected on the beach face and swash bar to determine the size distribution in the grid at Pingok Island. Table 12 indicates the bimodality of the samples, the median diameters being  $-2.5$  and  $1.45 \phi$ . The presence of a significant coarse fraction (33 percent pebbles and granules) is characteristic of most Alaskan Arctic beaches. At Barrow, Rex (1964) reported composite median diameters of beach sediment of  $-1.27 \phi$  and  $-0.05 \phi$  and at Cape Thompson Moore (1966) reported a composite modal diameter of  $-2.75 \phi$ .

Sorting of the sediments was generally good, showing a significant relationship between mean diameter and sorting (Fig. 55). Moore and Scholl (1961) reported that the coarse Cape Thompson beach sediments were well sorted. The relationship between mean diameter and skewness (Fig. 55) shows a tendency for negative skewness in the finer fractions and positive skewness in the coarser fractions, though considerable scattering exists in both fractions.

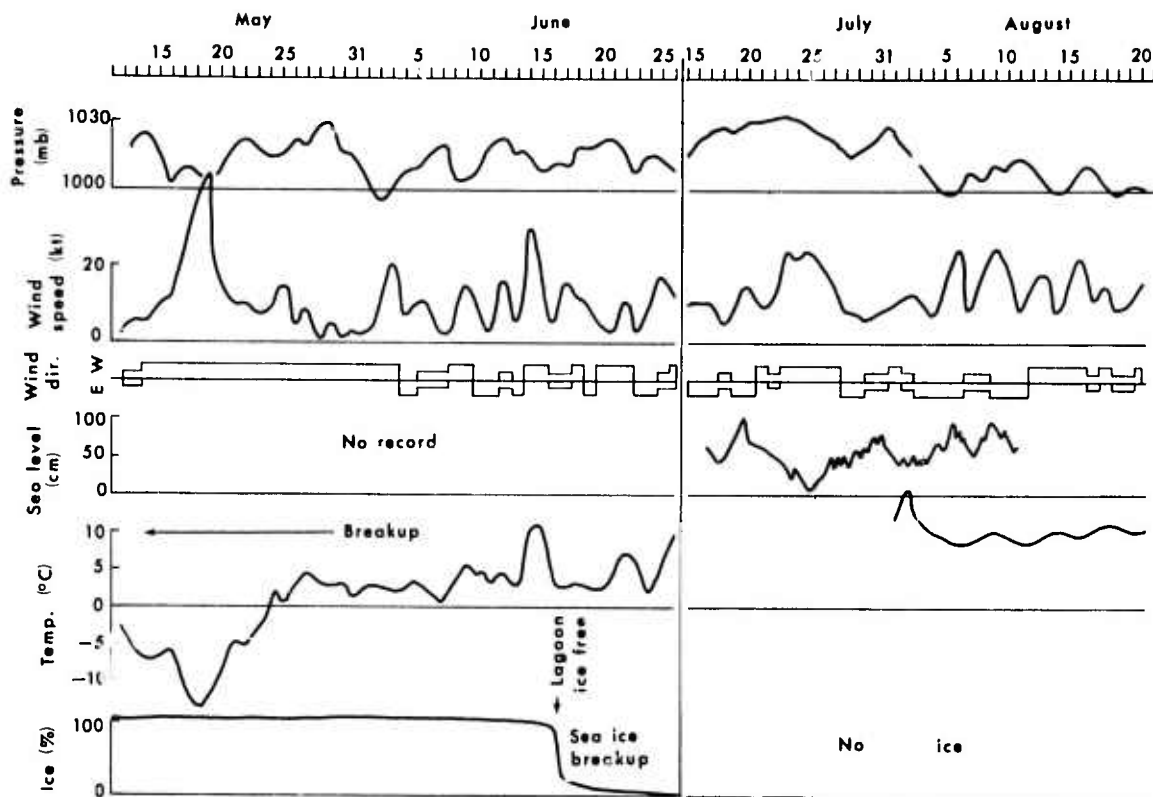


Figure 53. Plot of daily averages of selected marine and atmospheric parameters for Point Lay site, May 11 to June 26 and July 15 to August 21, 1972.

Figure 56 shows the location and grain size distribution of three sets of sediment samples across the swash bar and beach face. Three zones of sediment size and sorting are apparent. On the shallow inner bar (profile C, samples 6 and 7), sediments are medium grained, poorly sorted, and negatively skewed ( $M\phi = 1.5$ ,  $\sigma\phi = 0.7$ ,  $Sk\phi = -0.5$ ). The coarse size fraction increases shoreward onto the gravel swash bar (profiles C, D, and E, samples 1, 2, and 5), where the distribution was bimodal and positively skewed ( $M\phi = -1.4$ ,  $\sigma\phi = 2.3$ ,  $Sk\phi = 0.6$ ). Size decreased up the beach face (profiles C, D, E, samples 3 and 4), resulting in medium-grained, well-sorted, negatively skewed sediment at the swash limit ( $M\phi = 1.52$ ,  $\sigma\phi = 0.45$ ,  $Sk\phi = -0.1$ ).

The results indicate that the Pingok Island sediments (1) are typical of Alaskan Arctic beach sediments; (2) possess size-sorting and size-skewness relationships similar to those exhibited by non-arctic beaches; and (3) are zoned by size across the surf zone.

#### Two-Dimensional Beach Response

The type and magnitude of two-dimensional beach response are directly related to the input wave conditions. These conditions in the Arctic are in turn a function of the available fetch and prevailing winds, as discussed in a previous section. Fetch is dependent on the position of the pack ice.

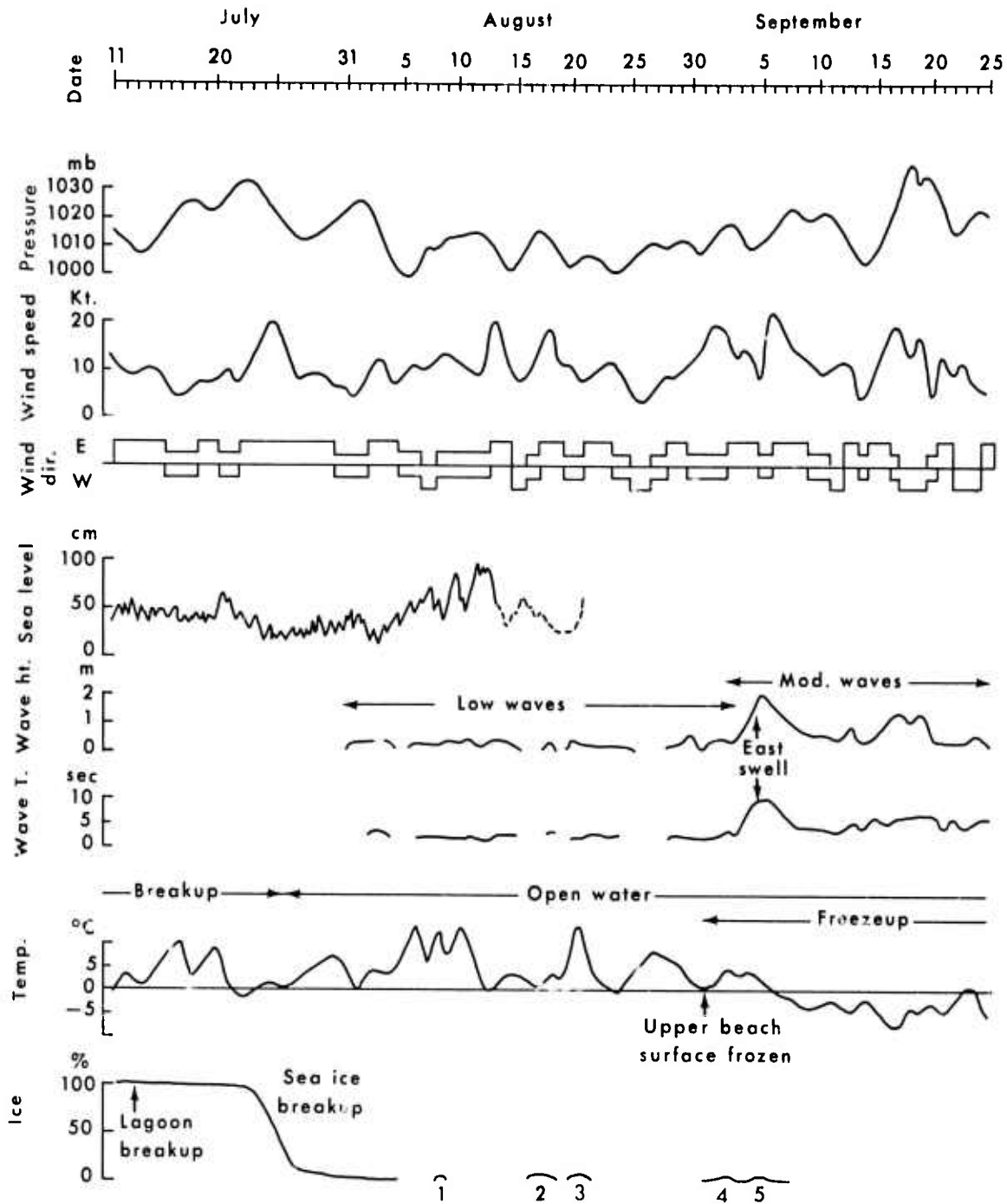


Figure 54. Plot of daily averages of selected marine and atmospheric parameters at Pingok Island site, July 11 to September 25, 1972.

Table 11  
 Summary of Daily Means of Selected Marine and Atmospheric Parameters  
 at Point Lay and Pingok Island

Date	Quadrant*	Wind			Mean Pressure	Mean Temp. (°C)	Waves		
		Speed <sup>#</sup> (kt)	Direction T.N.	Per-cent-age			H (cm)	T (sec)	Per-cent-age
<u>Point Lay</u>									
May 1-31	N-E 315-135°	13	42°	85	1015	-4			
	W 136-314°	9.5	209	15					
June 1-30	N-E W	12 7	44 225	65 30	1009	4.6			
			calm	5					
July 15-31	N-E W	16 10	64 234	50 50					
Aug. 1-31	N-E W	11 15	55 244	63 32	1007	9.4			
			calm	5					
<u>Pingok Island</u>									
July 11-31	E 1-180° W 181-360°	10.1	38°	85	1013.5	1.5			
		5.9	284°	15					
Aug. 1-31	E W	11.0 8.7	50° 276°	63 37	1009.3	2.4	12 24	1.9 1.6	52 23
Sept. 1-25	E W	12.7 13.5	66° 279°	63 37	1019.0	-1.3	67 50	5.4 5.3	58 42

\*Wind and wave characteristics are summarized according to the quadrant from which they arrived.

<sup>#</sup>Wind speed is average of all speeds.

To measure beach response beach grids were established, and the location of the grids was dependent on the planar morphology of the beach and proximity to the field camp. The Pingok Island beach varies considerably in width owing to the presence of shoreline rhythms. Therefore, three grids (I, II, and III in Fig. 57) were established to check for lateral variation in beach response. To record the cross-sectional characteristics and lateral variability of beaches and barriers of the adjacent Jones and Return islands, eleven profiles were surveyed at representative sites across six islands or their beaches (Fig. 2, numbers 1 to 11).

At Pingok Island two distinct periods of wave intensity and beach response

Table 12

## Composite of Pingok Island Beach Sediment

	$\phi$	Percentage	Median $\phi$ Diameter
Pebbles	-2 to -6	20	
Granules	-1 to -2	13	-2.5
Very Coarse Sand	0 to -1	7	
Coarse Sand	0 to -1	13	
Medium Sand	1 to 2	37	
Fine Sand	2 to 3	10	1.45
Very Fine Sand	3 to 4	Tr.	

occurred during 1972. Short, low waves dominated from breakup to September 4, and significantly larger waves arrived until at least September 26. Both periods can be directly related to the position of the pack ice. Prior to September 3, the pack ice remained relatively close to shore (10-20 km), but an easterly storm (September 4-8) moved the ice offshore in excess of 100 km, permitting the generation of swell and moderately large wind waves. The maximum possible fetch to the east of Pingok Island during this period was 1,000 km.

Beach response during the low-wave periods (average wave height 16 cm, average period 1.8 seconds) was confined to a 5-10-meter-wide surf zone. The maximum length of swash uprush was 12 meters; the swash reached an elevation of 0.5 meter above sea level. The surf zone consisted of a submerged gravel swash bar upon which waves broke as plunging or spilling breakers; the beach face, composed of bimodal sediments; and the area near the swash limit, where either a miniature gravel berm or small erosional scarp was formed.

Variation in the prevailing wind, wind waves, and sea level conditions effected rapid response of the beach. The mean variation in sea level associated with alternating easterly and westerly winds was 22 cm, and maximum range was 90 cm. Westerly winds raised sea level, moving the surf zone up the shore, and easterly winds moved it down. As a result, if easterly winds were followed by westerly winds, the upper beach features were preserved. However, in the reverse situation, the lower beach features were submerged and reworked by the swash. During periods of falling water level a series of berms and/or scarps was formed across the beach face, often only centimeters apart, whereas during higher water level periods only a single berm or scarp was present at the swash limit. Figures 58A and 58B show miniature beach features generated by low waves. During the 32-day period between breakup and September 3, eight separate berms and four scarps were formed along grid I.

The net effect of the high-frequency beach response to small wave agitation was a superficial disturbance of the lower beach face. Along grid I the net change in beach volume per unit surface from July 22 to September 3 ranged from 0.03 to 0.2 m<sup>3</sup>, and cumulative totals ranged from 0.1 to 1.0 m<sup>3</sup> (Fig. 59). The overall two-dimensional beach configuration was unaffected.

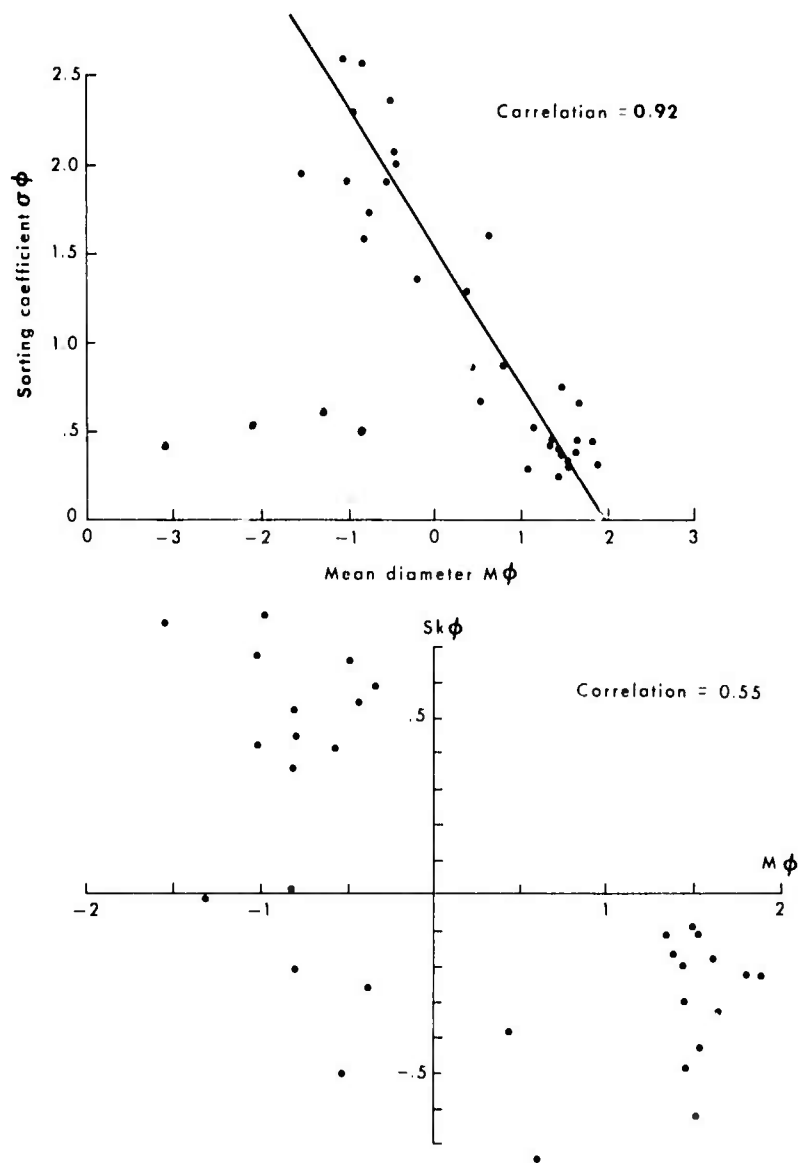


Figure 55. Relationship between mean grain diameter and sorting coefficient, and mean grain diameter and skewness, for Pingok Island beach samples.

The extent of such small wave conditions in the Arctic is considerable. Evidence along the Jones Islands (Fig. 2) indicates that during the entire 1971 open-water period similar conditions dominated, the swash never overtopping the beach crest (0.75-1.0 meter above sea level). At Barrow, Hume and Schalk (1964) have reported years (e.g., 1955) when the sea ice remained in during the entire open-water period, and other seasons when an average seasonal wave height of 17 cm was recorded.

Along the Alaskan North Slope, such small wave conditions are more likely to occur and persist along the northwestern coast above Point Franklin and along the

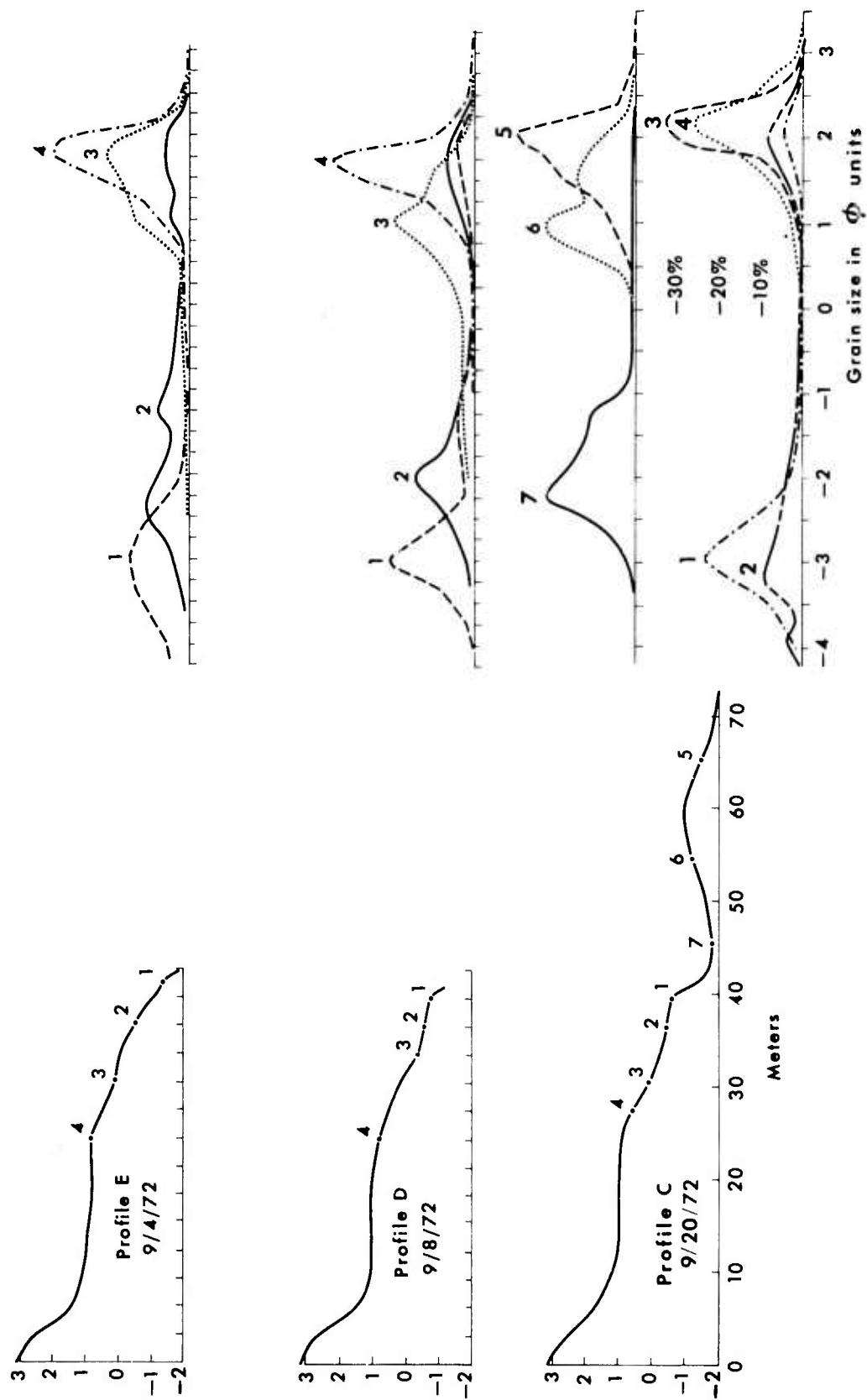


Figure 56. Variation in grain size distribution across three beach sections on Pingok Island, grid I. Numbers on beach profiles refer to grain size distribution curves on right.

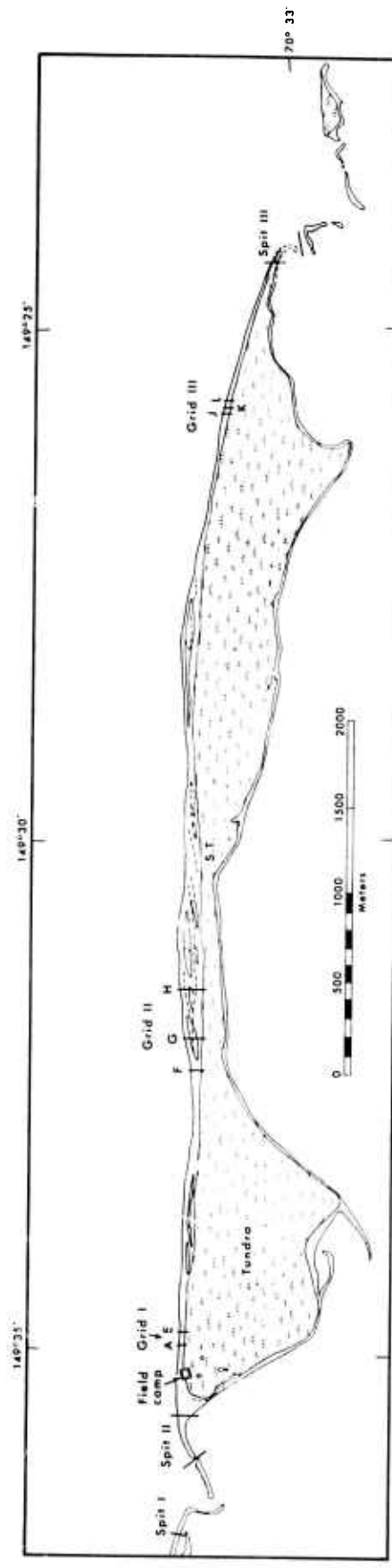


Figure 57. Map of Pingok Island showing location of the field camp, beach grids (I, II, and III), profiles A-L, and spits surveyed (I, II, III).



A. View of the lower beach face showing gravel bands backed by a miniature berm. The gravel bands represent earlier berms that were flattened by rising swash. Pingok Island, August 10, 1972.



B. Miniature ridge-and-runnel system backed by a small erosion scarp. The line of driftwood on the beach represents the 1971 limit of wave activity. Waves are approximately 15 cm high. Pingok Island, August 14, 1972.

Figure 58. Photographs illustrating details of small-scale beach features formed during low wave action.

eastern coast between Barrow and Jago Spit. In these areas, the pack ice limits the fetch (Fig. 38).

The second period of beach response at Pingok Island resulted from an offshore movement of the pack ice, reinforced by an easterly storm (September 4-9). The larger fetch (approximately 100-200 km) permitted the generation of moderate swell (height 2.0-2.5 meters, period 9-10 seconds) by the storm, followed by moderate wind waves (average height 1 meter, period 4-5 seconds). The generation of such swell is rare along the eastern coast, and even moderate-sized wind waves occur infrequently (E. Reimnitz and J. DiMaio, personal communications), though the latter are characteristic along the central and southern portions of the western coast, including the Point Lay area. Figure 59 indicates the immediate response in wave height and beach volume changes at Pingok Island during the period August 1 through September 25. The volume of beach change during the storm increased by an order of magnitude over the lower energy conditions that existed previously.

The two-dimensional beach response monitored at Pingok Island during these periods of higher wave energy follows closely the beach-profile transition model developed by Sonu and van Beek (1971) and Sonu and James (1973). This model (Fig. 60) predicts sequential changes in beach profile according to their configuration. Beach change (accretion or erosion) can occur only in the direction of the arrows.

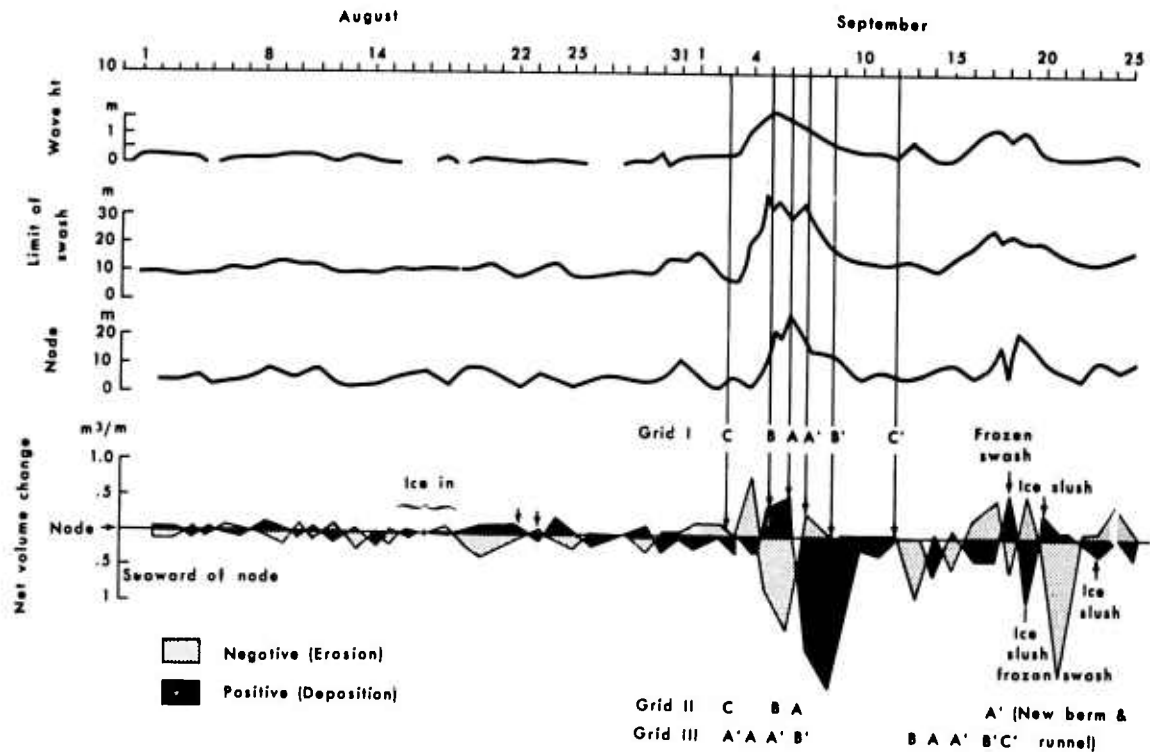


Figure 59. Plot of wave height, swash limit, erosion-deposition node, and beach volume change at Pingok Island, grid I. The swash limit and node are measured landward from the seaward limit of the grid. The curve on the node graph indicates the position on the beach with reference to the grid where no change in beach volume has taken place. The net volume change curve shows the volume of sediment eroded or deposited above or below the node.

Daily beach surveys on grid I, Pingok Island, showed that sequential beach profile changes underwent a regular transitional sequence following this model. Figure 61 shows selected beach profiles (A, B, C, D, and E on grid I) during the period September 3 through September 25. The beach initially had a convex configuration; increasing wave energy resulting from the storm passage generated an erosional profile change, C → B → A, during the period September 4-6. Wave energy began subsiding on September 6 and rapid accretion generated an A' → B' → C' profile transition during the period September 6-21. At grid II (Fig. 62) a similar profile transition took place during and after the storm. Profile G, grid II, had an initial convex configuration, and during the period September 3-18 it followed the model sequence, ending with a B' configuration, the development of a prominent berm and runnel. The berm and runnel are shown in Figure 63. Grid III (Fig. 64) profiles displayed similar transitions and took 13 days to move through the sequence A' → A → A' → B' → C'.

Figure 59 illustrates the close relationship between wave height, swash limit, position of the erosion-deposition node, and the volume of beach change at Pingok Island during the open-water period. Both erosion and deposition occurred on either side of the node between most daily measurements. Note that the greatest amount of change occurred during two periods, September 3-12 and September 19-22, both following

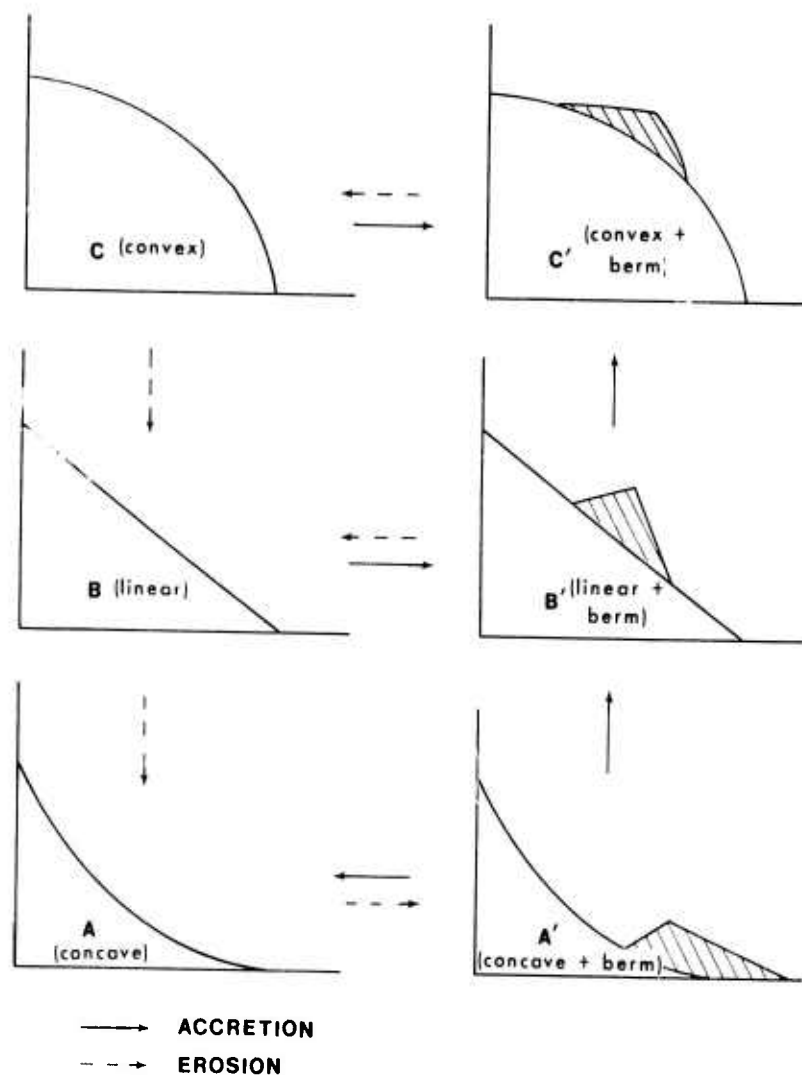


Figure 60. Schematic diagram showing characteristic sequence of beach profile change (after Sonu and van Beek, 1971).

periods of moderate wave action. Only when one trend exceeded the other did a depositional or erosional transition occur. Even during periods of considerable beach erosion, upper beach deposition occurred (September 5, Fig. 59). At both sides a similar pattern of volume change was observed. Rising waves caused lower beach deposition and upper beach erosion (C → B, Fig. 59); this was soon followed by erosion across most of the beach (B → A, Fig. 59). With a decrease in wave action, rapid deposition on the lower beach occurred for several days (A → A' → A → A' → B' → C', Fig. 59), accompanied by minor upper beach erosion. This latter erosion resulted from a runnel forming behind the berm.

These cycles indicate four important aspects of Alaskan Arctic beaches:

- (1) The arrival of moderately high waves initiates a transition sequence in

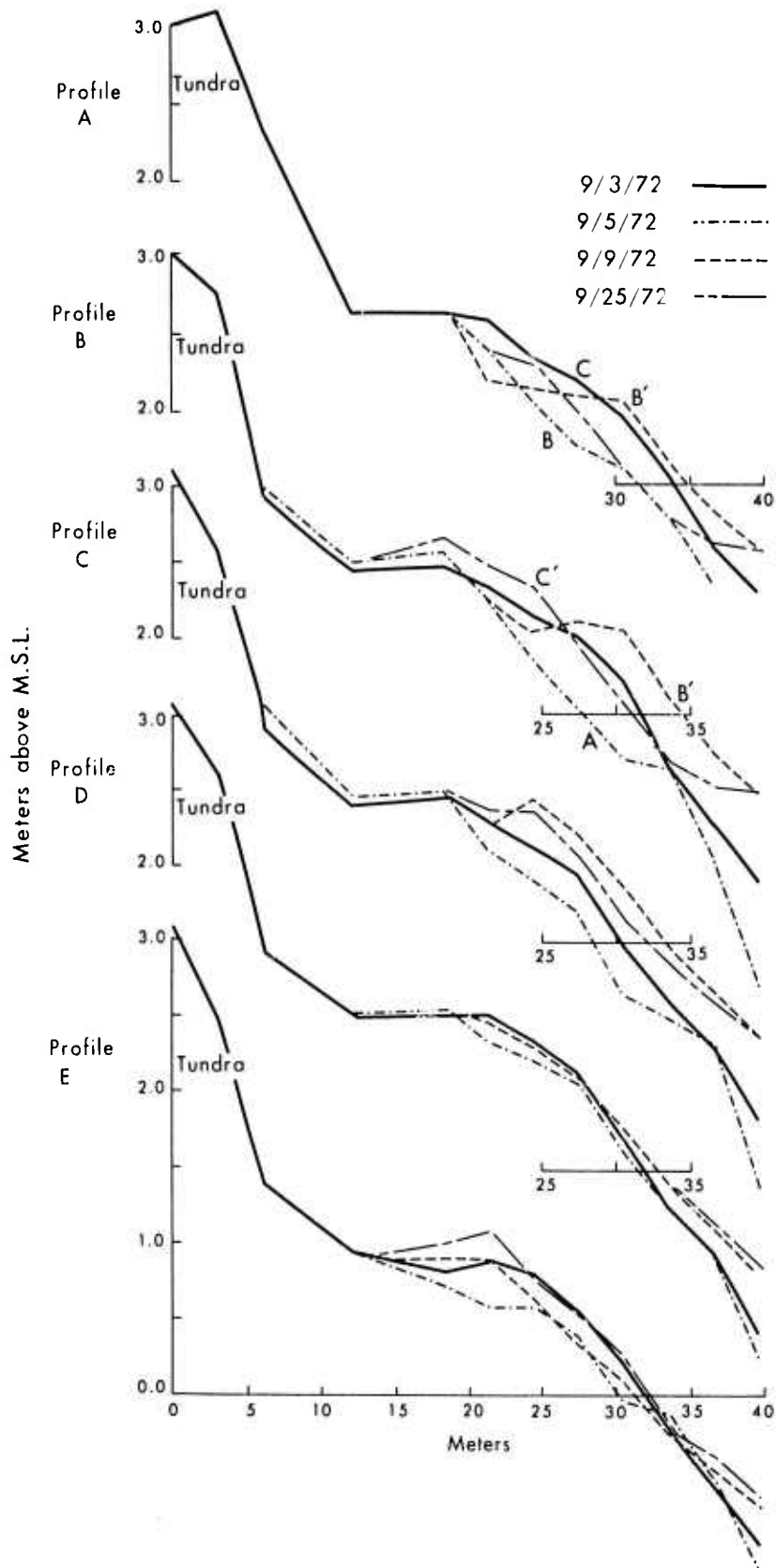


Figure 61. Selected changes in beach configuration along profiles A, B, C, D, and E, grid I, Pingok Island, during the period September 3-25, 1972. Letters refer to shape of profile indicated on Figure 60. Location of profiles shown on Figure 57.

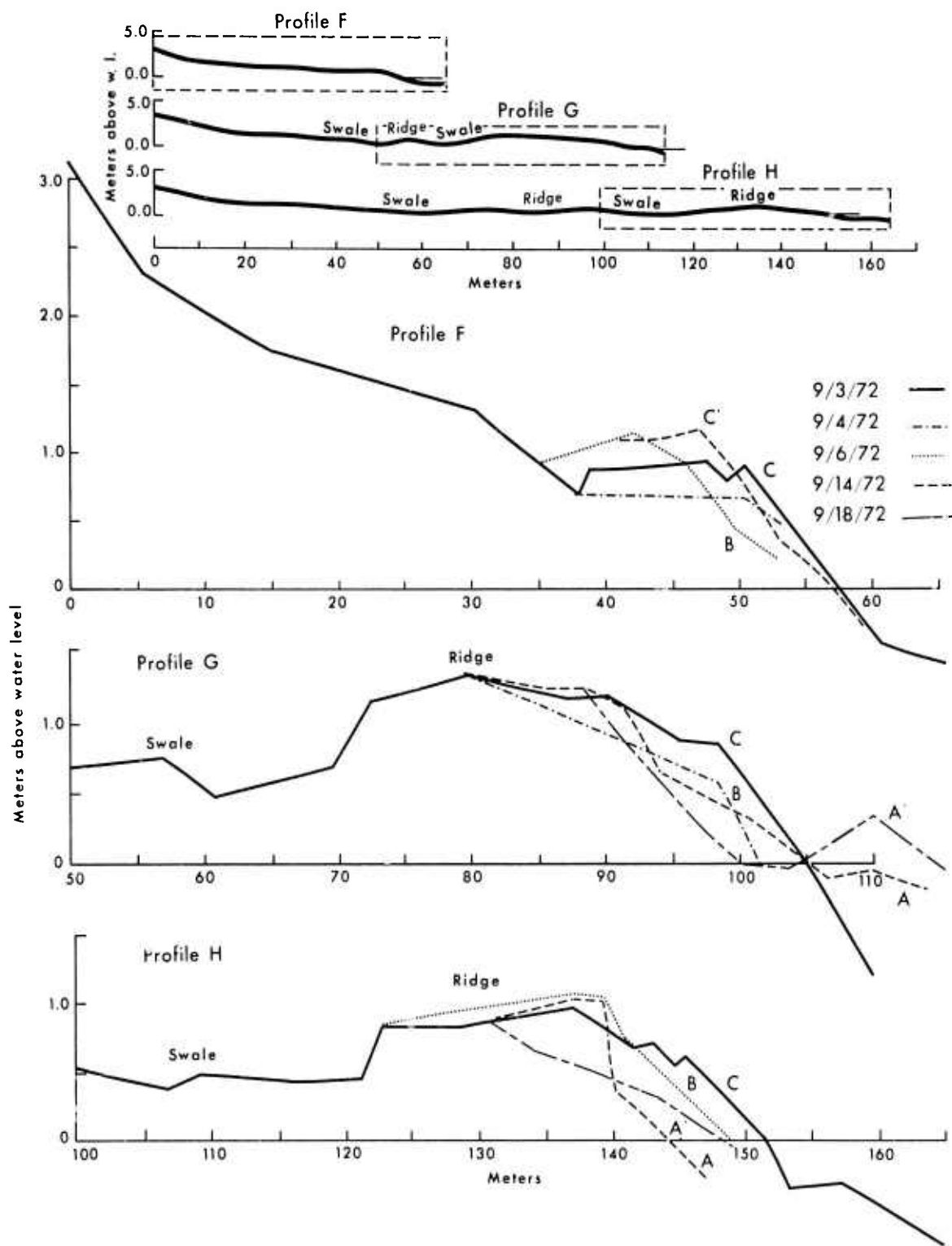


Figure 62. Changes in beach profiles F, G, and H, grid II, Pingok Island. The position of the three profiles on the total beach is shown in the upper inset. Location of profiles shown on Figure 57.



Figure 63. Photograph of recently formed ridge-and-runnel system on Pingok Island. This topography was developed on a concave beach following storm erosion and was formed during a period of only a week.

beach configuration which fits within the general beach cycle transition model developed on mid-latitude beaches by Sonu and van Beek (1971). This implies that active beach configuration will respond to a given process intensity in an identical manner to that on non-arctic beaches.

- (2) Variation in the sequence and number of transitions between the Pingok Island beach grids indicates that additional longshore parameters influence the sequence. This was anticipated by Sonu and James (1973), who suggested that longshore adjustments need to be made to the model. The cause of this longshore variation on Pingok Island is probably related to the presence of the rhythmic features and outer bars.
- (3) The dependence of cycle initiation at Pingok Island on infrequent summer storm waves produced a long waiting time within profile states (September 1970 - September 1972) which was followed by rapid profile transitions, thus attesting to the erratic and unpredictable nature of arctic process conditions. This was also noted by Owens and McCann (1970).
- (4) Because of number (3), beach response during the short open-water period is of great importance in the Arctic inasmuch as significant changes generated by a major summer storm will have protracted

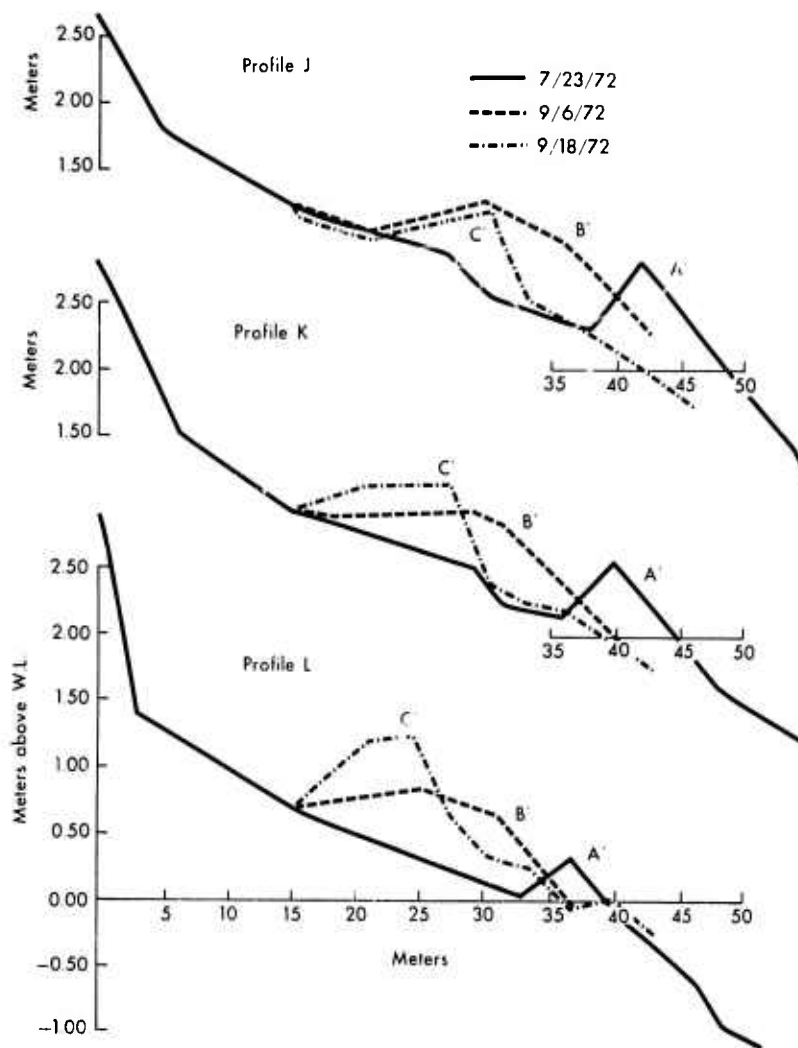


Figure 64. Selected changes in profiles J, K, and L, grid III, Pingok Island. Location of profiles shown on Figure 57.

influence on the morphology when followed by calmer open-water seasons.

#### Offshore Bars

The dominant easterly winds and westerly currents along the eastern coast interact with the sediments forming a gentle offshore slope (1:100-1:150) to generate a net westerly movement of sediment. This sediment is moved in the surf zone by wave agitation, swash action, and wave-generated currents, and seaward of the surf zone by wave orbital motion and coastal currents. The two separate zones and mechanisms of transport result in two different responses of the movable bed. One is reflected in the high-frequency beach response described in the previous section, the other in the formation of outer bars. The outer bars along Pingok and Leavitt

islands are typical of this low-frequency response.

A series of thirty-five offshore profiles (Fig. 65) was run off Pingok and Leavitt Islands with a Raytheon fathometer. Four distinct outer bars (I-IV, Fig. 65) were readily apparent in both plan and profile views. The presence of the bars has generated four shoreline rhythms: the horns labeled A, B, C, and D and bays A<sub>1</sub>, B<sub>1</sub>, C<sub>1</sub>, D<sub>1</sub>, and E<sub>1</sub> in Figure 65. In each case, the bars intersect the shoreline at an angle between 8 and 10° and are skewed to the west as a result of dominant easterly waves and westerly setting currents. Note that each bar ends seaward at a point nearly opposite the region where a downdrift bar attaches to the shoreline, causing the bars to overlap. The bars average 4.0 km in length, 200 meters in width, and 2.5-3.0 meters in height, and the crests are 3-4 meters below the surface. The crest deepens to 4-5 meters at its downcurrent limit, where the bar attains a maximum distance from shore of 400 meters.

In section the bars are asymmetrical. The shoreward slope is steep, resting at the angle of repose, whereas the seaward slope is gentler (see profiles in Fig. 65). The bars are best developed immediately downcurrent of the shoal, where the width is narrowest, the crest highest (3 meters), and asymmetry most pronounced. The bars become more symmetrical, widen, and decrease in height at their alongshore limit. In addition to the four outer bars, several secondary deformations of the bed, both seaward and landward of the bars, are present. These deformations have produced some secondary bars, shoals, and troughs but do not display the regularity or relief of the larger bars.

Figure 66A shows an aerial view of waves breaking on the outer bar (Bar III, Fig. 65) at Pingok Island. The photograph vividly shows the attaching of the outer bar to the shoreline and is typical of the other bars in the vicinity. Figure 66B, taken July 8, 1972, shows the rhythmic shoreline that develops as a result of the outer bars. Note also the well-developed ridge-and-swale system shown in the foreground. This has resulted from previous migration of bars and will be discussed in a following section.

Study of rhythmic topography has recently received growing attention. Sonu (1973) summarized these studies and put forward a scheme of outer and inner bar systems, shown in Table 13. The asterisks (Table 13) indicate the agreement of the Pingok-Leavitt bar system with those described by Sonu. Note that, although the bars display the features characteristic of Sonu's "Outer-Bar Rhythm" (Table 13), they also display a large number of the characteristics ascribed to the "Inner-Bar rhythm." The reason for this discrepancy is that the bars described by Sonu are based on field work along moderate-energy coasts, where waves are capable of developing distinct inner-bar systems. Under such conditions, the inner bar development is primarily associated with wave breaking and wave-generated currents in the surf zone. These bars act normal to the shore and tend to migrate diagonally onto the beach, producing the associated shoreline rhythms. The circulation systems related to the formation of the outer bars extend to, but cannot penetrate the breakerline. With the disintegration of the formative mechanism, the outer bars terminate seaward of the breakerline. Along the Alaskan Arctic Coast, however, the small to moderate waves break at the foot of the beach. Therefore, the surf zone is restricted to a relatively narrow zone adjacent to the beach. As a result, the mechanisms, which affect the development of the outer bars can extend almost to the shoreline and thereby produce shoreline rhythms associated with outer bars. The arctic bars represent the first known evidence of outer bars consistently extending to and actively modifying the shoreline in the absence of inner bars. However, it is expected that similar morphology will result wherever the above processes and bed characteristics are present.

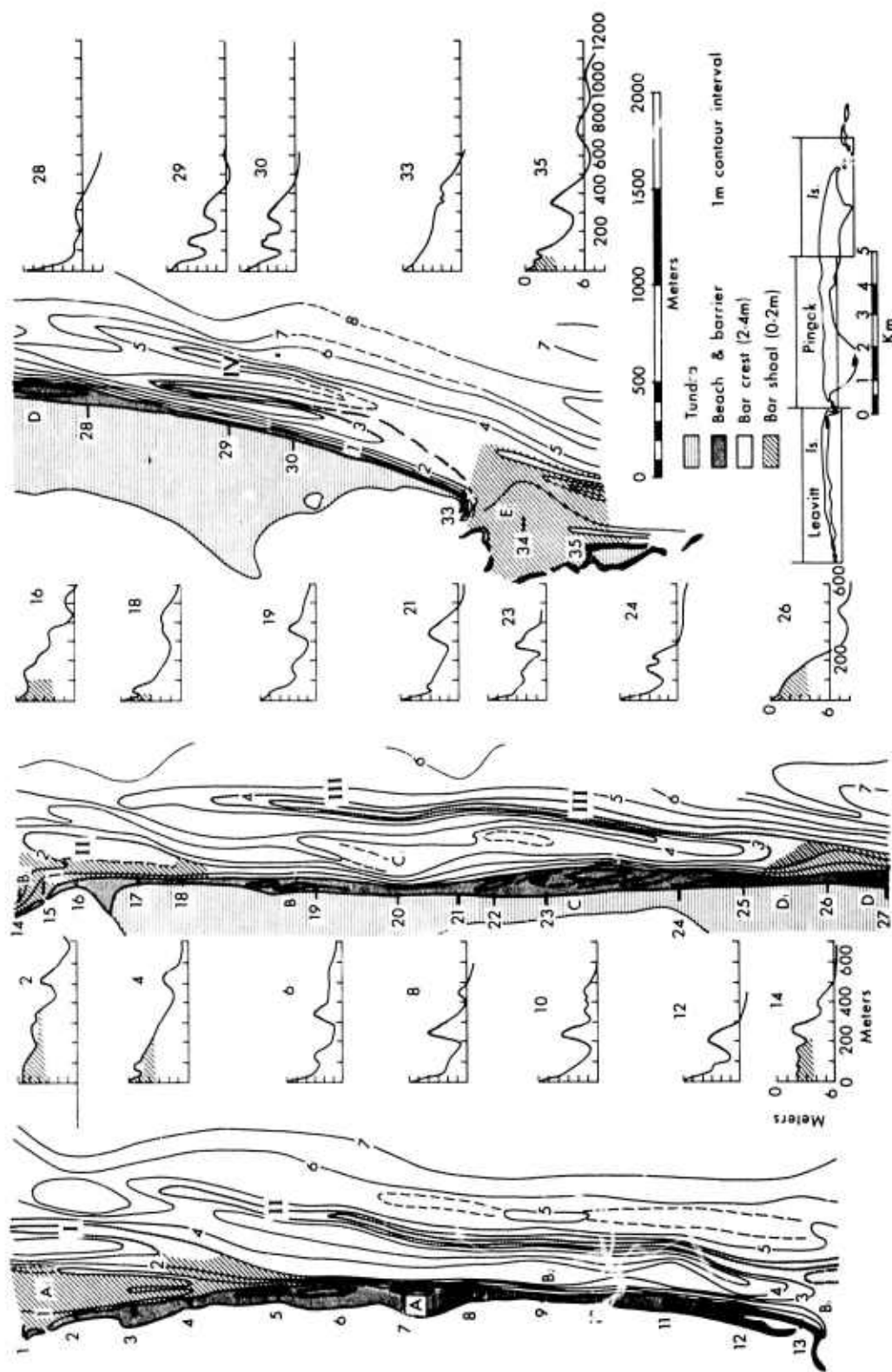


Figure 65. Nearshore bathymetry off Pingok and Leavitt islands (August-September 1972). Note the presence of outer bars which extend to the shore, generating shoals and shoreline rhythms. Bar profiles on the right are in line with their respective beach ranges (1-35). I, II, III, and IV mark the position of outer bars; A-D represent the horns of the shoreline rhythms; and A1-E1 represent the bays of the shoreline rhythms.



A. Waves breaking on the outer bar (bar III in Fig. 65). Note the point where the bar merges with the shoreline.



B. View east along Pingok Island showing the shoreline rhythms (horns C and D in Fig. 65). Note the ridge-and-swale systems in the foreground.

Figure 66. Photographs illustrating the outer bar and shoreline rhythms along Pingok Island.

Figure 67 shows a series of profiles along different ranges (range 26-18) of outer bar III shown in Figure 65. This structure strongly resembles that described by Sonu (1973) for the inner bar structure along the Florida coast. The major difference is scale. The bar begins as a convex shoal (range 26), then moves offshore and assumes its asymmetrical shape (range 25). Moving downcurrent, the bar continues farther offshore, maintaining the asymmetry and heightening the crest (ranges 21 and 23). Finally it disintegrates as a broad, symmetrical shoal (range 18) located opposite a new bar that has developed on the shore.

#### Bar Formation

The presence of offshore bars represents the response of a movable bed to wave agitation coupled with coincident coastal currents. Low waves in the Arctic, moving across the nearshore zone, do not break on the offshore bars except during severe storms or periods of exceptionally high waves. Normally waves pass over the bars and break only on the swash bar at the foot of the beach. However, currents associated with wave orbital motion over the bar crests are capable of putting some of the sediment into suspension or slightly lifting it off the bottom. This material

Table 13

## Distinctions Between Outer- and Inner-Bar Rhythmic Topographies

	Outer-Bar Rhythm (300-3,000 m) <sup>#</sup>	Inner-Bar Rhythm (Order of 10 <sup>2</sup> m) <sup>*</sup>
Shape	*Predominantly symmetrical *Continuous series	*Skewed shape frequent Discontinuous series more frequent
Correlation with shoreline rhythm	Often out of phase between bar and shoreline rhythms Shoreline rhythm may be smooth Bar points not necessarily contiguous to shore (Ridge-and-swale topography preserved on shoreline rhythms) (Landward extent of shoreline rhythms difficult to delimit on low barrier islands)	*Usually in phase *Shoreline rhythms always present *Oblique shoals anchored at horns
Modification and movement	*Bar rhythm relatively stable after formation *Bar and shoreline rhythms may migrate independently *Little movement normal to shore	Both bar and shoreline rhythms ephemeral No sustained longshore migration Active shoreward migration and climb on shore under swell activities
Correlation with near-shore currents	*Tends to skew downdrift under longshore currents *Generates circulation of moderate speeds	*Oblique bar develops a gentle upstream slope and steep lee slope Generates strong circulations and meandering currents with rips

<sup>#</sup>Wave length at Pingok 5-6,000 meters.

<sup>\*</sup>Agreement with Pingok-Leavitt bars and aerial observations of eastern coast bars. (Characteristics in parentheses are unique to arctic bars and were inserted by the writers.) (After Sonu, 1973)

can then be acted on by wind- or tide-driven coastal currents. Bajorunes (1970) has stressed that, though wave power and nearshore currents are the main elements in sediment transport, wave action places the sand in suspension and currents determine the direction of movement. Off Pingok Island, wind-generated coastal currents ranged in velocity from 30 to 50 cm/sec, a speed capable of moving most of the sediment without wave agitation. If the coastal currents are dominant in one direction, then

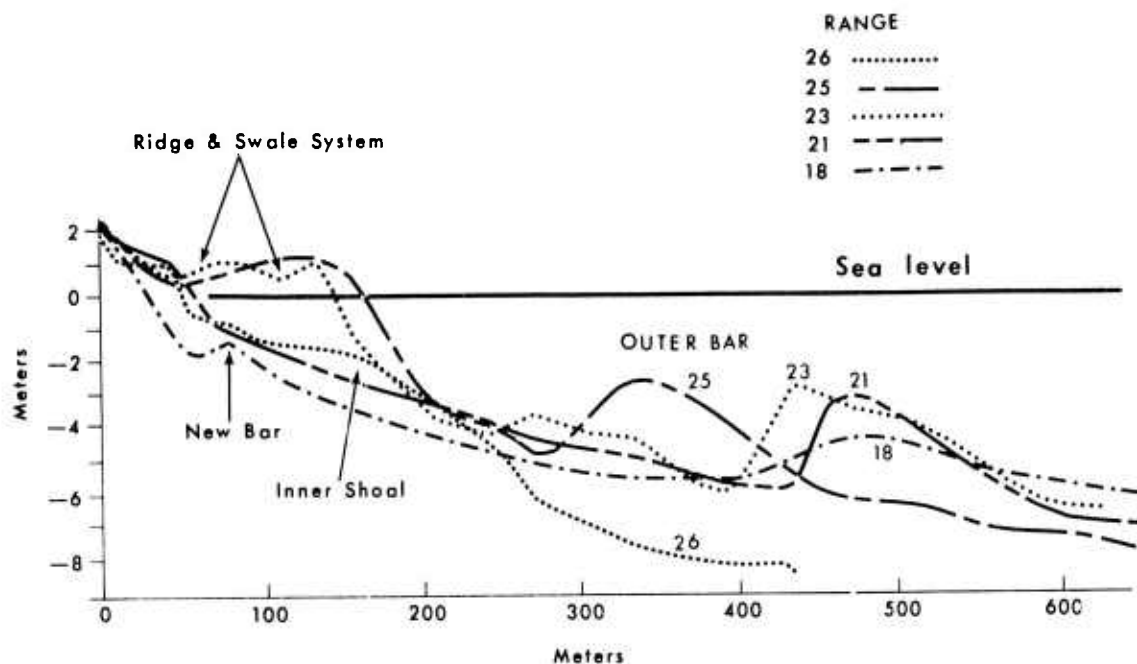


Figure 67. Selective bar profiles showing the pattern of bar development (see Fig. 65 for location of ranges).

a net movement of sediment will occur in that direction.

E. Reimnitz (personal communication) observed during numerous dives on the bars off Pingok Island that the sediment consists of medium to fine sand on the bar crest and coarse sand and gravel on the lee side and in the troughs. This sediment pattern agrees with the lag deposits observed by Swift et al. (1972) on Virginia Beach, where the troughs were floored with primary lag deposits of coarse, pebbly sand, the crests with secondary lag medium to fine sand, and the flanks with fine to very fine wave-winnowed sands. These deposits and the asymmetrical profile of the bars indicate that the direction of bar movement is toward the leeward face.

Thus it is probable that the waves and coastal currents generate mass movement of the bed, but how they interact with the bed to generate and maintain the bars is less certain. Swift et al. (1972) have suggested three mechanisms of bar genesis, one of which--spiral flow systems--may be applicable in the present situation. These currents are "secondary flow" patterns consisting of an accelerating descending flow and a gentle ascending flow. In association with a movable bed, erosion would reinforce this flow. This flow could be generated over the bars in question, but whether it results from the presence of the bars or formed the bars is unknown.

In addition, evidence along the west coast indicates that the pattern of bar spacing and orientation shows a relationship to the angle of wave approach, bars tending to be more transverse where waves approach at a sharp angle and to be parallel to the coast where waves arrive parallel. It is therefore suggested that the mechanism of bar formation and maintenance is closely linked to both the dominant incident wave and to the coincident wind-generated coastal currents, with waves determining the pattern of bar development and both wave orbital and coastal currents

providing the mechanism of arranging the sediment into this pattern. In addition, periods of exceptionally high waves may generate accelerated changes in the bar morphology.

#### Bar Migration

Changes in the configuration of Pingok and Leavitt islands are shown in Figures 68A-68D. The lateral migration of the Pingok-Leavitt bars was estimated from comparison of 1950 and 1955 aerial photographs (Figs. 68B and 68C) and the 1972 field surveys (Fig. 68D). Over the 22-year period, the points where the bars intersected the shoreline had rates of migration of between 1,000 and 2,000 meters, averaging 70 meters per year. However, the seasonal rates are expected to be extremely variable because of their dependence on the prevailing wind and wave conditions and because of the occurrence of occasional severe storms. Moody (1964) observed that sand ridges off the Delaware coast migrated as much as 50 meters during the great Ash Wednesday storm of 1962. Off Pingok Island, sequential bottom profiles (Fig. 69) showed that considerable movement of the bars occurred during the period of high easterly waves (September 4-9). The outer portion of bar II (Fig. 65) migrated 300 meters onshore, and the inner portion of bar III (Fig. 65) migrated 100 meters onshore. If such rates were typically associated with storms, it might be assumed that occasional severe storms control bar migration. It is more likely a combination of the normal and the exceptional conditions that effects the migration.

Given the average seasonal rate of 70 meters per year, the bars would migrate one wave length (4,500 km) in approximately 65 years. The bar wave length and migration rate agree with a summary of worldwide bar lengths and migrations, as shown on Figure 70. Arctic bars have a spacing and migration rate similar to that of bars on higher wave energy coasts. This agreement suggests that the mechanisms of bar formation, nearshore waves and coastal currents, are similar between the areas, though associated with two significantly different wave environments.

#### Beach Modification Associated with Bars

The subaerial beach along Pingok and the adjacent islands ranges in width from 5 to 190 meters. Typical profiles are shown in Figures 71 and 72. On the barrier islands this includes the entire island, from lagoon to seashore. This variation is associated with shoreline rhythms generated by the bars, as indicated in the previous section. Migration of the bars and shoreline rhythms produces corresponding changes in beach width.

Migration of the rhythms during 1972 could not be determined from the Pingok beach profiles. This is to be expected inasmuch as the long-term migration is a low-frequency beach response which may take several seasons to produce a net variation in beach width. However, stranded on the upper beach surface are ridge-and-swale systems associated with previous migration of shoreline rhythms. Figure 65 shows these systems on Leavitt and Pingok islands, and Figure 66B shows an aerial photograph of these features. Similar relict systems were also observed on Spy Island, Bertoncini, Bodfish, Cottle, and Long islands. The ridges extended laterally for up to 500 meters, paralleling the downcurrent side of the horns. Ridge width ranged from 10 to 40 meters, and maximum elevation was 1.5 meters above sea level. The swales ranged in width from 10 to 30 meters and were 0.25-0.5 meter in height.

Figure 73 illustrates schematically the development of the ridge-and-swale systems. As the bar and shoreline rhythm move alongshore (dashed to solid lines), erosion and beach retreat take place on the upcurrent side of the rhythm and

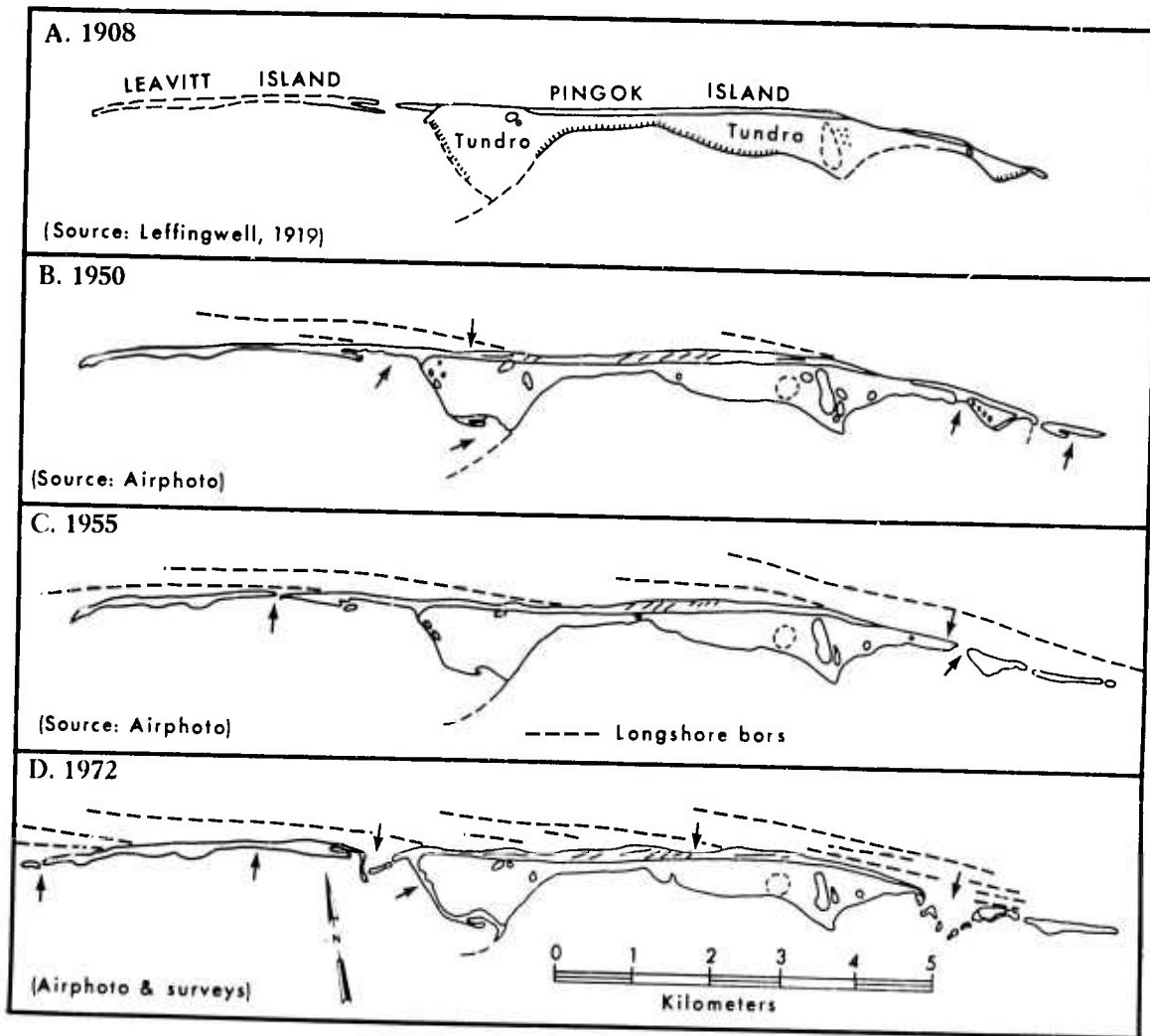


Figure 68. Pingok and Leavitt islands shown in 1908, 1950, 1955, and 1972. Dashed lines seaward of the beach indicate outer bars. Arrows point to areas of significant change between dates.

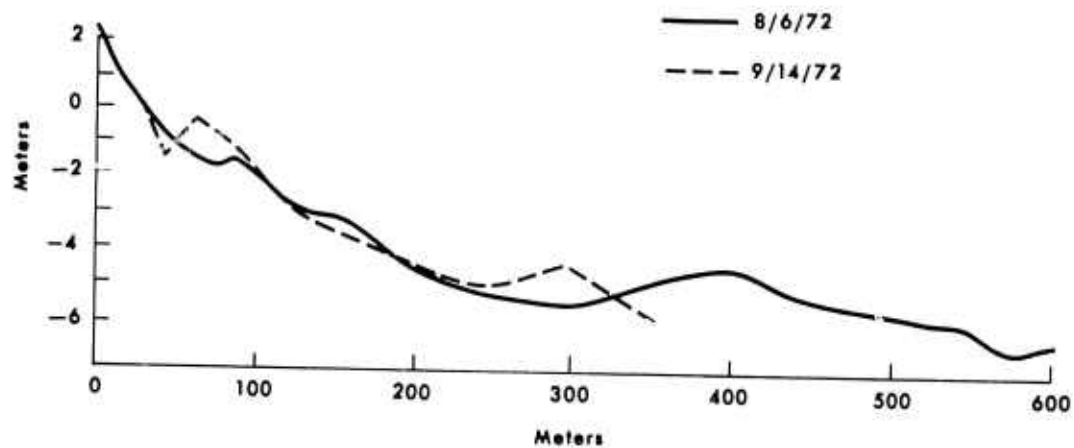


Figure 69. Sequential profiles along range 17 showing the onshore migration of two bars. This migration occurred during the period of moderately high easterly waves.

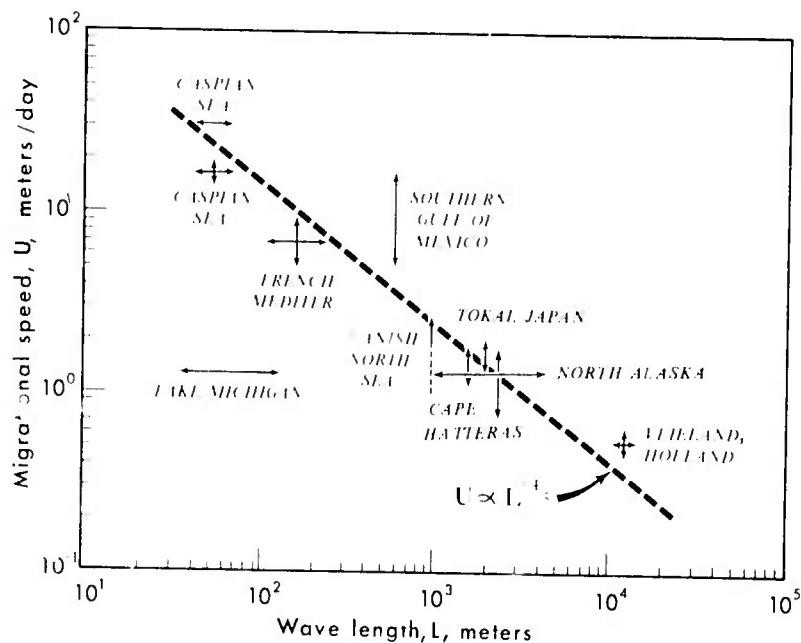


Figure 70. Rates of migration of cusp-type sand waves versus wave length. (Modified from Sonu, 1968)

deposition and beach growth on the downcurrent side. If, in the area of deposition, a new berm-and-runnel system develops, continued growth of the beach will build the berm into a beach ridge, stranding the swale behind it. Continuous growth of the beach and occasional development of a new berm and runnel generate a series of abandoned ridge-and-swale systems paralleling the downcurrent beach ( $R_1 - R_4$ , Fig. 73).

Such systems are not always apparent along the shoreline inasmuch as long-term beach retreat will remove them. In addition, upcurrent erosion causes truncation of the seaward end of the ridge-and-swale systems (Fig. 73).

Along Pingok Island four new berm-and-runnel systems up to 320 meters in length were built along the western half of the beach in September 1972 (Fig. 63). The new berms represented seaward growth of the beach and abandonment of the previous beach face. Assuming that conditions are favorable, i.e., that they are located in an area of beach growth, and no severe storms occur for a few seasons, they could be built upward and outward over a period of years into a new ridge, the runnel being elevated to a swale. However, severe storms or continued erosion would readily remove the berm, as occurred at grid III (Fig. 64). Therefore, infrequent severe storms, followed by seasons of low wave conditions, may be a triggering mechanism of berm-ridge development. Each new ridge represents rapid deposition following a storm, and its continued growth reflects subsequent calmer periods.

The preservation of these abandoned ridge-and-swale systems over a period of

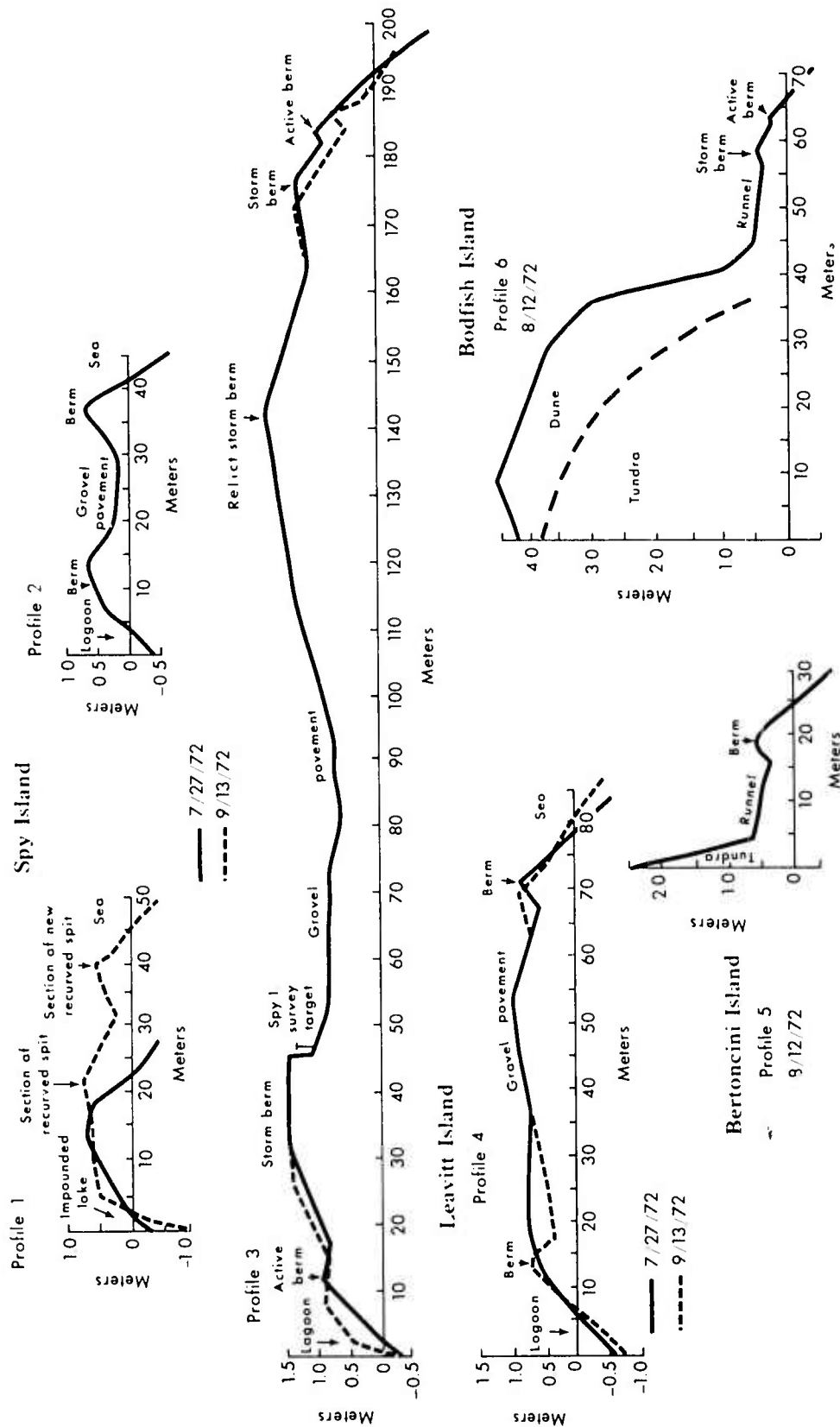


Figure 71. Beach profiles across Spy Island (1, 2, and 3), Leavitt Island (4), Bertoncini Island (5), and Bodfish Island (6). See Figure 3 for locations.

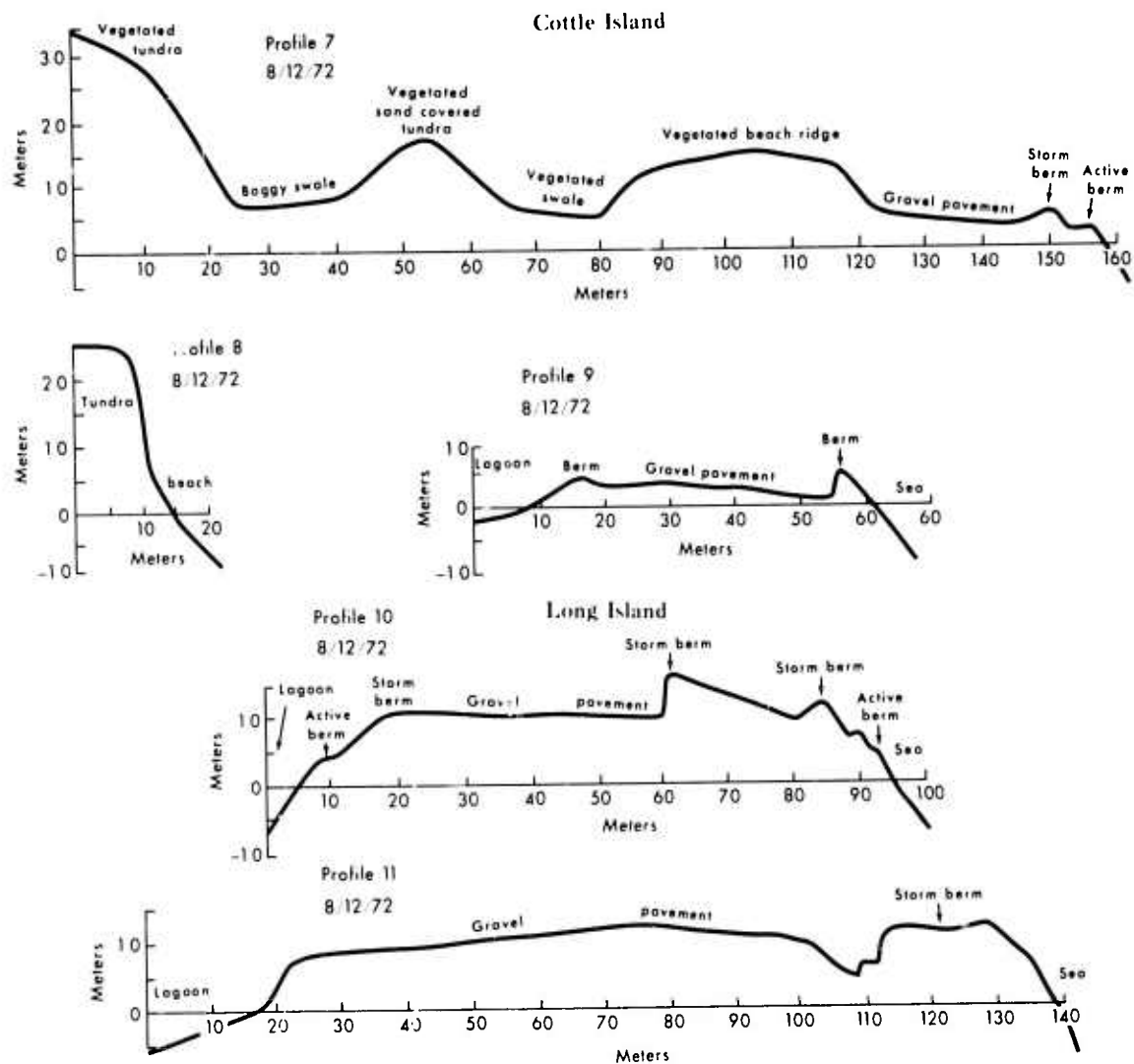


Figure 72. Beach profiles across Cottle Island (7, 8, and 9) and Long Island (10 and 11). See Figure 3 for locations.

decades is unique to the Arctic. In low latitudes, eolian and storm activity tend to rework the beach ridges. In the Arctic, however, several factors favor their preservation:

- (1) Disturbance by severe storms is rare, and even the 1970 westerly storm which covered the beach did not modify them.
- (2) The beach is frozen for 10 months of the year, protecting the systems from eolian and wave activity.
- (3) The coarse fraction in the beach sediments forms a gravel pavement on the ridges once surface deflation has occurred. This pavement prevents further eolian erosion.

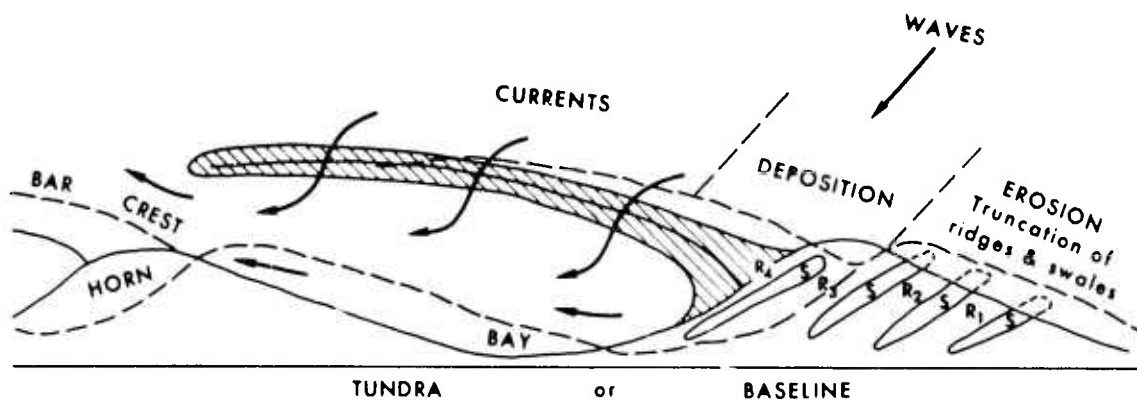


Figure 73. Schematic diagram showing migration of outer bar and shoreline rhythm and development of beach ridge-and-swale systems.

- (4) The swales are filled with water during much of the open-water season as a result of ice and snow melt trapped by the impermeable permafrost, forming perched lakes (Walker, 1967). The water prevents eolian erosion, though wind-generated waves and currents rework the bottom.

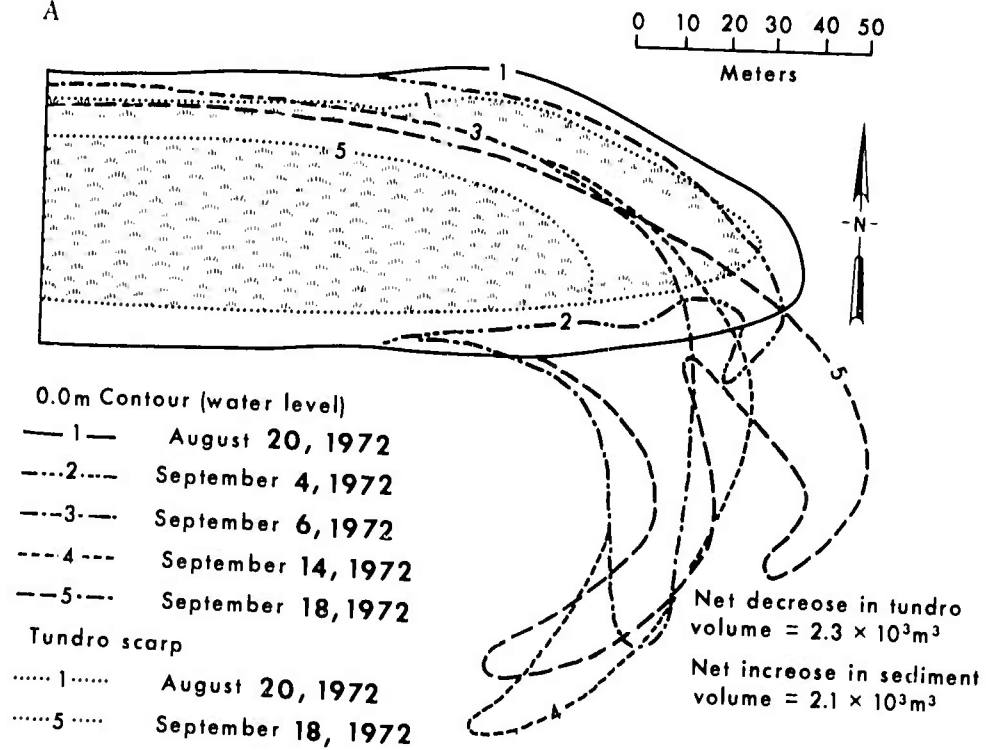
#### Inlet Morphology

Inlets originate as breaches in wave-built barriers. Breaching occurs most commonly during river breakup, when meltwater floods the lagoons, and during severe westerly storms. If offshore bars are present, breaching tends to occur downdrift of the horns, where the shoreline is narrowest. Subsequent longshore transport of sediment into the breaches and wave reworking will tend to narrow the inlets and produce a well-defined channel-and-inlet shoreline. Their continued maintenance is related to lagoon geometry, amount of longshore sediment transport, tidal range, and nearshore bar morphology.

Along the eastern coast, low wave energy, strong littoral currents, and a short open-water period result in irregular, discontinuous barrier chains backed by wide lagoons (average width 2.5 km,  $\sigma$  2.6 km). Inlets are numerous (one for every 5 km of barrier) and wide (average width 540 meters,  $\sigma$  700 meters). The normally low easterly and westerly waves are of insufficient strength to close the inlets. During September 1972, however, unusually high waves generated on the order of  $10^4 \text{ m}^3$  of sediment transport along the Jones Islands. In a 3-week period wave action and associated sediment transport effected major changes in inlets to either side of Pingok Island and the western ends of Leavitt and Spy islands.

The inlet on the eastern end of Pingok Island was modified considerably during this period of time. The inlet spit underwent severe thermal and mechanical erosion, the low tundra bluffs retreated as much as 50 meters, and a well-developed recurved inlet spit was formed (Fig. 74A). Thermal erosion and initiation of the recurved inlet spit had begun prior to September 4 but at a relatively slow rate. Following the arrival of high waves on September 4, accelerated tundra retreat and rapid spit growth took place. A total of  $2,300 \text{ m}^3$  of tundra was removed, and  $2,100 \text{ m}^3$  of sediment was

A



B

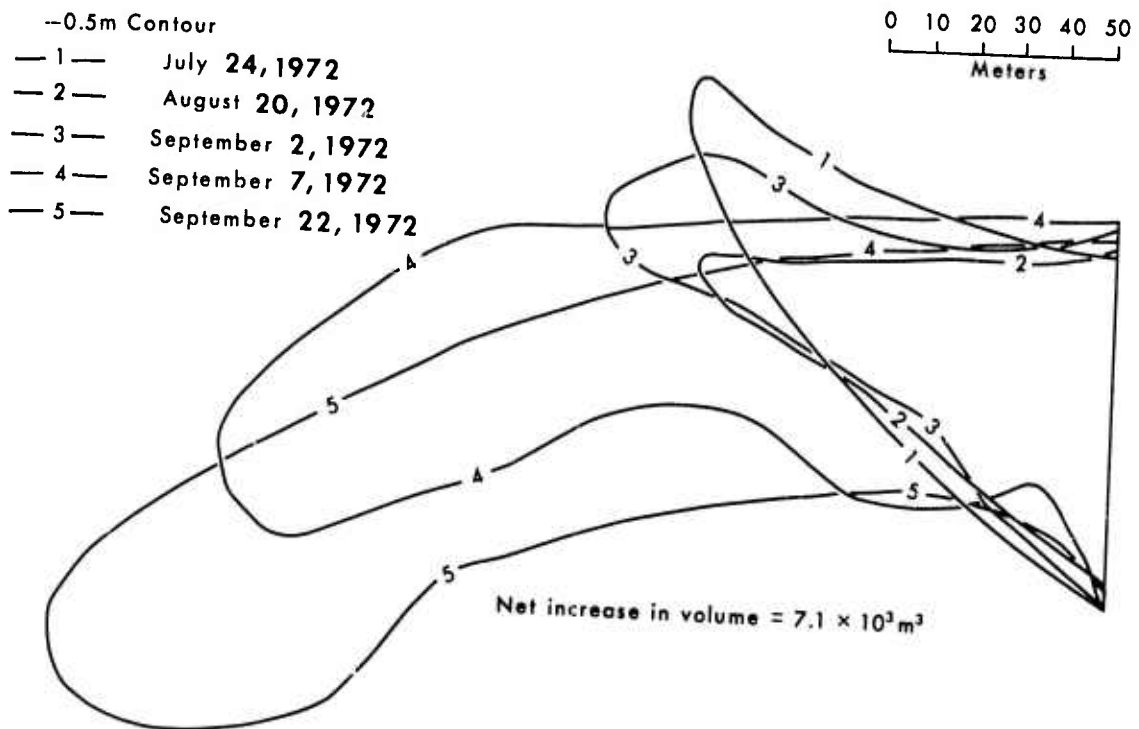


Figure 74. Spit development at eastern (A) and western (B) ends of Pingok Island. Sequential contours are leveled to a common datum.

deposited on the spit. Two well-defined inlet channels 2 meters deep developed, one adjacent to the spit and one in the center, and emerged shoals filled much of the previously wide, shallow inlet.

Similar changes occurred in the inlet on the western end of Pingok Island. This inlet is located landward of an offshore bar, and immediately east is a well-developed shoreline rhythm. The inlet was initially breached during the September 1970 westerly storm. By July 1972 the inlet was 400 meters wide and had an ill-defined channel along the western bank of only 2-meter depth. The spit at the eastern side was initially curved seaward (Fig. 74B), suggesting dominance of lagoon outflow and westerly waves over northeasterly waves during 1971. Prior to September 4, the spit maintained its approximate size, curving into the lagoon when easterly conditions persisted and curving seaward when westerly conditions were dominant. However, during and following the period of higher wave action, the spit increased in size significantly, extended more than 150 meters into the inlet, and had a net increase in volume of  $7,100 \text{ m}^3$  by September 22 (Fig. 74B). In addition, a second 250-meter-long exposed shoal was built up in line with the spit and extended farther into the lagoon. The western bank (Leavitt Island) of the inlet extended as a recurved spit more than 200 meters into the lagoon. The growth of the spits narrowed the inlet from 400 meters to 70 meters over a period of 6 weeks and moved a minimum of  $30,000 \text{ m}^3$  of sediment into the inlet and lagoon. The development of each spit was triggered by rapid deposition following passage of a severe storm.

Over a longer time period, the eastern coast inlets exhibit considerable variation. Along Pingok Island and Leavitt Island (Fig. 68) the long-term inlet variation may be a response to bar migration inasmuch as each inlet on the 1955 and 1972 photographs occurs in the bay area of a shoreline rhythm. The Tapkaluk Islands (Fig. 75) show similar variability over a 5-year period, the inlets again occurring downcurrent of the shoreline rhythms. Long Island (Fig. 76), while showing little long-term variation in island morphology, possesses considerable variability in inlet shape and location. The inlet between Long and Cottle islands appears to be narrowing as a spit associated with an outer bar migrates eastward from Long Island. The breaching in Egg Island (Fig. 76) can be attributed probably to river meltwater overflow during breakup of the Kuparuk River, 3.5 km to the south. P. Barnes (personal communication) observed river floodwater flowing through breaches in the island during breakup.

#### Island Migration

The barrier and tundra islands of the Alaskan Arctic Coast are bounded by dynamic inlets and are subject to infrequent, rapid, unidirectional sediment transport. This results in a net migration of the island in the direction of sediment movement, with inlet migration generating numerous short-term changes in island shape, especially in length. The scale of the aerial photographs utilized in this study was not of mapping quality, and quantification of island migration does not appear to be warranted.

Pingok, Leavitt, Tapkaluk, Long, and Egg islands (Figs. 68, 75, and 76) exhibit only slight migration over the period of comparisons in this study (22 to 64 years). Dygas et al. (1972) estimated that between 1949 and 1971  $7.1 \times 10^5 \text{ m}^2$  was eroded from the eastern end of Pingok Island. Assuming deposition of the same magnitude and frequency occurs at the western end, Pingok Island could migrate one island length in approximately 1,000 years, at an average rate of 6 meters per year. Actual rates obviously fluctuate considerably inasmuch as during the 1972 study the eastern end eroded 40 meters and the western end grew 150 meters.

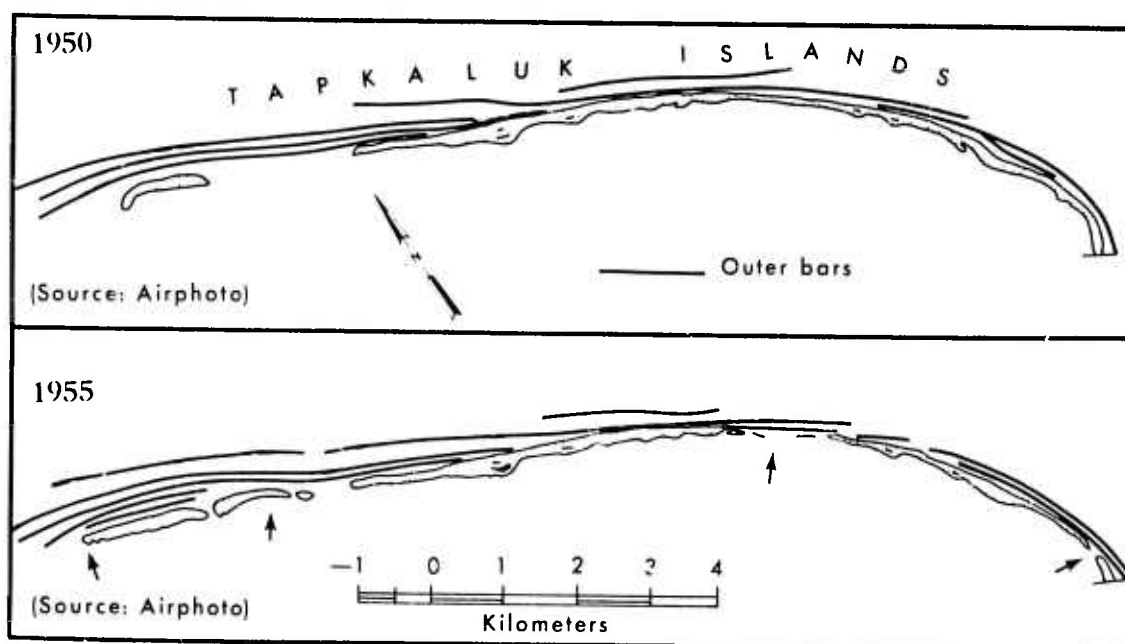


Figure 75. The Tapkaluk Islands shown in 1950 and 1955. Solid lines represent outer bars. Arrows point to areas of significant change in island shape between dates.

The Maguire Islands (Fig. 77), situated 130 km east of Pingok Island, lie 5 km offshore and are well exposed to easterly wave approach. Between 1908 and 1950, all four islands migrated westward an average of 1,000 meters, or approximately 25 meters per year. Between 1950 and 1955 the western end of Duchess, Alaska, and Challenge islands (Fig. 77) extended by 500, 300, and 150 meters, respectively, or an average of 190 meters per year. This greater average can be attributed to seasonal variations in inlet morphology. In addition, the islands have undergone considerable variation in width, inlet position, and bar migration. The bars along the islands (Fig. 77) have an average spacing or wave length of 700 meters (range 200-1,000 meters), suggesting that they migrate at a faster rate than the Pingok-Leavitt bars. The seaward shore of the islands also attests to the influence of the bars, which have produced a series of prominent shoreline rhythms. The westerly currents have also produced shorter rhythms and bars on the lagoon side of Alaska Island.

#### POINT LAY

Beach response was monitored only intermittently during the 1972 study because of logistics problems. Grid I, near the camp, was surveyed fifty-two times during the period May 25 - October 13 (76 days), whereas the profiles on Pingok Island were normally surveyed once daily except during periods of rapid change, when they were surveyed several times in a 24-hour period. The absence of well-developed bars in the nearshore resulted in a rather straight shoreline, and hence fewer alongshore variations were apparent at this site. During the 1971 aerial reconnaissance flights a single offshore bar was apparent but obviously was destroyed prior to freezeup. Offshore fathometer profiles run during 1972 did not reveal the bar to be present at the site of the grid. Farther north of the camp, however, the bar was present, but monitoring of this site on a continuous basis was not possible.

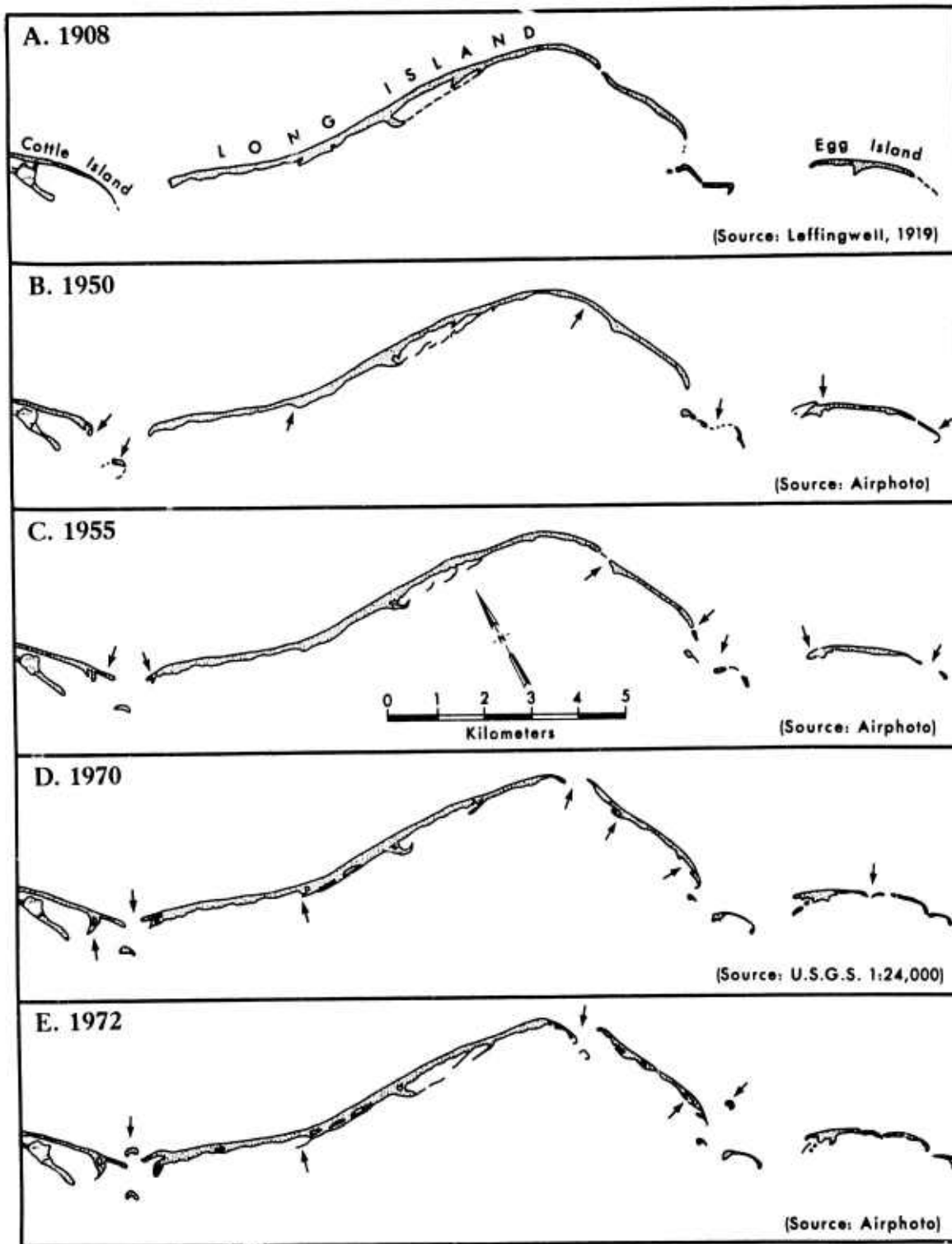


Figure 76. Eastern Cattle Island, Long Island, and Egg Island, shown in 1908, 1950, 1955, 1970, and 1972. Arrows point to areas of significant island change between dates.

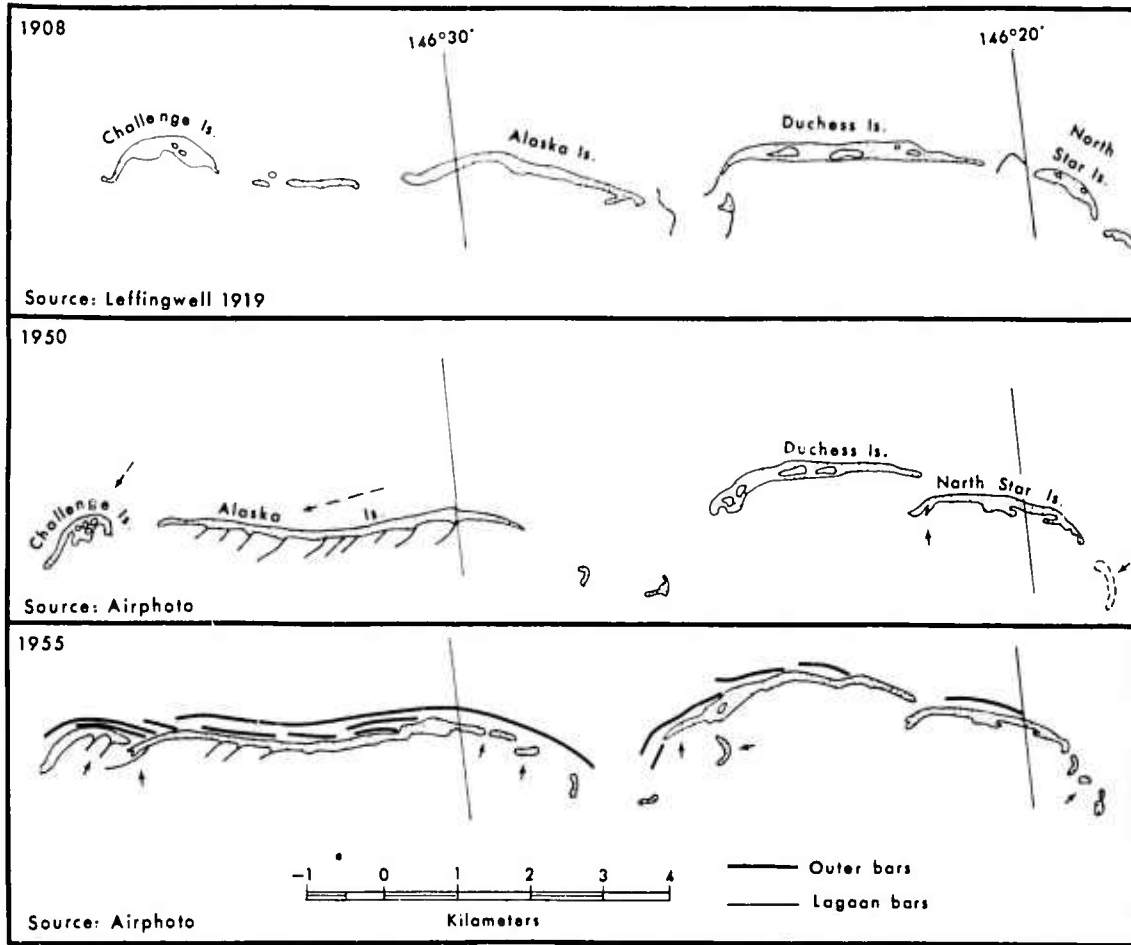


Figure 77. The Maguire Islands, shown in 1908, 1950, and 1955. Solid arrows point to areas of significant change between 1950 and 1955. Dashed arrows indicate the trend of island migration between 1908 and 1950.

Some of the general comments on beach change discussed in the previous section on Pingok Island apply to the Point Lay site and will not be discussed again. Figure 53 shows the daily averages of selected marine and atmospheric parameters at Point Lay. Westerly and northerly winds dominated throughout the study period.

#### Two-Dimensional Beach Response

The beach at Point Lay is relatively straight and continuous and has no littoral bars. As a result, subaerial beach profile change is primarily caused by wave action. The recurrence of moderately high waves is related to the wind and fetch characteristics and to passage of occasional storms. Figure 78 shows changes in beach volume at the Point Lay site. Variations in wind direction occurred in cycles of 1-7 days at Point Lay, and the beach responded accordingly. Strong southwesterly winds were responsible for the greatest change in profile, and three westerly storms (August 5-7 and 8-11, October 8-12) caused the most severe change in beach configuration.

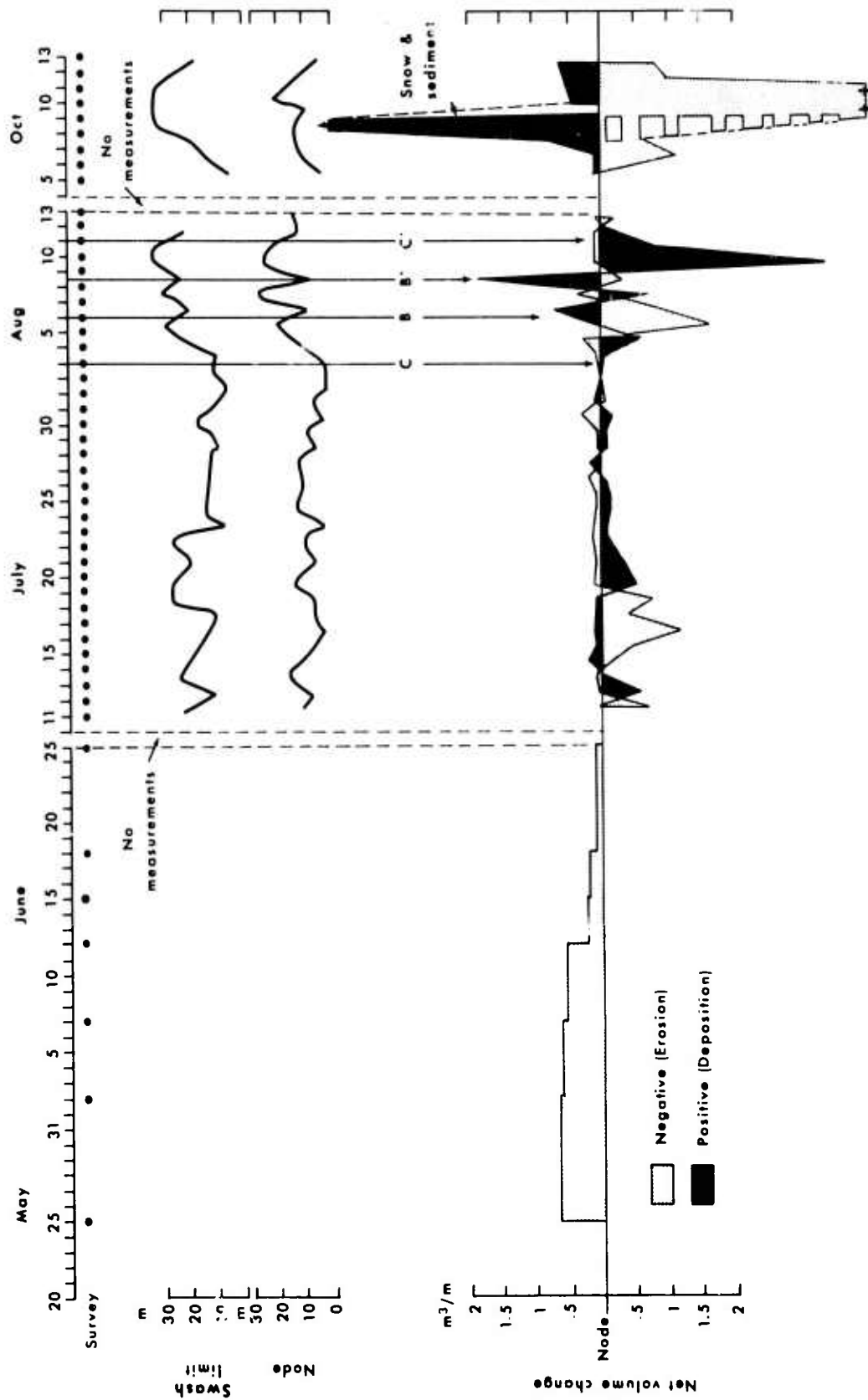


Figure 78. Plot of swash limit, erosion-deposition node, and beach volume changes at Point Lay, grid I. (See Fig. 59 for explanation of terms.) Beach volume changes between May 25 and June 25 represent beach subsidence as a result of ice melt. Changes from July 11 to August 13 are a result of wave action. Changes from October 5 to 13 include layers of sediment-covered snow.

The response of the beach to input wave frequencies follows the beach profile transition model developed by Sonu and van Beek (1971), which was discussed in a previous section. Following beach thaw, the surface of the beach was depressed by melting of ice and subsidence (May 25 - June 25). This process, combined with extremely low wave action and strong alongshore drift between the ice and the shoreline, resulted in a convex profile. This profile persisted with only minor changes during the period June 25 - August 4. Rising wave action associated with the passage of a severe westerly storm initiated an erosional transition (C → B, Fig. 78) in which the beach configuration was transformed to a linear profile. After passage of the storm, a decrease in wave action resulted in beach accretion and transition through profiles B → B' → C' (Fig. 78). This four-step transition, C → B → B' → C', took 8 days and ended with a convex berm profile.

The third westerly storm, October 8-12, caused similar profile transitions, but the change in beach volume was much greater (Fig. 78). In addition, during this period snow and ice were incorporated into the beach sediment. The long delay in freezing of nearshore waters precluded monitoring of this site until final freezeup.

#### Inlet Morphology

Along the western coast, wave energy is sufficiently high throughout the open-water period to move sediment rapidly through the inlets and into the lagoon. The barrier islands are long and continuous, and inlets are few in number and when present are narrow. There is an average of one inlet per 12 km of barrier, and the mean width of the inlets is 130 meters (standard deviation = 670 meters). Normally, broad tidal deltas are found on the lagoon side of the inlet and smaller tidal deltas on the seaward side. During the winter period, pressure ridges commonly develop along the seaward edge of these tidal deltas.

Along the Kasegaluk Lagoon section, the barrier island had eight inlets in the spring of 1972. Comparison of 1955 aerial photographs with 1972 aerial reconnaissance showed that four of these inlets were formed during the intervening period and four others had been sealed off. Inlet breaching along such a narrow lagoon is likely to be related to river melt flooding the lagoon and breaking through low points along the barrier chain.

The inlet in the vicinity of the Point Lay camp site was breached by river meltwater in the late 1960's. At the beginning of the 1972 field season, the inlet was 182 meters wide and the channel depth averaged 5.2 meters (Fig. 79A). Wave action in the middle of July caused appreciable alongshore drift, and the spit on the southern side of the inlet built up, narrowing the inlet to approximately 30 meters. On August 4-5, 1972, a severe southwesterly storm generated a 50-cm rise in sea level, and waves 2.0-2.5 meters high and 4-6 seconds in period pounded the coast. These conditions moved a minimum of 10,000 m<sup>3</sup> of sediment into the inlet and built a 1.5-meter-high beach across the inlet, sealing it within a 36-hour period (Fig. 79B). It is apparent that the inlets along the western coast are formed rapidly by river meltwater breaching and sealed quickly by severe wave action and attendant high alongshore sediment transport. This is considerably different from the situation described along the eastern coast.

#### DISCUSSION

Arctic beach response to open-water processes exhibits considerable variability both in section and in plan. The magnitude of two-dimensional response is directly related to wave height, which is in turn dependent upon the prevailing winds and position of the pack ice. Low waves (less than 30 cm and 1.0-2.5 seconds in period)

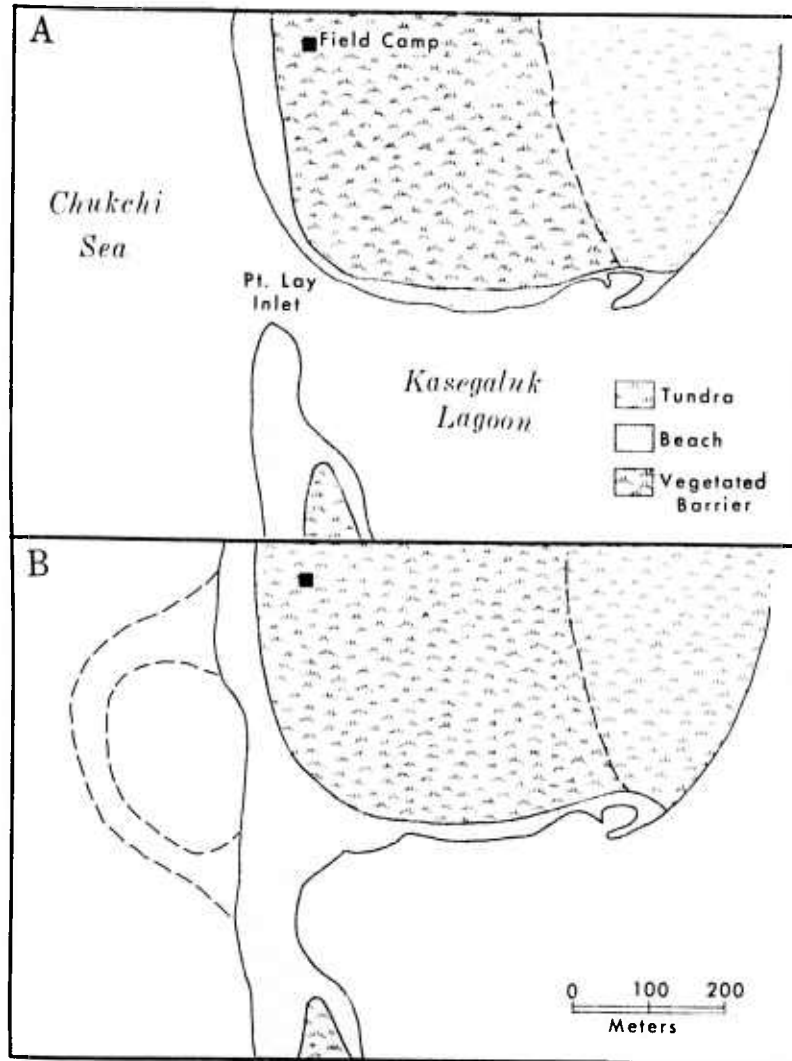


Figure 79. Changes in the inlet at the Point Lay site. A. Inlet configuration traced from aerial photographs supplied through the courtesy of the Bureau of Land Management, Department of Interior (Alaska State Office). Photo taken July 4, 1972. B. Closure of the inlet traced from photographs taken by NARL on September 19, 1972. Note the complete sealing of the inlet and the position of the former inlet bar.

generate small-scale beach forms which only superficially disturb the beach to a height of 0.5 meter above sea level. During periods of higher waves (height greater than 50 cm, period 4-10 seconds), the entire beach responds, the beach configuration moving through a transition sequence that is dependent upon wave growth and subsidence. The sequence agrees with the general model developed by Sonu and van Beek (1971) for mid-latitude beaches. On the east coast, low waves predominate. Infrequent higher waves will generate a beach response an order of magnitude larger than that produced by low waves. Along the west coast the higher waves (0.5 to 1.5 meters

in height, 3 to 6 seconds in period) predominate.

In plan, beach and nearshore morphology is dominated by the presence of outer bars which leave the shoreline and extend lateral to the shore for several kilometers before terminating seaward at a distance several hundred meters from shore. Shoreline rhythms associated with the bars control beach width. Downcurrent of the horns, successive generation of berm-and-runnell systems produces beach ridge-and-swale systems. Upcurrent erosion truncates these systems.

Alongshore movement of sediment on the order of  $10^4 \text{ m}^3$  moved along the Pingok and Point Lay beaches during 1972. The net direction of movement is to the west along the eastern coast and to the north along the western coast. Longshore sediment movement results in narrowing and finally closing of the inlets. Inlets along the eastern coast are breached primarily by two processes: those opposite river mouths form by overflowing river meltwater, and those removed from river mouths are breached primarily by storm action during periods of higher sea level (up to 3 meters). The inlets along the western coast form primarily as a result of river meltwater breaching. Sealing of the inlets results primarily from wave action associated with passage of storm fronts.

The islands on the eastern coast erode on their eastern ends and deposit on their western ends, resulting in net westerly migration. The rate of migration varies considerably from an estimated 6 meters per year (Pingok Island) to 25 meters per year (Maguire Islands).

A good relationship exists between the period of time over which the above morphological changes take place (i.e., beach response, bar migration, inlet migration, sediment movement, island migration, etc.) and the associated migration of material per unit time (Fig. 80). As is to be expected, the longer the time period, the greater the volume of sediment migration and the larger the forms involved. However, the slope of the regression line ( $V \propto T^{10/7}$ ) indicates that the summation of individual short-term migration forms does not account for the volume involved over longer term periods. This implies that the long-term changes are associated with combinations of the shorter term changes.

#### Freezeup

Freezeup is a transitional period from summer to winter conditions during which the water and land freeze, forming a continuous ice cover. Along the Alaskan Arctic Coast, freezeup begins in mid-September and extends into October on the eastern and northwestern coasts. Along the southwestern coast, it commences in October and extends into November and December. Significant seasonal variability, however, is common.

This section will discuss the general sequence of freezeup along the coast, its effect on the beach and nearshore zone, and the resultant ice and ice-sediment features produced in these zones. Discussions will deal primarily with the Pingok Island site.

Freezeup commences when temperatures fall consistently below 0 C. Days on which both the maximum air temperature does not rise above 0 C and ice on the surface of the water does not thaw are called "ice days." In this study, "non-ice days" are those when neither of the above occurs. The low temperature causes freezing of the water in the top few centimeters of land and water surfaces. Gradual freezing of the active layer, water bodies, and condensed water vapor does not in itself affect the beach topography [though subsequent thermal expansion of the ice

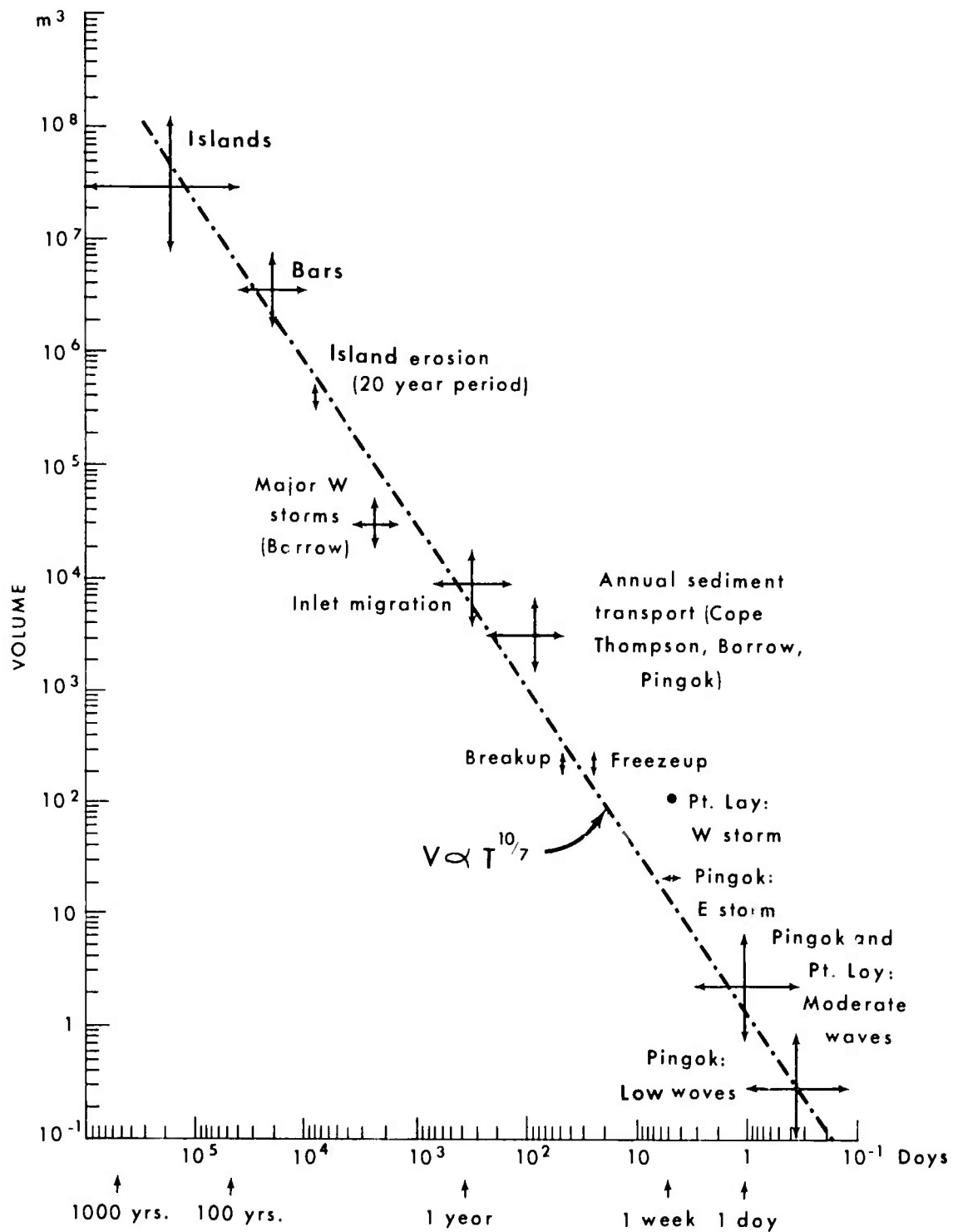


Figure 80. Relationship between period of morphological response and volume of material per unit time.

cover may affect pressure ridging and ice push (Zumberge and Wilson, 1953)]. Unique arctic beach features are produced, however, when normal coastal processes are coupled with a freezing environment. The features result from deposition and growth of ice and ice-sediment structures in the beach and in the nearshore zone. The magnitude and occurrence of the structures depend on incoming wave energy, tidal range, coastal currents, and proximity to freshwater bodies. If calm sea conditions accompany freezeup, they preclude the development of all wave- and swash-dependent forms.

The freezeup sequence and its effects on the beach and nearshore morphology will be examined in the following chronological order: frozen upper beach surface, snow cover, ice cakes, lagoon ice slush, frozen swash, foam and spray, frozen beach face, sea frazil ice, ice push, and pressure ridges.

#### FROZEN UPPER BEACH SURFACE

With the onset of ice days (early September along the eastern and northwestern coasts, late September along the southwestern coast), the exposed beach surface between the prevailing swash limit and the vegetated backshore freezes first. Prior to the onset of ice days, temperatures oscillate above and below 0 C, producing diurnal freeze and thaw of the upper beach surface. Below the beach surface, freezing will move downward with the progression of winter, eventually reaching permafrost.

The initial freezing of the beach surface on Pingok Island occurred on September 1 (minimum air temperature -3 C); subsequent temperature fluctuations (-3 to 6.5 C) produced diurnal freezing and thawing of the surface until September 24. Two periods of ice days (September 14-22 and September 25) kept the beach frozen throughout the day. Though the beach was completely frozen on the last day of the Pingok study (September 25), subsequent thaw was possible.

#### SNOW COVER

Snow plays an important role in the freezeup process; it prevents eolian reworking of the beach sediment, insulates the frozen crust, and often is incorporated into the internal beach structure. This latter process was observed at Point Lay in October 1972. After a 5-20-cm-thick layer of snow had been deposited on the beach, sea level and wave height rose significantly under the influence of westerly winds, and swash washed over the snow-covered upper beach. Swash did not melt the snow; rather, a thin layer of sediment was deposited directly on top of the snow. As sea level fell and waves subsided, water percolating through the sediment began to freeze and solidify. At the same time, below 0 C temperatures began freezing swash on the upper beach face, forming a thin ice crust. Subsequent non-ice days melted both the snow and swash structures. However, if air temperature had not risen significantly, it is likely that the structures would have been preserved within the winter beach.

#### ICE FORMATION

Snow cover and the formation of sea and lagoon ice are the most noticeable effects of freezeup. These blanket the land and water with a frozen, snow-capped mantle. Ice, however, is present along the Alaskan Arctic Coast throughout the year, though type and extent vary seasonally. During summer the ice pack, consisting of ice more than 2 years old and at least 2.5 meters thick, lies tens of kilometers off the eastern coast and hundreds of kilometers off the western coast. Onshore winds transport small ice floes (a small ice floe is a single piece of sea ice 10-200 meters in diameter) and ice cakes (ice floe smaller than 10 meters in diameter) from the pack to the nearshore. New ice (including sheet ice, frazil, ice slush, medium

winter ice, ice rind, and pancakes) begins forming with the onset of ice days. Frazil first appears on brackish water lagoons and riverine areas (salinity 5-20 ‰) as a result of the higher freezing point of brackish water and protection from agitation. It may form in the lagoons weeks before the adjacent higher salinity (salinity 20-32 ‰), wave-agitated sea surface freezes.

Ice crystals first form on calm, supercooled water. The ice crystals, called frazil, coalesce into a thin crust called sheet ice. As the crust thickens to 1-2 cm, it is termed ice slush. Pancakes are produced by fracturing of ice slush into circular pieces of ice up to 3 meters in diameter. Additional freezing and thickening of ice slush to a thickness of approximately 5 cm produces ice rind. Continued thickening to 15-30 cm produces medium winter ice. By the end of winter, newly formed winter ice thickens to between 15 cm and 2 meters.

#### Ice Cakes

Along the Alaskan Arctic Coast, sea ice moves onshore with westerly winds (Wendler, 1973) and the resultant shoreward Ekman drift. Conversely, easterly winds move ice seaward. Ice cakes moving into the nearshore zone are eventually grounded and sorted according to their draft, the largest cakes being grounded farthest from shore and the smallest being washed onto the beach. Off Pingok Island and along much of the Alaskan Arctic Coast, cakes first ground on the outer bars (see Fig. 48B). During open water they disintegrate within 4-5 days through melt and mechanical abrasion. Well-developed microrelief features produced by grounding ice in depths from 6 to 14 meters are described by Rex (1955). Reimnitz et al. (1972) found similar features scouring the bottom from the beach to the 75-meter contour.

Off Pingok Island, the pack ice initially moved out 10-20 km, and alternating westerly and easterly winds moved ice inshore and offshore seven times between August 6 and September 25. Larger cakes grounded on bars, but masses of smaller cakes reached the beach, causing significant wave dampening to occur during low wave conditions (maximum wave period 2.5 seconds). Only small pieces of ice (less than 50 cm in diameter) with a shallow draft were washed onto the beach. During high wave conditions (period 4-10 seconds, height 0.5-2.5 meters) waves battered large cakes in the surf zone and pushed smaller cakes (up to 2 meters in diameter) onto the beach, depositing them up to 1 meter above sea level. Figure 81A shows ice cakes which were deposited, sorted, and partially buried during high-wave conditions. Reimnitz et al. (1972) described ice cakes being stranded on barrier islands up to 4 meters above sea level. Their deposition was associated with a severe westerly storm in September 1970 which raised sea level 3 meters. Kettle holes resulted from the melting of ice stranded during this storm. Ward (1959) described beach ramparts 1.2 meters high formed of drifting ice during summer. Deposition of an ice boulder ridge on Pingok Island is discussed later.

If wave agitation is such as to cause movement of stranded ice boulders without significant transport, swash and backwash will scour beach-sediment beneath the boulders, causing the boulders to sink into the beach. Subsequent sediment deposition by swash will bury the boulders, and on non-ice days the boulders will rapidly melt unless insulated by complete burial. Figure 81B shows the melting crests of partially buried boulders. These boulders are already causing beach subsidence. Note that the exposed boulders are coated by wind-blown sand, which decreases their albedo and accelerates melt. Preservation of these ice boulders through winter is dependent on their relative positions on the beach, their size, depth of burial, and time of deposition relative to freezeup. Those deposited farthest from the shoreline under the thickest sediment cover during freezeup are most likely to be preserved. Boulders deposited and embedded on Pingok Island on September 5 (Fig. 81A)



A. Ice boulders deposited on the beach at Pingok Island during a period of high wave action. Note the decrease in size of boulders higher on the beach and their partial burial. September 6, 1972.



B. Melting ice boulders and beach subsidence on Pingok Island. These boulders were deposited and covered with sediment 2 days earlier, as shown on Figure 81A. September 8, 1972.



C. Lagoon ice slush moving out of Simpson Lagoon. Note the tracks (a and b) left in the slush as it moves past grounded ice cakes. Photo by Don Saunders, NARL, October 4, 1972.



D. Two ice slush berms on Pingok Island. Note floating lagoon ice slush in the swash zone, and remnant frozen swash and foam on the upper beach (white band). September 24, 1972.

Figure 81. Photographs illustrating types of nearshore ice accumulations.

after freezeup had begun were partially preserved on September 25, although continuous ice days had not begun.

Ice boulders preserved through winter will melt during breakup the following year. Melt of the boulders causes collapse of the beach surface and the formation of kettle holes (Fig. 81B). Kettle holes have been described on Baffin Island by Tarr (1897), in Spitsbergen by Thompson (1953), in Antarctica by Nichols (1961) and Kirk (1966), near Nome by Greene (1970), and in lakes in the southern part of Canada by Dionne and Laverdière (1972). Holes ranging from a few centimeters to 10 meters in diameter and up to 1.5 meters deep were observed on Pingok Island. Numerous holes were observed along much of the northwestern and northeastern Alaskan coast during spring 1972. Kettle holes on the northeastern coast were remnants of boulders deposited during the 1970 storm (Reimnitz et al., 1972). Wave activity during 1971 had been too low to reach them. Kettle holes on the northwest coast (north of Wainwright) were the result of ice boulders deposited during a storm in fall 1971.

#### Lagoon Ice Slush

Frazil first appeared on Simpson Lagoon, behind Pingok Island, on September 18. It initially occurred in pockets along the lagoon shore and spread rapidly over most of the lagoon surface during the relatively cold, calm nights of September 19 and 22, thickening into ice slush. Beginning on September 19, wind and tide currents regularly flushed tens of square kilometers of ice slush out through the inlets and into the nearshore zone. This occurred daily in the Jones Island area, and in September and October 1972 was observed occurring at numerous inlets along the northeastern Alaskan coast, with tongues of ice slush extending over 10 km laterally along the coast. Figure 81C shows ice slush moving out of the inlet between Long and Egg islands.

Waves moving through ice slush, which may cover all the nearshore water surface, are attenuated and at times prevented from breaking by the weight of the ice. This is shown in Figure 81D. The currents and wave-induced movement breaks ice slush into small pancakes 1-20 cm in diameter and 1-2 cm thick.

Often when ice slush enters the surf zone it is washed onto the beach as pancakes. Because of their buoyancy, flatness, and relatively small size, pancakes are deposited at the swash limit, accumulating in piles large enough to be termed ice slush berms (Fig. 81D). The term "ice slush berm" has been applied to the structure inasmuch as it resembles in size, shape, and location on the beach face the regular beach berm deposited under similar wave conditions. Sediment is deposited with the ice, at times scattered throughout the berm and at other times completely burying it.

Because the lagoon ice slush develops before sea ice slush, at a time when wave activity is likely to be more intense, it is more often deposited on the ocean beach. When sea ice slush forms, wave activity is much reduced by the ice cover, and the beach may already be protected by ice. However, occasional severe late-season storms are capable of breaking up the new ice and generating large waves and rises in sea level that erode the beach, as occurred in late fall 1972, and in their waning period rapidly deposit frozen swash and sea ice on the beach, building a storm ice foot.

Thus formation of ice slush in the lagoons plays an important role in the freezeup process in the nearshore. The flushing of this slush through inlets and into nearshore waters drastically reduces nearshore wave action and will more than likely cause nearshore waters to freeze somewhat earlier than in regions where

inlets are absent. In addition, deposition of this slush and associated pancakes is worked onto the beach, many of the ice berms being incorporated into the beach structure.

#### Frozen Swash, Foam, and Spray

Swash, foam, and spray will begin to freeze on the beach face when air and water temperatures fall below 0 C, especially if accompanied by strong winds, which increase the chill factor. On Pingok Island, the first freezing swash was simultaneous with lagoon freezing on September 19. Air temperature was -4 C and water temperature was -1 C. Swash began freezing within 15 seconds on gravel and about 20 seconds on sand, forming continuous frazil in about 30 seconds. Subsequent swash runup destroyed the frazil, and the process began again. With falling sea level or decreasing wave energy, frazil was preserved on the beach face, forming a frozen beach matrix if mixed with sediment or a separate ice layer if not. These processes occurred several weeks before frazil or sea ice slush formed on the ocean surfaces.

Sea spray blown onto the beach during sub-zero temperatures freezes, forming a thin frazil ice layer. Foam generated by breaking waves and deposited at the swash limit as foam banks is readily preserved on ice days, rapidly freezing into solid ice and often being embedded with sediment. On Pingok Island, foam banks (Fig. 82A) were deposited contiguous with sediment, resulting in irregular sand and foam interbedding (Fig. 82B). Following deposition of the foam and sediment, waves began to subside and a layer of sediment and occasional pancakes was deposited on top of the foam. The foam had solidified sufficiently to prevent warping by the sediment. A sample of this frozen foam had a salinity of 5 ‰. If much more salt were removed during the winter, it might prove difficult to differentiate frozen foam from snow, which had a salinity of less than 1 ‰ in the spring beach.

#### FROZEN BEACH FACE

Freezing of the beach face within the swash zone coincides with freezing of swash, the frozen swash often acting as a cementing agent for embedded sand and gravel and ice boulders. Freezing produces a hard, smooth crust on the beach face down to the low-tide swash limit. During low water or low wave activity, the beach may freeze close to sea level. Subsequently, it may be eroded or covered by sediment (Fig. 82C). During erosion, slabs of frozen beach crust may be broken off and deposited farther up the beach. If accretion occurs, the frozen surface is buried and insulated against thaw and may be preserved through winter.

Deposition of ice on the beach in the form of frozen snow, ice boulders, ice slush, and frozen swash spray and foam was observed occurring contiguously with deposition of sediment and freezing of the beach face. Under ideal conditions of ice days and upper beach face accretion, ice-sediment deposition is rapid; most of that shown in Figure 82B was deposited in a few hours. This is shown schematically in Figure 83A. The frozen layers solidify into a moderately resistant ice-cemented sand structure. Increasing thickness of the structure augments insulation of subsurface layers, protecting them against thaw on non-ice days. On such days, non-frozen layers of sand and gravel may be deposited over frozen layers. Moore (1966) applied the term "kaimoo" to this feature, but confusion exists in the literature as to the exact use of this term (McCann and Carlisle, 1972). Greene (1970) and Short and Wiseman (1973) described some forms resulting from melting of such structures.



A. Frozen swash and foam on Pingok Island. Note the fresh foam line at the swash limit and sediment-covered swash to the right. September 19, 1972.



B. Beach trend at Pingok Island showing interfingering of frozen foam and sediment. This foam zone is the one illustrated in Figure 82A after burial. Seaward to the left. September 21, 1972.



C. Frozen beach face (center) containing partially buried ice boulders and slabs of frozen sand eroded from the forward edge. Snow, frozen swash, and ice boulders cover the beach in the background; freshly deposited unfrozen gravel is in the foreground. Pingok Island. September 19, 1972.



D. Beach section at Point Lay. June 5, 1972. Note the buried ice layers and beach subsidence resulting from melt of the ice foot in the foreground (layer 1 in Fig. 83B).

Figure 82. Photographs illustrating processes and resulting forms during freezeup.

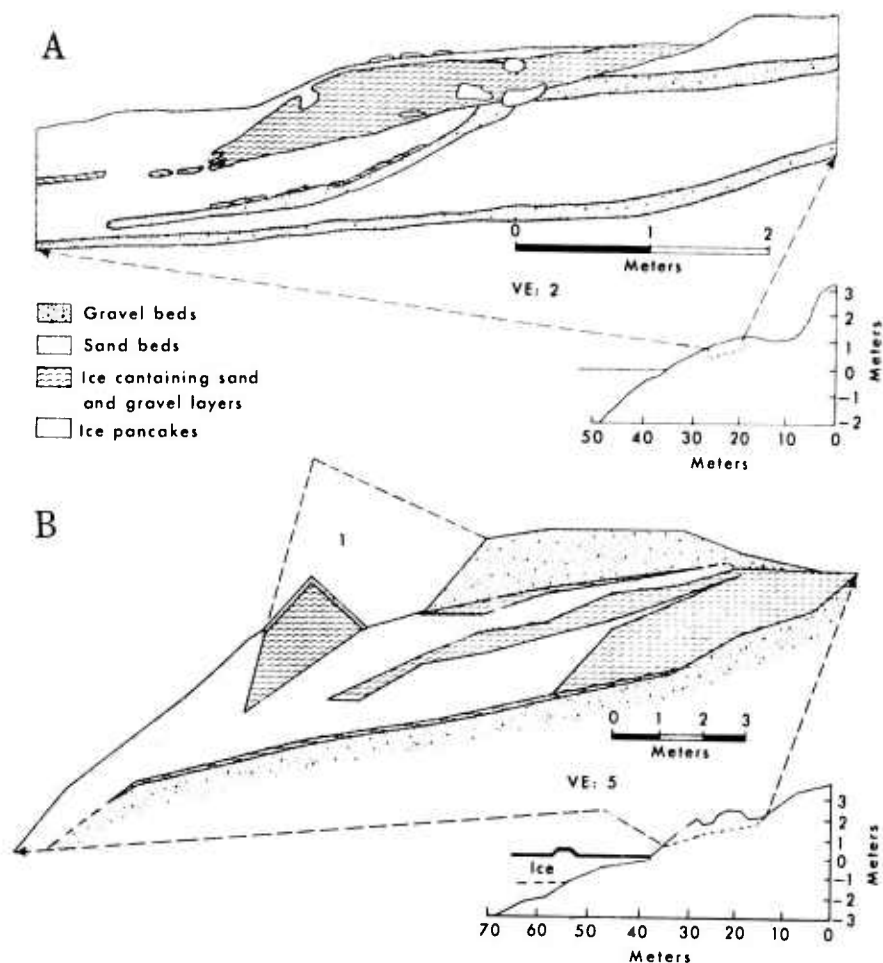


Figure 83. A. Beach section at Pingok Island made on September 21, 1972. B. Beach section at Point Lay made on June 7, 1972. The dashed line is the estimated surface of layer 1 on May 25, prior to melt.

#### Observation of a Winter Beach

The Point Lay beach was surveyed and sectioned in spring 1972 prior to break-up (Figs. 82D and 83B). The section revealed ice-sediment interbedding. In Figure 82B the thin white stringers consist of snow and frozen swash that have been incorporated in the beach in the manner described above. The thicker layer seen in a trench on Point Lay, shown in Figure 83B (layer 1), is a storm ice foot. The other ice layers in this trench had very low salinities (less than 1 ‰), suggesting their origin as snow. Layering was smooth, unlike the mottled frozen foam structures seen forming at Pingok Island (Fig. 82B). In addition, the 1971-1972 freezeup period at Point Lay was accompanied by numerous periods of abnormally high sea level (LIZ-2 DEW Line site personnel, personal communication), suggesting a mechanism of sediment deposition over snow, high on the beach. Short and Wiseman (1973) described sedimentary structures resulting from melt of these ice layers.

## LATE FREEZEUP FEATURES

Freezing of the sea surface was late in the Alaskan Arctic in 1972. Complete freezeup of the nearshore waters had not occurred at Pingok Island by October 1 or at Point Lay by November 1 (P. Barnes, personal communication). Average date of the freezeup at Point Lay is November 4 (Hartwell, 1971). As of the beginning of December, the open water extended for tens of kilometers offshore at Barrow, Alaska. Because of its lateness, the complete sequence of freezeup was not observed. Processes and forms important in the final stage of freezeup are as follows:

- (1) Sea frazil and ice slush rapidly accumulate in the intertidal zone as an ice foot. This feature has been described more than any other arctic shore structure. A good review of past work is given by McCann and Carlisle (1972). Formation of a 1-meter-high storm ice foot was observed at Barrow on October 4, 1972, and air photos taken of the Jones and Return islands (October 4, 1972) indicate that an ice foot ridge was formed above the shoreline and ice extended seaward for several meters along most of the shore (Fig. 84A). New ice had also formed above shoal sections of inner bars, suggesting the ice was bottomfast in these areas.
- (2) Infrequent severe westerly storms have been recorded in September (Reimnitz et al., 1972), October (Hume and Schalk, 1967), and November (as occurred at Barrow in 1972). The Pingok Island area was also affected by a severe storm, possibly the November Barrow storm, in late fall 1972. The effects of the storm were preserved through the winter and were measured during field studies made prior to thaw in May 1973. Figure 85A shows the beach at grid I on May 15, 1973, and the last profile made on September 25, 1972. Figure 85B is a photograph of the ice boulder ridge. Only the surface snow covering the beach sediment was removed, and it is possible that ice-sediment interbedding existed in the beach sediments. The surface of the beach was covered by graded ice boulders, the smallest (average diameter 15 cm) deposited on the upper beach, grading into larger boulders (average diameter 30-100 cm), and finally into an ice boulder ridge at the beach crest. These ice boulders were formed from new winter ice with a maximum thickness to 50 cm and diameter of 1-10 meters. These boulders commonly had sediment embedded in their bases, suggesting that they were shorefast before erosion. The ridge was quite distinctive and relatively continuous the entire length of Pingok and Leavitt islands. The largest boulder observed on Pingok Island measured 10 m X 10 m X 30 cm and was deposited 1.5 meters above sea level, attesting to the rise in sea level accompanying the storm. A small ice foot, similar to that seen at Barrow, fronted the ridge, and at the base, 0.5 meter above sea level, the shorefast ice extended 15 meters seaward to the sea ice. In all, a minimum of 12 m<sup>3</sup> per unit width of ice was deposited on the beach. This was in turn covered by 10-50 cm of snow.
- (3) Ice-pushed ridge formation has been described by Nichols (1963), Hume and Schalk (1964), and Owens and McCann (1970). Hume and Schalk described push as occurring at any time of the year, but Owens and McCann believe it is a summer or fall event. In the study area, the only significant ice push was preserved in the winter beach along the western coast. Ridges up to 15 meters



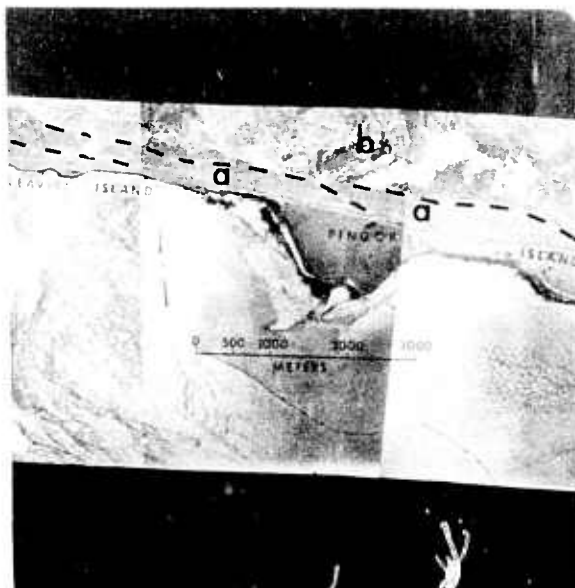
A. Bodfish Island, showing newly developed ice foot and ice forming over sections of the bar. October 4, 1972. Photo by Don Saunders, NARL.



B. Ice push (approximately 15 meters high) on barrier 7 km north of Point Lay. Note distinct zones: exposed foredune (foreground) and two shoreline pressure ridges on either side of ice push. Frozen sea surface is in upper portion of photograph. Width of photo is approximately 1 km. May 17, 1972.



C. Two parallel pressure ridges formed over outer bars. Inner ridges are result of shoreline pressure ridging, ice foot, and snow-covered foredune. Open water to west. Location 8 km south of Point Franklin. May 17, 1972.



D. Mosaic of Pingok Island showing the effect of bars on sea ice patterns in nearshore zone. Ice inside of bars (a) is solid and unfractured; ice seaward (b) is highly fractured and contorted.

Figure 84. Aerial photographs illustrating late freezeup features on the Alaskan Arctic Coast.

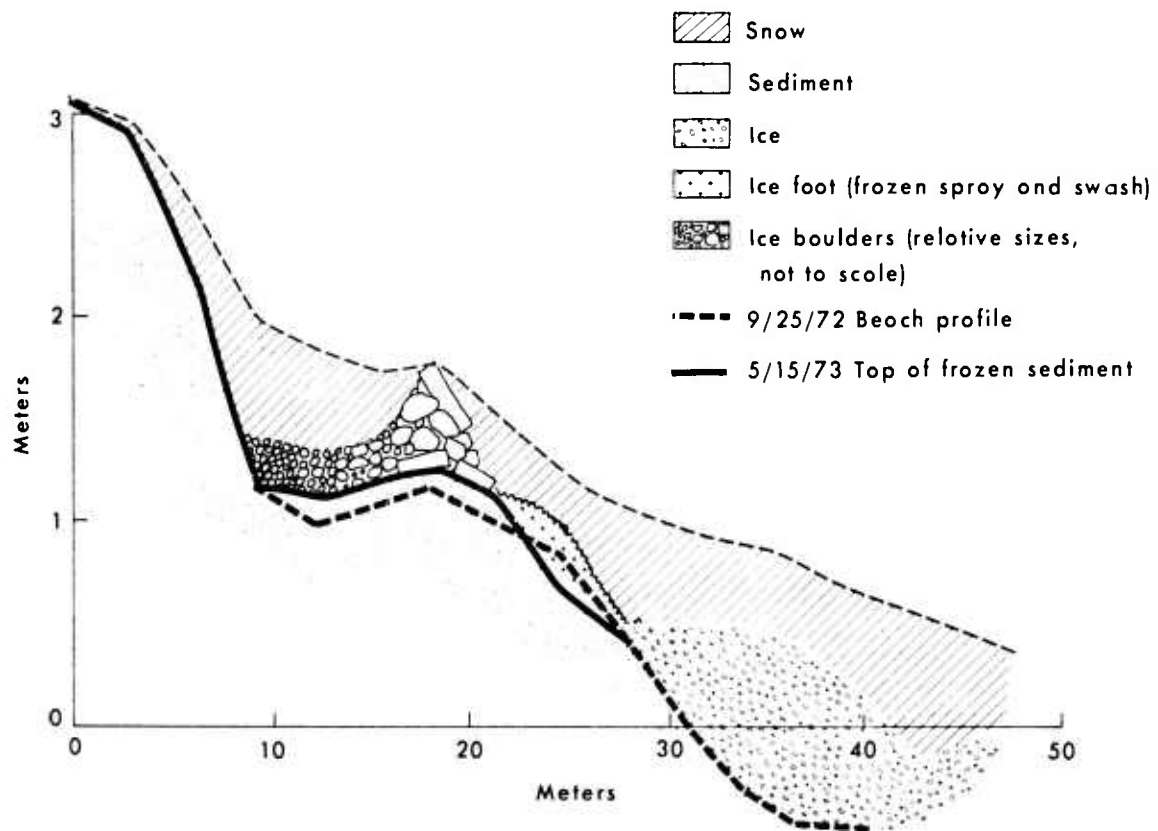


Figure 85A. Section across Pingok Island winter beach following complete 1972 freezeup.



Figure 85B. View west (sea to the right) along the ice boulder ridge on Pingok Island, May 14, 1973. See diagram above.

high, 400 meters long, and 150 meters wide, containing sediment up to 10 meters above sea level, were observed (Fig. 84B). The push never extended past the foredune. Minor ice push at the water line was observed at Point Lay during breakup; the ice was propelled against the shore by currents.

- (4) Shoreline pressure ridges, consisting of buckled new winter ice, form above the sea ice/shorefast ice boundary (Fig. 84B). These ridges are a result of floating ice riding up onto the fast ice during a storm. Along the central western coast, including Point Lay, these ridges, along with a storm ice foot and foredune, stood out as distinctive linear features paralleling the generally featureless winter beach. The inner pressure ridge shown on Figure 84B was the result of ice push at the shoreline.
- (5) Nearshore pressure ridges form on the periphery of tidal delta shoals opposite inlets and on outer bars as a result of ice grounding. Subsequent movement of the sea ice outside the bars pushes ice onto and builds up the distinctive ridges over the bars. The two outer pressure ridges shown in Figure 84C near Point Franklin are positioned just seaward of offshore bars. Ice seaward of the outer bar tends to be fractured and contorted, whereas ice landward of the bars is protected from movement and remains through the winter as a continuous unit. Figure 84D shows the relatively smooth ice (a) inside the bars and fractured ice (b) seaward of the bars. Continuous pressure ridges were observed above the Pingok-Leavitt islands bars in May 1973.

#### DISCUSSION

Around the Alaskan Arctic Coast, freezeup introduces ice and snow into the beach and nearshore zones. Ice slush formed on brackish water bodies is flushed into the adjacent nearshore zone, facilitating its deposition prior to the formation of sea ice slush. Lagoon ice slush has greater potential influence along the eastern coast, where rivers, lagoons, and inlets are more numerous. If wave activity and sea level fluctuations coincide with the presence of ice on the sea surface, the ice may be deposited on the beach as distinctive ice or ice-sediment structures. These structures include ice boulders, ice slush berms, ice-sediment interbedding, ice foot, and ice ridges.

Ice and ice-sediment features occur with high frequency along the western coast, where wave activity often extends into freezeup. Along the eastern coast, freezeup is more often accompanied by calm seas, which preclude the development of wave- and swash-dependent forms.

#### Summary

In general, arctic beach and nearshore morphology is primarily related to processes operating during the open-water season, when wave action is relatively free of ice influence. The extent and duration of this season varies both spatially and seasonally. On the western coast, where it extends for 3-4 months, the pack ice moves out hundreds of kilometers and moderate westerly and lower northerly wave conditions dominate. As a result, the coast has a continuous wave-aligned shoreline. On the eastern coast, open water exists for only 2-3 months, the pack ice moving out only tens of kilometers. Low easterly and westerly waves dominate. The resulting shoreline is irregular and discontinuous. In addition, fluvial influence is significant,

producing wide, shoal coastal lagoons and supplying sediment to the nearshore zone.

The following conclusions appear to be the most significant findings associated with the study of beach processes and responses at the two sites:

- (1) The morphology of the western coast (Cape Lisburne to Point Barrow) reflects moderate westerly and low northerly wave influence, which have interacted to generate large cape systems (three in number). Northerly waves dominate the southern portion of each cape, whereas southwesterly waves dominate the northern sections. This results in a convergence of nearshore transport systems at the capes and divergence in the central part of the systems, where tundra erosion is common.
- (2) The morphology of the eastern coast (Point Barrow to Demarcation Point) reflects the low wave energy, strong alongshore currents, and high fluvial influence. The coast is irregular and broken and has four separate barrier island chains, irregular tundra shorelines, and two large deltas protruding into shoal embayments.
- (3) Waves and coastal currents have generated migratory outer bars along approximately 50 percent of the entire coast, especially off the barrier islands and tundra shorelines. Bar formation is closely related to both the dominant incident waves and coincident wind- and wave-generated currents. Waves determine the pattern of bar development, and both wave orbital motion and coastal currents provide a mechanism of arranging the sediment into this pattern.
- (4) Three sequential periods of process type and intensity occur seasonally along the coast: breakup, open water, and freezeup, each related to the variation in air temperature above and below 0 C.
- (5) Breakup of the coastal zone can be defined in terms of three inter-related zones: river breakup, sea ice breakup, and beach thaw. The timing and extent of the overall breakup are dependent upon the timing and extent of temperature rise above 0 C. The entire breakup sequence took 4-5 weeks at Point Lay and 7-8 weeks at Pingok Island.
- (6) River meltwater causes early breakup in the adjacent lagoons and nearshore zones. The area affected is a function of river discharge, coastal configuration, bottom slope, and coastal currents.
- (7) Sea ice breakup is initiated by above 0 C temperatures, which melt and progressively weaken the ice. The ice breaks up and moves out under the driving force of offshore winds.
- (8) Sea ice grounded on the outer bars delays nearshore breakup by up to 2 weeks.
- (9) Beach thaw requires from 3 to 8 weeks, depending on the amount of ice on and in the beach. Ice within the beach melts slowly, causing subsidence of the overlying beds, and generates unique arctic beach features, including kettle holes, gravel pits, ice foot depressions and scarps, distorted bedding, and microfans and microdeltas. Eolian action rapidly modifies many of the subsidence features.
- (10) During the open-water period, low wave conditions (height less than 30 cm, period 1.0-2.5 seconds) cause superficial disturbance of the beach face

up to 0.5 meter above sea level. Miniature beach forms are generated, though no net change in the beach configuration occurs. Low waves are associated with both easterly and westerly winds on the eastern coast and with northerly winds on the western coast.

- (11) Higher wave conditions (height 0.5-2.2 meters, period 4-10 seconds) are generated by westerly winds on the western coast and occasional storms on the eastern coast. The changes in two-dimensional beach configuration, associated with the arrival of the waves, agree with a general model of beach profile change developed by Sonu and van Beek (1971).
- (12) The magnitude of volume change on Pingok Island during several days of severe wave action ranged from 1 to 10 m<sup>3</sup>/m, an order of magnitude greater than during low wave conditions.
- (13) Unusually high swell and wind waves generated along the eastern coast during September 1972 caused a net change in beach volume equal to the normal beach volume change under westerly waves on the western coast.
- (14) Offshore bars of various configurations dominate much of the nearshore morphology. Along Pingok-Leavitt islands, bars extend from the shore at an angle of 8-10° to a distance of 4-600 meters seaward over a lateral distance of 4-5 km. The bars effect shoreline rhythms with amplitudes of up to 200 meters and average wave lengths of 4,000 meters. Along the coast, spacing of en echelon bars ranges from 0.2 to 20.0 km.
- (15) Planar beach morphology is dominated by the presence and migration of shoreline rhythms. Beaches and islands are broadest behind shoreline horns and narrowest adjacent to bays. On Pingok Island, beach widths ranged from less than 5 meters in bays to 165 meters on horns.
- (16) Beach ridge-and-swale systems oriented at angles to the shoreline are generated by the migration of these shoreline rhythms. Net deposition on the downcurrent side of the horns, coupled with infrequent storms, generates a series of berms and runnels which, as the shoreline progrades seaward, are abandoned as beach ridge-and-swale systems. Truncation of older ridge-and-swale systems occurs on the upcurrent bay side.
- (17) Inlet morphology along the eastern coast is related to breaching of the barriers by river floodwater during breakup and rising sea level during severe westerly storms. Breaching is more likely to occur in the bay areas of shoreline rhythms where the beach or barrier island is narrowest. Along the western coast inlet breaching is more commonly caused by river floodwater.
- (18) Longshore sediment transport of the order of 10<sup>4</sup> m<sup>3</sup> (minimum estimate) occurred at Point Lay and Pingok Island during the 1972 open-water season. This appears to be normal for Point Lay but exceptional for Pingok Island.
- (19) Sediment movement narrowed and closed off several inlets. Inlet migration (breaching and closing) occurs at the rate of one every 1-10 years.

- (20) Island migration to the west is occurring along the eastern coast at rates of between 6 and 25 meters per year.
- (21) Freezeup began in mid-September at Pingok Island and in early October at Point Lay. The upper beach freezes first, and snow cover follows. Next, the surface of the brackish water lagoons freezes. Lagoon ice slush is regularly flushed into the nearshore zone.
- (22) If wave activity and sea level fluctuations continue into freezeup, lagoon and sea ice slush, ice cakes, frozen swash, foam, and spray may be deposited on the beach face as ice and ice-sediment structures up to 3 meters above sea level.
- (23) Calm conditions during freezeup will preclude the development of any beach ice structures, and the summer beach will be preserved until breakup.
- (24) Late-summer storms (September-November) may generate ice foot ridges, storm ice foot, ice push, shoreline ice ridges, and nearshore pressure ridges over the outer bars.
- (25) Throughout the year, the strong Coriolis parameter accentuates the following parameters: sea set-up and set-down; onshore and offshore movement of ice; lagoon flushing, including lagoon ice slush through set-up and set-down; and in general the zonation of beach response, relatively higher on the beach during westerly conditions and lower during easterly.
- (26) Several process-response relationships and morphological characteristics are highlighted by or unique to arctic conditions and deserve consideration in further investigations. These include the following:
  - (a) The freezing of the beach through winter, which allows sectioning and examination of the beach and nearshore zone (to the 2-meter contour) without wave or water interference;
  - (b) The effect of wind set-up and set-down on shifting the swash zone across the beach face during both low and high waves;
  - (c) The pronounced bimodal nature of the sediments, which lend themselves to investigations of this common beach sediment characteristic and its relation to variation in two- and three-dimensional beach configuration;
  - (d) The prominent flotsam (driftwood) lines deposited during severe westerly storms and associated dieback of vegetation, which provide a means of accurately delimiting the extent of storm surges;
  - (e) Relict ridge-and-runnel systems preserved on the horns, which shed additional light on migration of shoreline rhythms and recent changes in beach morphology;
  - (f) The effect of the outer bars on shoreline rhythms, beach width, inlet morphology, and island stability;

- (g) Freezing of the beach face and permafrost and the induced changes in beach permeability unique to arctic beaches.

In total, the results show that the beach and nearshore morphology reflect the dominating influence of waves and coincident wind-generated currents and, to a lesser extent, tides, eolian and fluvial action, and the strong Coriolis effect. Moderate to high waves cause response of the entire beach and generate significant longshore transport. Low waves effect minor beach response. In the nearshore zone, waves and wind-generated currents affect the formation of outer bars, which dominate the nearshore morphology and produce shoreline rhythms. These processes are restricted in influence to the open-water period. Freezing temperatures coupled with the above generate unique arctic ice and ice-sediment structures which dominate the winter beach. Melt of these structures during breakup leaves, at most, superficial disturbance of the wave-dominated morphology.

## CHAPTER VI

### CONCLUSIONS

The Alaskan Arctic Coast project commenced in May 1971 and continued through June 1973. The major objective of the project was to improve understanding of the temporal and spatial variability of the coastal process environments and shoreline responses along this coast and to document specific nearshore processes and beach responses at two field sites, Point Lay and Pingok Island. The project consisted of three phases: data acquisition from maps, aerial photographs, and field reconnaissance (May-December 1971); specific field studies at the Point Lay and Pingok Island sites (April-October 1972); and data reduction and analysis (November 1972 - June 1973). The study required inputs from and investigations by scientists in various disciplines, including meteorology, nearshore hydrodynamics, wave mechanics, morphodynamics, beach dynamics, and geomorphology. Each of the investigators carried out a program within his own field of interest, but attempts were made to integrate these studies so as to satisfy the basic goal of the overall project.

Specific conclusions from each of the studies can be found in each chapter, but the more salient are discussed below:

- (1) A low-level jet was found to exist in wind profiles over a nearshore ice pressure ridge. This finding contrasted significantly with the logarithmic wind profiles measured over smooth ice. The presence of the jet implies an increased drag on the ice surface resulting from the disruption of the wind field by the topography. The presence of such a drag force should be important in determining the location of lead formation, which contributes to local weather modification and fog development. Thus, for accurate predictions of lead location, ice motion, or details of local weather, one must take into account the variation in the drag on the ice over the variable ice topography rather than utilizing a single, flat-ice drag coefficient.
- (2) Determinations of instantaneous drag coefficients and roughness lengths over the nearshore snow-covered ice showed extreme variability. This variability results from wind-blown snow, which causes dynamic changes in local topography. Thus, even over relatively flat ice, there is no single characteristic drag coefficient. This could complicate attempts to model the transfer of momentum from the atmosphere to the ice.
- (3) A constant drag coefficient ( $1.71 \times 10^{-3}$  at 10 meters) was determined for air-sea momentum transfer in the nearshore waters of the Chukchi Sea. This drag coefficient was nearly identical to that found by Banke and Smith (1971) in the nearshore waters of the Beaufort Sea. Therefore, a constant drag coefficient appears to be applicable to air-sea interaction studies of arctic nearshore waters during ice-free periods.
- (4) It was apparent, from the nearshore physical oceanographic measurements,

that air-sea interactions are of paramount importance in determining the dynamic characteristics of nearshore waters. In particular, the momentum transfer from wind to water exerts a strong control on the variations in intensity and direction of nearshore currents during the open-water season. Nearshore currents are much stronger and more variable under ice-free conditions than are the currents beneath shorefast ice at the same location. Current direction in both cases, however, is essentially parallel to the coast. Thus, wind-driven currents dominate the open-water nearshore circulation, and wind-driven coastal currents, in combination with shoreline irregularities, result in intense water level set-up and set-down at and along the coast. Although astronomical tides are present along the Arctic Coast, meteorological tides are far greater in magnitude and contribute significantly to patterns of nearshore circulation.

- (5) Measurements of nearshore waves at the two sites indicate that major wave energy inputs to the coastline are associated with the passage of storms. During the ice-free period of 1972 three storms were witnessed at Point Lay, and one was observed at Pingok Island. This suggests that such mechanisms for producing high wave energy are not uncommon. The along-shore wave power during a single storm at Point Lay was  $2.0 \times 10^8$  ergs/sec/cm, as contrasted to an alongshore power of  $1.0 \times 10^6$  ergs/sec/cm during nonstorm conditions. Such shoreline energy differences play an important role in alongshore sediment transport. The same amount of sediment was transported in one day during storm conditions as average waves would transport in 142 days, or the entire ice-free period. Thus, the vast majority of the sediment moved along the coast is associated with storms, and shoreline response is primarily the result of these storms.
- (6) Wave measurements during nonstorm conditions both east and west of Point Barrow indicate that open water distances are sufficiently large to insure that local wind-generated waves are not fetch limited by the ice pack. To the west of Barrow, during storm conditions wind-generated waves are again not fetch limited by the pack ice, but they may be fetch limited by the size of the storm. East of Barrow, storm-generated waves may be fetch limited by either the size of the storm or the width of offshore open water, depending on the direction of the winds.
- (7) Intense changes in the characteristics of nearshore water masses occur because of impoundment and flushing of waters in the lagoons by storm tides. Flushing of lagoon waters through the inlets introduces low-salinity, warm, turbid water into the nearshore zone, producing a sharp pycnocline or totally replacing the indigenous waters. During the period of freezeup the flushing of fresher lagoon water into the nearshore zone plays an important role in the timing of freezeup of the adjacent nearshore zone and beach. The introduction to the nearshore area of lagoon slush ice through inlets during moderately high wave action results in considerable amounts of ice being incorporated within the beach deposits and thus controls the beach morphology during freezeup as well as during the subsequent thaw period.
- (8) Comparisons of nearshore wave energy and morphologic parameters between the Chukchi and Beaufort seacoasts showed statistically significant contrasts. Variability studies revealed the following:
  - (a) Structural lineaments correlate with coastal morphology and shoreline configuration along the Chukchi Sea coast, the most conspicuous

lineaments parallel the coast, whereas along the Beaufort seacoast they are normal to the coast;

- (b) Barrier systems are straight and continuous along the western coast, irregular and arcuate along the eastern coast;
  - (c) Nearshore wave energy is significantly higher on the western coast than on the eastern coast. Under average wind-generated wave conditions, the volume of sediment change during the open-water period on the western coast is an order of magnitude greater than that along the eastern coast. Sediment volume changes during storms are much more significant and may be several orders of magnitude greater than during nonstorm periods on either coast;
  - (d) The landforms and morphology along the western coast are more nearly in equilibrium with the prevailing energy regimes than those of the eastern coast. Thus, the shoreline along the eastern coast is more subject to major temporal change.
- (9) Dynamic offshore bars were found to be present along at least 50 percent of the entire coastline. Of these, the en echelon type (those that attach at one end to the shoreline), having separations of several kilometers alongshore, variable lengths, and multiple linear, parallel, alongshore bars, are most common. In regions where offshore bars are not present, the nearshore zone is characterized by rocky terraces, mudflats associated with river mouths, rapidly retreating tundra scarps, and featureless nearshore topography.
- (10) The presence of offshore bars plays a significant role in controlling (a) the location of nearshore ice grounding, (b) the formation and location of new inlets or tidal passes, (c) subaerial beach characteristics such as beach slope, width, and trafficability, and (d) rates of erosion and deposition along the shoreline.
- (11) Barrier islands along the eastern coast are migrating to the west at rates of from 6 to 25 meters per year, according to maps and aerial photographs dating back to 1908. Yearly migration rates along any barrier, however, may greatly exceed the annual average. During a 6-week period of observations the western end of Leavitt Island extended a distance of 150 meters.
- (12) The rate of nearshore sea ice breakup is highly variable along the coast and is locally accelerated in regions adjacent to major river systems, in the vicinity of inlets, and in regions devoid of offshore bars. Sea ice breakup is delayed by up to several weeks in the presence of offshore bars or when an ice foot or ice-pushed features are present along the shoreline. These latter features can be detected prior to breakup by aerial reconnaissance or remote-sensing techniques.
- (13) The passage of storms or significant wave action during the freezeup period results in appreciable volumes of ice being incorporated into the beach deposits and forming a distinctive ice ridge at the beach crest that can be recognized on aerial photographs. The incorporated ice delays thaw of the beach during breakup and upon thawing leaves an extremely hummocky, irregular, and soft beach surface that persists until remolded by significant wave action during the open-water season. This beach morphology is unique to arctic beaches and is quite distinctive

on aerial photographs.

- (14) Nearshore pressure ridging or ice grounding occurs over the offshore bars, thus presenting an excellent opportunity for remotely sensing the presence and location of bars in the nearshore. The offshore bars act as barriers to ice movement, causing the sea ice offshore to display a fractured, mosaic pattern, whereas shoreward of the bars the sea ice is relatively smooth and unfractured. Commonly, ridges of broken ice occur directly over the bars.

The 2-year study of arctic coastal processes and shoreline responses raised many more questions than it answered. It indicated, however, that a thorough understanding of the interactions between the air, sea, land, and ice is essential before accurate predictions of the process environments and shoreline responses along the Alaskan Arctic Coast can be made.

#### REFERENCES

- Aagaard, K., 1964, Features of the physical oceanography of the Chukchi Sea in the autumn. M.S. thesis, Univ. of Washington, Seattle.
- Adkison, W. L., and M. M. Brosgé, eds., 1970, Proceedings of the geological seminar on the North Slope of Alaska, 1970. Pacific Section, Am. Assoc. Petrol. Geologists, and North California Geological Soc., 212 pp.
- Arctic Institute of North America, 1963, Proceedings of the Arctic Basin Symposium. October 1962, Hershey, Pa. Centreville, Md. (Tidewater Publ. Co.), 313 pp.
- Are, Felix, 1972, The reworking of shores in the permafrost zone. In (W. P. Adams and F. M. Helleiner, eds.) International Geography. Toronto, Ontario, Canada (Univ. of Toronto Press), 1:78-79.
- Arnborg, L., H. J. Walker, and J. Peippo, 1967, Suspended load of the Colville River, Alaska, 1962. *Geografiska Annaler*, 49(A):131-144.
- Arya, S. P. S., 1973, Air friction and form drag on arctic sea ice. Univ. of Washington, Arctic Ice Dynamic Joint Experiment (AIDJEX) Bull. 19, pp. 43-57.
- Bajorunes, L., 1970, Littoral transport and energy relationships. Proc., 12th Coastal Engr. Conf., Washington, D.C. Am. Soc. Civil Engrs., pp. 787-798.
- Baker, B. B., W. R. Deebel, and R. D. Geisenderfer, 1966, Glossary of oceanographic terms. U.S. Naval Oceanographic Office, Washington, D.C., 2nd ed., 204 pp.
- Banke, E. G., and S. D. Smith, 1971, Wind stress over ice and over water in the Beaufort Sea. *J. Geophys. Res.*, 76:7368-7374.
- Barnes, P. W., 1972, Preliminary results of geologic studies in the eastern central Chukchi Sea. In (M. C. Ingham et al., eds.) WEBSEC-70, An ecological survey in the eastern Chukchi Sea. U.S. Coast Guard Oceanographic Report 50, CG373-50, pp. 87-110.
- \_\_\_\_\_, and E. Reimnitz, 1972, River overflow onto the sea ice off the northern coast of Alaska, spring 1972 (abstract). *Trans. Am. Geophys. Union*, 53(11): 1020.
- Beal, M. A., 1968, The seasonal variation in sea level at Barrow, Alaska. In (J. E. Sater, coordinator), Arctic drifting stations. Arctic Inst. of North America, pp. 327-341.
- Bird, J. B., 1967, Physiography of arctic Canada. Baltimore, Md. (Johns Hopkins Univ. Press), 336 pp.
- Black, R. F., 1951, Eolian deposits of Alaska. *Arctic*, 4(2):89-111.

- Black, R. F., 1964, Gubik formation of Quaternary age in northern Alaska. U.S. Geol. Surv. Prof. Paper 302(C), 91 pp.
- Bretschneider, C. L., 1954, Field investigation of wave energy loss in shallow water ocean waves. U.S. Army Corps of Engrs. Beach Erosion Board Tech. Memo. 46:1-21.
- \_\_\_\_\_, and R. O. Reid, 1954, Modification of wave height due to bottom friction, percolation and refraction. U.S. Army Corps of Engrs. Beach Erosion Board Tech. Memo. 45, 36 pp.
- Brewer, M. C., 1958, The thermal regime of an arctic lake. Trans. Am. Geophys. Union, 39(2):278-284.
- Bruun, P., and F. Gerritsen, 1960, Stability of coastal inlets. Amsterdam (North Holland), 123 pp.
- Coachman, L. K., 1963, Water masses of the Arctic. Proc., Arctic Basin Symposium, October 1962, Hershey Pa. Arctic Inst. of North America. Centreville, Md. (Tidewater Publ. Co.), pp. 143-167.
- \_\_\_\_\_, and J. L. Newton, 1972, Water and ice motion in the Beaufort Sea, spring 1970. Univ. of Washington, Arctic Ice Dynamic Joint Experiment (AIDJEX) Bull. 12:61-91.
- Coachman, L. K., and R. B. Tripp, 1970, Currents north of Bering Strait in winter. Limnology and Oceanography, 15(4):625-632.
- Coleman, J. M., and L. D. Wright, 1972, Analysis of major river systems and their deltas: procedures and rationale, with two examples. Louisiana State Univ., Coastal Studies Inst. Tech. Rept. 95, 125 pp.
- Csanady, G. T., 1972, The coastal boundary layer in Lake Ontario. Part I, The spring regime. J. Phys. Oceanography, 2(1):41-53.
- Davies, R. A., Jr., 1970, Ice effects along coastal Lake Michigan. Symposium on Effects of Extreme Conditions on Coastal Environments, unpublished manuscript. 3 pp.
- Dietz, R. S., and G. Shumway, 1961, Arctic Basin geomorphology. Bull. Geol. Soc. Am., 72:1319-1330.
- Dillon, W. P., and J. T. Conover, 1965, Formation of ice-cemented sand blocks on a beach and lithologic implications. J. Sediment. Petrol., 35(4):964-969.
- Dionne, J. C., 1969, Tidal flat erosion by ice at La Pocatiere, St. Lawrence Estuary. J. Sediment. Petrol., 39(3):1174-1181.
- \_\_\_\_\_, and Camille Laverdière, 1972, Ice formed beach features from Lake St. Jean, Quebec. Canadian J. Earth Sci., 9(8):979-990.
- Dolan, R., and J. Ferm, 1968, Crescentic landforms along the Atlantic coast of the United States. Science, 159:627-629.
- Dygas, J. A., R. Tucker, and D. C. Burrell, 1972, Geological report on the heavy minerals, sediment transport, and shoreline changes of the barrier islands

- and coast between Oliktok Point and Beechy Point. In (P. J. Kinney et al., eds.) Baseline data study of the Alaskan Arctic aquatic environment. Univ. of Alaska, Inst. of Marine Sci., Rept. R-72-3, pp. 61-121.
- Ekman, V. W., 1905, On the influence of the earth's rotation on ocean currents. Arkiv för matematik, astronomi, och fysik. Band 2, No. 11.
- Farrelly, W., 1972, Form and sediments of an Antarctic Beach. Unpublished M.A. thesis, Univ. of Canterbury, New Zealand, 109 pp.
- Fleming, R. H., and D. Heggarty, 1966, Oceanography of the southeastern Chukchi Sea. In (N. J. Wilimovsky and J. N. Wolfe, eds.) Environments of the Cape Thompson Region, Alaska. U.S. Atomic Energy Comm., Oak Ridge, Tenn., pp. 697-754.
- Friedman, G. M., 1967, Dynamic processes and statistical parameters compared for size frequency distribution of beach and river sands. J. Sediment. Petrol., 37:327-354.
- Galvin, C. J., 1970, Ice-cemented sand slabs on middle Atlantic coast beaches. Symposium on Effects of Extreme Conditions on Coastal Environments, unpublished manuscript.
- Garrett, J., 1969, Some new observations on the equilibrium region of the wind wave spectrum. J. Marine Res., 27(3):273-277.
- Giddings, J. L., Jr., 1952, Driftwood and problems of arctic sea currents. Am. Philos. Soc. Proc., Philadelphia, 96:129-142.
- Greene, H. G., 1970, Micro-relief of an arctic beach. J. Sediment. Petrol., 40:419-427.
- Grigor'ev, N. F., 1964, Features of the formation of coasts under conditions of polar climates. National Committee Soviet Geography, Moscow, pp. 148-158.
- Groen, P., and G. W. Groves, 1962, Surges. In (M. N. Hill, ed.) The sea. New York (Interscience Publishers), I:611-646.
- Hartwell, A. D., 1971, Coastal conditions of arctic northern Alaska. Cold Regions Res. and Engr. Lab (CRREL), Hanover, N.H., Special Rept. Draft, Advanced Research Projects Agency (ARPA) Order 1615, 26 pp.
- Hess, S. L., 1959, Introduction to theoretical meteorology. New York (Holt, Rinehart, and Winston), 355 pp.
- Horn, D. R., 1967, Recent marine sediments and submarine topography, Sverdrup Islands, Canadian Arctic Archipelago. Ph.D. dissertation, Univ. of Texas, Austin, 362 pp.
- Hume, J. D., and Marshall Schalk, 1964a, The effects of ice-push on arctic beaches. Am. J. Sci., 262:267-273.
- \_\_\_\_\_, 1964b, Nearshore environment, processes and sedimentation, Barrow, Alaska. Unpublished manuscript, 20 pp.
- \_\_\_\_\_, 1967, Shoreline processes near Barrow Alaska: A comparison of the normal and the catastrophic. Arctic, 20(2):86-103.

- Hunkins, K., 1962, Waves on the Arctic Ocean. *J. Geophys. Res.*, 67(6):2477-2489.
- \_\_\_\_\_, 1965, Tide and storm surge observations in the Chukchi Sea. *Limnology and Oceanography*, 10(1):29-39.
- Ingham, M. C., and B. A. Rutland, 1972, Physical oceanography of the eastern Chukchi Sea off Cape Lisburne - Icy Cape. In (M. C. Ingham et al., eds.) WEBSEC-70, An ecological survey in the eastern Chukchi Sea, September-October 1970. U.S. Coast Guard Oceanographic Report 50, CG373-50, pp. 1-86.
- Inman, D. L., 1952, Measure for describing the size distribution of sediments. *J. Sediment. Petrol.*, 22(3):125-145.
- Kelley, J. J., Jr., and D. F. Weaver, 1969, Physical processes at the surface of the arctic tundra. *Arctic*, 22(4):425-437.
- Kinney, P. J., D. M. Schell, J. Dygas, R. Nenahlo, and G. E. Hall, 1972, Nearshore currents. In (P. J. Kinney et al., eds.) Baseline data study of the Alaskan Arctic aquatic environment. Univ. of Alaska, Inst. of Marine Sci., Rept. R-72-3, pp. 29-48.
- Kinsman, Blair, 1965, Wind waves. New York (Prentice-Hall), p. 23.
- Kirk, R. M., 1966, Beach observations at Cape Royds, Ross Island, McMurdo Sound, Antarctica, 1965-66. Univ. of Canterbury, New Zealand, Geography Dept., New Zealand Antarctica Soc. Rept. to Canterbury Branch, 23 pp.
- Kluev, E. V., 1965, The role of permafrost in the dynamics of bottom relief of the polar seas. *Okeanologiya*, 5(5):863-869.
- Komar, P. D., and D. L. Inman, 1970, Longshore sand transport on beaches. *J. Geophys. Res.*, 75:5914-5927.
- Lachenbruch, A. H., 1960, Thermal contraction cracks and ice wedges in permafrost. In *Short Papers in Geological Sci.*, U.S. Geol. Surv. Prof. Paper 400-B, B404-B406.
- LaFond, E. C., and D. W. Pritchard, 1952, Physical oceanographic investigations in the eastern Bering and Chukchi seas during summer of 1947. *J. Marine Res.*, 11:69-86.
- Leffingwell, E. de K., 1919, The Canning River region, northern Alaska. U.S. Geol. Surv. Prof. Paper 109, 251 pp.
- Lewellen, R. T., 1965, Characteristics and rates of thermal erosion, Barrow, Alaska. Unpublished Master's thesis, Univ. of Denver, Colorado, 181 pp.
- \_\_\_\_\_, 1970, Permafrost erosion along the Beaufort Sea coast. *Arctic Inst. of North America*, Washington, D.C. (Univ. of Denver microfilm), 4 pp.
- \_\_\_\_\_, 1972A, Studies on the fluvial environment, arctic coastal plain province, Northern Alaska. Published by the author, Littleton, Colorado, v. 1, 282 pp.
- \_\_\_\_\_, 1972B, The occurrence and characteristics of nearshore permafrost, Northern Alaska. Progress Rept. for Arctic Inst. of North America, 77 pp.

- MacCarthy, G. R., 1953, Recent changes in the shoreline near Point Barrow, Alaska. *Arctic*, 6:44-51.
- Maher, J.C., and W. M. Trollman, 1970, Geological literature on the North Slope of Alaska. Am. Assoc. Petrol. Geologists, Tulsa, Okla., 132 pp.
- Matthews, J. B., 1970, Tides at Point Barrow. *The Northern Engr.*, 2(2):12-13.
- \_\_\_\_\_, 1971, Long period gravity waves and storm surges on the Arctic Ocean continental shelf (abstract). *Proc., Joint Oceanographic Assembly, Tokyo, 1970*, pp. 332-333.
- McCann, S. B., 1972, Magnitude and frequency of processes operating on arctic beaches, Queen Elizabeth Islands, N.W.T. In (W. P. Adams and F. M. Helleiner, eds.) *International Geography*. Toronto, Ontario, Canada (Univ. of Toronto Press), 1:41-43.
- \_\_\_\_\_, and R. J. Carlisle, 1972, The nature of the ice-foot on the beaches of Radstock Bay, south-west of Devon Island, N.W.T, Canada. *Inst. of British Geographers Spec. Publ.* 4:175-186.
- McCann, S. B., and E. H. Owens, 1969, The size and shape of sediments in three arctic beaches, S. W. Devon Island, N.W.T., Canada. *Arctic and Alpine Res.*, 1(4):267-278.
- \_\_\_\_\_, 1970, Plan and profile characteristics of beaches in the Canadian Arctic Archipelago. *Shore and Beach*, 38(1):26-30.
- McManus, D. A., and J. E. Creager, 1963, Physical and sedimentary environments on a large spitlike shoal. *J. Geol.*, 71:498-512.
- Miller, R. L., T. G. Payne, and G. Gryc, 1959, Geology of possible petroleum provinces in Alaska. *U.S. Geol. Surv. Bull.* 1094, 131 pp.
- Moigin, A., 1965, A contribution to the study of the shore and bottom of Kongsfjorden (Veslspitsbergen), 79 N. *Cahiers Oceanographiques*, 17(8):543-563.
- \_\_\_\_\_, and A. Guilcher, 1967, A coastal sandspit in an arctic periglacial environment: the Sars sandspit (Svalbard). *Norois*, 14(56):548-568.
- Moody, J. W., 1964, Coastal morphology and processes in relation to the development of submarine sand ridges off Bethany Beach, Delaware. Unpublished thesis, Johns Hopkins Univ., Baltimore, Md., 167 pp.
- Moore, G. W., 1960, Observations of coastal processes in the vicinity of Cape Thompson, Alaska, from May 3 to May 9, 1960. *U.S. Geol. Surv. Rept.* TEI-764, pp. 24-28.
- \_\_\_\_\_, 1961, Sorting of beach sediment, Northwestern Alaska. In *Short Papers in the Geologic and Hydrologic Sciences*, U.S. Geol. Surv. Prof. Paper 424C, pp. C198-C200.
- \_\_\_\_\_, 1966, Arctic beach sedimentation. In (N. J. Wilimovsky and J. N. Wolfe, eds.) *Environments of the Cape Thompson Region, Alaska*. U.S. Atomic Energy Comm., Oak Ridge, Tenn., pp. 587-608.

- \_\_\_\_\_, and D. W. Scholl, 1961, Coastal sedimentation in northwestern Alaska. U.S. Geol. Surv. Rept. TEI-779, pp. 43-65.
- Munk, W., 1963, Long ocean waves. In (M. N. Hill, ed.) The sea. Vol. 1, pp. 647-663. New York (Wiley).
- Munn, R. E., 1966, Descriptive micrometeorology. New York (Academic Press), 245 pp.
- Nichols, R. L., 1953, Marine and lacustrine ice-pushed ridges. J. Glaciology, 2(13):172-175.
- \_\_\_\_\_, 1961, Characteristics of beaches formed in polar climates. Am. J. Sci., 259:694-708.
- \_\_\_\_\_, 1968, Coastal geomorphology, McMurdo Sound, Antarctica. J. Glaciology, 7(51):449-478.
- Norrman, J. O., 1964, Lake Vättern - Investigation on shore and bottom morphology. Geografiska Annaler, Hafte 1-2, Series A, Nr. 194, 238 pp.
- O'Sullivan, J. B., 1961, Quaternary geology of the arctic coastal plain, northern Alaska. Ph.D. thesis, Iowa State Univ., Ames, 191 pp.
- Owens, E. H., and S. B. McCann, 1960, The role of ice in the arctic beach environment with special reference to Cape Ricketts, Southwest Devon Island, N.W.T., Canada. Am. J. Sci., 268:397-414.
- Pollard, Raymond, 1973, Interpretation of near-surface current meter observations. Deep-Sea Res., 20(3):261-268.
- Popov, E. A., 1959, The effect of ice bodies and shore ice on coastal dynamics. Trudy okeanogr. Kom. Akad. Nauk. SSSR 4.
- Raasch, G. O., ed., 1961, Geology of the Arctic: Proceedings, First International Symposium on Arctic geology, January 1960, Calgary. Toronto, Ontario, Canada (Univ. Toronto Press), 2 vols, 732 pp.
- Reimnitz, E., and K. F. Bruder, 1972, River discharge into an ice-covered ocean and related river sediment dispersal, Beaufort Sea, coast of Alaska. Bull. Geol. Soc. Am., 83:861-866.
- Reimnitz, E., P. Barnes, T. Forgatsch, and C. Rodeick, 1973, Influence of grounding ice on the arctic shelf of Alaska. Marine Geology, 13(5):323-334.
- Reimnitz, E., S. C. Wolf, and C. A. Rodeick, 1972, Preliminary interpretation of seismic profiles in the Prudhoe Bay area, Beaufort Sea, Alaska. U.S. Geol. Surv., open-file report, 11 pp.
- Rex, R. W., 1955, Micro-relief produced by sea ice grounding in the Chukchi Sea near Barrow, Alaska. Arctic, 8:177-186.
- \_\_\_\_\_, 1964, Arctic beaches: Barrow, Alaska. In (R. L. Miller, ed.) Papers in Marine Geology, pp. 384-400.
- \_\_\_\_\_, and E. J. Taylor, 1953, Littoral sedimentation and the annual beach cycle of the Barrow, Alaska, area. Stanford Univ., ONR Final Rept., Contract Nonr 225(09), 67 pp.

- Ruggles, K. W., 1969, The wind field in the first ten meters of the atmosphere above the ocean. Mass. Inst. Technology, Rept. 69-1, 108 pp.
- Sater, J. E., and collaborators, 1963, The Arctic Basin. Arctic Inst. of North America, Washington, D.C., 319 pp.
- Schalk, Marshall, 1957, Beach and nearshore studies: Point Barrow, Alaska (July 1954 - January 1957). Woods Hole Oceanographic Inst., manuscript rept., 43 pp.
- \_\_\_\_\_, 1963, Study of nearshore bottom profiles east and southwest of Point Barrow, Alaska: comparison of profiles in the Point Lay and Plover Island areas. Arctic Inst. of North America Projects ONR-217, 241, final rept. Unpublished manuscript.
- \_\_\_\_\_, and J. D. Hume, 1966, Sea ice movement of beach material in the vicinity of Point Barrow, Alaska (abstract). J. Geophys. Res., 66(8):2558-2559.
- Scott, R. F., 1969, The freezing process and mechanics of frozen ground. Cold Regions Research and Engr. Lab. (CRREL), Hanover, N.H., Monograph 11-D1, 65 pp.
- Searby, H. W., Climate of Alaska. In Climatology of the United States: Climates of States. Dept. of Commerce, ESSA, Environmental Data Service. 23 pp.
- Short, A. D., 1973, Beach dynamics and nearshore morphology of the Alaskan Arctic Coast. Unpublished Ph.D. dissertation, Louisiana State Univ., Baton Rouge, 140 pp.
- \_\_\_\_\_, and Wm. J. Wiseman, Jr., 1972, Freezing effects on arctic beaches. Louisiana State Univ., Coastal Studies Bull. 7, Tech. Rept. 128, pp. 23-31.
- Smith, S. D., 1972, Wind stress and turbulence over a flat ice floe. J. Geophys. Res., 77(21):3886-3901.
- Snedecor, G. W., and W. G. Cochran, 1967, Statistical methods. Ames, Iowa (Iowa State Univ. Press), 593 pp.
- Sonu, C. J., 1969, Collective movement of sediment in littoral environment. Proc., Eleventh Coastal Engr. Conf., London, pp. 373-400.
- \_\_\_\_\_, 1972, Bi-modal composition and cyclic characteristics of beach sediment in continuously changing profiles. J. Sediment. Petrol., 42(4):852-857.
- \_\_\_\_\_, 1973, Three dimensional beach changes. J. Geol., 81(1):42-64.
- \_\_\_\_\_, and W. R. James, 1973, A Markov model for beach profile changes. J. Geophys. Res., 78(9):1462-1471.
- Sonu, C. J., and J. L. van Beek, 1971, Systematic beach changes on the Outer Banks, North Carolina. J. Geol., 79(4):416-425.
- Spelizman, L. A., 1959, Vegetation of the arctic slope of Alaska. U.S. Geol. Surv. Paper 302-B, 58 pp.
- Spichkin, V. A., 1961, The mechanics of fast (land) ice breakup. Leningrad, Arkticheskiĭ i antarkicheskiĭ n-issl. inst. Trudy, Vol. 256, pp. 12-27.
- Sverdrup, H. V., 1927, Dynamics of tides on the North Siberian Shelf. Geofiziske Publikasjoner, 4(5):1-75.

- Swift, D. J. P., B. Holliday, N. Avignon, and G. Shideler, 1972, Anatomy of a shoreface ridge system, False Cape, Virginia. *Marine Geol.*, 12(1):59-84.
- Tarr, R. S., 1897, The Arctic sea ice as a geological agent. *Am. J. Sci.*, 183:223-229.
- Tedrow, J. C. F., and J. Brown, 1967, Soils of Arctic Alaska. In (H. E. Wright, Jr., and W.H. Osburn, eds.) *Arctic and alpine environments*, pp. 283-293, Bloomington, Indiana (Indiana Univ. Press).
- Tedrow, J. C. F., J. V. Drew, D. E. Hill, and L. A. Douglas, 1958, Major genetic soils of the arctic slope of Alaska. *J. Soil Sci.*, 9(1):33-45.
- Thompson, H. R., 1953, Geology and geomorphology in the southeastern Nordaustland (North-East Land), Spitsbergen. *Proc., Geologists Assn.*, 64:293-312.
- Tolstov, A. N., 1961, A region of great wash-outs and thermokarst. *Problemy Severa*, 4:151-156.
- Truxillo, S. G., 1970, Development of a resistance-wire wave gauge or shallow-water wave and water-level investigations. Louisiana State Univ., Coastal Studies Bull. 4, p. 73.
- U.S. Navy Hydrographic Office, 1958, Oceanographic atlas of the polar seas, Part II, Arctic. 149 pp.
- Voronov, P. S., Reinin I. V. Lastochkin, and V. I. Yakushev, 1970, Orientation and origin of lineaments. In (M. I. Belov, ed.) *Problems of polar geography*. Vol. 285 (translation, Israel Program for Scientific Translations, Jerusalem).
- Walker, H. J., 1967, River bank dunes in the Colville Delta. Louisiana State Univ., Coastal Studies Bull. 1, pp. 7-14.
- \_\_\_\_\_, 1969, Some aspects of erosion and sedimentation in an arctic delta during breakup. *Assoc. Internat. d'Hydro. Sci., Actes du Colloque de Bucarest, Hydrologie des Deltas*, pp. 209-219.
- \_\_\_\_\_, 1972, Salinity changes in the Colville River delta, Alaska, during breakup. In *International Symposium on the Role of Snow and Ice in Hydrology*, Banff, Canada, 7 pp.
- \_\_\_\_\_, 1973, Spring discharge of an arctic river determined from salinity measurements beneath sea ice. *Water Resources Res.*, 9(2):474-480.
- \_\_\_\_\_, and J. M. McCloy, 1967, Morphologic change in two arctic deltas. *Arctic Inst. of North America Research Paper* 49.
- Ward, W. H., 1959, Ice action on shores. *J. Glaciology*, 3(25):437.
- Washburn, A. L., 1956, Classification of patterned ground and review of suggested origins. *Bull. Geol. Soc. Am.*, 67(7):823-866.
- Wendler, G., 1973, Sea ice observations by means of satellite. *J. Geophys. Res.*, 78(9):1427-1448.
- Werner, M. A., and Marshall Schalk, 1959, Comparative study of shallow-water sediments in the vicinity of Barrow, Alaska (abstract). *Bull. Geol. Soc. Am.*, 70(12):1798.

Wilimovsky, N. J., and J. N. Wolfe, eds., 1966, Environments of the Cape Thompson Region, Alaska. U.S. Atomic Energy Comm., Oak Ridge, Tenn., 1250 pp.

Wright, L. D., 1970, Circulation, effluent diffusion, and sediment transport, mouth of South Pass, Mississippi River delta. Louisiana State Univ., Coastal Studies Inst., Tech. Rept. 84, 56 pp.

Zumberge, J. H., and J. T. Wilson, 1953, Quantitative studies on thermal expansion and contraction of lake ice. J. Geol., 61:374-383.